Ministry for Primary Industries
Manatū Ahu Matua

Characterisation and length-based assessment model for scampi (*Metanephrops challengeri*) in the Bay of Plenty (SCI 1) and Hawke Bay/Wairarapa (SCI 2)

New Zealand Fisheries Assessment Report 2014/33
Ian Tuck

ISSN 1179-5352 (online)
ISBN 978-0-478-43710-2 (online)

July 2014

New Zealand Government

Growing and Protecting New Zealand

Requests for further copies should be directed to:

Publications Logistics Officer
Ministry for Primary Industries
PO Box 2526
WELLINGTON 6140

Email: brand@mpi.govt.nz
Telephone: 0800 00 83 33
Facsimile: 04-894 0300

This publication is also available on the Ministry for Primary Industries websites at:
http://www.mpi.govt.nz/news-resources/publications.aspx
http://fs.fish.govt.nz – go to Document library/Research reports

© Crown Copyright - Ministry for Primary Industries

TABLE OF CONTENTS

EXECUTIVE SUMMARY

Tuck, I.D. (2014). Characterisation and length-based population model for scampi (*Metanephrops challengeri*) in the Bay of Plenty (SCI 1) and Hawke Bay/Wairarapa (SCI 2).

***New Zealand Fisheries Assessment Report 2014/33.* 170 p.**

Stock assessments of the Bay of Plenty (SCI 1) and Wairarapa / Hawke Bay (SCI 2) scampi stocks have been undertaken through MPI project DEE201002SCIB. This work has revised existing models for these stocks, developed within previous MPI projects. The assessments presented for both stocks were accepted.

Fishery characterisations were undertaken, and a range of CPUE indices were estimated for each stock, on the basis of spatial and temporal stratification of the previous models. Previous models have examined incorporating considerable spatial structure, but following preliminary investigations, the SFAWG recommended only developing single area models for these stocks, and fitting an annual CPUE index rather than separate time step indices. Sensitivity to natural mortality, commercial fishery selectivity and the assumption of equilibrium conditions at the start of the fishery were investigated, with base models for both stocks taken as those with M fixed at 0.2 and 0.3.

For SCI 1, SSB is estimated to have increased through the late 1980s or early 1990s, peaking around 1994, and then declining until the early 2000s, and remaining stable at around 70% SSB_0 thereafter. MCMC posteriors suggest 0% probability that SSB_{2012} is below 40% SSB_0. Annual fishing intensity has consistently been estimated to be below F 40% B_0. Future catches between 100 and 140 tonnes (to 2018) are predicted to reduce the SSB relative to SSB_{2012}, but remain above 40% SSB_0.

For SCI 2, SSB is estimated to have increased through the early 1990s, peaking in 1992, and then declining to a minimum in 2003, increasing slightly until about 2008, with a more marked increase after this. MCMC posteriors suggest 0% probability that SSB_{2012} is below 40% SSB_0. Annual fishing intensity peaked in 2002 (when it may have exceeded F 40% B_0) but has declined considerably in recent years, while SSB as a proportion of SSB_0 has increased. Future catches between 100 and 140 tonnes (to 2018) are predicted to reduce the SSB relative to SSB_{2012}, but remain above 40% SSB_0.

1. INTRODUCTION

This report undertakes a fishery characterisation for the Bay of Plenty (SCI 1) and Hawke Bay/Wairarapa (SCI 2) scampi stocks, and applies the previously described Bayesian, length-based, two-sex population model to these stocks. Previous characterisations of scampi stocks are described by Tuck (2009). The first attempt at developing a length-based population model for any scampi stock was conducted for SCI 1 (Cryer et al. 2005), implemented using the general-purpose stock assessment program CASAL v2.06 (September 2004). This model for SCI 1 was developed further and the same model structure was also applied to SCI 2 in a later project (Tuck & Dunn 2006). The current study used CASAL v 2.22 (Bull et al. 2008) with a slightly modified selectivity option. Developments in the model implementation and structure have been largely based on suggestions raised at the MFish funded Scampi Assessment Workshop (Tuck & Dunn 2009), and subsequently at Shellfish Fisheries Assessment Working Group (SFAWG) meetings. Assessments for SCI 1 and SCI 2 using this model were accepted in 2011 (Tuck & Dunn 2012).

We describe the available data and how they were used, the parameterisation of the model, and model fits and sensitivity. This report fulfils Ministry of Fisheries project DEE201002SCIB "*Stock assessment of scampi*", undertaking a first assessment of SCI 1 and SCI 2. The objective of this project was to conduct a stock assessment, including estimating yield, for SCI 1 and SCI 2 in 2012–13.

1.1. The Bay of Plenty (SCI 1) and Hawke Bay/Wairarapa (SCI 2) scampi fisheries

Scampi is fished all around New Zealand, in nine fishery management areas (Figure 1). The SCI 1 and SCI 2 fisheries are two of New Zealand's four main scampi fisheries (the others being SCI 3 and SCI 6A), and over the last 5 years (2007–08 to 2011–12) have contributed an average of 105 and 92 tonnes annually, with landings from SCI 1 remaining relatively stable while those from SCI 2 have increased in recent years. The TAC for SCI 1 is 120 tonnes, for SCI 2 is 100 tonnes (having been reduced from 200 tonnes in 2011), and the total TAC for all management areas is 1191 tonnes.

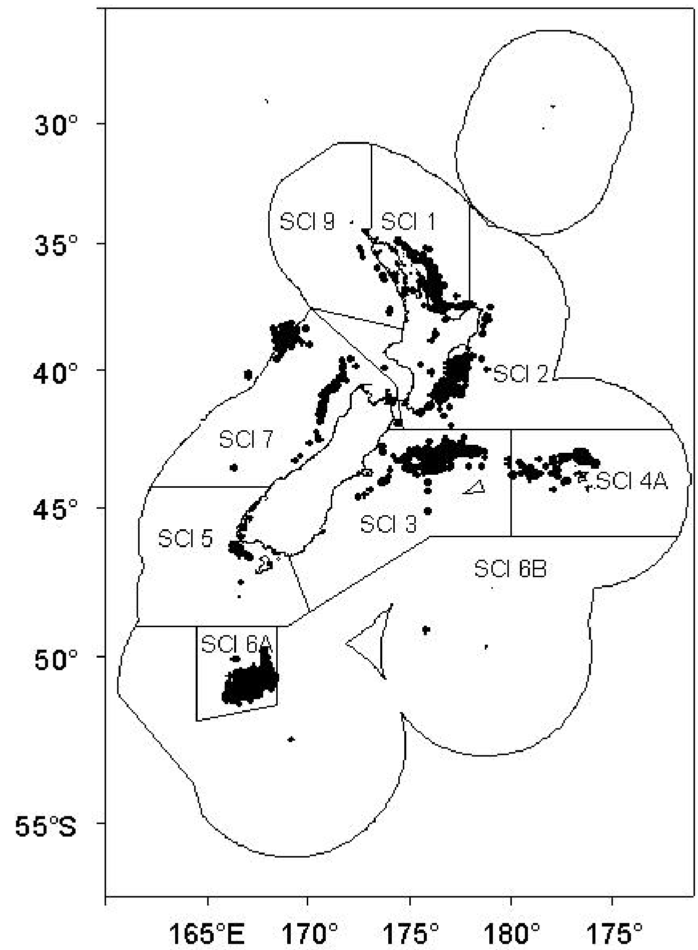

Figure 1: Spatial distribution of the scampi fishery since 1988–89. Each dot shows the mid point of one or more tows recorded on TCEPR with scampi as the target species.

The spatial distribution of the targeted scampi fishing within SCI 1 is focussed in an relatively narrow continuous band (interrupted at Mayor Island) within the Bay of Plenty (Figure 2), generally ranging from 300–500 m depth. More isolated patches have also been fished in some years, to the north and east, but in the same depth range. Targeted scampi fishing in SCI 2 has been focussed in two separate patches, from Hawke Bay to (roughly) Blackhead Point, and from Cape Turnagain to Castle Point, again generally ranging from 300–500 m depth (Figure 3). Smaller isolated patches have also been fished on occasion to the north and south. In both areas, surveys have focussed on the main areas of the fishery, and survey strata coverage is illustrated in the respective figures.

Management areas have remained consistent for SCI 1 and SCI 2 throughout the history of the fishery. Prior to the 1991–92 fishing year there were no limits on scampi catches. For the 1991–92 fishing year, Individual Quotas (IQs) were introduced for both areas (allocated on the basis of the permit holders' catch in 1990–91). These IQs were maintained with the introduction of ICE regulations in 1999, and continued until the Court of Appeal ruled in October 2001 that the scampi ICE regulations were unlawful, after which all scampi stocks were managed under competitive catch limits, until the species was introduced into the QMS (October 2004), since which time all scampi fisheries have been managed with individual quotas.

Previous fishery characterisations have been undertaken for these areas in Cryer & Coburn (2000) and Tuck (2009).

SCI 1

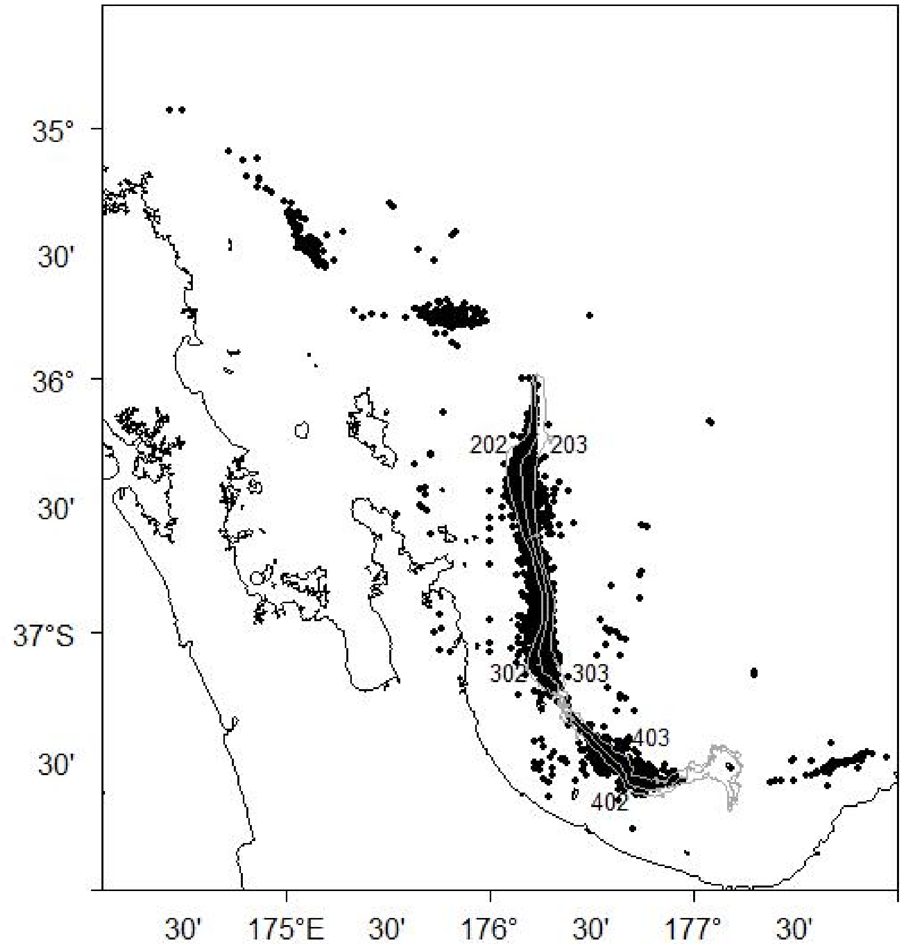

Figure 2: Spatial distribution of the scampi fishery within management area SCI 1 since 1988–89. Each dot shows the mid point of one or more tows recorded on TCEPR with scampi as the target species. The extents of the six scampi survey strata are shown in grey with associated labels.

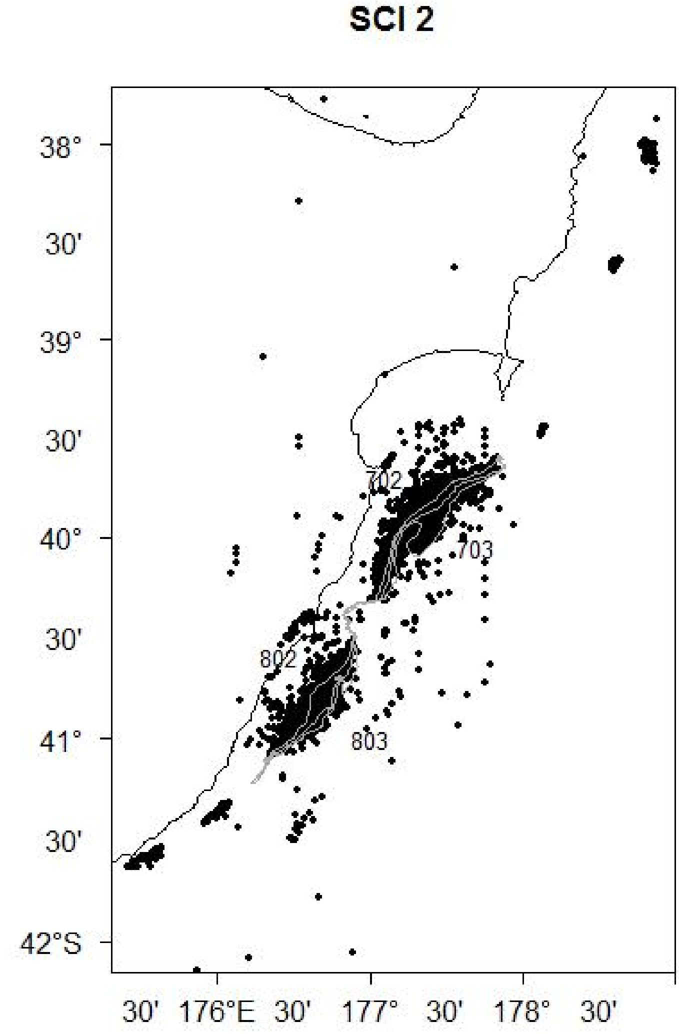

Figure 3: Spatial distribution of the scampi fishery within management area SCI 2 since 1988–89. Each dot shows the mid point of one or more tows recorded on TCEPR with scampi as the target species. The extents of the four scampi survey strata are shown in grey with associated labels.

2. FISHERY CHARACTERISATION AND DATA

2.1. Commercial catch and effort data

Scampi fishers have consistently reported catches on the Trawl Catch, Effort, and Processing Returns (TCEPR) form since its introduction in 1989–90, providing a very valuable record of catch and effort on a tow by tow basis.

Data were extracted from the MPI TCEPR database, requesting all tows where scampi (SCI) was the nominated target species, or was reported in the catch. Previous analyses using TECPR data have only extracted and groomed the most recent year's data, and appended these to previously groomed data. Following a suggestion of the SFAWG, a full extract of all years was requested from MPI for this analysis. Errors in TCEPR records are reducing in frequency, but do occur, and the raw records were groomed in the following manner. For each record, the reported data were used to estimate the duration of the trawl shot, the distance between the start and finish locations, and the mid point between the start and finish locations. Tows with zero scampi catch were excluded. All tows with zero hours tow duration recorded (but some scampi catch) were reset to the median tow duration for the trip. All tows with a tow distance greater than 100 km were reset to the median of the mid point of tows on the same day, adjacent days, or the trip, depending on available data.

Subsequent analyses were conducted on this "groomed" version of the data set (98701 records), representing over 90% of all scampi landings, as it is considered to be the most appropriate to investigate patterns in the fishery, given that it represents the targeted scampi fishery, and latitude and longitude data are available for spatial aspects of the analysis. Previous characterisations have used a slightly different grooming approach (to that discussed above), details of which are provided in Tuck (2009). Comparisons of unstandardized CPUE data for the previous and revised grooming approaches are presented for SCI 1 and SCI 2 in Appendix 1. The revised grooming slightly reduces the estimated CPUE prior to 2003 (due to rounding of the haul duration data), but the medians of the annual values appear identical after this. Other management areas show the same pattern (not presented).

2.1.1. SCI 1

Total annual landings for the fishery, and the percentage by the target scampi fishery are presented in Table 1, and the distribution of fishing activity within the SCI 1 area over time is presented in Figure 4 and Figure 5. The area over which the assessment model is applied is defined at the survey strata (300–500 m depth range in the main area of the fishery)(Figure 2), and over 96% of the targeted scampi catch has been reported from this area in all years (Table 1). The core area has consistently been fished over the history of the fishery, with smaller isolated patches (particularly to the north) fished in some years. The core (modelled) area has accounted for over 90% of scampi targeted catch in all years, except 1997–98 (81%). Boxplots of the unstandardized CPUE (Figure 6) show catch rates initially increasing in the mid 1990s, peaking in 1996, declining to about 2000, and then remaining relatively stable to the present date.

The breakdown of catch by survey strata and fishing year is presented for SCI 1 in Figure 7. In general, the shallower strata (202, 302 and 402 – 300–400 m) contributed more catch than the deeper strata, and fishing was less consistent in the southern area (strata 402 and 403).

Table 1: Reported commercial landings (tonnes) from the 1987–87 to 2011–12 fishing years for SCI 1, catch estimated from scampi target fishery, and estimated catch from modelled area (survey strata).

	Landings (MHR)	Target catch (TCEPR)	% SCI target	Estimated catch (modelled area)	% catch (modelled area)
1986–87	5.00				
1987–88	15.00				
1988–89	60.00				
1989–90	104.00	102.88	99%	102.06	99%
1990–91	179.00	162.86	91%	154.64	95%
1991–92	132.00	128.31	97%	125.33	98%
1992–93	114.00	115.95	102%	108.93	94%
1993–94	115.00	111.62	97%	105.65	95%
1994–95	114.00	113.65	100%	106.53	94%
1995–96	117.00	116.38	99%	111.79	96%
1996–97	117.00	114.01	97%	112.80	99%
1997–98	107.00	114.99	107%	92.74	81%
1998–99	110.00	112.41	102%	108.18	96%
1999–00	124.00	116.06	94%	107.77	93%
2000–01	120.00	117.14	98%	108.90	93%
2001–02	124.00	109.85	89%	103.58	94%
2002–03	121.00	95.81	79%	95.01	99%
2003–04	120.00	115.90	97%	115.47	100%
2004–05	114.00	100.08	88%	99.89	100%
2005–06	109.00	93.84	86%	93.72	100%
2006–07	110.00	101.30	92%	101.21	100%
2007–08	102.00	93.12	91%	93.05	100%
2008–09	86.00	81.00	94%	80.97	100%
2009–10	111.41	104.98	94%	102.22	97%
2010–11	113.87	107.89	95%	105.50	98%
2011–12	114.47	107.34	94%	107.03	100%

Monthly patterns of effort and catch are presented by subarea in Figure 8 and Figure 9. The fishery was managed with competitive catch limits between 2001–02 and 2003–04. During this period, effort and catches were focussed in the first few months of the fishing year, but prior to and since this time, fishing has been distributed throughout the year (particularly more recently).

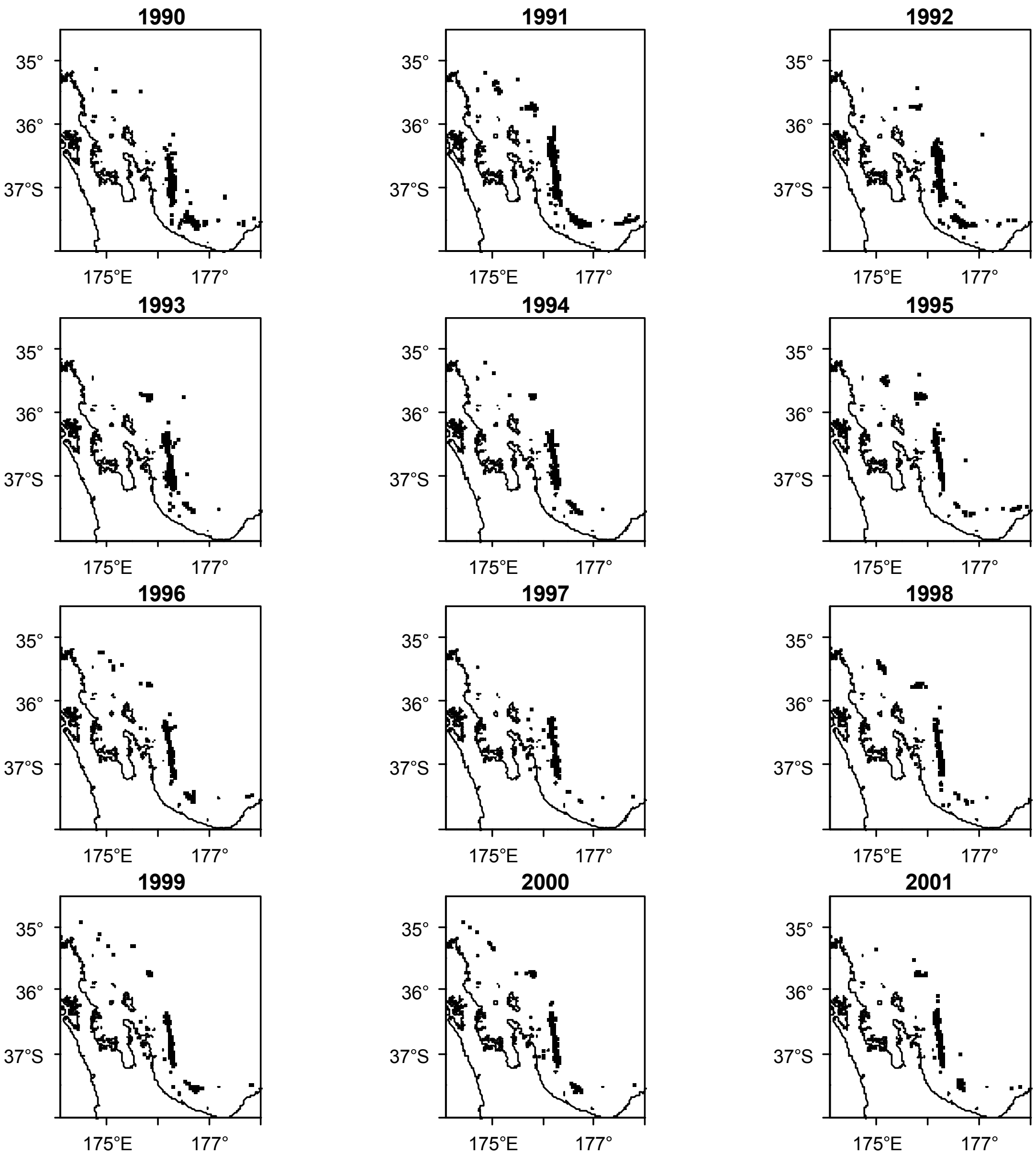

Figure 4: Spatial distribution of the main area of the SCI 1 scampi trawl fishery from 1989–90 to 2000–01. Each dot represents the mid point of one or more tows reported on TCEPR. General area covered by plots indicated within Figure 5.

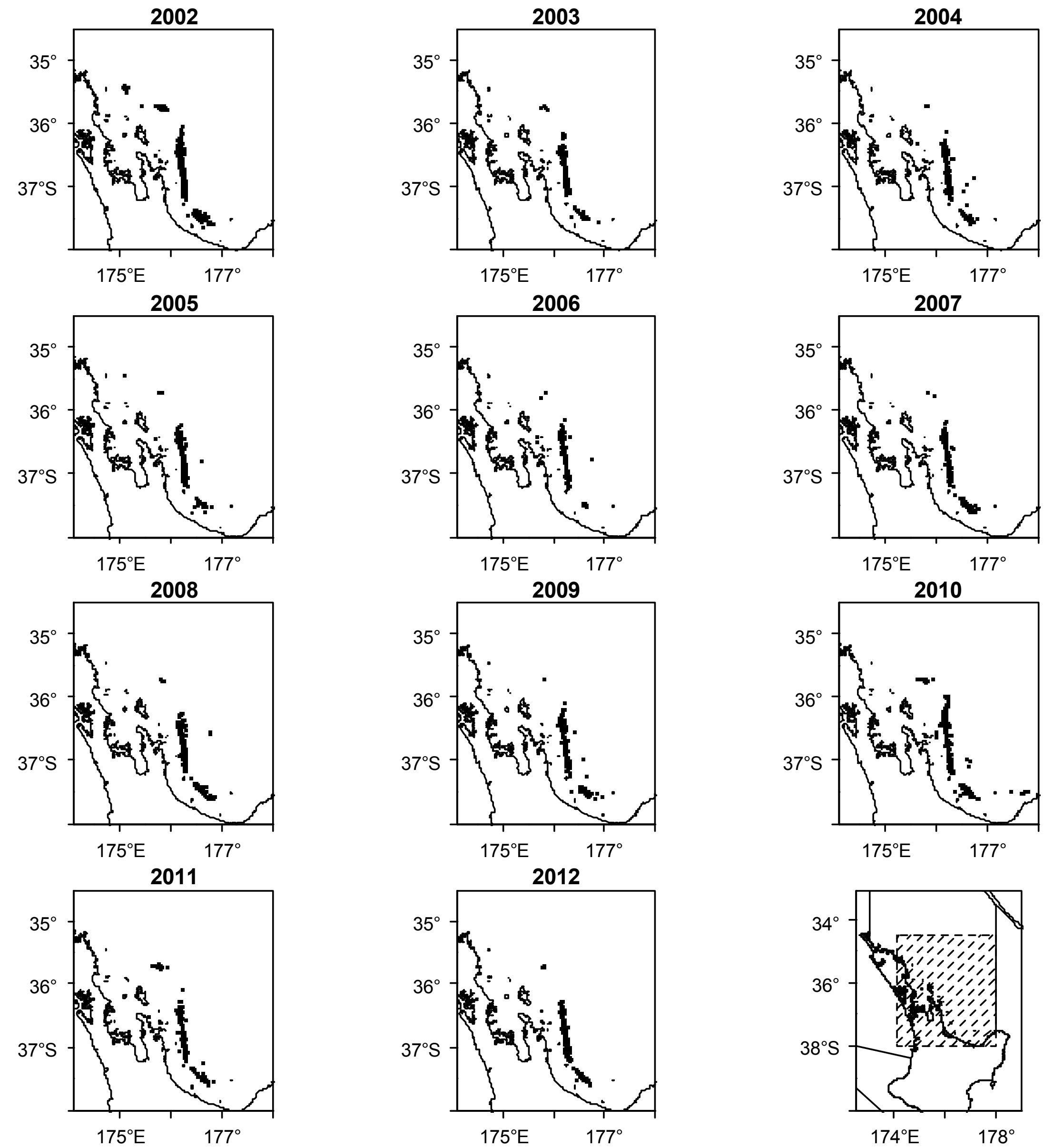

Figure 5: Spatial distribution of the main area of the SCI 1 scampi trawl fishery from 2001–02 to 2011–12. Each dot represents the mid point of one or more tows reported on TCEPR. General area covered by plots indicated by shaded box in bottom right plot.

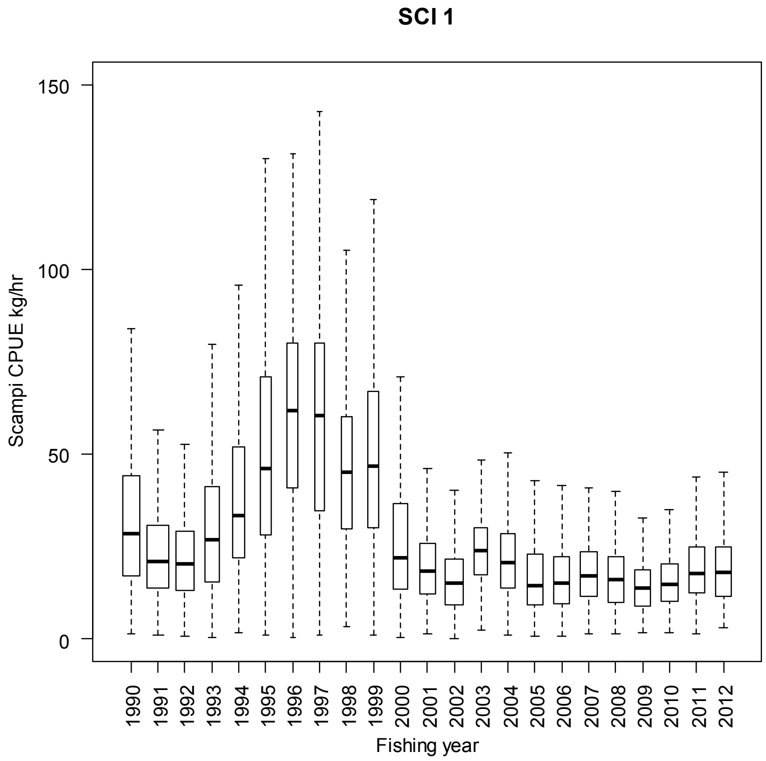

Figure 6: Boxplot (with outliers removed) of individual observations from TCEPR of unstandardized catch rate (catch (kg) divided by tow effort (hours)) with tows of zero scampi catch excluded, by fishing year for the SCI 1 fishery. Box width proportional to square root of number of observations.

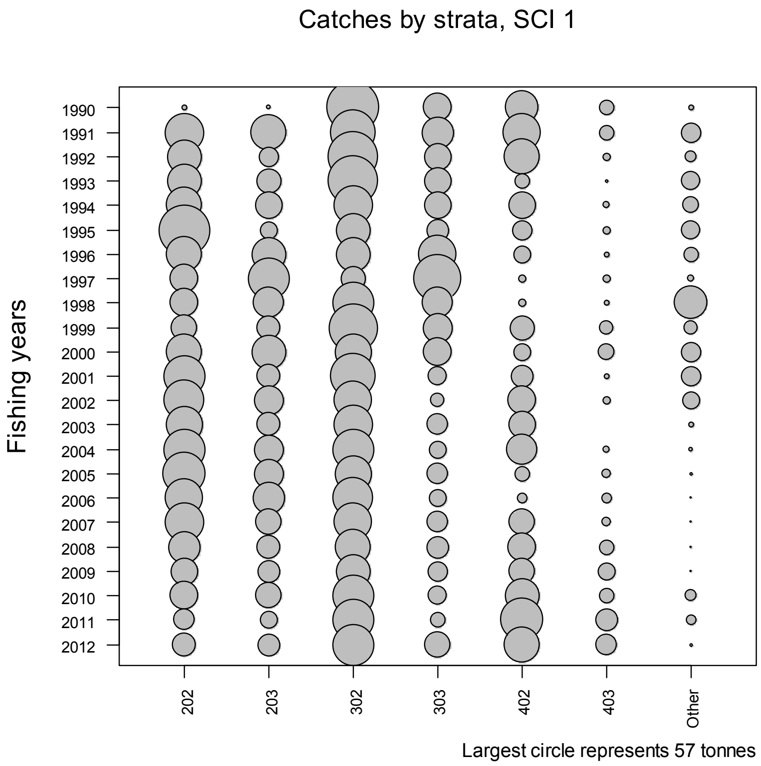

Figure 7: Annual catch breakdown by survey strata (and outside modelled area) and fishing year for SCI 1.

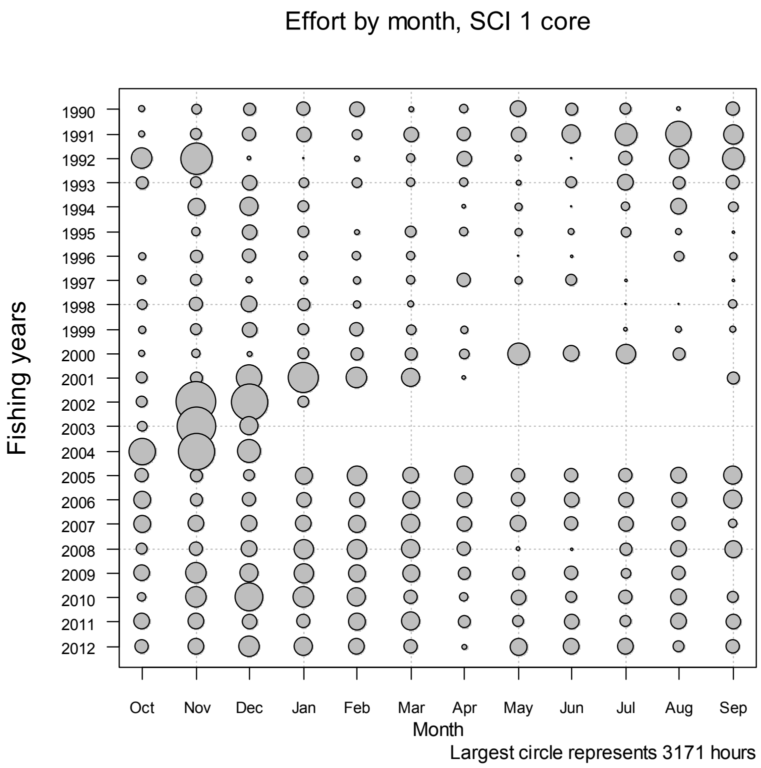

Figure 8: Monthly pattern of fishing effort in the scampi targeted fishery by fishing year for the core (modelled) area of SCI 1.

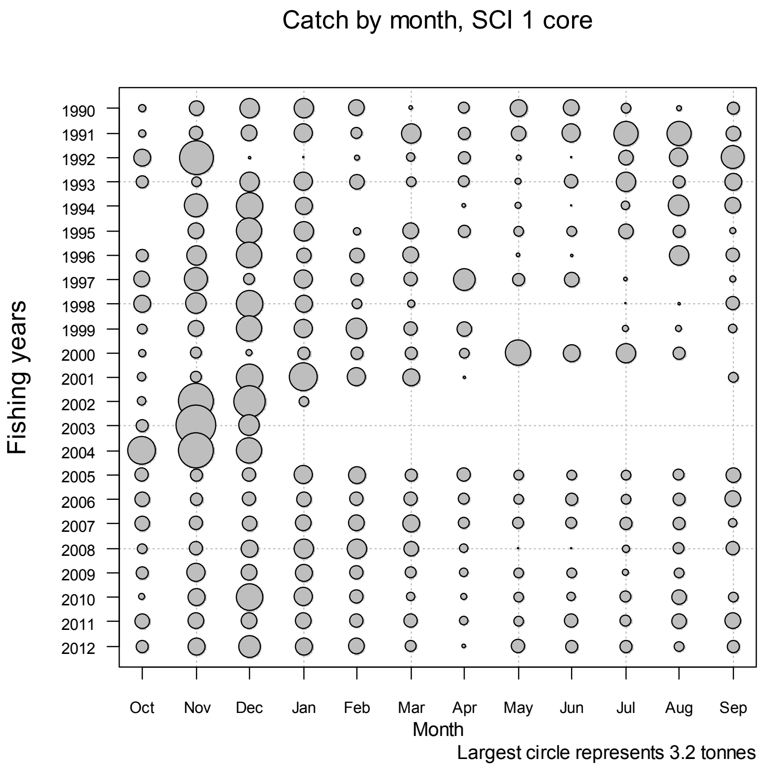

Figure 9: Monthly pattern of scampi catches in the scampi targeted fishery by fishing year for the core (modelled) area of SCI 1.

2.1.2. SCI 2

Total annual landings for the fishery, and the percentage by the target scampi fishery are presented in Table 2, and the distribution of fishing activity within the SCI 2 area over time is presented in Figure 10 and Figure 11. The area over which the assessment model is applied is defined by the survey strata (300–500 m depth range in the main area of the fishery)(Figure 3), and over 96% of the targeted scampi catch has been reported from this area in all years (Table 2). The main fishery comprises two distinct grounds (Hawke Bay and Wairarapa), and these core areas have consistently been fished over the history of the fishery, with smaller isolated patches (both to the north and south) fished in some years. The core (modelled) area has accounted for over 90% of scampi targeted catch in all years, except 2004–05 (80%). A boxplot of the unstandardized CPUE (Figure 12) shows that catch rates were initially stable, increased in 1995, declined steadily to 2002, increased slightly to 2008, and have shown a greater increase in more recent years (to levels similar to those recorded in the early 1990s).

Table 2: Reported commercial landings (tonnes) from the 1987–87 to 2011–12 fishing years for SCI 2, catch estimated from scampi target fishery, and estimated catch from modelled area (survey strata).

	Landings (MHR)	Target catch (TCEPR)	% SCI target	Estimated catch (modelled area)	% catch (modelled area)
1986–87	0.00				
1987–88	5.00				
1988–89	17.00				
1989–90	138.00	140.79	102%	137.41	98%
1990–91	295.00	261.12	89%	248.93	95%
1991–92	221.00	212.02	96%	191.27	90%
1992–93	210.00	208.77	99%	199.38	96%
1993–94	244.00	230.51	94%	222.26	96%
1994–95	226.00	233.83	103%	219.73	94%
1995–96	230.00	229.86	100%	227.09	99%
1996–97	213.00	214.15	101%	208.57	97%
1997–98	224.00	227.86	102%	218.47	96%
1998–99	233.00	240.59	103%	234.12	97%
1999–00	193.00	190.27	99%	187.38	98%
2000–01	146.00	190.59	131%	186.79	98%
2001–02	247.00	229.49	93%	219.09	95%
2002–03	134.00	113.52	85%	109.15	96%
2003–04	64.00	56.36	88%	55.87	99%
2004–05	71.00	61.47	87%	49.26	80%
2005–06	77.00	70.28	91%	68.56	98%
2006–07	80.00	73.12	91%	72.02	99%
2007–08	61.00	56.89	93%	56.18	99%
2008–09	52.00	49.15	95%	48.95	100%
2009–10	125.41	119.75	95%	119.06	99%
2010–11	128.20	119.93	94%	119.49	100%
2011–12	98.80	88.21	89%	87.74	99%

The breakdown of catch by survey strata and fishing year is presented for SCI 1 in Figure 13. The two shallower strata (702 and 802 – 300–400 m) contributed far more catch than the deeper strata, with the deeper strata off the Wairarapa coast (strata 803) contributing little in most years.

Monthly patterns of effort and catch are presented by subarea in Figure 14 and Figure 15. As with SCI 1, the fishery was managed with competitive catch limits between 2001–02 and 2003–04. During this period, effort and catches were focussed after the SCI 1 fishery was completed (catch limit taken).

Fishing has generally been far less consistently distributed through the year than in SCI 1, and in recent years there has been very little activity in the fishery between April and August.

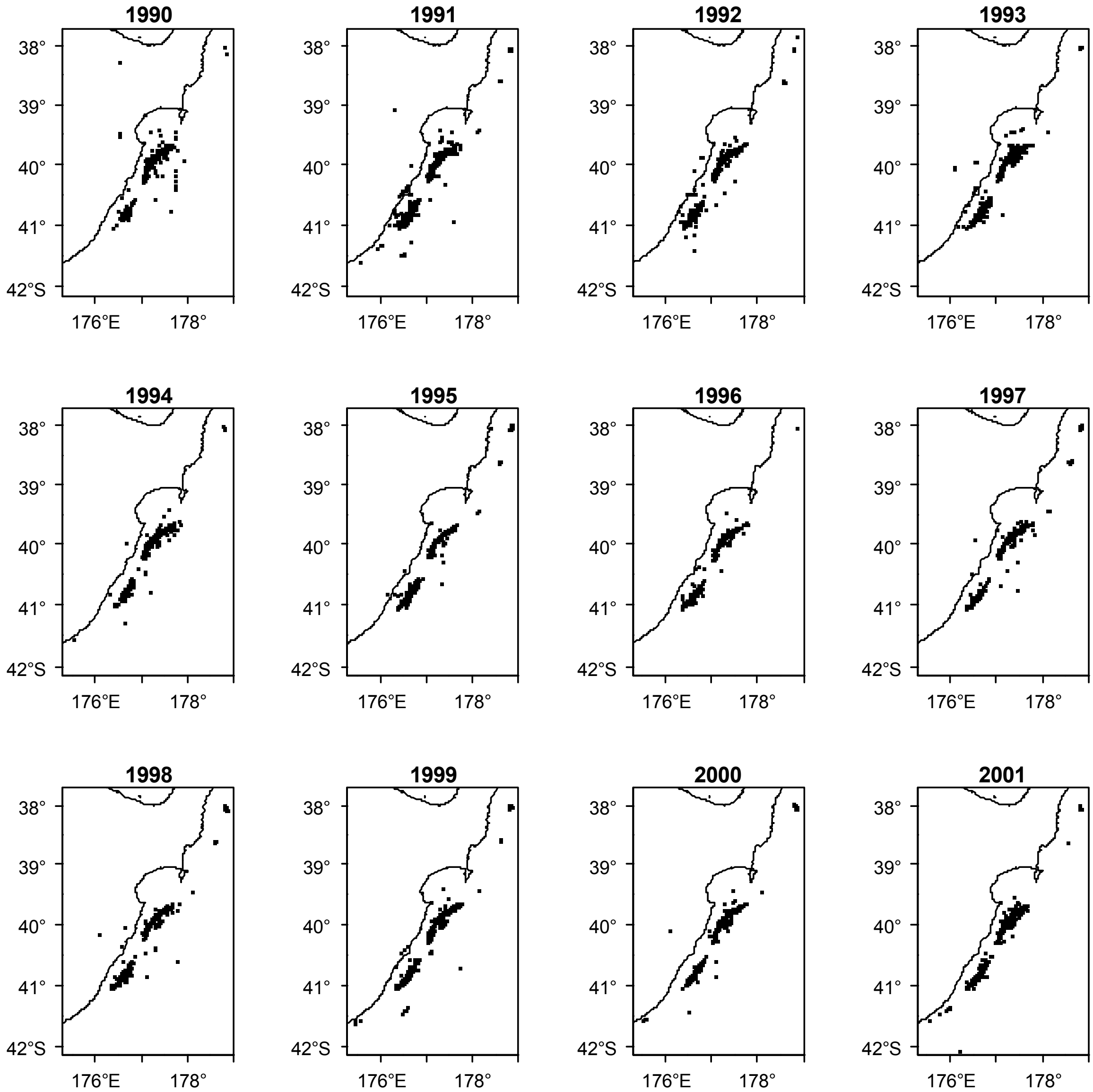

Figure 10: Spatial distribution of the main area of the SCI 2 scampi trawl fishery from 1989–90 to 2000–01. Each dot represents the mid point of one or more tows reported on TCEPR. General area covered by plots indicated within Figure 11.

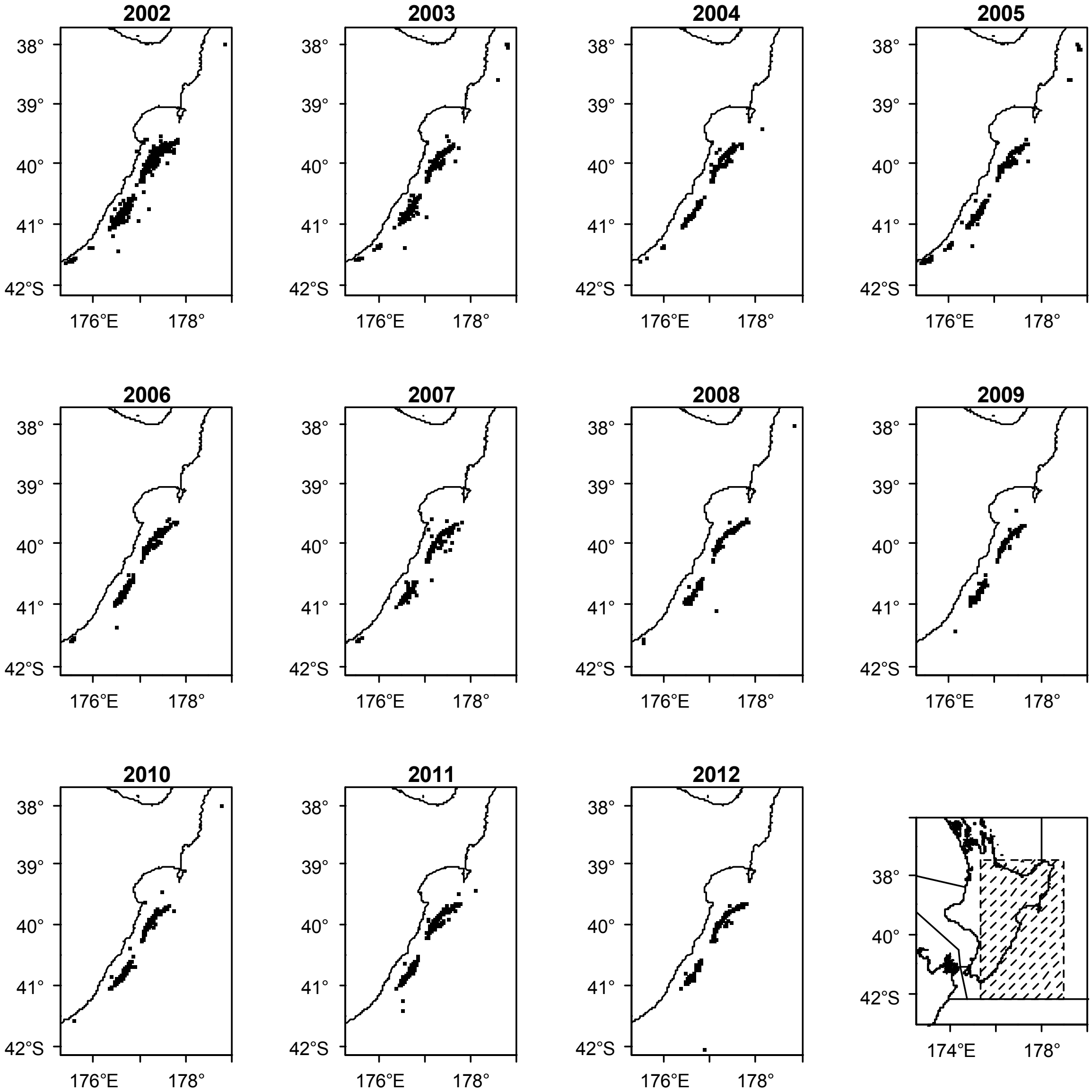

Figure 11: Spatial distribution of the main area of the SCI 2 scampi trawl fishery from 2001–02 to 2011–12. Each dot represents the mid point of one or more tows reported on TCEPR. General area covered by plots indicated by shaded box in bottom right plot.

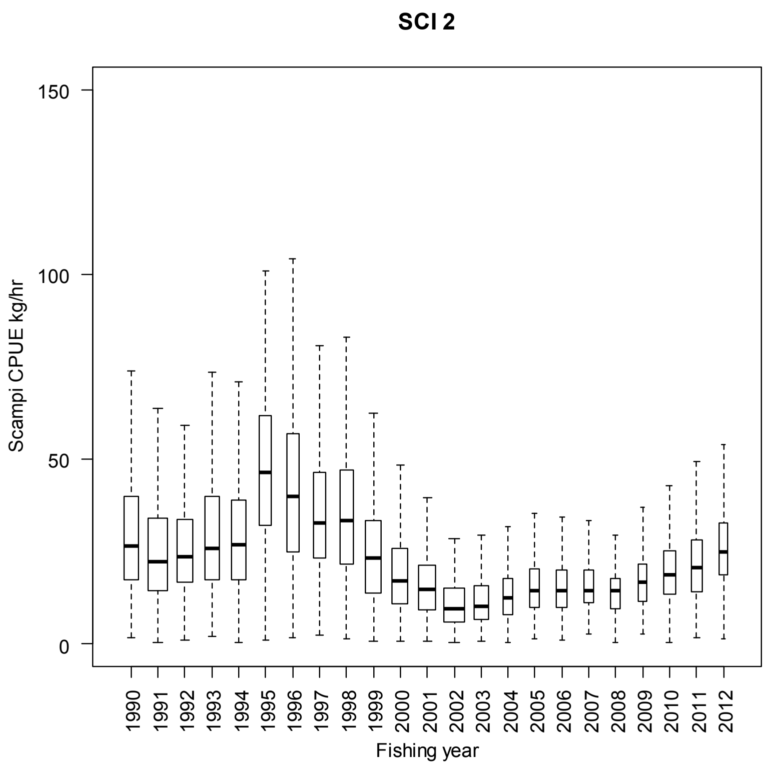

Figure 12: Boxplot (with outliers removed) of individual observations from TCEPR of unstandardized catch rate (catch (kg) divided by tow effort (hours)) with tows of zero scampi catch excluded, by fishing year for the SCI 2 fishery. Box width proportional to square root of number of observations.

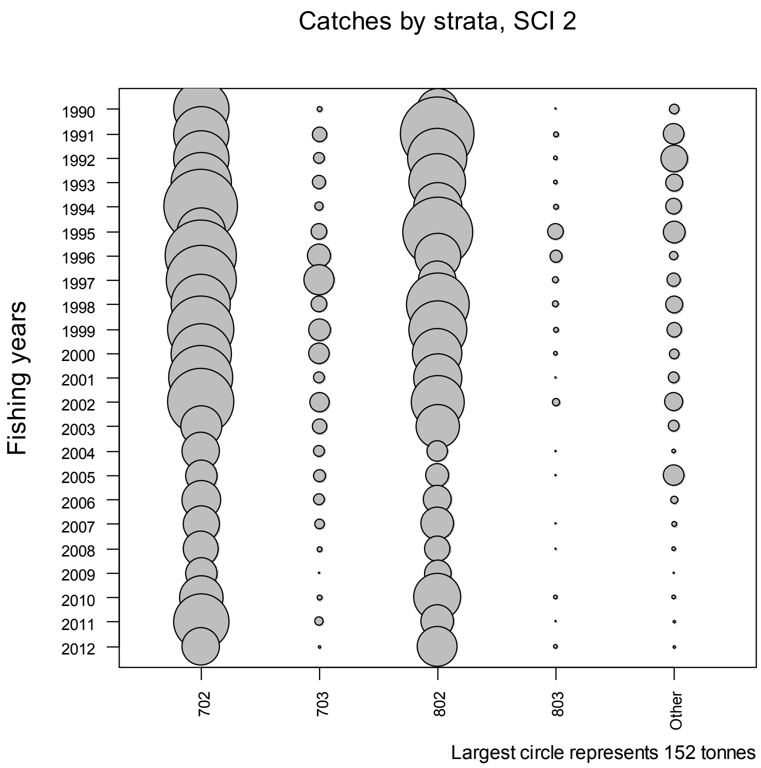

Figure 13: Annual catch breakdown by survey strata (and outside modelled area) and fishing year for SCI 2.

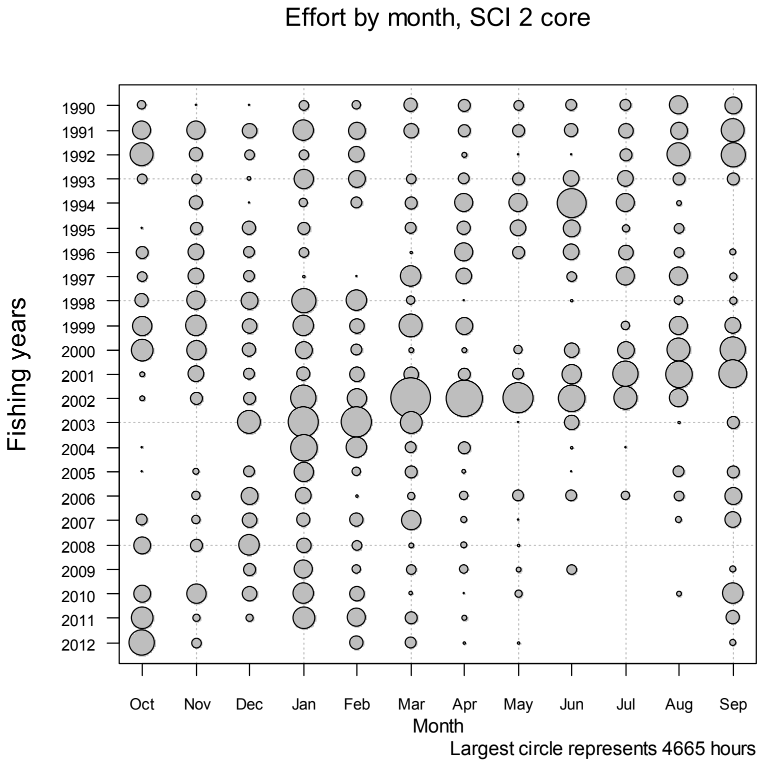

Figure 14: Monthly pattern of fishing effort in the scampi targeted fishery by fishing year for for the core (modelled) area of SCI 2.

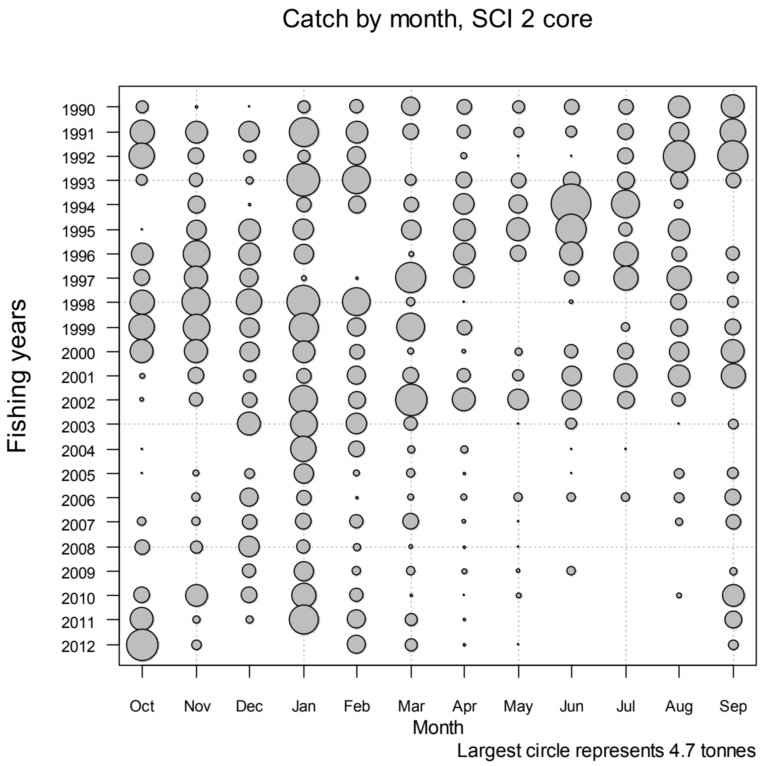

Figure 15: Monthly pattern of scampi catches in the scampi targeted fishery by fishing year for the core (modelled) area of SCI 2.

2.2. Seasonal patterns in scampi biology

Previous development of the length based model for scampi has shown that determination of appropriate time steps for the model is important in fitting to length and sex ratio data in particular (Tuck & Dunn 2006, 2009, 2012). Scampi inhabit burrows, and are not available to trawling when within a burrow. Catchability varies between the sexes on a seasonal basis in relation to moulting and reproductive behaviour, and leads to seasonal changes in sex ratio in catches.

2.2.1. Sex ratio

Current knowledge of the timing of scampi biological processes in SCI 1 and SCI 2 are summarised in Table 3 (Tuck 2010). From patterns in ovary and egg stage observed from commercial and research trawl sampling, along with the proportion of soft animals (Figure 16) and ovigerous females, mature female moulting appears to occur around October and November, just after the hatching period (August and September), with mating occurring at this time and new eggs being spawned onto the pleopods in November – January. The main male moulting is completed well before the female moult (since mating occurs post moult for females, but the males must have completed the moult to mate), and appears to be concentrated in April and May (Figure 17), but may start as early as February. There is also some evidence of male moulting in September – November, generally for smaller (less than 40mm CL) animals.

The combination of biological processes for males and females lead to different relative availabilities of the two sexes through the year, resulting in the pattern of sex ratio (displayed as proportion males) shown in Figure 18. Males are markedly less abundant than females in catches between February and April (male catches being reduced during their moulting period), but females also dominate catches to a lesser extent between May and September.

Table 3: Summary of scampi biological processes for SCI 1. Source; Tuck (2010) and more recent survey data.

	Jan	Feb	Mar	Apr	May	Jun	Jul	Aug	Sep	Oct	Nov	Dec
Male moult		?	?	X	X							
Female moult										X	X	
Mating										X	X	
Eggs spawn	X										X	X
Eggs hatch								X	X			

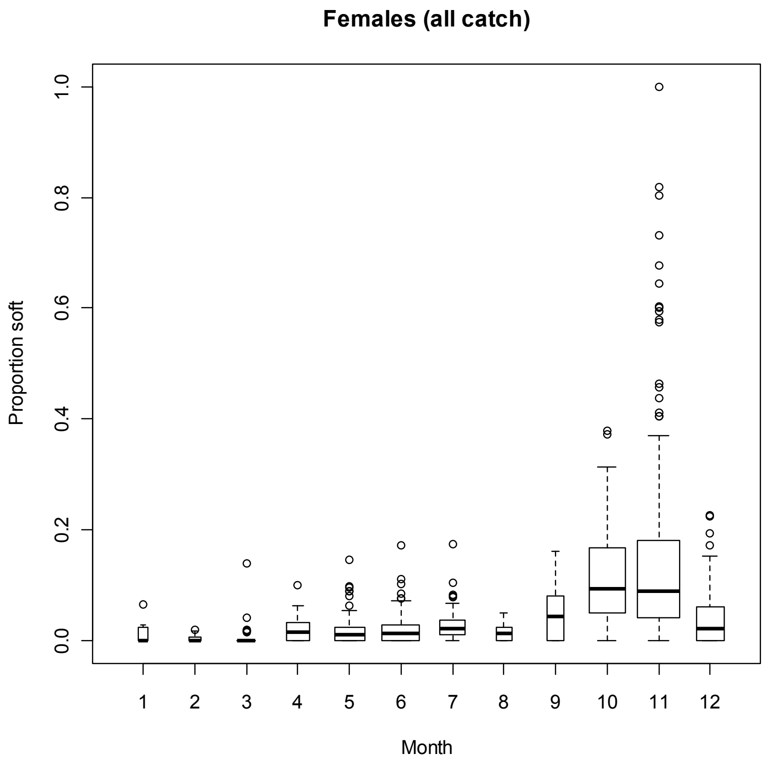

Figure 16: Proportion of females with soft carapace by month, from observer sampling in the SCI 1 and SCI 2 fisheries. Box widths proportional to square root of number of observations.

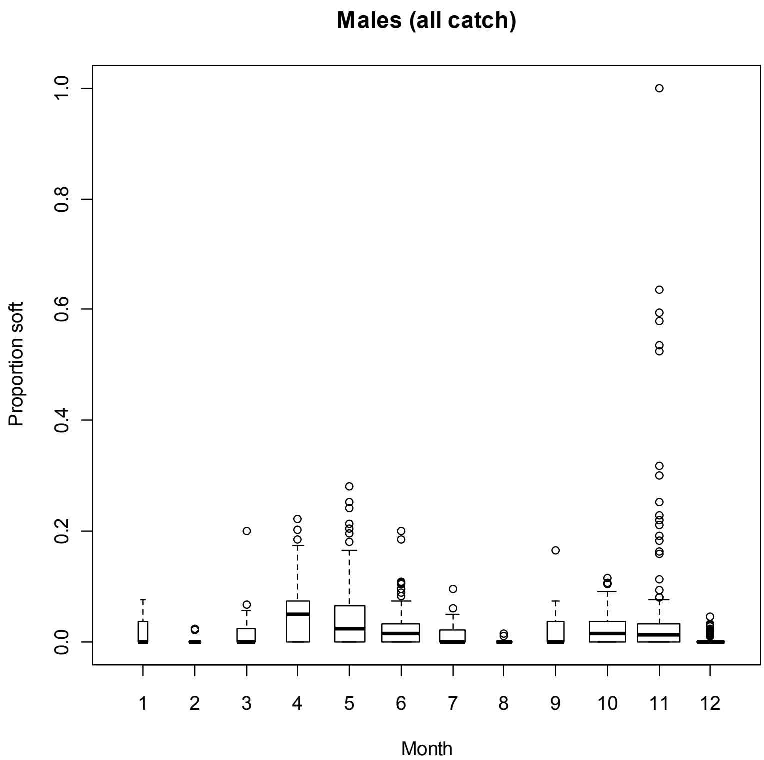

Figure 17: Proportion of males with soft carapace by month, from observer sampling in the SCI 1 and SCI 2 fisheries. Box widths proportional to square root of number of observations.

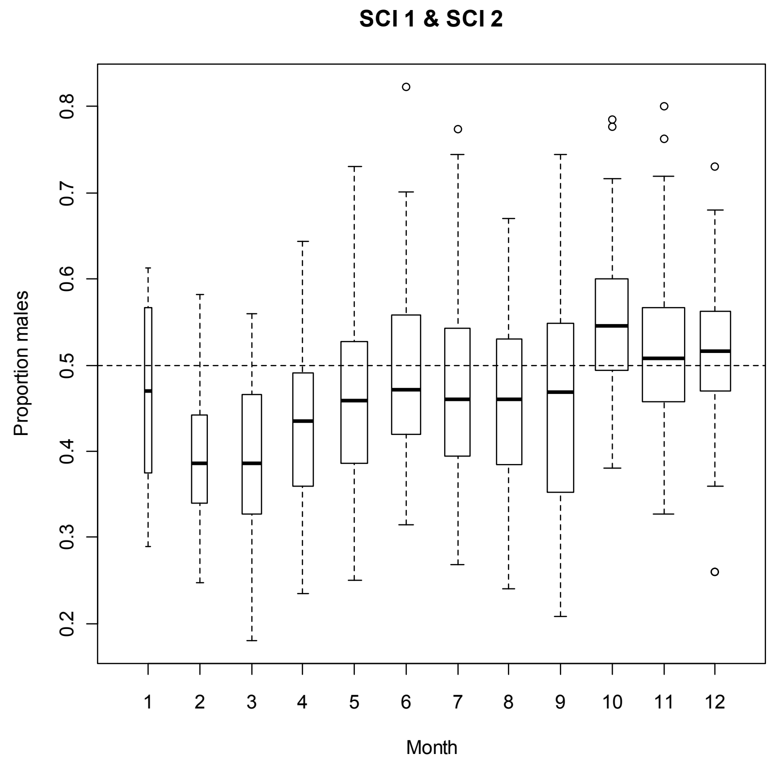

Figure 18: Boxplots of proportion of males in catches by month from observer sampling in the SCI 1 and SCI 2 fisheries. Box widths proportional to square root of number of observations.

2.2.2. Time steps in assessment model

On the basis of our understanding of the timing of biological processes for scampi in this area, and the seasonal pattern in sex ratio, three time steps are proposed for the assessment model, as defined in Table 4. Catch data, stock abundance indices and length frequency distributions have been collated and estimated in relation to these time steps, for inclusion in the assessment model.

Table 4: Annual cycle of the population model for SCI 1 and SCI 2, showing the processes taking place at each time step, and their sequence within each time step. Fishing and natural mortality that occur together within a time step occur after all other processes, with 50% of the natural mortality for that time step occurring before and 50% after the fishing mortality. Natural mortality is apportioned to time steps in relation to their duration (as a fraction of the year). Fishing mortality is apportioned to time steps according to reported landings.

Step	Period	Process
1	October – January	Growth (both sexes) Natural mortality Fishing mortality
2	February – April	Recruitment Maturation Natural mortality Fishing mortality
3	May - September	Natural mortality Fishing mortality

2.3. Standardised CPUE indices

2.3.1. Core vessels – SCI 1

A plot of vessel activity (number of scampi targeted tows recorded) over time is presented for SCI 1 in Figure 19. One vessel has been active and dominant throughout the history of the fishery, while some others have contributed for a number of years. Some vessels were only active in the fishery during the late 1990s and early 2000s (partly associated with the period of competitive catch limits between 2001–02 and 2003–04). Only three vessels have been routinely active in the fishery in recent years.

Figure 20 (upper plot) shows the proportion of the total catch (over the history of the fishery) in relation to number of years vessels contributing that catch have been active in the fishery, and on the basis of this, a cut off of 10 years of activity has been selected to identify seven core vessels. The lower plot of Figure 20 shows the proportion of catch accounted for in each year by vessels active for over 5 or 10 years. Other than 2001–02 and 2002–03, the core vessels (active for over 10 years) have accounted for over 80% of targeted scampi catches, and often over 90%.

2.3.2. Core vessels – SCI 2

A plot of vessel activity (number of scampi targeted tows recorded) over time is presented for SCI 2 in Figure 21. A number of vessels have been regularly active in the fishery, and none is dominant. A few vessels joined the fishery associated with the period of competitive catch limits between 2001–02 and 2003–04, but to a lesser extent than for SCI 1. Four vessels have been routinely active in the fishery in recent years.

Figure 22 (upper plot) shows the proportion of the total catch (over the history of the fishery) in relation to number of years those vessels contributing that catch have been active in the fishery, and on the basis of this, a cut off of 10 years of activity has been selected to identify nine core vessels. Vessel numbers from SCI 1 core vessels do not relate to vessel numbers for SCI 2, but all of the core vessels from SCI 1 are included in the SCI 2 list. The lower plot of Figure 22 shows the proportion of catch accounted for in each year by vessels active for over 5 or 10 years (no difference between the lines). Other than 2001–02, the core vessels (active for over 10 years) have accounted for over 80% of targeted scampi catches, and often over 90%.

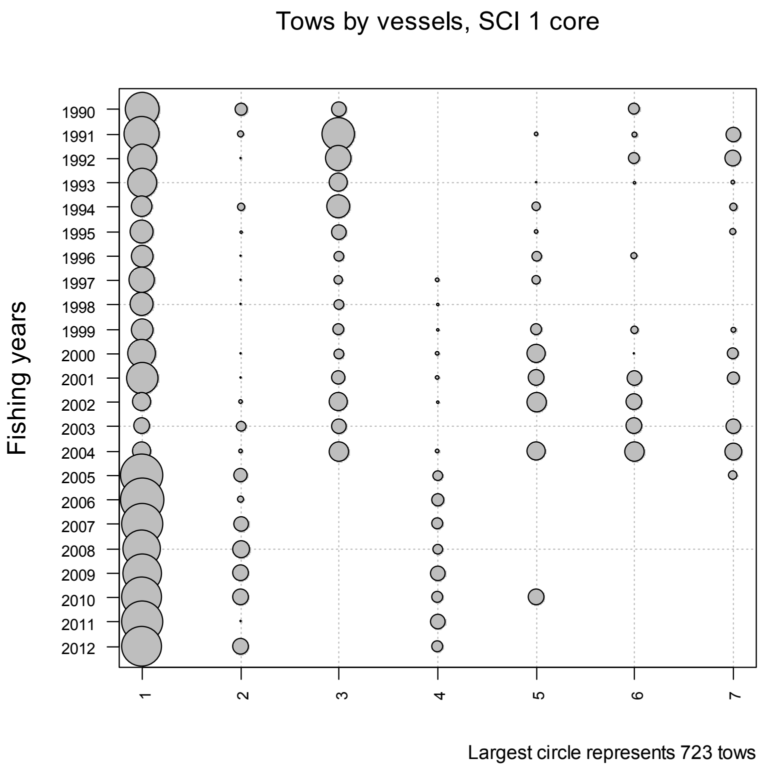

Figure 19: Pattern of fishing activity by vessel and fishing year for SCI 1. The area of the circles is proportional to the number of tows recorded.

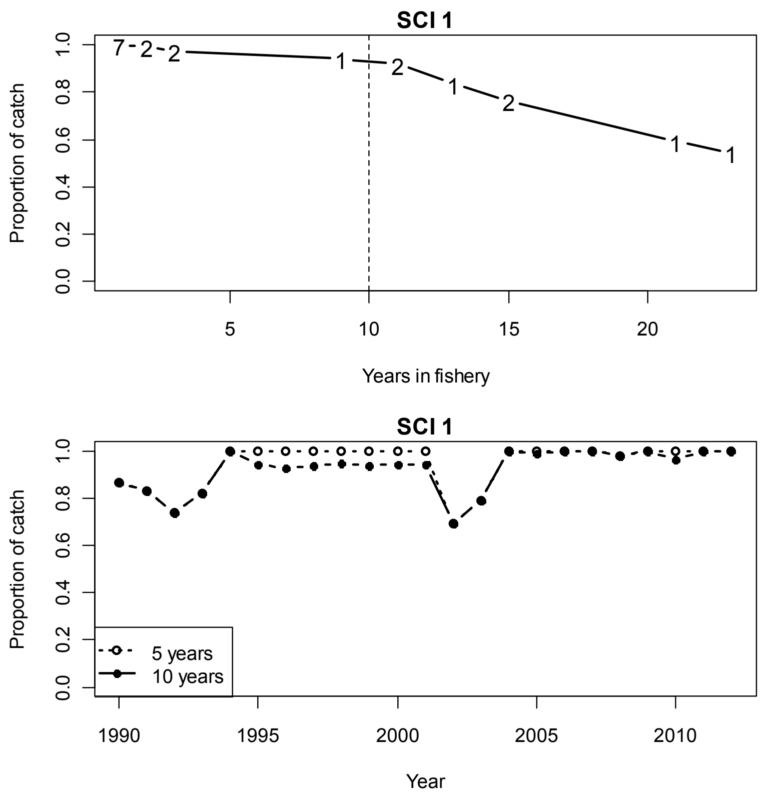

Figure 20: Catch breakdown by vessel. Upper plot - Proportion of total scampi catch (all years) plotted against the number of years the vessels reporting that catch have been active in the fishery. Numbers indicate number of vessels active for that duration. Vertical dotted line represents cut off for core vessels. Lower plot – Proportion of annual catch reported by vessels active in the fishery for 5 and 10 years.

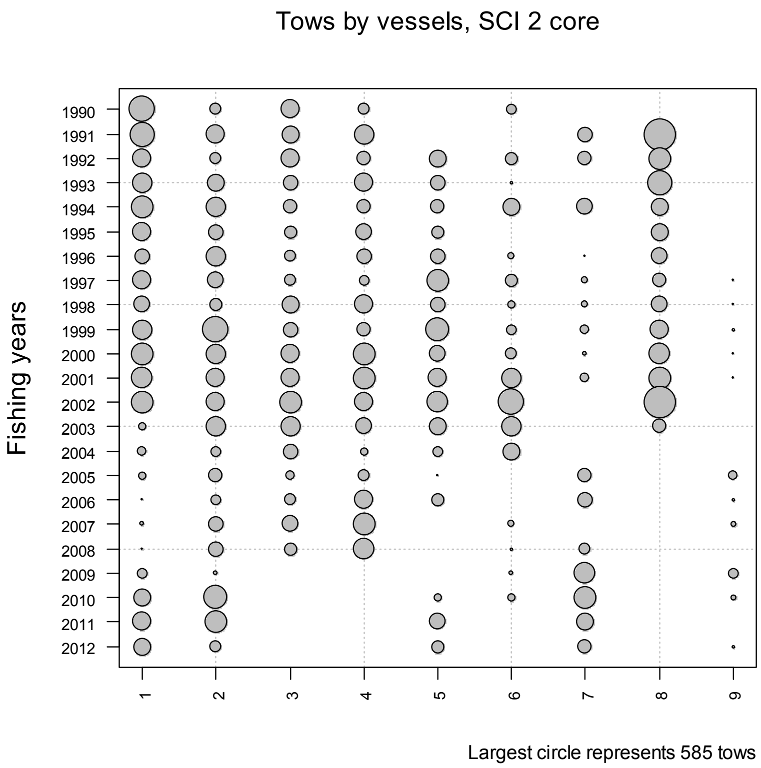

Figure 21: Pattern of fishing activity by vessel and fishing year for SCI 2. The area of the circles is proportional to the number of tows recorded.

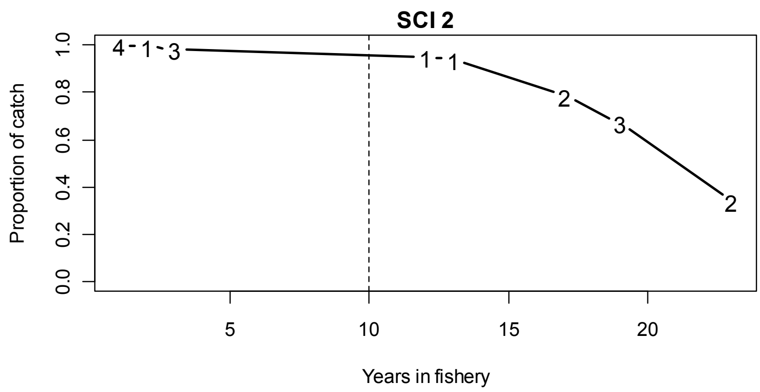

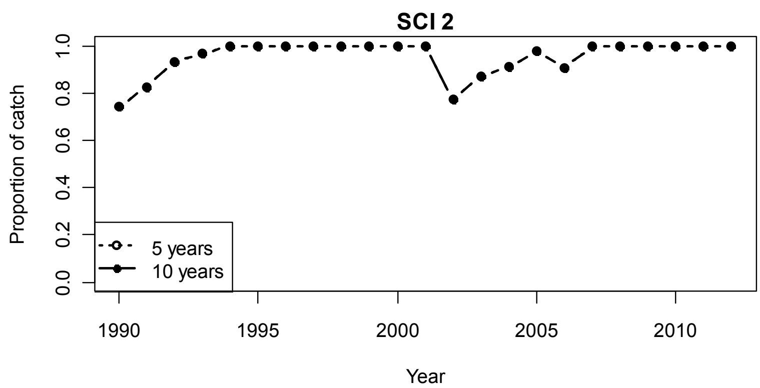

Figure 22: Catch breakdown by vessel. Upper plot - Proportion of total scampi catch (all years) plotted against the number of years the vessels reporting that catch have been active in the fishery. Numbers indicate number of vessels active for that duration. Vertical dotted line represents cut off for core vessels. Lower plot – Proportion of annual catch reported by vessels active in the fishery for 5 and 10 years.

2.3.3. Exclusion of poorly sampled time periods

Following the approach developed for SCI 3 (Tuck 2013), time steps that were poorly sampled by the fishery were excluded from the standardisation of the CPUE, on the basis that a small number of tows in an area, or at a particular time, may not provide a good index of abundance. Records were excluded from the analysis when there were less than 10 tows recorded by core vessels within a time step in a year (Figure 23).

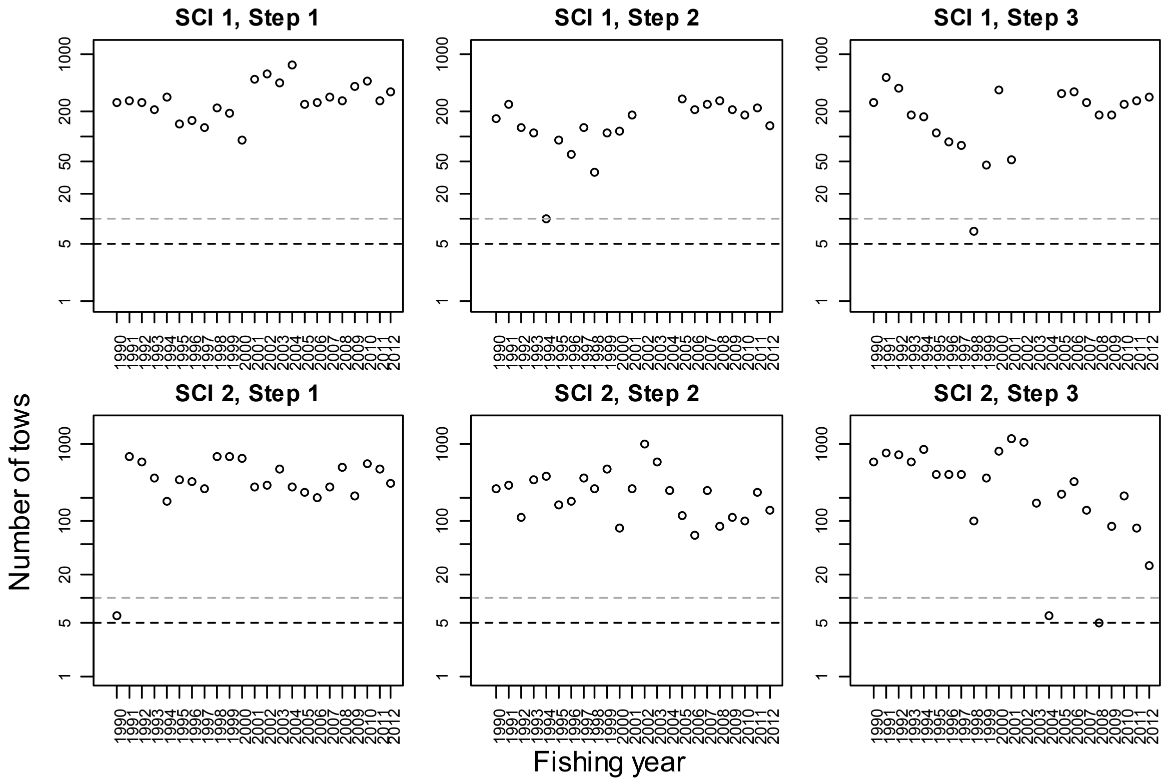

Figure 23: Numbers of commercial tows available within the core vessel dataset by time step and fishing year for SCI 1 (upper row) and SCI 2 (lower row). Dashed lines represent arbitrary cut offs at 5 and 10 tows.

2.3.4. Calculation of indices

Previous assessment of SCI 1 and SCI 2 have fitted separate abundance indices for different survey strata and time steps (Tuck & Dunn 2012), but more recently the SFAWG has suggested a simplification of the model structure. Therefore, a range of standardised indices were calculated for each fishery, namely an annual index and three time step indices for the whole fishery, and separate indices for each stratum in each time step (as applied previously). For each index, scampi catch of core vessels within the appropriate area and time step was modelled using combined spatial and temporal strata (forced), vessel, time of day, state of moon, depth and fishing duration. For the three time step indices, spatial strata was included in the model as a term, while for the annual index, spatial strata and time step were included.

The time of day of each tow was calculated in relation to nautical dawn and dusk (time when the sun is 12 degrees below the horizon in the morning and evening), as calculated by the *crepescule* function of the *maptools* package in R. Individual tows were characterised on the basis of whether they included dawn (shot before dawn, hauled after dawn and before dusk), day (shot after dawn, hauled before dusk), dusk (shot before dusk, hauled after dusk and before dawn) or night (shot after dusk and hauled before dawn). Longer tows including more than one period (i.e. shot before dusk and hauled after dawn were excluded from this part of the analysis (excluding 45 records from a total of over 17 000 for SCI 1, and 82 records from a total of over 26 000 for SCI 2).

Individual hauls were also categorised in terms of moon state, on the assumption that tidal current strength at the sea floor will be related to the lunar cycle. Tows were categorised by their date in relation to the lunar cycle, as Full moon (more than 26 days since full moon, or less than 3 days since full moon), Waning (4 – 11 days since full moon), New moon (12 – 18 days since full moon), and Waxing (19 – 26 days since full moon).

Core vessels were selected as described above, by examining the scampi fleet’s activity over the history of the fishery, and selecting vessels that had consistently contributed over a number of years, and together, had contributed a significant proportion of the overall catches over the whole fishery, and in each year.

Within the core vessels identified, two have changed gear configuration (twin rig to triple rig) in recent years, and two have changed engine power over the history of the fishery. On the basis of previous investigations (Tuck 2013), engine power was fitted within the model (as a factor), and gear configuration as a two level factor (twin or triple rig). Gear configuration for a particular vessel and date was determined on the basis of information provided by the fishing industry as to when vessels changed from twin to triple, and all tows after this date are defined as triple rig. It is acknowledged that vessels may change configuration within a trip depending on gear damage or fishing conditions, but it is not thought that this is recorded consistently enough over the history of the fishery within the TCEPR records to be useable.

In addition, examination of the data for SCI 3 (Tuck 2013) identified a distinct shift in trawl duration between 2002–03 and 2006–07 (from about 5 hours to 7 hours). This shift (in SCI 3) was fleet-wide, and associated with a modification to the top of the trawl to reduce the bycatch (John Finlayson, Sanford Ltd. *pers comm.*), enabling vessels to fish for longer on each tow. Boxplots of tow duration over time have been examined for each of the core vessels identified for SCI 1 and SCI 2 (Figure 24), and rather than the relatively rapid shift in trawl duration recorded by the same vessels in SCI 3 (Figure 25), within SCI 1 and SCI 2, the increase in haul duration appears to have been more gradual, starting in the early 1990s, and stabilising at about 7 hours by the late 1990s or early 2000s. Once the bycatch modification to the gear was introduced by a vessel (around 2004–05), it was used in all fisheries, but it does not appear to have had an effect on tow duration in SCI 1 and SCI 2. For each vessel, the timing of the gear modification was estimated from examination of tow durations in SCI 3, and fitted as a two level factor in the model.

Catch indices were derived using generalised linear modelling (GLM) procedures (Vignaux 1994, Francis 1999), using the statistical software package R. The response variable in the GLM was the natural logarithm of scampi catch. The fishing-year (combined with any time step or spatial strata for the index) was entered as a categorical covariate (explanatory) term on the right-hand side of the model. Standardised CPUE abundance indices (canonical) were derived from the exponential of the fishing-year covariate terms as described in Francis (1999).

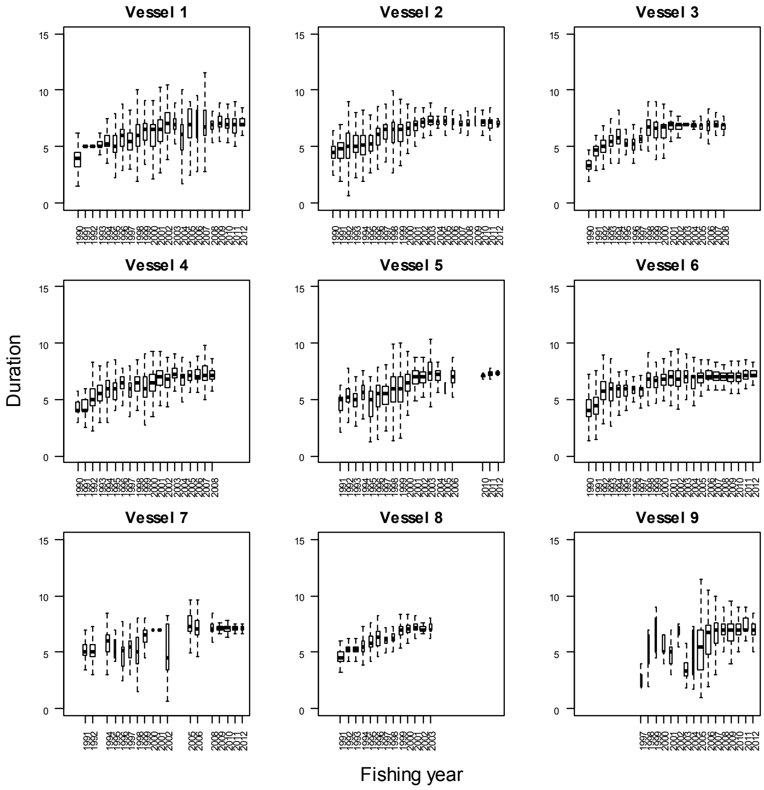

Figure 24: Boxplots of tow duration (hours) for scampi targeted fishing in SCI 1 and SCI 2 (combined) for the nine core vessels identified for SCI 2. Box widths proportional to square root of number of observations.

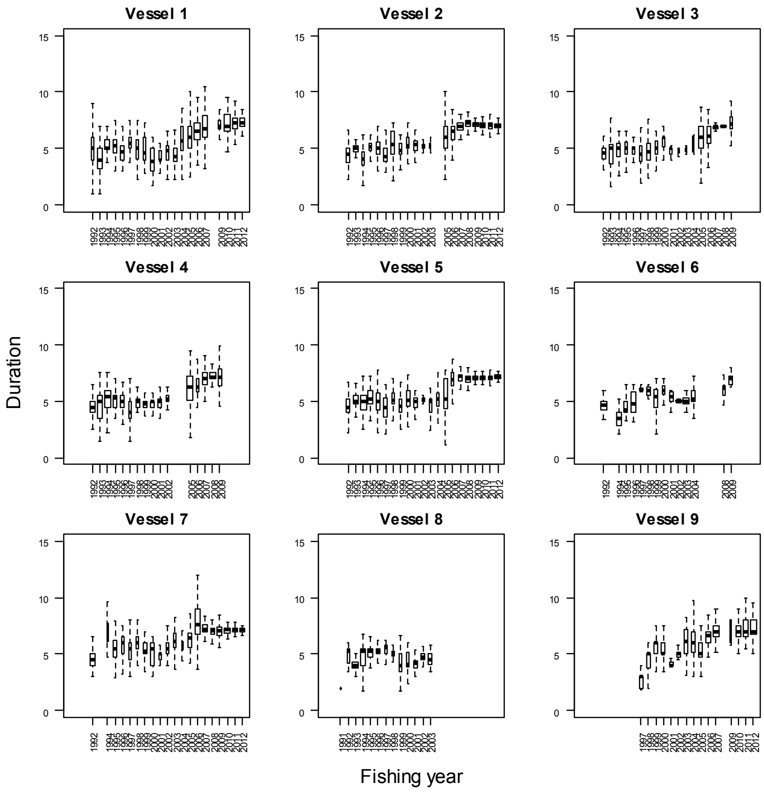

Figure 25: Boxplots of tow duration (hours) for scampi targeted fishery in SCI 3 for the nine core vessels identified for SCI 2. Box widths proportional to square root of number of observations.

In order to accommodate a non-linear relationship with the response variable (log catch), the continuous variables (effort and depth) were "offered" to the GLM's as third order polynomials. Vessel, time of day, state of tide, twin or triple rig, bycatch modification and vessel power were "offered" to the GLM's as factors. A forward fitting, stepwise, multiple-regression algorithm was used to fit GLM's to groomed catch, effort and characterisation data. The stepwise algorithm generates a final regression model iteratively and uses a simple model with a single predictor variable, fishing year, as the initial or base model. The reduction in residual deviance relative to the null deviance is calculated for each additional term added to the base model. The term that results in the greatest reduction in residual deviance is added to the base model if this results in an improvement in residual deviance of more than 1%. The algorithm repeats this process, updating the model, until no new terms can be added. Diagnostic plots for the final models are presented in Appendix 2 (Bentley et al. 2012).

2.3.5. SCI 1 indices

Stratum time step indices

Stepwise regression analysis of the dataset to estimate the stratum time step CPUE indices for SCI 1 resulted in a final model with fishing year, time of day, effort and vessel retained (Table 5). The model explained 45% of the variation in the data. Effort was the most influential variable, at 12%, with time of day and vessel having influences of about 6 to 7%. The standardised and unstandardized annual indices are shown in Figure 26 (with standardised indices scaled to the median of the unstandardised records for each stratum time step combination). The two sets of indices generally follow a very similar pattern in all years, with only a few occasions where the standardised index is markedly below the unstandardised.

Table 5: Analysis of deviance table and overall influence for standardisation model selected by stepwise regression for stratum time step indices for SCI 1.

	Df	Deviance explained	Additional deviance explained (%)	Overall influence (%)*
NULL				
fishing_year_step_area	221	2032.74	29.79	
Time of day	3	551.27	8.08	7.52
Effort	3	411.87	6.04	12.61
Vessel	6	70.63	1.03	5.85

*- Overall influence as in table 1 of Bentley et al. (2012)

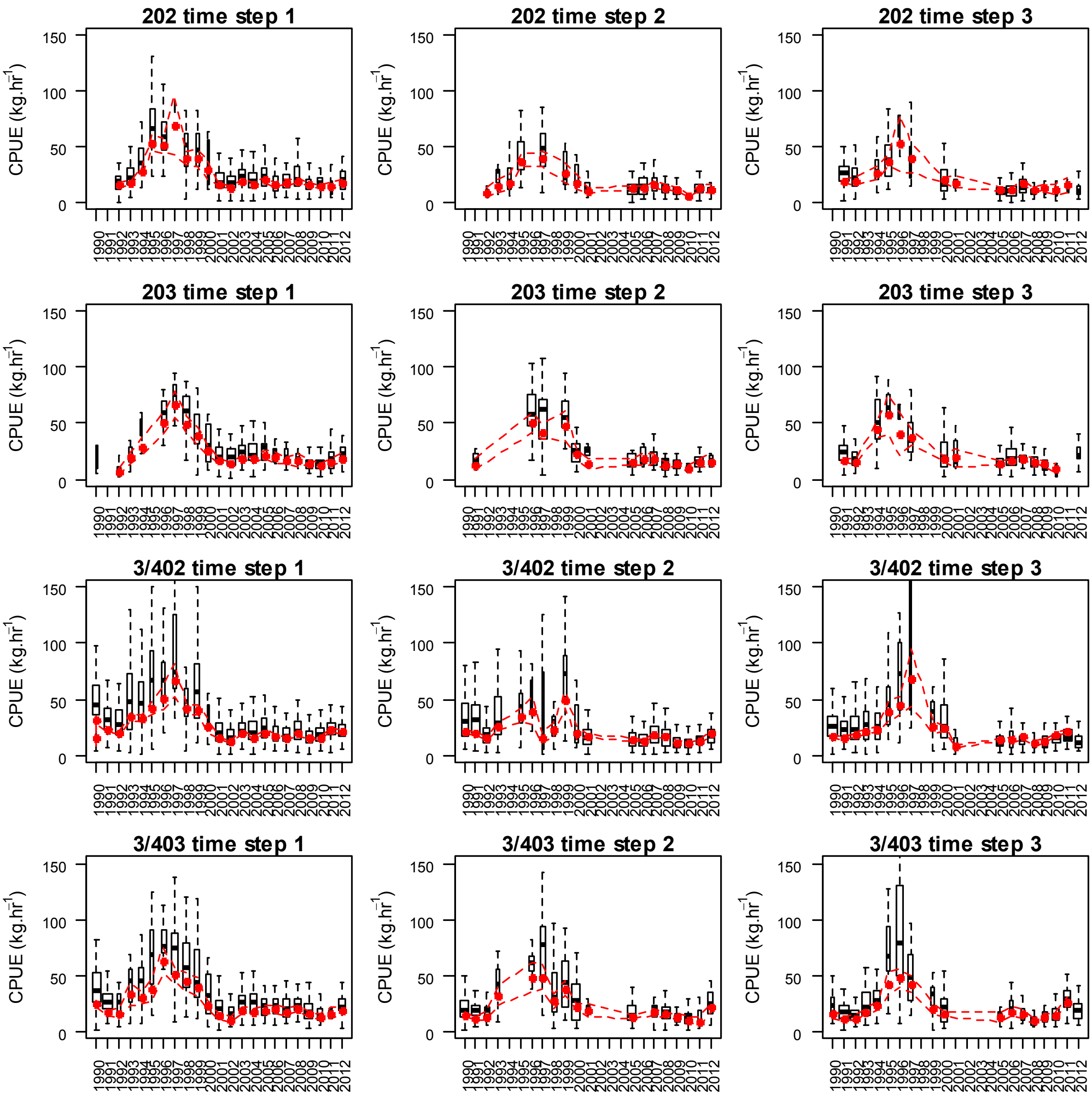

Figure 26: Boxplots of unstandardized CPUE for the core vessels in SCI 1 by fishing year (by stratum and time step), overlaid by standardised CPUE indices (scaled to the median of the unstandardised data).

Time step indices

Stepwise regression analysis of the dataset to estimate an annual CPUE index for SCI 1 resulted in a final model with fishing year step, time of day, and effort retained (Table 6). The model explained 41% of the variation in the data. Effort was the most influential variable, at 12%, with time of day having an influence of about 7%. The standardised and unstandardized annual indices are shown in Figure 27 (standardised indices scaled to the median of the unstandardised records for each time step). The two sets of indices follow a very similar pattern, although standardised index is consistently below the unstandardized during the early part of the series, particularly in time step 1, but also in the other time steps during years of particularly high CPUE. In more recent years, there is very little difference between the indices.

Table 6: Analysis of deviance table and overall influence for standardisation model selected by stepwise regression for time step indices for SCI 1.

	Df	Deviance explained	Additional deviance explained (%)	Overall influence (%)*
NULL				
fishing_year_step	61	1781.14	25.98	
TOD	3	599.93	8.75	7.41
poly(effort, 3)	3	420.83	6.14	11.71

*- Overall influence as in table 1 of Bentley et al. (2012)

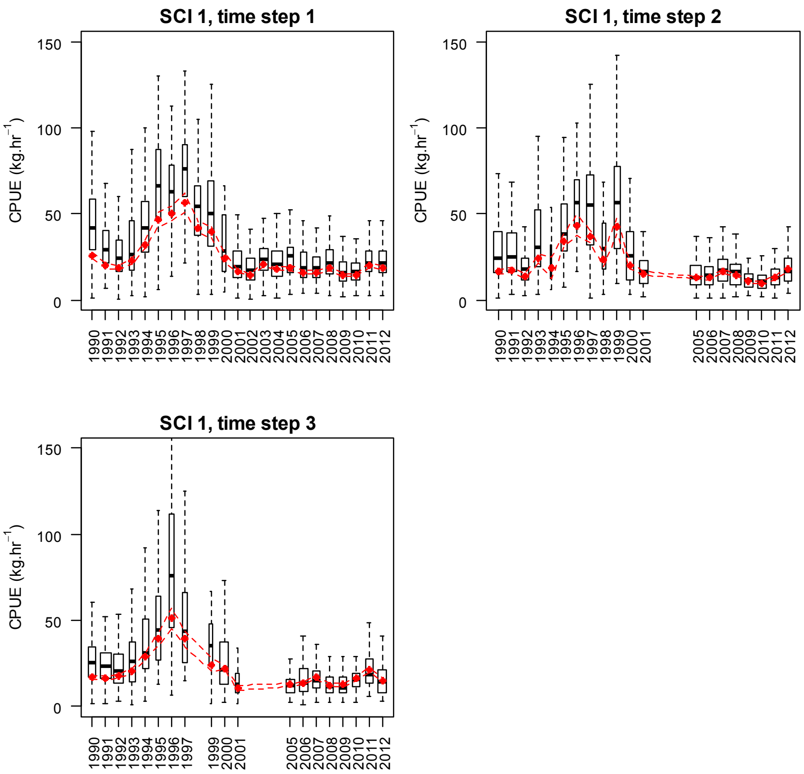

Figure 27: Boxplots of unstandardized CPUE for the core vessels in SCI 1 by fishing year (by time step), overlaid by standardised CPUE indices (scaled to the median of the unstandardised data).

Single annual index

Stepwise regression analysis of the dataset to estimate an annual CPUE index for SCI 1 resulted in a final model with fishing year, time of day, effort and time step retained (Table 7). Model diagnostics are presented in Appendix 2. The model explained 39% of the variation in the data. Effort was the most influential variable, at 10%, with time of day and time step having influences of about 4%. The standardised and unstandardized annual indices are shown in Figure 28. The two indices follow a very similar pattern, although standardised index is consistently above the unstandardized during the early part of the series (as fishing duration was increasing), and the unstandardized is above the standardised from 2001 to 2004 (when most fishing was concentrated in time step 1). The relative effects of the explanatory variables (excluding fishing year) are shown in Figure 29. Expected catch rates are highest during the day, and lowest at night, being about half of the daytime rate. Expected catch increases for tow durations up to about 8 hours, but then declines. Catch rates are highest in time step 1, falling to about 80% of this level in time steps 2 and 3.

Table 7: Analysis of deviance table and overall influence for standardisation model selected by stepwise regression for an annual index for SCI 1.

	Df	Deviance explained	Additional deviance explained (%)	Overall influence (%)*
NULL				
fishing_year	22	1403.55	20.47	
TOD	3	733.97	10.70	4.21
poly(effort, 3)	3	429.41	6.26	10.39
model_step	2	102.35	1.49	3.39

*- Overall influence as in table 1 of Bentley et al. (2012)

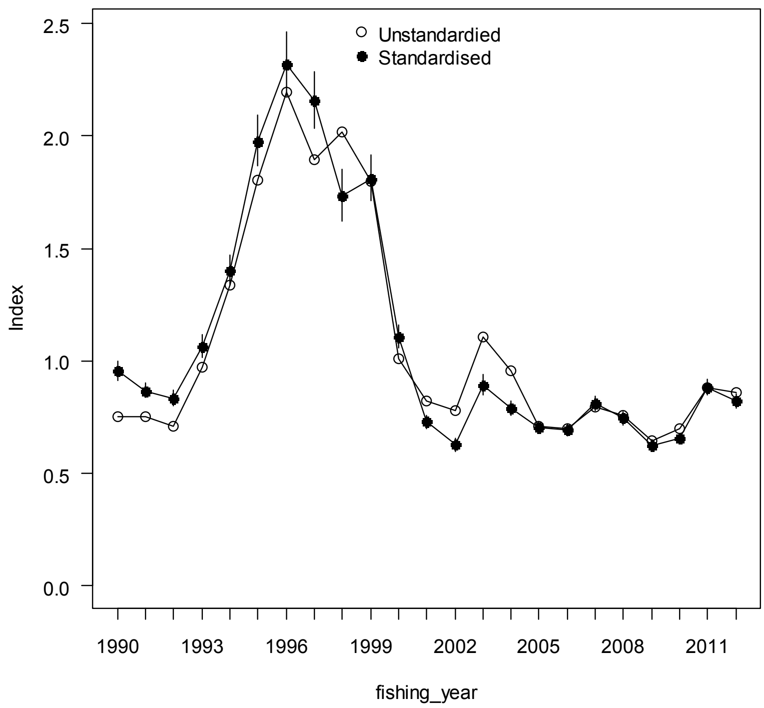

Figure 28: Comparison of standardised (Table 7) and unstandardized annual CPUE index for SCI 1.

As discussed, previous assessment models for scampi have fitted indices stratified spatially and temporally (Tuck & Dunn 2012), but the SFAWG proposed investigation of simplified model structures. Consistency in the patterns shown in the indices were examined between strata within time step, and the Working Group agreed that realistic options for weighting individual spatial strata would not generate a composite time step indices greatly different from the three time step indices presented in Figure 27. Preliminary assessment models were presented to the Working Group fitting to the single annual standardised index (Figure 28), and the three time step indices (Figure 27). Model outputs were very similar, and the Working Group agreed that the annual index (Table 7, Figure 28) should be used within the models as the index of abundance from the CPUE data.

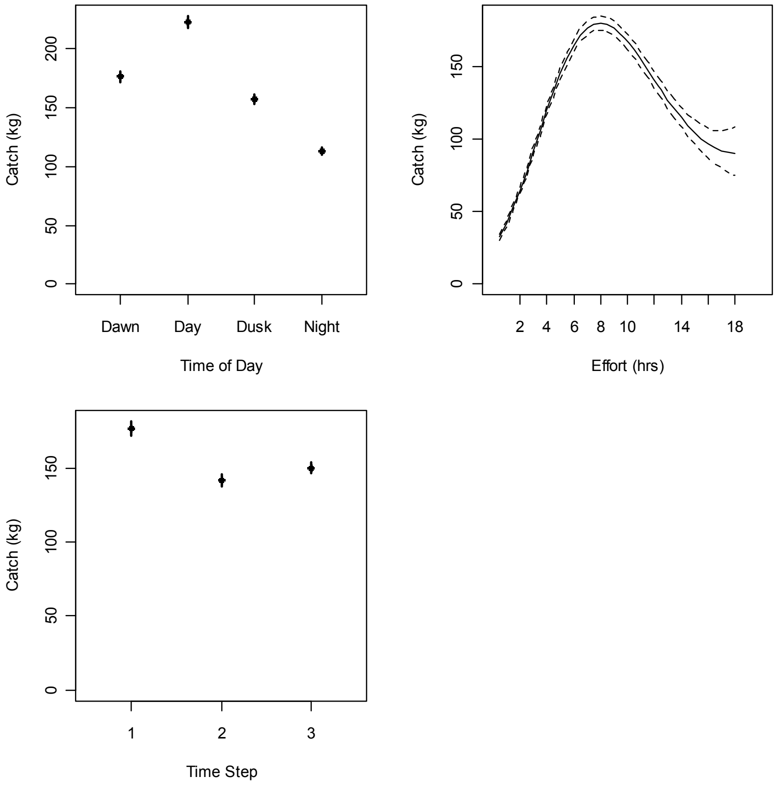

Figure 29: Termplot (in natural space) for annual index standardisation model (Table 7), showing relative effects of time of day, effort (tow duration), and time step.

2.3.6. SCI 2 indices

Stratum time step indices

Stepwise regression analysis of the dataset to estimate the stratum time step CPUE indices for SCI 2 resulted in a final model with fishing year, time of day, effort and vessel retained (Table 8). The model explained 45% of the variation in the data. Effort was the most influential variable, at 11%, with time of day and vessel having influences of about 3 to 4%. The standardised and unstandardized annual indices are shown in Figure 30 (standardised indices scaled to the median of the unstandardised records for each stratum time step combination). As with the equivalent SCI 1 model, the two sets of indices generally follow a very similar pattern in all years, with only a few occasions where the standardised index is markedly below the unstandardised.

Table 8: Analysis of deviance table and overall influence for standardisation model selected by stepwise regression for stratum time step indices for SCI 2.

	Df	Deviance explained	Additional deviance explained (%)	Overall influence (%)*
NULL				
fishing_year_step_area	179	4349.8	36.10	
poly(effort, 3)	3	569.2	4.72	10.73
TOD	3	308.6	2.56	4.33
vessel	8	132.4	1.10	2.91

*- Overall influence as in table 1 of Bentley et al. (2012)

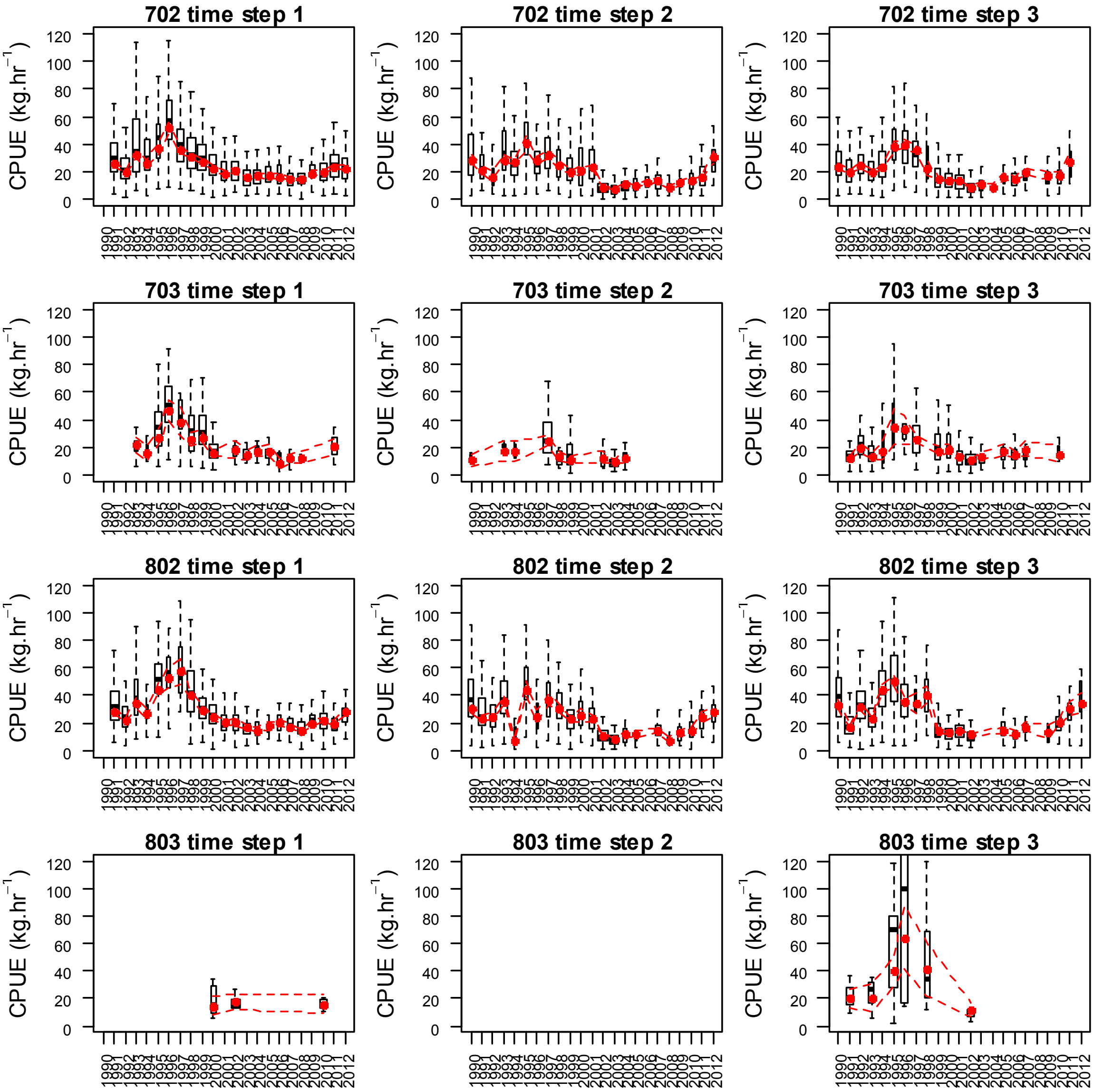

Figure 30: Boxplots of unstandardized CPUE for the core vessels in SCI 2 by fishing year (by stratum and time step), overlaid by standardised CPUE indices (scaled to the median of the unstandardised data).

Time step indices

Stepwise regression analysis of the dataset to estimate an annual CPUE index for SCI 2 resulted in a final model with fishing year step, effort, time of day, and vessel retained (Table 9). The model explained 42% of the variation in the data. Effort was the most influential variable, at 10%, with time of day and vessel having an influence of about 3%. The standardised and unstandardized annual indices are shown in Figure 31 (standardised indices scaled to the median of the unstandardised records for each time step). The two sets of indices follow a very similar pattern, although standardised index is often below the unstandardized during the early part of the series, particularly in time step 1. In more recent years, there is very little difference between the indices.

Table 9: Analysis of deviance table and overall influence for standardisation model selected by stepwise regression for time step indices for SCI 2.

	Df	Deviance explained	Additional deviance explained (%)	Overall influence (%)*
NULL				
fishing_year_step	65	3965.8	32.70	
poly(effort, 3)	3	610.2	5.03	10.47
TOD	3	316.7	2.61	3.78
vessel	8	148.7	1.22	3.29

*- Overall influence as in table 1 of Bentley et al. (2012)

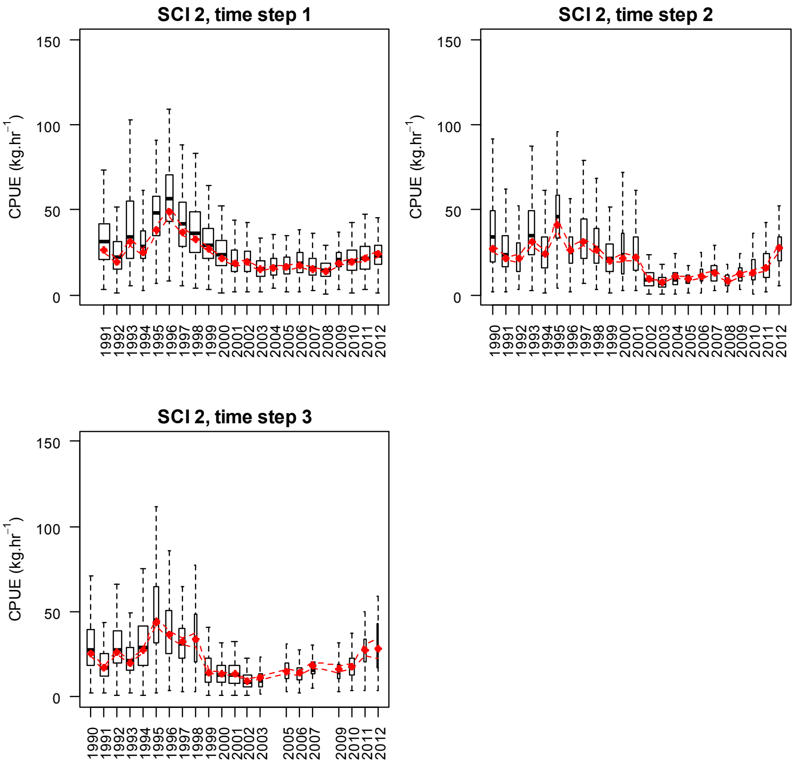

Figure 31: Boxplots of unstandardized CPUE for the core vessels in SCI 2 by fishing year (by time step), overlaid by standardised CPUE indices (scaled to the median of the unstandardised data).

Single annual index

Stepwise regression analysis of the dataset to estimate an annual CPUE index for SCI 2 resulted in a final model with fishing year, time of day, effort, time step and vessel retained (Table 10). Model diagnostics are presented in Appendix 3. The model explained 37% of the variation in the data. Effort was the most influential variable, at 11%, with time step an influence of 4%, and time of day and vessel having influences of about 2%. The standardised and unstandardized annual indices are shown in Figure 32. The two indices follow a generally similar pattern, although this standardised index is consistently above the unstandardized during the early part of the series (as fishing duration was increasing), and has been below the unstandardized index since the early 2000s (when a greater proportion of the overall catch has been taken in the first time step of the fishing year). The relative effects of the explanatory variables (excluding fishing year) are shown in Figure 33. Expected catch rates are highest during the day, and lowest at night, being just over two thirds of the daytime rate. Expected catch increases for tow durations up to about 8 to 10 hours, but then declines. Catch rates are highest in time step 1, falling to just under 80% of this level in time steps 2 and 3. Seven of the vessels were reasonable similar in their catch rate, but two vessels were markedly different, one above (124%) and one below (72%) the rest.

Table 10: Analysis of deviance table and overall influence for standardisation model selected by stepwise regression for an annual index for SCI 2.

	Df	Deviance explained	Additional deviance explained (%)	Overall influence (%)*
NULL				
fishing_year	22	2775.22	22.89	
poly(effort, 3)	3	642.96	5.30	10.95
TOD	3	583.15	4.81	1.81
model_step	2	334.74	2.76	4.00
Vessel	8	209.2	1.73	2.17

*- Overall influence as in table 1 of Bentley et al. (2012)

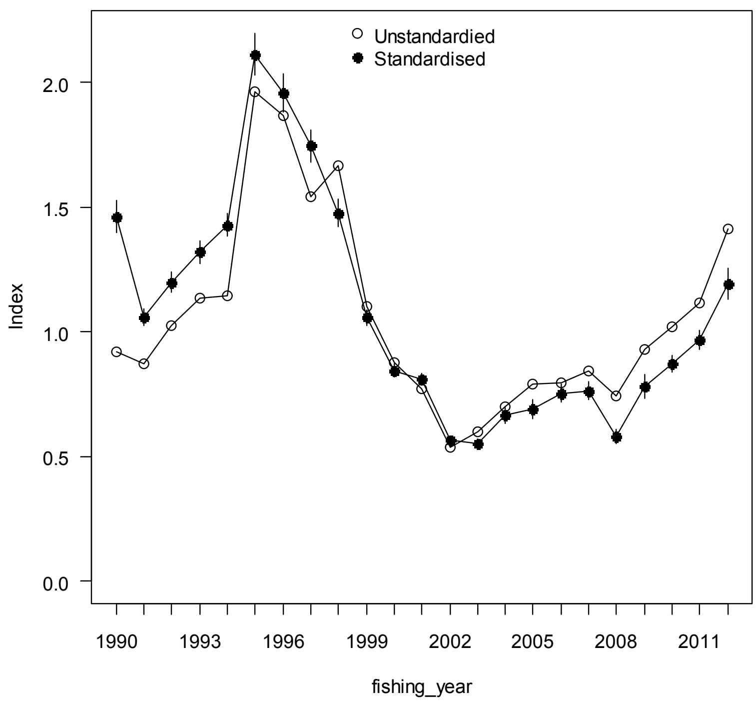

Figure 32: Comparison of standardised (Table 10) and unstandardized annual CPUE index for SCI 2.

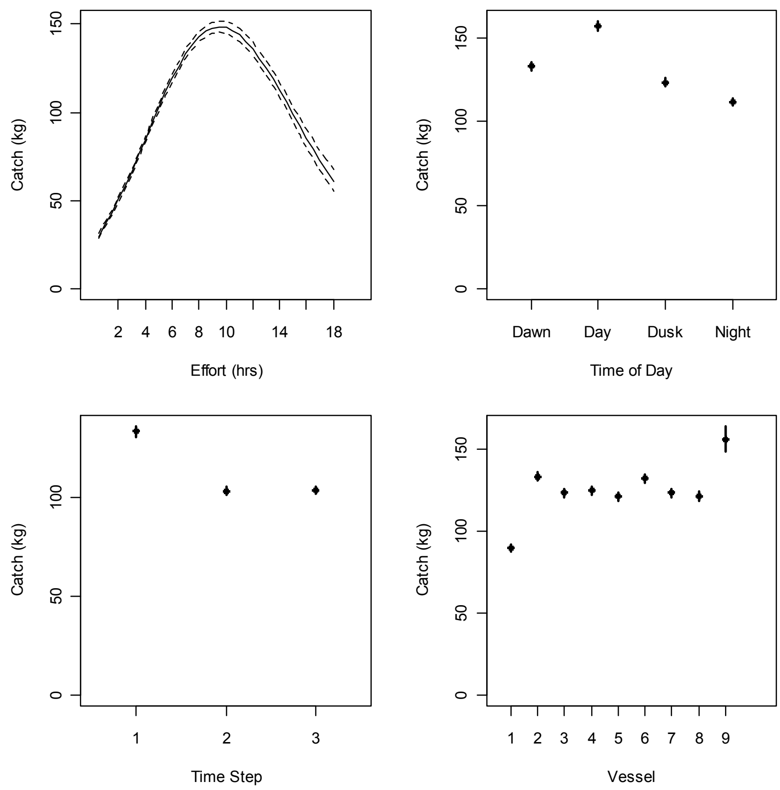

Figure 33: Termplot (in natural space) for annual index standardisation model (Table 10), showing relative effects of effort (tow duration), time of day, time step, and vessel.

As with the SCI 1 indices, consistency in the patterns shown in the indices were examined between strata within time step, and the Working Group agreed that realistic options for weighting individual spatial strata would not generate a composite time step indices greatly different from the three time step indices presented in Figure 31. Preliminary assessment models were presented to the Working Group fitting to the single annual standardised index (Figure 32), and the three time step indices (Figure 31). Model outputs were very similar, and the Working Group agreed that the annual index (Table 10, Figure 32) should be used within the models as the index of abundance from the CPUE data.

3. MODEL STRUCTURE

3.1. Spatial and seasonal structure, and the model partition

The model partitions scampi by sex, and length class. Growth between length classes are determined by sex-specific, length-based growth parameters. Individuals enter the partition by recruitment and are removed by natural mortality and fishing mortality. The model's annual cycle is based on the fishing year and is divided into the three time-steps described above (Table 4). The choice of three time steps was based on current understanding of scampi biology and sex ratio in catches. Note that model references to "year" within this report refer to the modelled or fishing year, and are labelled as the most recent calendar year, e.g. the fishing year 1998–99 is referred to as "1999" throughout. Previous models for SCI 1 and SCI 2 have included spatial structure (Tuck & Dunn 2012), but following the characterisation and preliminary model investigation, the SFAWG recommended a single area model for both assessments.

The model uses capped logistic length based selectivity curves for commercial fishing and research trawl surveys, assumed constant over years, but allowed to vary with sex and time step (where necessary). While the sex ratio data suggest that the relative catchability of the sexes vary through the year (hence the model time structure adopted), there is no reason to suggest that assuming equal availability, selectivity at size would be different between the sexes. Therefore the two sex selectivity implementation developed within CASAL for the SCI 1 and SCI 2 assessments (Tuck & Dunn 2012) was applied. This allows the L_{50} (size at which 50% of individuals are retained) and a_{95} (size at which 95% of individuals are retained) selectivity parameters to be estimated as single values shared by both sexes in a particular time step, but allows for different availability between the sexes through estimation of different a_{max} (maximum level of selectivity) values for each sex. At the suggestion of the Working Group, sensitivities were also examined to using double normal capped selectivity curves for the commercial fishery, to allow domed selectivity (no link between the parameters for each sex). Photographic survey abundance indices are not sex specific, and a standard logistic length based selectivity curve is applied.

3.2. Biological inputs

3.2.1. Growth

Scampi growth has been estimated from wild-tagged scampi in SCI 1 (Cryer & Stotter 1997, 1999) and aquarium-reared scampi from SCI 2 (Cryer & Oliver 2001) (Figure 34).

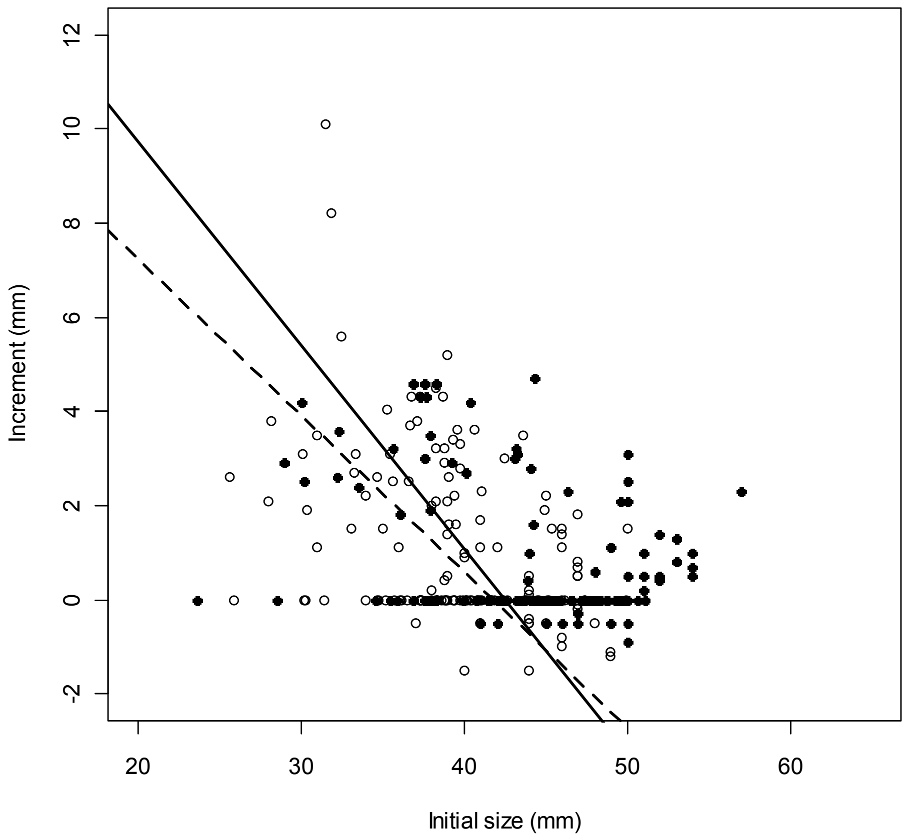

Figure 34: Growth increment data from scampi tagging in SCI 1 and SCI 2, and aquarium studies. Solid and hollow symbols represent males and females. Solid (males) and dotted (females) lines represent best fits to data from combined growth studies.

In the initial developments of the of the scampi assessment model (Cryer et al. 2005), the combined data set were analysed externally and the estimated growth parameters for each sex fixed within the model. However, given the strong influence growth has on length based models, and the scatter around the externally fitted relationships in Figure 34, more recently the fitting of the growth data has been included within this model (Tuck & Dunn 2012). The growth increment data from SCI 1 and SCI 2 have been combined into a single dataset, and are fitted independently in the two assessment models.

On the basis of the time steps within the model structure, the tag data can be split into three release events. Recaptures of tagged scampi from these releases are tabulated by recapture time step in Table 11. Within the analysis, animals from both wild release and aquarium studies have been combined, although the numbers of animals are provided separately in Table 11.

Table 11: Numbers of scampi recaptured by release and recapture time step (SCI 1 and 2).

Release/Recapture	1996-3	1997-1	1997-2	1997-3
1996-2		20	7	13
1996-3*	12	15 (28)	2 (21)	42 (30)
1997-1			15	80

* - recaptures from1996-3 release include 79 animals in aquaria and 71 from wild releases. For recaptures, numbers in parenthesis represent aquarium animals.

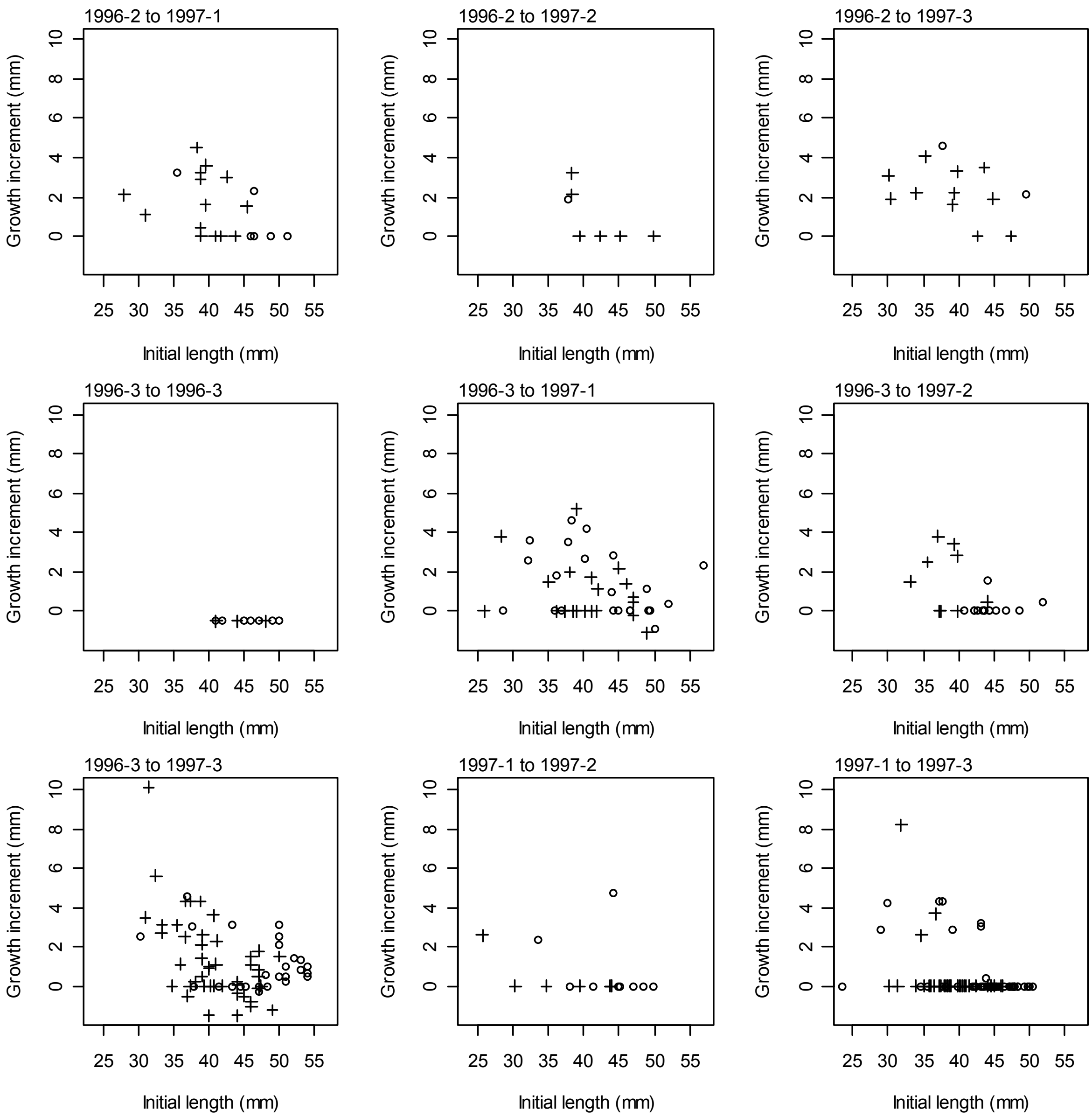

Figure 35: Plot of initial length against growth increment by combination of release and recapture time steps. Males represented by hollow symbols, females represented by crosses.

For the nine combinations of release and recapture the length increment is plotted by sex against initial length in Figure 35. The model structure has a growth period assigned to the start of time step 1 for both sexes, and a growth period assigned to the start of time step 2 for males (when two growth periods are included). Therefore no growth would be expected for those animals released in 1996-3 and recaptured in 1996-3, or females released 1997-1 and recaptured in 1997-2 or 1997-3 (although 4 of 40 females showed some growth). The animals released and recaptured in 1996-3 have been excluded from the model for simplicity. The data available, particularly for males (Figure 17), suggest some evidence of two periods of moulting. The sensitivity of the model to allowing two growth periods per year were examined in a previous assessment (Tuck & Dunn 2012).

3.2.2. Maturity

The proportion of females mature at each 1 mm size class have been recorded during all research surveys since 1993. These data have been combined for females from SCI 1 and 2, assuming internal gonad stages 2–5 to be mature, and stage 1 to be immature. No data are available for the maturity of male scampi, so their maturity ogive was assumed identical to that of females, although studies on *N. norvegicus* have suggested that male maturity may occur at a larger size (although possibly the same age) than females (Tuck et al. 2000). Maturity is not considered to be a part of the model partition, but proportions mature were fitted within the model based on a logistic ogive with a binomial likelihood (Bull et al. 2008).

Analysis of the proportion ovigerous data, modelled as a function of length, was conducted within a GLM framework, with a quasibinomial distribution of errors and a logit link (McCullagh & Nelder 1989),

$$\text{logit}(m)=a+bl$$

which equates to the logistic model. The model was weighted by the number measured at each length. After obtaining estimates for the parameters *a* and *b*, the length at which 50% are mature (L_{50}) was calculated from:

$$L_{50} = -\frac{a}{b}$$

with selection range (SR) calculated from:

$$SR = \frac{(2.\ln(3))}{b}$$

Female maturity data for SCI 1 and 2 are summarised in Figure 36 (Tuck & Dunn 2006). The L_{50} estimate for the pooled SCI 1 and SCI 2 data was 29.7 mm, with a selection range a_{25} to a_{75} of 5.3mm. The maturity curve fitted to these data is plotted in Figure 37.

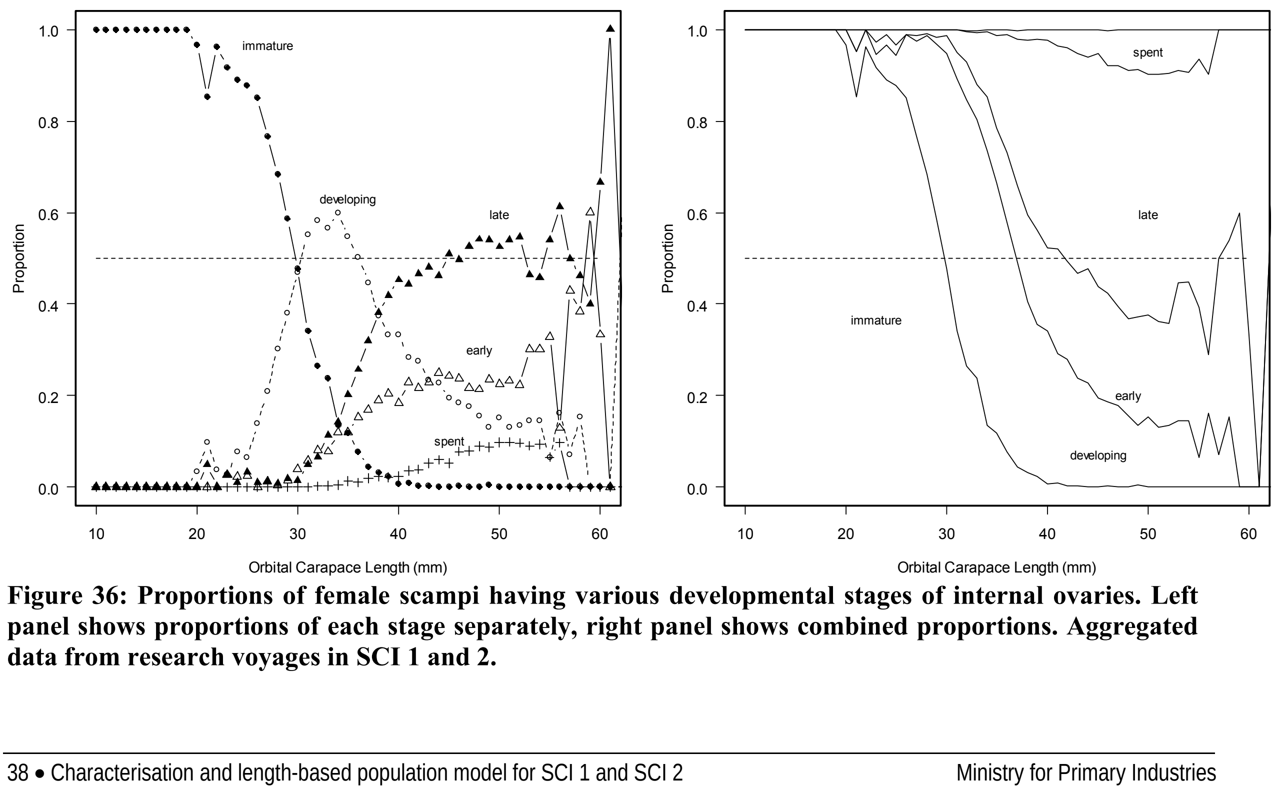

Figure 36: Proportions of female scampi having various developmental stages of internal ovaries. Left panel shows proportions of each stage separately, right panel shows combined proportions. Aggregated data from research voyages in SCI 1 and 2.

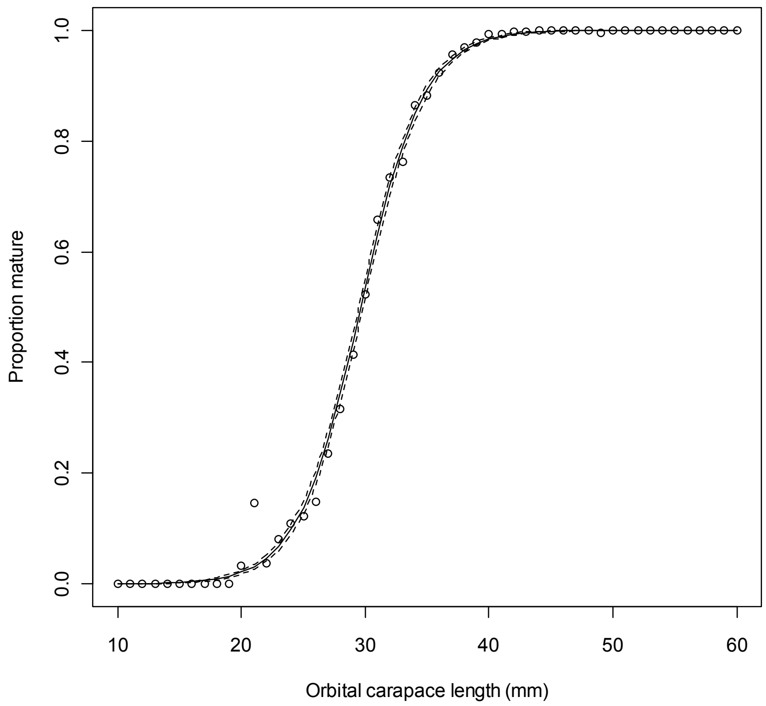

Figure 37: Proportions of female scampi with mature gonad stages at length, from all research trawling in SCI 1 and SCI 2. Solid line represents logistic curve fitted to the data (L_{50} 29.7 mm and selection range 5.3 mm). Dashed line represents ± 1 s.e.

3.2.3. Natural mortality

The instantaneous rate of natural mortality, M, has not been estimated directly for any scampi species, but estimates have been made based on the estimate of the K parameter from a von Bertalanffy growth curve (Cryer & Stotter 1999) using a correlative method (Pauly 1980, Charnov et al. 1983). Morizur (1982) used length distributions from 'quasi-unexploited' *Nephrops* stocks to obtain estimates for annual *M* of 0.2–0.3. The values most commonly assumed for assessment of *Nephrops* stocks in the Atlantic is 0.3 for males and immature females, and 0.2 for mature females (assumed less vulnerable to predation during the ovigerous period)(Bell et al. 2006). For New Zealand scampi, M has previously been fixed at 0.2 (Tuck & Dunn 2012). Within the current assessment, an attempt was made to estimate M within the model, but sensitivities were also examined with M fixed at 0.2, 0.3 and 0.4.

3.3. Catch data

Data for the model were collated over the spatial and temporal strata as defined in the model structure. Catches in these modelled areas represent over 96% of scampi catches from both SCI 1 and SCI 2. Details of catches by time step, and breakdown by survey strata, are provided for SCI 1 in Table 12, and SCI 2 in Table 13.

Table 12: Catch breakdown by time step for each fishing year for SCI 1, along with breakdown by survey strata within each time step.

	Step 1					Step 2					Step 3				
	Catch	202	203	3/402	3/403	Catch	202	203	3/402	3/403	Catch	202	203	3/402	3/403
1987						2	0%	0%	50%	50%	3	0%	1%	18%	81%
1988						6	0%	0%	50%	50%	9	0%	1%	18%	81%
1989						22	0%	0%	50%	50%	38	0%	1%	18%	81%
1990	47	1%	1%	71%	28%	19	0%	1%	67%	32%	38	1%	0%	90%	9%
1991	43	1%	0%	74%	25%	35	1%	2%	82%	15%	101	36%	28%	22%	14%
1992	68	12%	5%	68%	15%	13	2%	2%	85%	11%	51	32%	11%	45%	12%
1993	44	41%	5%	48%	5%	21	4%	0%	82%	14%	49	15%	21%	40%	23%
1994	75	31%	4%	54%	11%	1	61%	0%	35%	3%	39	12%	36%	28%	24%
1995	59	48%	3%	39%	11%	24	60%	3%	31%	6%	31	51%	15%	17%	17%
1996	67	39%	16%	23%	22%	22	1%	59%	17%	23%	28	6%	4%	43%	47%
1997	58	5%	28%	16%	51%	38	29%	36%	8%	26%	21	11%	30%	10%	48%
1998	88	22%	24%	35%	18%	9	0%	6%	41%	53%	10	2%	2%	69%	28%
1999	62	17%	12%	58%	14%	39	9%	13%	52%	26%	9	0%	0%	53%	47%
2000	22	17%	36%	17%	30%	24	8%	26%	10%	56%	78	31%	19%	42%	8%
2001	82	35%	11%	45%	9%	32	28%	7%	59%	5%	5	41%	16%	42%	1%
2002	124	32%	17%	45%	6%										
2003	121	29%	13%	48%	10%										
2004	120	30%	15%	48%	7%										
2005	46	41%	22%	28%	9%	34	31%	13%	35%	22%	34	39%	20%	37%	4%
2006	40	25%	6%	53%	16%	26	34%	9%	57%	1%	43	36%	44%	12%	8%
2007	43	33%	10%	44%	13%	34	16%	9%	61%	14%	32	45%	24%	26%	5%
2008	48	29%	4%	49%	18%	33	15%	8%	59%	18%	20	24%	44%	21%	11%
2009	50	21%	11%	47%	21%	18	24%	16%	48%	12%	17	9%	18%	53%	20%
2010	65	26%	21%	47%	6%	15	4%	4%	68%	24%	31	3%	2%	77%	19%
2011	48	5%	6%	86%	3%	23	33%	15%	50%	2%	43	1%	1%	64%	34%
2012	58	14%	9%	63%	14%	19	6%	4%	67%	23%	37	9%	14%	42%	35%

Table 13: Catch breakdown by time step for each fishing year for SCI 2, along with breakdown by survey strata within each time step.

	Step 1					Step 2					Step 3				
	Catch	702	703	802	803	Catch	702	703	802	803	Catch	702	703	802	803
1987															
1988											5	68%	0%	32%	0%
1989						1	0%	0%	100%	0%	16	68%	0%	32%	0%
1990	16	99%	0%	1%	0%	38	39%	1%	60%	0%	81	70%	1%	29%	0%
1991	137	34%	0%	66%	0%	55	27%	0%	73%	0%	89	44%	9%	47%	1%
1992	65	58%	1%	42%	0%	20	19%	0%	81%	0%	115	44%	3%	52%	0%
1993	73	69%	3%	28%	0%	60	40%	1%	59%	0%	68	41%	5%	54%	1%
1994	30	67%	3%	30%	0%	53	97%	1%	2%	0%	153	59%	1%	40%	1%
1995	66	34%	9%	58%	0%	42	35%	1%	62%	2%	104	25%	2%	67%	6%
1996	107	67%	13%	18%	1%	27	80%	0%	20%	0%	93	55%	2%	39%	4%
1997	61	70%	6%	23%	0%	69	57%	11%	31%	0%	78	73%	18%	8%	1%
1998	151	53%	4%	43%	0%	43	33%	3%	64%	0%	21	14%	3%	78%	6%
1999	127	56%	6%	38%	1%	68	43%	3%	54%	0%	32	64%	15%	21%	0%
2000	101	43%	8%	49%	1%	15	51%	0%	49%	0%	74	73%	6%	20%	0%
2001	28	62%	0%	38%	0%	32	63%	0%	37%	0%	83	63%	4%	34%	0%
2002	65	64%	2%	31%	2%	98	50%	1%	49%	0%	73	59%	14%	26%	1%
2003	77	45%	3%	52%	0%	37	32%	8%	60%	0%	14	80%	19%	1%	0%
2004	39	72%	8%	19%	0%	24	70%	4%	26%	0%					
2005	33	65%	9%	25%	0%	9	59%	3%	38%	0%	15	45%	16%	38%	1%
2006	36	48%	1%	51%	0%	6	96%	1%	3%	0%	33	70%	13%	18%	0%
2007	36	37%	4%	59%	0%	26	61%	1%	38%	0%	17	67%	11%	22%	0%
2008	55	61%	2%	37%	0%	5	82%	2%	15%	0%					
2009	32	55%	1%	44%	0%	11	36%	0%	64%	0%	10	92%	0%	8%	0%
2010	85	41%	0%	58%	1%	10	49%	1%	51%	0%	29	62%	3%	35%	0%
2011	82	76%	3%	21%	0%	29	77%	1%	23%	0%	17	45%	1%	54%	0%
2012	61	48%	1%	51%	1%	31	50%	0%	48%	2%	7	3%	0%	97%	0%

3.4. CPUE indices

The annual CPUE indices estimated within the standardisation (SCI 1: Figure 28, SCI 2: Figure 32) were fitted within the model as abundance indices. There has been considerable discussion on whether CPUE is proportional to abundance for scampi (Tuck 2009), with rapid increases in both CPUE and trawl survey catch rates for a number of stocks in the early to mid 1990s (and changes in sex ratio in trawl survey catches) initially being considered related to changes in catchability. Later analysis (Tuck & Dunn 2009) suggested that the observed changes in sex ratio were related to slight changes in the survey timing in relation to the moult cycle. Similar patterns in CPUE are observed over the same period for rock lobster (Starr 2009, Starr et al. 2009), and scampi in SCI 3 (Tuck 2013), which may suggest broad scale environmental drivers influencing crustacean recruitment. The CPUE patterns for SCI 1 are mirrored by trawl survey catch rates, suggesting that they do not reflect fisher learning. While not considered appropriate for use as an index in the model (Tuck 2013), the middle depths (Tangaroa) trawl survey scampi abundance index shows a very similar temporal pattern to the standardised CPUE indices for SCI 3, also supporting the suggestion that the increases in scampi catch rate observed during the 1990s reflect scampi abundance rather than fisher learning.

3.5. Research survey indices

Trawl surveys were first conducted from the RV *Kaharoa* in SCI 1 and SCI 2 in 1993, and have been conducted intermittently (in conjunction with photographic surveys in more recent years). Surveys have been conducted between January and April, but timing within this period has varied between years.

3.5.1. Photographic surveys

Photographic surveys of SCI 1 and SCI 2 (Cryer et al. 2003, Tuck et al. 2006, Tuck et al. 2009, Tuck et al. 2013) have been used to estimate the absolute abundance (in numbers) of burrows thought to belong to scampi in 1998, 2000–2003, 2008 and 2012 (for SCI 1) and 2003–2006 and 2012 (for SCI 2). The surveys provide two indices of scampi abundance, one based on major burrow openings, and one based on visible scampi. Both indices are subject to uncertainty, either from burrow detection and occupancy rates (for burrow based indices) or emergence patterns (for visible scampi based indices). The burrow index has been used to date within assessments for SCI 1 and SCI 2 (Tuck & Dunn 2012). Survey estimates are provided for SCI 1 in Table 14 and SCI 2 in Table 15. Surveys of SCI 1 only covered part of the main fishery area until 2012, and the data are fitted within the model as two separate series, with separate *q* values, with the *q* for the total area informed by a prior, and the ratio between the *q*s for the total and part surveys constrained by the @ratio_qs_penalty in CASAL. Details of the estimation of the priors and the ratio are provided in Section 3.7. Although the photographic surveys have occurred in time step 1 and 2, the survey abundance (based on burrow counts) should be relatively insensitive to moult cycle and reproductive behaviour driving the changes in sex ratio in catches, and therefore the indices are fitted as occurring at the end of time step 1.

Table 14: Time series of photo survey scampi stock estimates (millions) and CV for SCI 1. Estimates are provided for survey combined strata 302, 303, 402 and 403 (areas surveyed 1998–2008), and the larger area surveyed in 2012 (including survey strata 202 and 203). Time step relates to assessment model, with surveys in December – January allocated to step 1, and those in February – April allocated to step 2.

	302,303,402,403		Total area		
	Abundance	CV	Abundance	CV	Time step
1998	155.1	0.147			1
2000	96.7	0.125			2
2001	135.9	0.118			1
2002	128.2	0.080			2
2003	101.9	0.122			2
2008	107.1	0.075			2
2012	95.8	0.062	144.1	0.057	2

Table 15: Time series of photo survey scampi stock estimates (millions) and CV for SCI 2. Time step relates to assessment model, with surveys in December – January allocated to step 1, and those in February – April allocated to step 2.

	Abundance	CV	Time step
2003	114.5	0.122	2
2004	164.2	0.171	1
2005	106.3	0.112	2
2006	104.3	0.102	2
2012	168.9	0.086	2

3.5.2. Trawl surveys

Stratified random trawl surveys of scampi in SCI 1 and SCI 2, 200–600 m depth, were conducted in 1993, 1994, and 1995. Formal trawl surveys to estimate relative abundance were discontinued following this, because it was inferred from the results that catchability had varied among surveys, although it was later concluded that the changes were related to slight differences in survey timing (Tuck & Dunn 2009). Despite these concerns, research trawling continued in both areas for a variety of other purposes (in support of a tagging programme to estimate growth in 1995 and 1996, to assess selectivity of research and commercial mesh sizes in 1996, and trawl surveys have been conducted in support of photographic surveys since 1998). Identical gear has been used throughout the survey trawling. Survey coverage in SCI 1 has changed over time, with the early surveys covering the whole modelled area, but surveys in 1998, and from 2001 – 2008 only covering survey strata 302, 303, 402 and 403. Survey estimates (by area) are provided for SCI 1 in Table 16 and SCI 2 in Table 17. As with the photo survey for SCI 1, the trawl survey is fitted as two indices with separate *q*s, with the ratio between the *q*s for the total and part surveys constrained by the @ratio_qs_penalty (Section 3.7). Trawl surveys in both fisheries have occurred in time steps 1 and 2. In SCI 1, surveys in time step 2 have generally been early in the time step, and to reduce complexity, given the two levels of survey coverage, all trawl surveys were assumed to occur at the end of time step 1. In SCI 2, surveys have occurred later in time step 2, and have been fitted as separate indices in each time step.

Table 16: Time series of raised trawl survey scampi stock estimates (tonnes) by survey strata for SCI 1. Estimates are provided for survey combined strata 302, 303, 402 and 403 (areas surveyed 1998, 2001–2008), and the larger area surveyed in 1993–1995, 2000, 2012 (including survey strata 202 and 203). Time step relates to assessment model, with surveys in December – January allocated to step 1, and those in February – April allocated to step 2. N represents number of research tows in each survey.

	302,303,402,403			Total area			
	N	Biomass	CV	N	Biomass	CV	Time step
1993				36	271.6	0.117	1
1994				33	364.0	0.171	1
1995				37	510.4	0.150	1
1998	18	174.0	0.172				1
2000				15	225.1	0.328	2
2001	12	179.5	0.269				1
2002	13	130.6	0.236				2
2008	10	211.9	0.132				2
2012				19	186.6	0.210	2

Table 17: Time series of raised trawl survey scampi stock estimates (tonnes) by survey strata for SCI 2. Time step relates to assessment model, with surveys in December – January allocated to step 1, and those in February – April allocated to step 2. N represents number of research tows in each survey.

	N	Biomass	CV	Time step
1993	26	238.2	0.12	1
1994	27	170.0	0.16	1
1995	29	216.2	0.18	1
2003	7	28.0	0.33	2
2004	8	46.9	0.20	1
2005	8	50.8	0.35	2
2006	8	22.9	0.19	2
2012	14	164.2	0.28	2

3.6. Length distributions

3.6.1. Commercial catch at length data

Ministry of Fisheries observers have collected scampi length frequency data from scampi targeted fishing on commercial vessels in SCI 1 and SCI 2 since 1990–91. The numbers of tows for which length data are available are presented by fishing year and month in Table 18 (SCI 1), Table 19 (SCI 2).

For both fisheries, levels of sampling, and the pattern of sampling relative to the pattern of catches, vary between years, and the proportion of landings represented by the observer sampling varies considerably (Table 20). Where size compositions vary markedly between areas, low proportions of landings being represented by observer sampling may lead to biased estimates of catch composition.

For both fisheries, mean orbital carapace length (OCL) from observer sampling was modelled on year, survey strata and time step, with strata effects detected (improved residual deviance by more than 1%). Model results indicated that mean CL was 1 – 1.5 mm greater in some strata than others. Given the overall uncertainty in the observer samples, this margin of difference was not considered to be of concern by the WG.

Table 18: Number of commercial tows for which length distributions are available for SCI 1, by fishing year, time step and survey strata.

	Step 1				Step 2				Step 3			
	202	203	3/402	3/403	202	203	3/402	3/403	202	203	3/402	3/403
1991									8	60	25	8
1992		1	13	2					15			
1993	2		1									
1994											1	
1995									3			
1996	1		4						1			
1997						7		8				
1999					3	1	8	2				
2000									6	14	9	2
2002		2	1									
2004	1	1										
2005									7	6	2	1
2006	2	2	2	7					8	16		1
2007	4	2	13	1					11	2	5	1
2008	1	4	5	14			21	11				
2009	2	5	14	6								
2010	9		2	2	2		8	5	2	4	12	11
2011	1	3	20	2							20	2
2012			2	1			10	3				

Proportional length distributions (and associated CVs) were calculated using CALA (Francis & Bian 2011), using the approaches previously implemented in NIWA's *Catch-at-Age* software (Bull & Dunn 2002). Plots of the proportional length distribution are shown by year for SCI 1 by time step in Figure 38 to Figure 40, and for SCI 2 by time step in Figure 41 to Figure 44.

Table 19: Number of commercial tows for which length distributions are available for SCI 2, by fishing year, time step and survey strata.

	Step 1				Step 2				Step 3			
	702	703	802	803	702	703	802	803	702	703	802	803
1991									33	17	11	1
1992	9		5									
1993		1	2						7	2	18	
1994					1				32	2	24	
1995					4	2	18		7		25	5
1996	13								4		10	1
1997	28		6		1				5			
1999	3	1				2						
2000	51	8	22	1	18	7						
2002	20	26	29						1			
2004	36	2	16						7	1		
2005	25		12									
2006	11	2										
2007			6									
2008					3		1		1			
2009	10	2	8		7		3		2		1	
2010					6		6					
2011									4	2	4	
2012	4	1	12						3		3	

Table 20: Proportion of landings not represented by observer catch sampling.

	SCI 1			SCI 2		
	Step 1	Step 2	Step 3	Step 1	Step 2	Step 3
1991			0%			0%
1992	12%		68%	1%		
1993	11%			69%		1%
1994			72%		3%	1%
1995			49%		2%	2%
1996	38%		94%	33%		2%
1997		38%		7%	43%	27%
1998				43%	97%	
1999		0%		0%	54%	
2000			0%	1%		27%
2001				0%		34%
2002	38%			4%		
2003				52%		
2004	55%					
2005			0%	75%		
2006	0%		12%			
2007	0%		0%		1%	33%
2008	0%	23%		0%	2%	0%
2009	0%				0%	
2010	21%	4%	0%			0%
2011	0%		2%	0%		1%
2012	23%	10%		1%	52%	

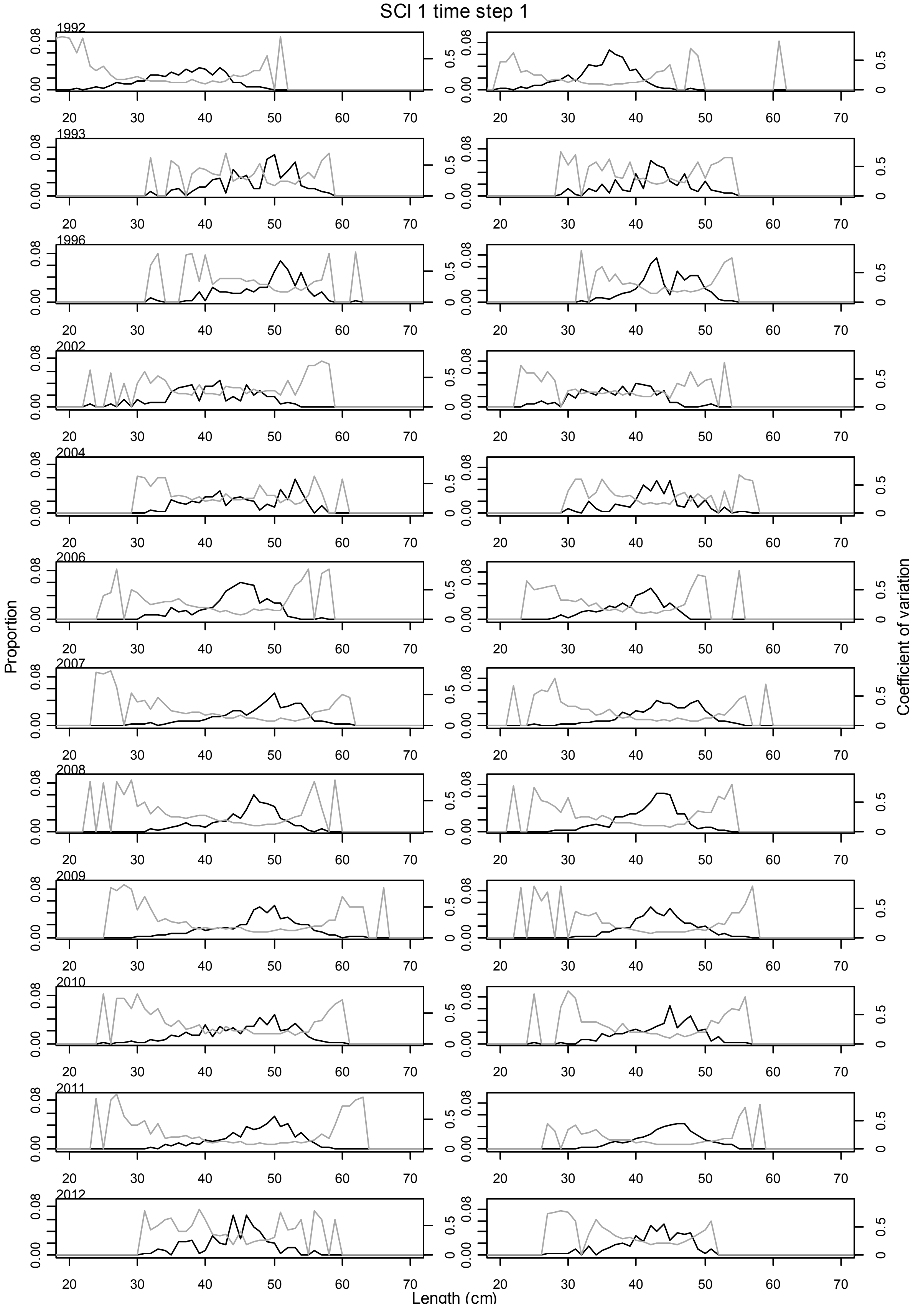

Figure 38: Proportional length frequencies (black line) and CVs (grey line) for commercial catches by model year and time step 1 for SCI 1. Males plotted on left, females on right.

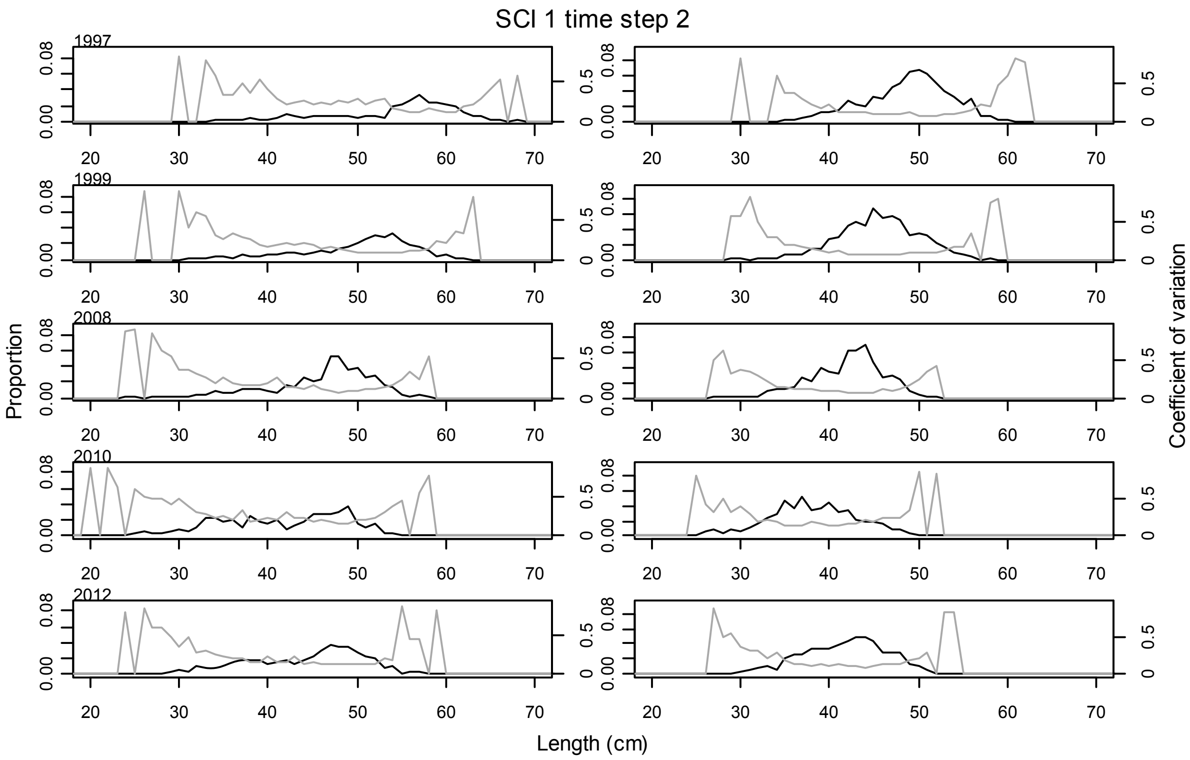

Figure 39: Proportional length frequencies (black line) and CVs (grey line) for commercial catches by model year and time step 1 for SCI 1. Males plotted on left, females on right.

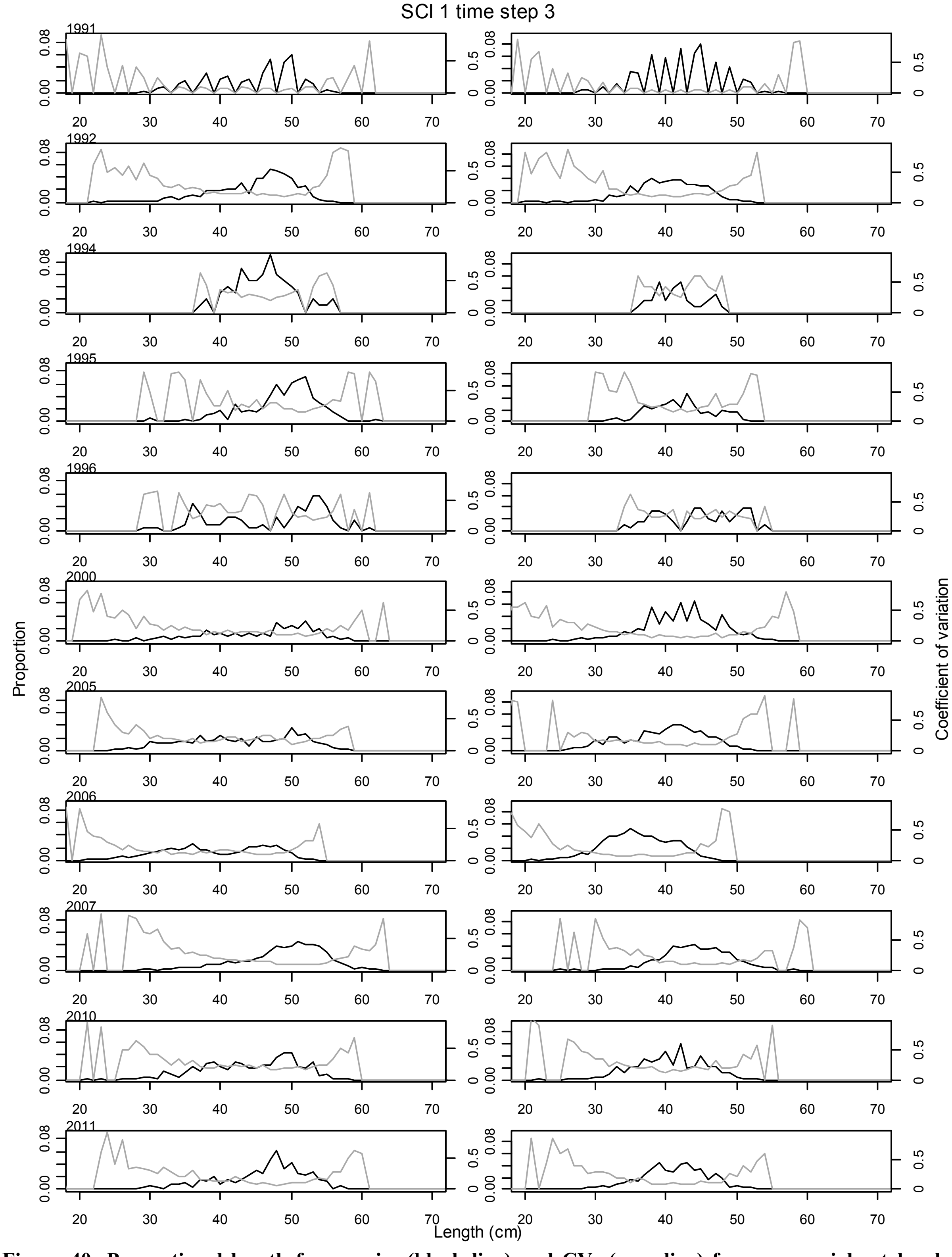

Figure 40: Proportional length frequencies (black line) and CVs (grey line) for commercial catches by model year and time step 3 for SCI 1. Males plotted on left, females on right.

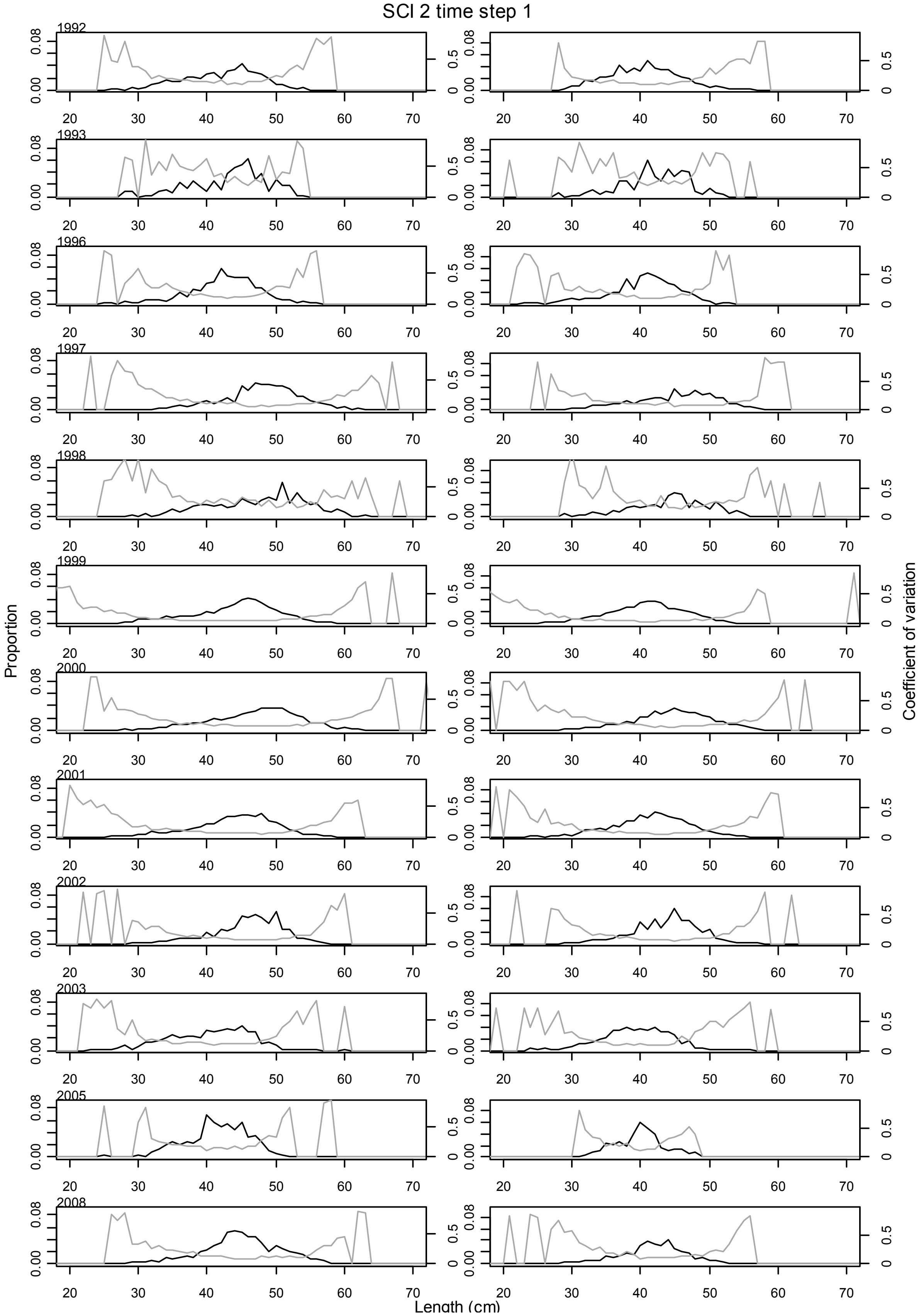

Figure 41: Proportional length frequencies (black line) and CVs (grey line) for commercial catches by model year and time step 1 for SCI 2, 1992 to 2008. Males plotted on left, females on right.

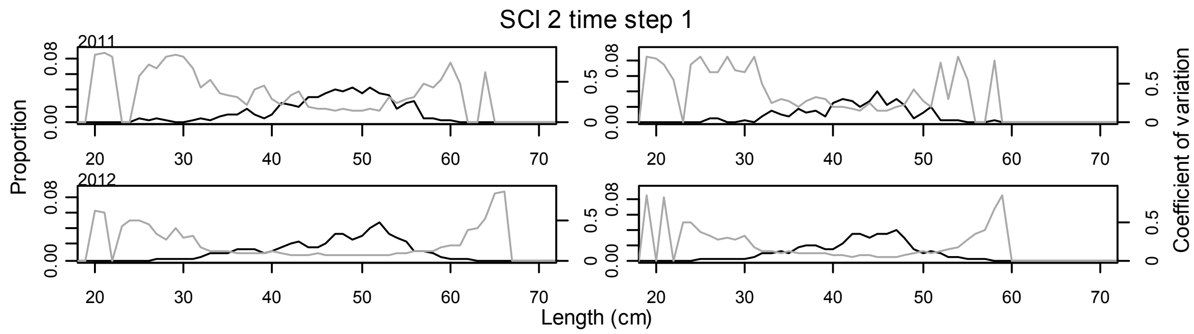

Figure 42: Proportional length frequencies (black line) and CVs (grey line) for commercial catches by model year and time step 1 for SCI 2, 2011 to 2012. Males plotted on left, females on right.

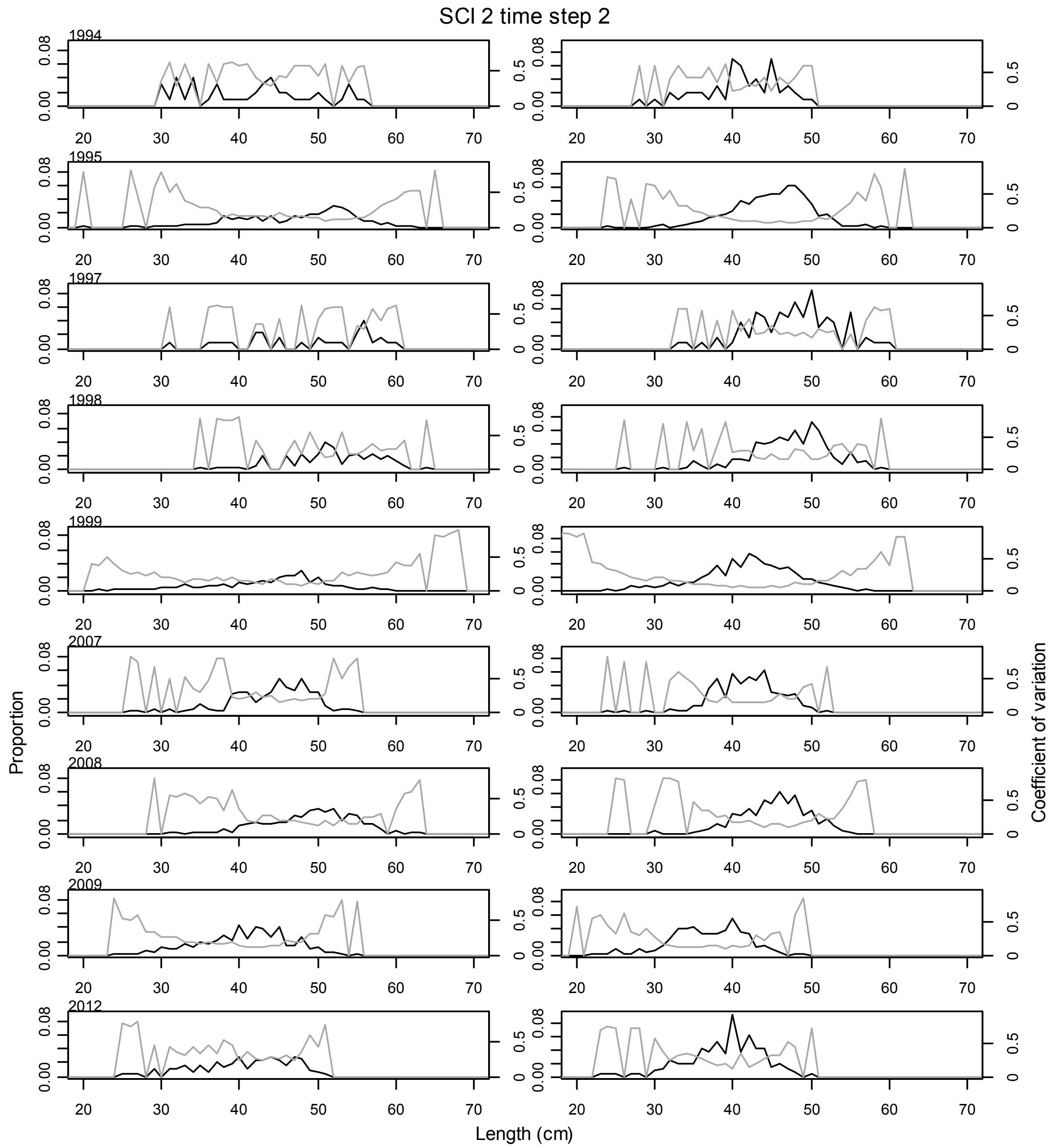

Figure 43: Proportional length frequencies (black line) and CVs (grey line) for commercial catches by model year and time step 2 for SCI 2. Males plotted on left, females on right.

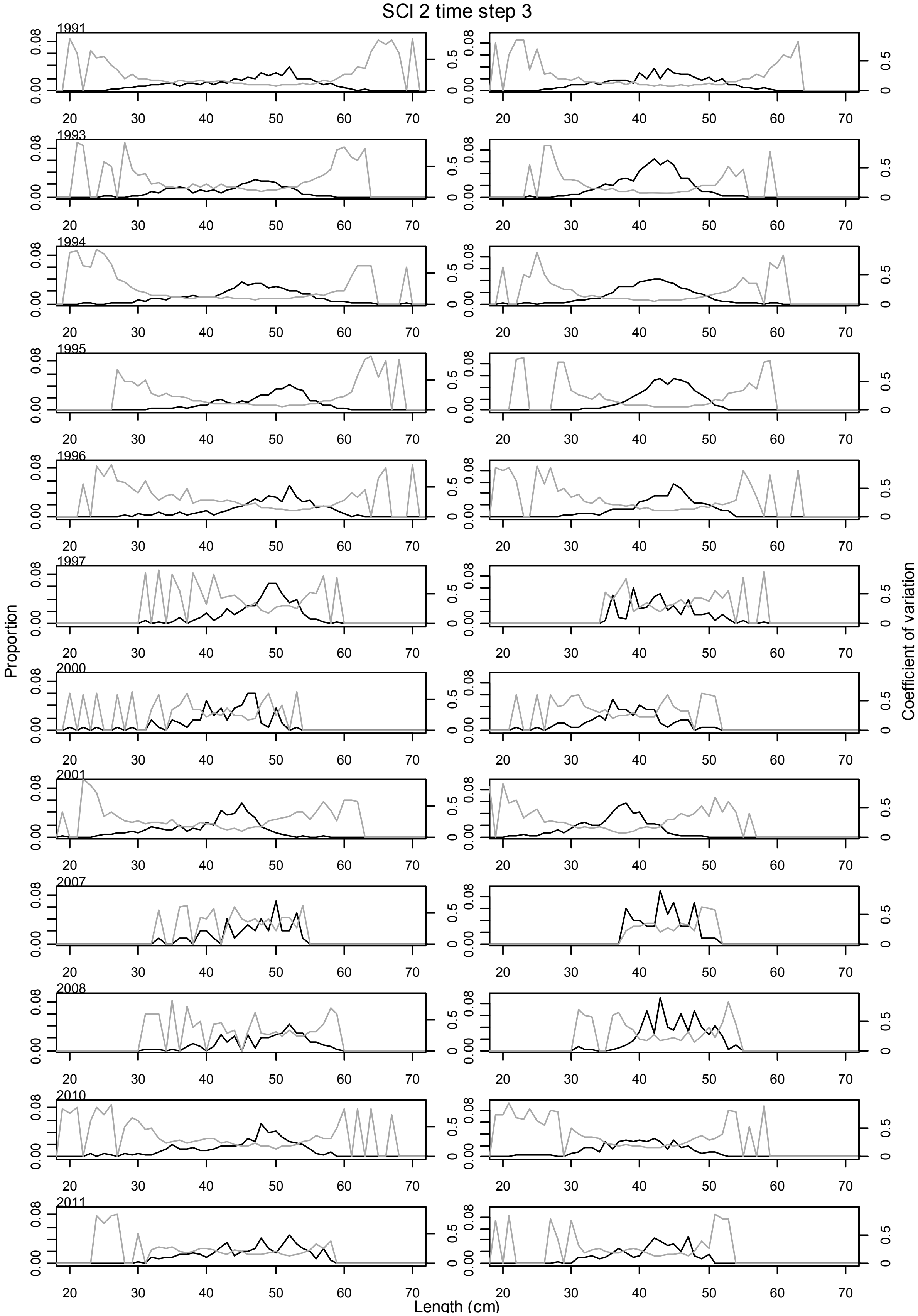

Figure 44: Proportional length frequencies (black line) and CVs (grey line) for commercial catches by model year and time step 3 for SCI 2. Males plotted on left, females on right.

3.6.2. Trawl survey length distributions

Length frequency samples from research trawling in both fisheries have been taken by scientific staff since 1993 (Table 16 and Table 17). Estimates of the length frequency distributions (with associated CVs) were derived using the NIWA CALA software (Francis & Bian 2011), using 1 mm (Orbital Carapace Length) length classes by sex, and are presented in Figure 45 and Figure 46.

3.6.3. Photo survey length distributions

Length frequency distributions were estimated for the relative photographic abundance series, by measuring the widths of a large sample of major burrow openings in the images, and converting these to orbital carapace lengths using a regression of OCL on major opening width (Cryer et al. 2005), augmented with additional data collected from more recent surveys. To estimate the CVs at length for each year, we used a bootstrap procedure, resampling with replacement from the original observations of burrow width, converting each observation to an estimated scampi size (in OCL), using an error term sampled from a normal distribution fitted to the regression residuals. Compared with the length frequency distributions from trawl catches, this procedure gave very large CVs, but we think this is realistic given the uncertainties involved in generating a length frequency distribution from burrow sizes. Estimates of the length frequency distributions (with associated CVs) for scampi generating burrows are presented for SCI 1 in Figure 47 and for SCI 2 in Figure 48.

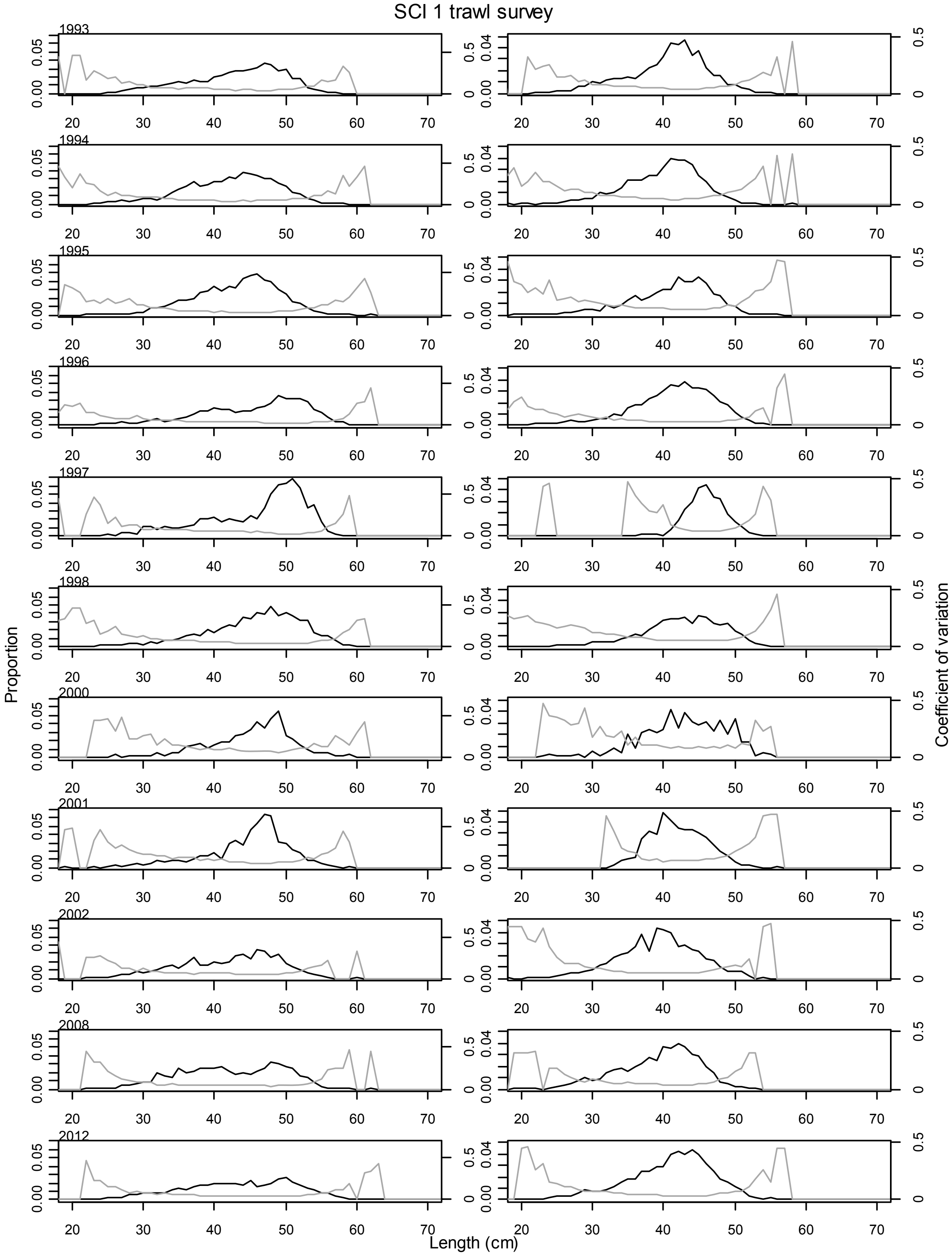

Figure 45: Proportional length frequencies (black line) and CVs (grey line) for research survey catches by model year for SCI 1. Males plotted on left, females on right.

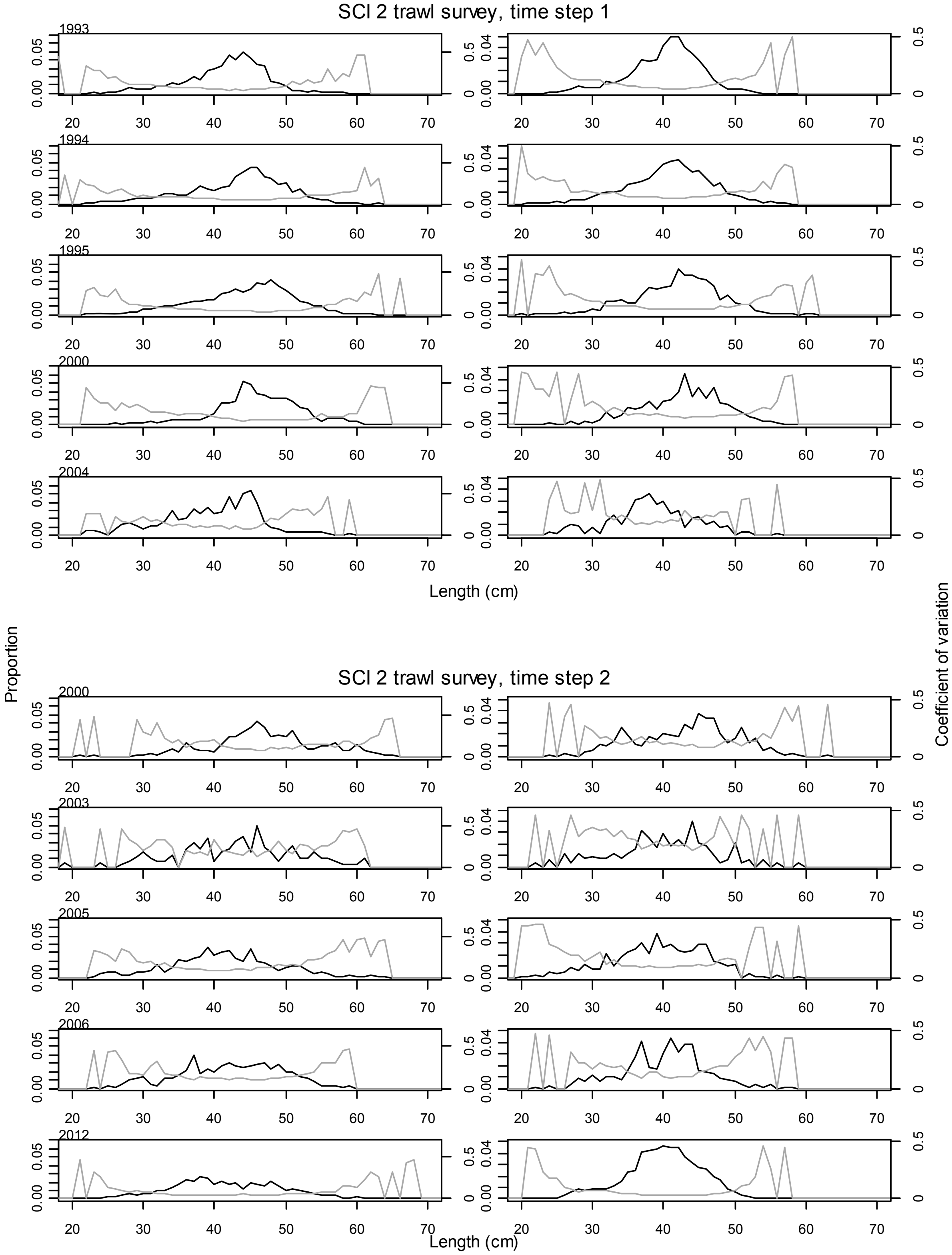

Figure 46: Proportional length frequencies (black line) and CVs (grey line) for research survey catches by model year and time step for SCI 2. Upper block, time step 1; lower block, time step 2. Males plotted on left, females on right.

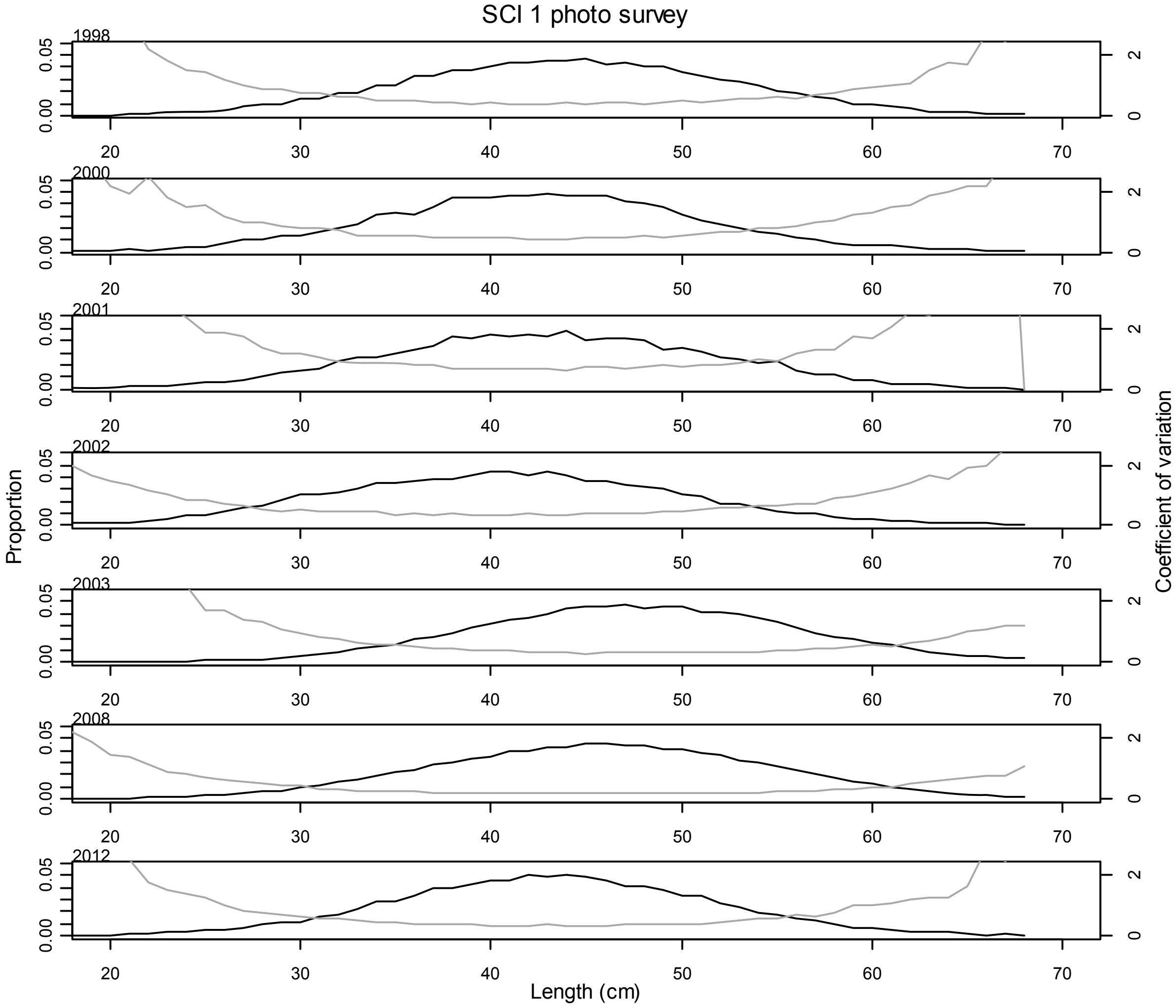

Figure 47: Proportional length frequencies and CVs for scampi responsible for burrows counted within photo survey for SCI 1.

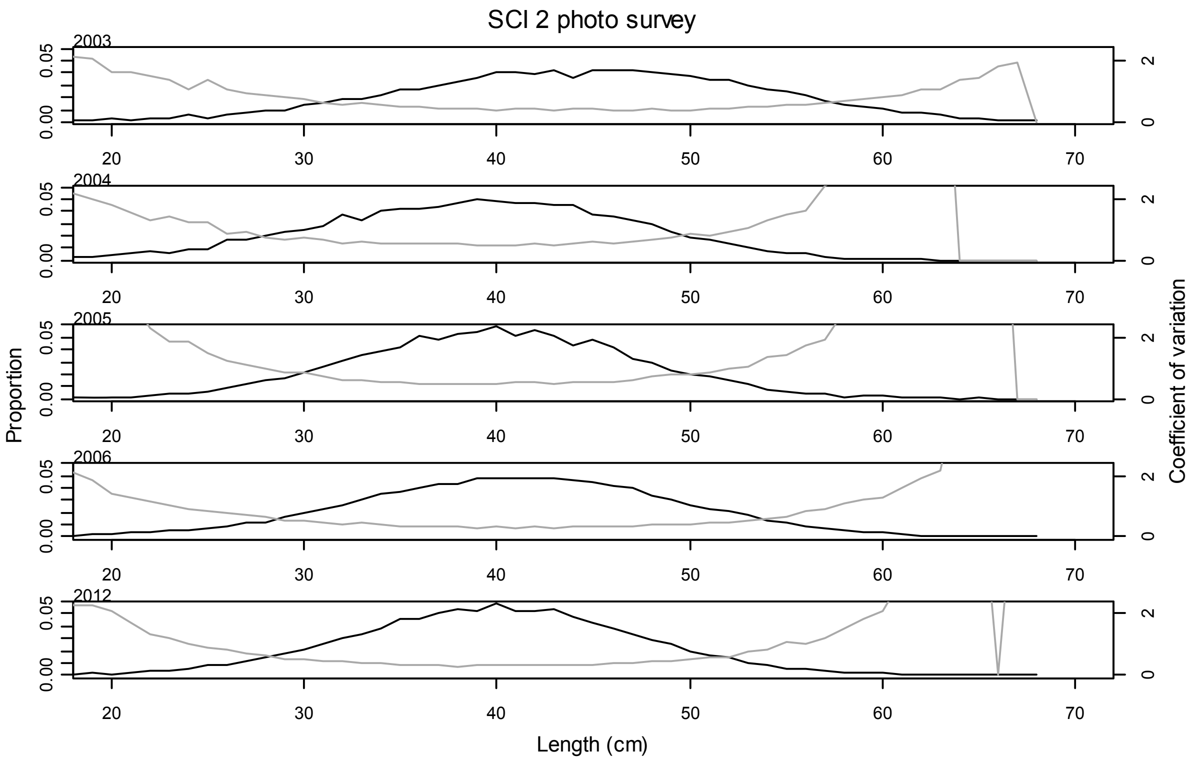

Figure 48: Proportional length frequencies and CVs for scampi responsible for burrows counted within photo survey for SCI 2.

3.7. Model assumptions and priors

Maximum Posterior Density (MPD) fits were found within CASAL using a quasi-Newton optimiser and the BETADIFF automatic differentiation package (Bull et al. 2008). Fitting was done inside the model except for the weighting of the abundance and length frequency data. For the length frequency data, observation-error CVs were estimated using CALA, converted to equivalent observation-error multinomial *N*s, and used within the model. The appropriate multinomial *N*s to account for both observation and process error were then calculated from the model residuals (method TA1.8), and these final *N*s were used in all models reported (Francis 2011). This generally resulted in small *N*s for the commercial length frequency data in particular, and therefore relatively low weighting within the model. For the CPUE indices, the approach proposed by Francis (2011) was initially investigated (estimating appropriate CVs by fitting a smoother to the index), but this led to high standard deviations in the normalised residuals, and so additional CV was added. Sensitivity analysis indicated that current stock status (% B_0) was not sensitive to CPUE weighting. CASAL was also used to run Monte-Carlo Markov Chains (MCMC) on the base models. MPD output was analysed using the extract and plot utilities in the CASAL library running under the general analytical package R.

The initial model was based on that described by Tuck & Dunn (2009, 2012). The model inputs include catch data, abundance indices (CPUE, trawl and photo surveys) and associated length frequency distributions. The parameters estimated by the base model include SSB_0 and R_0, and time series of SSB and year class strength, selectivity parameters for commercial and research trawling, and the photo survey, and associated catchability coefficients. To reduce the number of fitted parameters, the catchability coefficients (*q*'s) for commercial fishing, research trawling, and photographic surveys were assumed to be "nuisance" rather than free parameters. The only informative priors used in the initial model were for *q-Photo, q-Trawl*, the ratio of *q* values for *q-Photo* and *q-Trawl* for the whole and part areas of SCI 1, and the YCS vector (which constrains the variability of recruitment).

3.7.1. Scampi catchability

Previous priors for scampi catchability have been largely based on information on *Nephrops* emergence and occupancy rates from European studies conducted in far shallower waters than *Metanephrops* populations inhabit (Tuck & Dunn 2012), but the acoustic tagging study conducted at the Mernoo Bank in October 2010 offered an opportunity to estimate priors for occupancy and emergence from New Zealand data (Tuck 2013). Acoustic tagging was repeated within the SCI 1 and SCI 2 surveys, and the data collected within these studies have been used to estimate priors (Tuck et al. 2013).

Acoustic tags were fitted to scampi, and released with a moored hydrophone which recorded tag detections, when animals were emerged from burrows. Data were recorded over a period of up to 46 days for SCI 1, and 61 days for SCI 2 (Tuck et al. 2013). Tag detections showed distinct cyclical patterns (12.6 hour cycle), and the proportion of scampi detectable over the duration of the studies varied from 27 – 72% (2.5^{th} to 97.5^{th} percentile of range), with a median detection of 52% for SCI 1, and 66% for SCI 2. On the basis of shallow water trials with the acoustic tags, and scampi observations, it is assumed that these detections include scampi in burrow entrances and scampi walking free on the seabed (all of which would be visible to the photographic survey). Estimates of the density of major burrow openings, all visible scampi and scampi out of burrows are available from the surveys conducted in February / March 2012 in SCI 1 and SCI 2. An estimate of scampi density is provided by dividing the density of visible scampi by emergence.

Priors for three *q* terms have been estimated (Table 21). The *q_scampi* term (proportion of the scampi population represented by the count of visible scampi) is not used in these assessments, but is provided for completeness. The best estimate for each q term is based on the median estimate of emergence, while the upper and lower estimates are based on the 2.5th and 97.5th percentiles of the distribution of emergence values. The 2.5th, median and 97.5th percentiles of the estimated scampi density distribution are calculated by dividing the density of visible scampi by the emergence. This estimated density is used to calculate the priors.

3.7.2. Priors for *q*s

q-Photo

This is the proportion of the scampi population represented by the count of major burrow openings. The best estimate is 2.359 for SCI 1, and 3.483 for SCI 2 (major burrow openings divided by estimated scampi density). Upper and lower estimates are taken as the 2.5th and 97.5th percentiles of the distribution.

q-Trawl

This is the proportion of the scampi population represented by the trawl survey catches. The best estimate is 0.107 for SCI 1, and 0.07 for SCI 2 (scampi out of burrows divided by estimated scampi density). Upper and lower estimates are taken as the 2.5th and 97.5th percentiles of the distribution.

Ratio of *q*, part : whole survey (SCI 1)

As discussed above (Section 3.5), some surveys in SCI 1 have only covered four of the six survey strata that comprise the modelled area. These limited area surveys have been fitted as a separate index, with *q* constrained as a proportion of *q-Trawl* for the whole area survey, using the @ratio_qs_penalty command. The prior distribution for this ratio was estimated from the distribution of relative catch rates in the two areas by all scampi targeting commercial trips fishing in both areas, scaled by the relative size of the areas. The best estimate was that 80% of the biomass was within the limited survey area.

3.7.3. Estimation of prior distributions

The bounds and best estimate were assumed to represent the 2.5th, 50th and 97.5th percentiles of the prior distribution. These values were fitted within a binomial GLM (probit link) to estimate the slope and intercept of the cfd, which in turn were used to estimate the mean and standard deviation of the lognormal distribution of the prior. The distributions of the priors are presented for SCI 1 in Figure 49, and for SCI 2 in Figure 50. The distributions of the priors are somewhat tighter than those used in the previous assessment (Tuck & Dunn 2012), and the SFAWG has suggested further investigation into the estimation of these priors.

Table 21: Component factors for estimation of priors for q-Scampi, q-Photo, and q-Trawl.

	SCI 1			SCI 2			Source
	Lower	Best	Upper	Lower	Best	Upper	
Major opening	0.079	0.079	0.079	0.114	0.114	0.114	survey
Visible scampi	0.018	0.018	0.018	0.022	0.022	0.022	survey
Scampi "out"	0.004	0.004	0.004	0.002	0.002	0.002	survey
Scampi as % of openings		22%			19%		Visible/openings
% of scampi “out”		21%			11%		Out/visible
Emergence	27%	52%	72%	27%	66%	72%	Acoustic tags
Est scampi den	0.065	0.034	0.024	0.08	0.033	0.03	Visible/emergence
Est occupancy	82%	42%	31%	70%	29%	26%	Est den/major
q_Trawl	0.056	0.107	0.148	0.029	0.07	0.077	Out/Est den
q_scampi	0.27	0.52	0.72	0.27	0.66	0.72	Vis/Est den
q_photo	1.225	2.359	3.267	1.425	3.483	3.8	Major/Est den

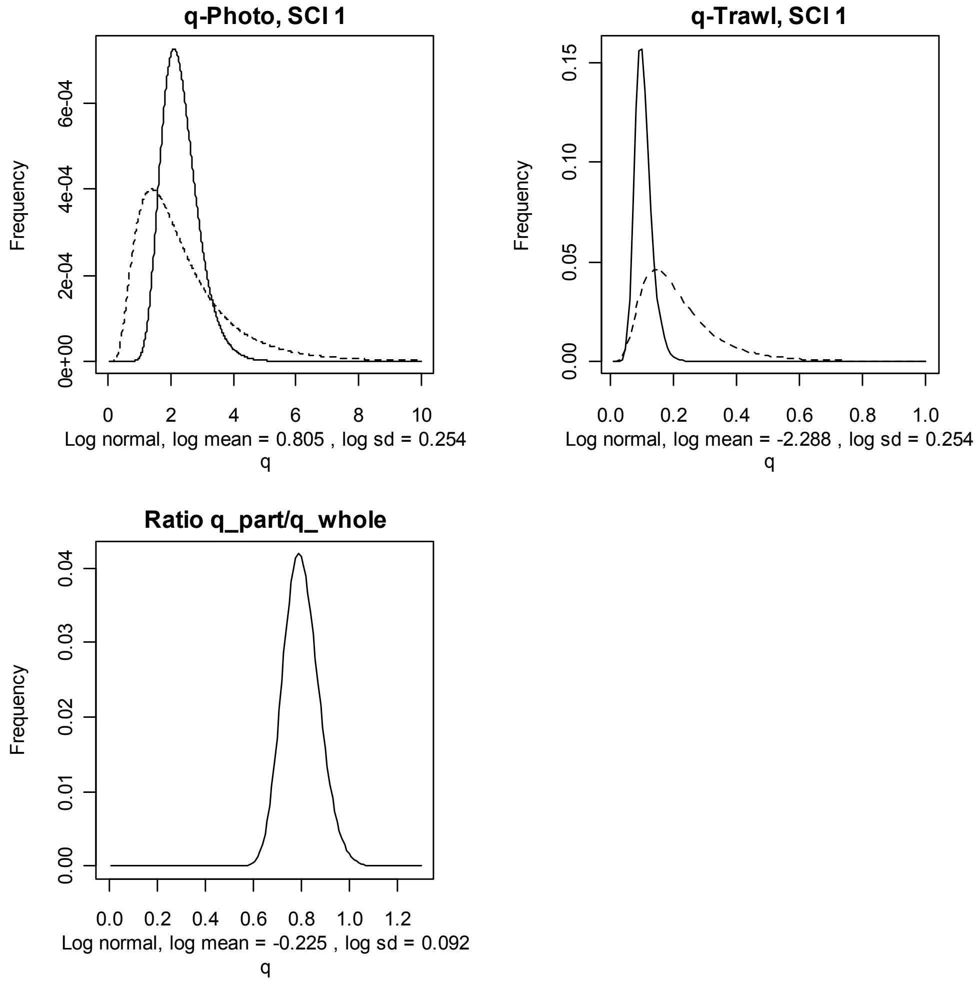

Figure 49: Estimated distribution of *q-Photo*, *q-Trawl*, and the ratio of q_part/q_whole for SCI 1. Dashed lines represent prior distributions used in previous assessment, based on a different estimation approach (Tuck & Dunn 2012).

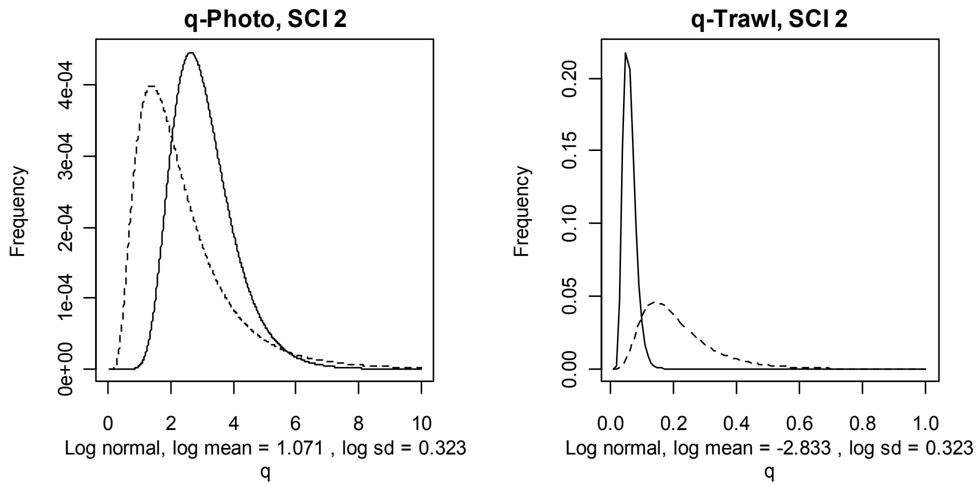

Figure 50: Estimated distribution of *q-Photo* and *q-Trawl* for SCI 2. Dashed lines represent prior distributions used in previous assessment, based on a different estimation approach (Tuck & Dunn 2012).

3.7.4. Recruitment

Few data are available on scampi recruitment. Relative year class strengths were assumed to average 1.0 up to the last two years, and are fixed at 1 for these. In the initial model development (Cryer et al. 2005) lognormal priors on relative year class strengths were assumed, with mean 1.0 and CV 0.2, and the sensitivity of year class strength (YCS) variation was examined in further developments (Tuck & Dunn 2006). More recent model investigations, particularly those fitting the CPUE indices, suggest that the constraint on variability in YCS may be too severe, and the SFAWG suggested increasing the CV (Tuck & Dunn 2012). In the current implementation, lognormal priors on relative year class strengths were assumed, with mean 1.0 and CV 1.0. The relationship between stock size and recruitment for scampi is unknown, and a Beverton Holt relationship with a steepness of 0.8 has been assumed. New Zealand scampi have very low fecundity (Wear 1976, Fenaughty 1989) (in the order of tens to hundreds of eggs carried by each female), so very successful recruitment is probably not plausible at low abundance. Recruitment enters the model partition as a year class, with a normally distributed OCL of mean 10 mm and CV 0.4.

4. SCI 1 - ASSESSMENT MODEL RESULTS

4.1. Initial models

As described in section 3.1, a single area model was applied, with an annual CPUE index, and the photo and trawl survey data both fitted as two separate indices, both in time step 1, but with different areas covered. Attempts to estimate natural mortality within the model were not considered reliable, and sensitivities to M, the shape of the commercial selectivity curve, and assumptions of equilibrium conditions at the start of the fishery, were examined. In addition, a model fitting to a simple trawl survey series only covering the consistently surveyed region was also examined (this sensitivity only being examined for SCI 1). Details of differences between models examined within sensitivity analyses are presented in Table 22. Key parameter and quantity estimates from the MPD fits for the models described in Table 23, and stock and recruitment trajectories for the models are presented in Figure 51.

Table 22: General details of models examined within sensitivity analyses for SCI 1.

Model	M	Commercial selectivity	Equilibrium conditions at start of fishery	Trawl survey indices
Base2	0.2	Logistic capped	Yes	Whole and Part region
Base3	0.3	Logistic capped	Yes	Whole and Part region
Base4	0.4	Logistic capped	Yes	Whole and Part region
BaseDome	0.3	Double normal capped	Yes	Whole and Part region
BaseBinit	0.3	Logistic capped	No	Whole and Part region
BaseTrawl	0.3	Logistic capped	Yes	Part region

Table 23: Estimated key parameters and quantities from MPD fits for SCI 1 sensitivity model runs.

	Base2	Base3	Base4	BaseDome	BaseBinit	BaseTrawl
M	0.2	0.3	0.4	0.3	0.3	0.3
SSB_0	4663	4779	7417	5638	5214	5797
SSB_{1986}	4663	4779	7417	5638	1875	5797
SSB_{2012}	3147	3459	5775	4106	3338	4306
SSB_{2012}/SSB_0	0.67	0.72	0.78	0.73	0.64	0.74
q-Photo	2.81	2.74	2.61	2.76	2.78	2.75
q-Trawl (whole area)	0.071	0.072	0.073	0.073	0.074	0.056
Ratio part:whole	0.71	0.76	0.78	0.73	0.76	-
Male g20	8.9	11.6	10.3	9.7	11.1	9.57
Male g40	1.65	2.25	2.17	2.07	2.19	1.98
Female g20	8.6	11.2	10.4	9.3	10.8	9.25
Female g40	0	0	0	0.16	0	0.05
Growth min_sigma	3.33	4.00	3.93	3.58	4.02	3.62

There was little difference between models in terms of fits to observed data. The different levels of natural mortality examined altered the magnitude of the estimated abundance increase and decline in the mid 1990s, but all models suggested biomass increased to the mid 1990s, declined to about 2000, remaining stable since that time. Domed selectivity improved the fits to the commercial length frequency data slightly, but neither this nor the BaseTrawl sensitivity differed significantly from the Base3 model. Relaxing the equilibrium assumption at the start of the fishery (BaseBinit) estimated a far lower biomass in 1986, but estimated a relatively smaller population decline in the late 1990s, and similar biomass estimates to the other models during the 2000s. Across the six models examined, estimates of SSB_0 varied from 4500 to 7500 tonnes, and although stock trajectories varied between models over the history of the fishery (Figure 51), the models were reasonably consistent in estimates of SSB_{2012}/SSB_0 (between 65 and 80% SSB_0). Patterns in YCS were very similar between the models, with all models estimating a large recruitment in the late 1980s, lower than average recruitment in the mid to late 1990s, and variable recruitment fluctuating about the long term average more recently.

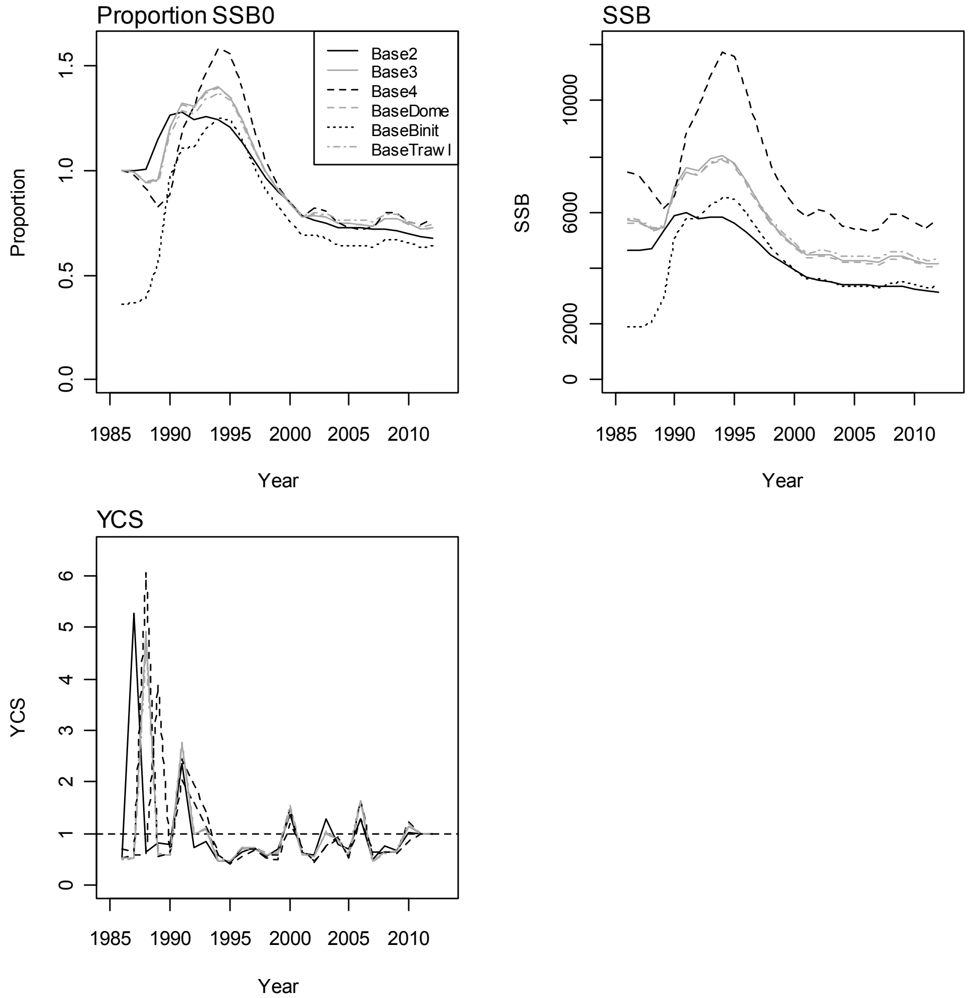

Figure 51: Plots of SSB as a proportion of SSB_0, SSB and year class strength (YCS) for MPD fits to the SCI 1 sensitivity model runs.

4.2. Comparison with 2011 assessment

As discussed above, the model structure applied here is a modification and simplification of that presented for the previous assessment of SCI 1 (Tuck & Dunn 2012), and data weighting approaches have also changed. In 2011, models 1C and 2C were accepted for SCI 1. Both models had M fixed at 0.2, but while model 1C was applied over a single area, model 2C was split into two spatial strata. Both models fitted separate CPUE and trawl survey indices for each time step and spatial components within the particular model.

None of the 2013 models included any spatial structure, and so no appropriate comparison can be made with model 2C. To enable appropriate comparison with model 1C, the Base2 model presented here was rerun with data truncated to 2010. Initial comparison with model 1C (equivalent model from Tuck & Dunn 2012) suggested a considerable discrepancy between the models, but when model 1C was revised using the same data weighting approach as the current models, stock trajectories were far more consistent (Figure 52). Although the overall level of biomass was lower in the revised 2011 model, stock status (SSB/SSB_0) followed a very similar pattern, particularly in more recent years. Catchability priors have also changed in the model since 2011 (Section 3.7.2), which may have contributed to the differences between the levels of absolute biomass estimated by the models.

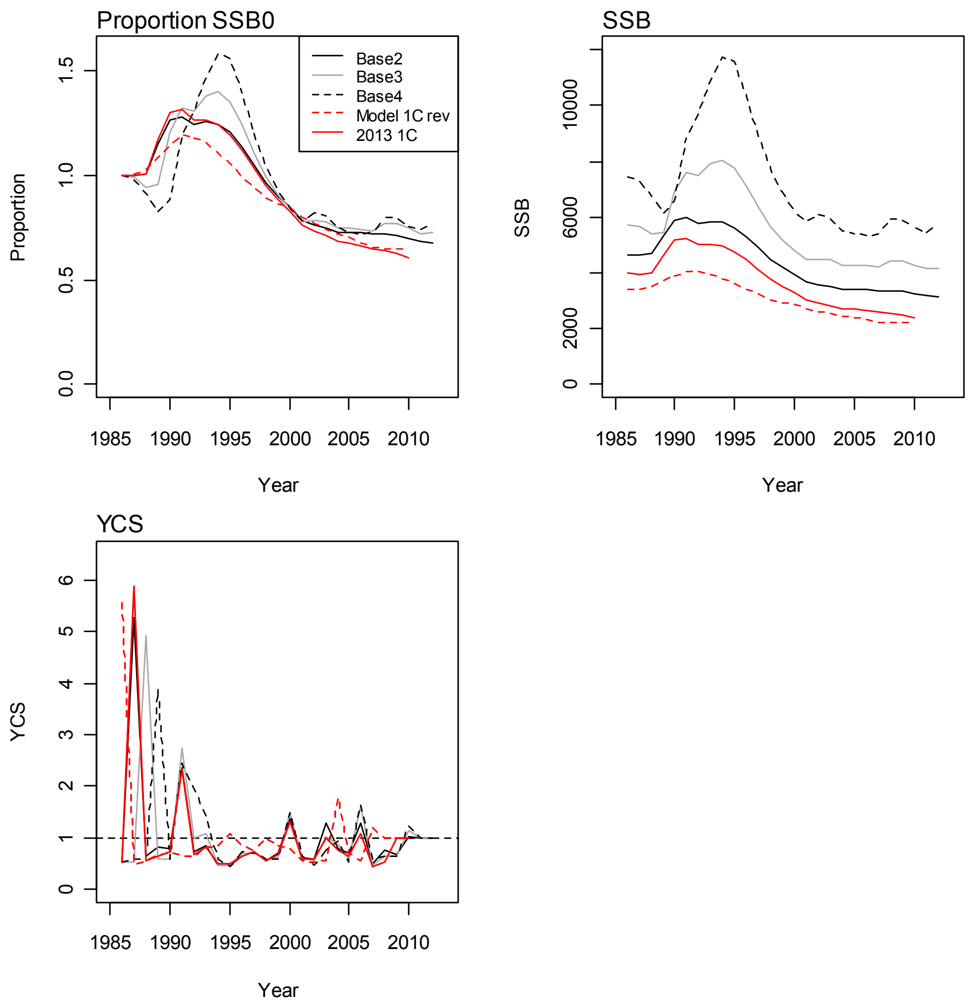

Figure 52: Plots of SSB as a proportion of SSB_0, SSB, and year class strength (YCS) for MPD fits for 2013 SCI 1 models (Base2, Base3 and Base4) for comparison with Base2 truncated to 2010 (2013 1C) and the previously accepted 2011 model 1C with updated data weighting (Model 1C rev).

4.3. Base models

On the basis of presentation of the sensitivity runs to the SFAWG, base models with M fixed at 0.2 and 0.3 were examined further. Various model output plots and diagnostics are presented as an Appendix for each model.

4.3.1. SCI 1 Base2 (Appendix 4)

The Base2 model (M = 0.2) estimated a SSB_0 of 4663 t, with SSB_{2012} 3147 t, 67% of SSB_0. Fits to the abundance indices and normalised residuals (A4. 1), show that the model did not match the observed increase and decline in CPUE in the mid 1990s, but fits to the trawl and photographic surveys (particularly over more recent years) were better. SSB is estimated to have increased in the late 1980s, remained relatively stable until 1995, declined through the later 1990s until about 2003, and then remained more stable (A4. 2). Strong year class strengths were estimated in 1986 and 1990 (to a lesser extent), with a period of below average recruitment until 1988, followed by a period with recruitment fluctuating around the long term average. Estimated selectivity curves matched observed changes in sex ratio between time steps, with males less available to trawling during time step 2. The L_{50} parameters for time step 2 (A4. 3) appear unrealistically large, but were the best fit to the limited sampling from this period. These parameters did not affect the perception of stock status (since the model simply estimated the required catchability to generate observed catches), but did need to be fixed at more appropriate values (from step 1) for estimation of equivalent annual F reference points. MPD estimates of trawl and photo survey catchability were within the prior distribution, as were the part:whole survey area ratios (A4. 4). Fits to the observer length frequencies were variable (A4. 5 – A4. 7), with the data weighting generally giving observer length frequency samples low effective sample size (A4. 8 – A4. 10), while fits to the trawl survey length frequencies were generally better (A4. 13), and effective sample size larger (A4. 14). The model appeared to consistently underestimate the proportion of larger scampi in the photo survey length frequencies (A4. 18).

The likelihood profile when B_0 is fixed shows a minimum at just under 5000 t (A4. 19), although it is relatively flat in this region of the curve. The data do not provide any consistent signal. The CPUE abundance index suggested a smaller SSB_0, while the proportions at length and catchability priors provided conflicting signals for the photo and trawl surveys. The other data sets appeared to provide little information on SSB_0.

MCMC runs

Three independent MCMC chains were started a random step away from the MPD for each model, and run for 4 million simulations, with every two thousandth sample saved, giving a set of 2000 samples. The three chains were examined for evidence of lack of convergence (A4. 20 – A4. 21), and concatenated and systematically thinned to produce a 2000 sample chain for projections. Posterior distributions of trawl and photo survey catchability were within the prior distribution (A4. 22), with the MPD estimates also located within the posterior distributions. The posterior trajectory of SSB (Figure 53) suggests a decline from about 1994 to about 2002, with the stock remaining stable after this. The median estimate of current status (SSB_{2012}/SSB_0) is 68%, with 0% probability that SSB_{2012} is below 40% SSB_0.

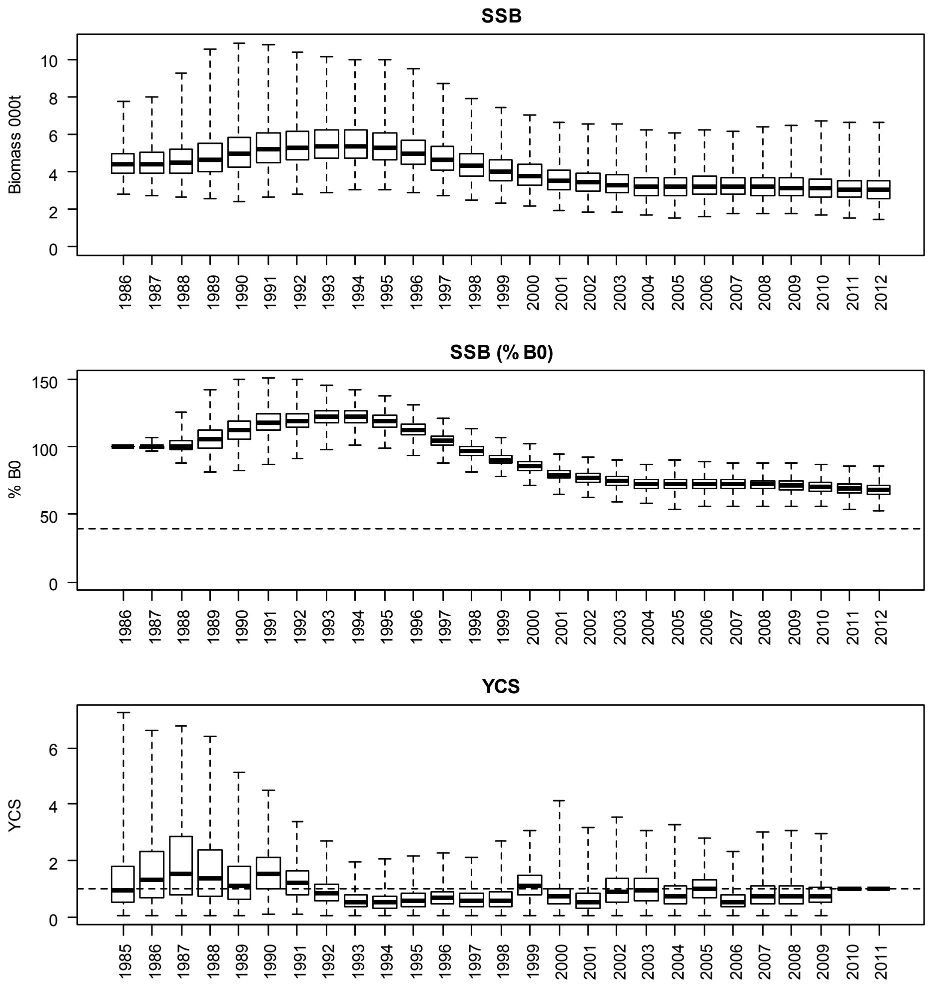

Figure 53: Posterior trajectory of SSB, SSB_{2012}/B_0 and YCS of MCMC run for SCI 1 Base2 model.

4.3.2. SCI 1 Base3 (Appendix 5)

The Base3 model (M = 0.3) estimated a SSB_0 at 4779 t, with SSB_{2012} 3459 t, 72% of SSB_0. Fits to the abundance indices and normalised residuals (A5. 1), show that the model fitted the observed increase and decline in CPUE in the mid 1990s slightly better than the Base2 model, and fits to the trawl and photographic surveys (particularly over more recent years) were reasonable. SSB is estimated to have increased from 1991 to 1995, declined through the later 1990s until about 2001, and then remained more stable (A5. 2). Strong year class strengths were estimated in 1988 and 1990/91 (to a lesser extent), with a period of below average recruitment around the mid 1990s, followed by a period with recruitment fluctuating around the long term average. Estimated selectivity curves were similar to those for the Base2 model, in that they matched observed changes in sex ratio between time steps, but also the estimates for the L_{50} parameters for time step 2 were unrealistically large. MPD estimates of trawl and photo survey catchability were within the prior distribution, as were the part:whole survey area ratios (A5. 4). Fits to the observer length frequencies were variable (A5. 5 – A5. 7), with the data weighting giving observer length frequency samples low effective sample size (A5. 8 – A5. 10), while fits to the trawl survey length frequencies were better (A5. 13), and effective sample size larger (A5. 14). As with the base2 model, the base3 model consistently underestimated the proportion of larger scampi in the photo survey length frequencies (A5. 18).

The likelihood profile when B_0 is fixed shows a minimum at just under 5000 t (A5. 19), although it is relatively flat in this region of the curve. The data do not provide any consistent signal. The CPUE abundance index suggested a smaller SSB_0, while the proportions at length and catchability priors provided conflicting signals for the photo and trawl surveys. CPUE and proportions at length appeared to have a greater influence than the priors.

MCMC runs

Three independent MCMC chains were started a random step away from the MPD for each model, and run for 4 million simulations, with every two thousandth sample saved, giving a set of 2000 samples. The three chains were examined for evidence of lack of convergence (A5. 20 – A5. 21), and concatenated and systematically thinned to produce a 2000 sample chain for projections. While there was some evidence that the SSB_0 and SSB_{2012} traces from the three chains had slightly different distributions, the SSB_{2012}/SSB_0 traces were consistent, and the medians of all three parameters were reasonably consistent. Posterior distributions of trawl and photo survey catchability were within the prior distribution (A5. 22), with the MPD estimates also located within the posterior distributions. The posterior trajectory of SSB (Figure 54) suggests a decline from about 1994 to about 2001, with the stock remaining stable after this. The median estimate of current status (SSB_{2012}/SSB_0) is 72%, with 0% probability that SSB_{2012} is below 40% SSB_0.

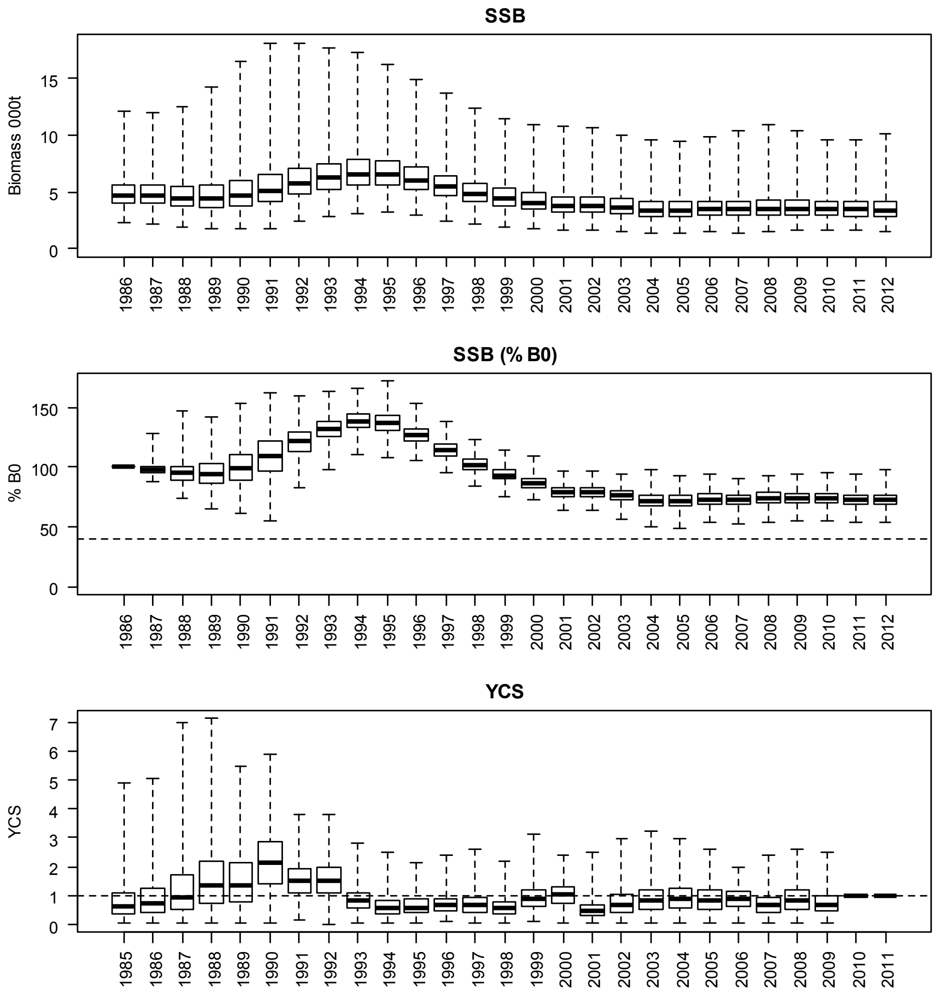

Figure 54: Posterior trajectory of SSB, SSB_{2012}/B_0 and YCS of MCMC run for SCI 1 Base3 model.

4.3.1. SCI 1 Fishing pressure

Annual fishing intensity (equivalent annual F) and the level of fishing that, if applied forever, would result in an equilibrium biomass of 40% SSB_0 (F 40% B_0) were calculated using methods described by

Cordue (2012). Plots of annual fishing intensity against proportion SSB_0 for both models (Figure 55 and Figure 56) show that although SSB has declined with the development of the fishery, it remains well above the 40% SSB_0 target, and annual fishing intensity remains well below F 40% B_0.

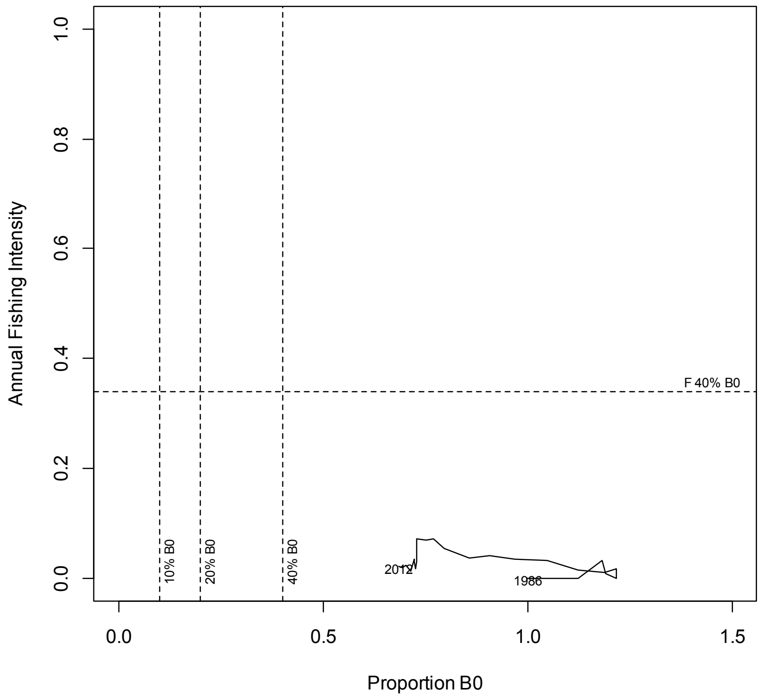

Figure 55: Trajectory of annual fishing intensity (equivalent annual F) plotted against proportion SSB_0 for the SCI 1 Base2 model, in relation to Harvest Strategy Standard target and limit reference points.

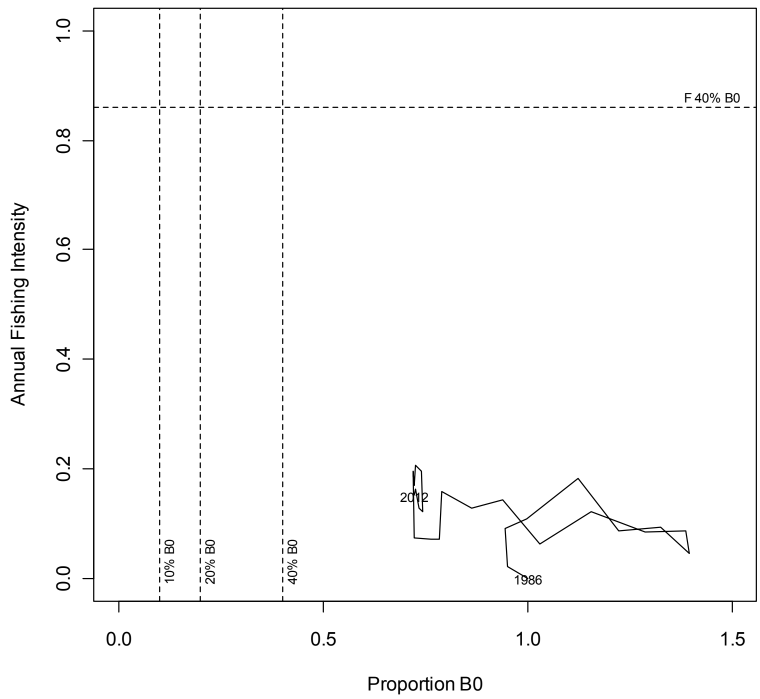

Figure 56: Trajectory of annual fishing intensity (equivalent annual F) plotted against proportion SSB_0 for the SCI 1 Base3 model, in relation to Harvest Strategy Standard target and limit reference points.

4.3.2. SCI 1 Projections

The assessments reported SSB_0 and $SSB_{current}$ and used the ratio of current and projected SSB to SSB_0 as preferred indicators. Projections were conducted up to 2018 on the basis of a range of catch scenarios (slightly above and below the current TACC of 120 t) (Table 24). Projections have been conducted randomly resampling year class strengths from the last decade of YCS estimated within the model (2000 – 2009). The probability of exceeding the default Harvest Strategy Standard target and limit reference points are reported (Table 25).

For both models presented (M=0.2 and M=0.3), future catches between 100 and 140 tonnes are predicted to reduce the SSB relative to SSB_{2012}, but remain above 40% SSB_0 (the most pessimistic prediction giving a 98% probability of SSB exceeding 40% SSB_0 by 2018).

Table 24: Results from MCMC runs showing B_0, B_{curr} B_{2016} and B_{2018} estimates at varying catch levels for SCI 1.

	Model	**M=0.2**	**M=0.3**
	B_0	4444	4681
	B_{curr}	3003	3294
	B_{curr}/B_0	0.68	0.71
100 tonnes	B_{2016}/B_0	0.66	0.71
	B_{2016}/B_{curr}	0.97	1.00
	B_{2018}/B_0	0.65	0.71
	B_{2018}/B_{curr}	0.97	1.00
110 tonnes	B_{2016}/B_0	0.65	0.70
	B_{2016}/B_{curr}	0.96	0.99
	B_{2018}/B_0	0.64	0.70
	B_{2018}/B_{curr}	0.95	0.98
120 tonnes (TACC)	B_{2016}/B_0	0.65	0.70
	B_{2016}/B_{curr}	0.96	0.98
	B_{2018}/B_0	0.64	0.70
	B_{2018}/B_{curr}	0.95	0.97
130 tonnes	B_{2016}/B_0	0.64	0.68
	B_{2016}/B_{curr}	0.95	0.96
	B_{2018}/B_0	0.63	0.68
	B_{2018}/B_{curr}	0.93	0.96
140 tonnes	B_{2016}/B_0	0.63	0.69
	B_{2016}/B_{curr}	0.93	0.97
	B_{2018}/B_0	0.62	0.68
	B_{2018}/B_{curr}	0.91	0.96

Table 25: Results from MCMC runs for SCI 1, showing probabilities of projected spawning stock biomass exceeding the default Harvest Strategy Standard target and limit reference points.

	100 tonnes	110 tonnes	120 tonnes (TACC)	130 tonnes	140 tonnes
M=0.2					
2016					
P(SSB<10% B0)	0.00	0.00	0.00	0.00	0.00
P(SSB<20% B0)	0.00	0.00	0.00	0.00	0.00
P(SSB>40% B0)	1.00	1.00	1.00	1.00	1.00
P(B2016 < B2012)	0.60	0.63	0.65	0.69	0.72
2018					
P(SSB<10% B0)	0.00	0.00	0.00	0.00	0.00
P(SSB<20% B0)	0.00	0.00	0.00	0.00	0.00
P(SSB>40% B0)	1.00	0.99	0.98	0.98	0.98
P(B2018 < B2012)	0.59	0.63	0.64	0.69	0.74
M=0.3					
2016					
P(SSB<10% B0)	0.00	0.00	0.00	0.00	0.00
P(SSB<20% B0)	0.00	0.00	0.00	0.00	0.00
P(SSB>40% B0)	1.00	1.00	0.99	0.99	0.99
P(B2016 < B2012)	0.49	0.54	0.54	0.59	0.58
2018					
P(SSB<10% B0)	0.00	0.00	0.00	0.00	0.00
P(SSB<20% B0)	0.00	0.00	0.00	0.00	0.00
P(SSB>40% B0)	0.99	0.99	0.99	0.99	0.98
P(B2018 < B2012)	0.51	0.54	0.55	0.59	0.59

4.3.3. Data weighting sensitivity

Within the base case model development the Francis (2011) approved approach (estimating appropriate CV by fitting smoother to CPUE) was initially applied, but led to high standard deviations of normalised residuals, and so additional CV was added to the CPUE datasets. Following presentation of the SCI 1 models to the MPI Plenary, further investigations were undertaken for the M=0.3 model giving more weight (lower CV) to the CPUE index. Commercial selectivity was constrained in time step 2 as discussed above, to allow estimation of reference F values. Following Francis (2011), lowess smoother fits to the CPUE index (Figure 57) were examined by eye, with the 0.4 smoother selected, giving a CV of 0.17 for the dataset. As with the previous models, process error of 0.2 was added to trawl and photographic surveys, and length frequency data were reweighted iteratively using method TA1.8 (Francis 2011).

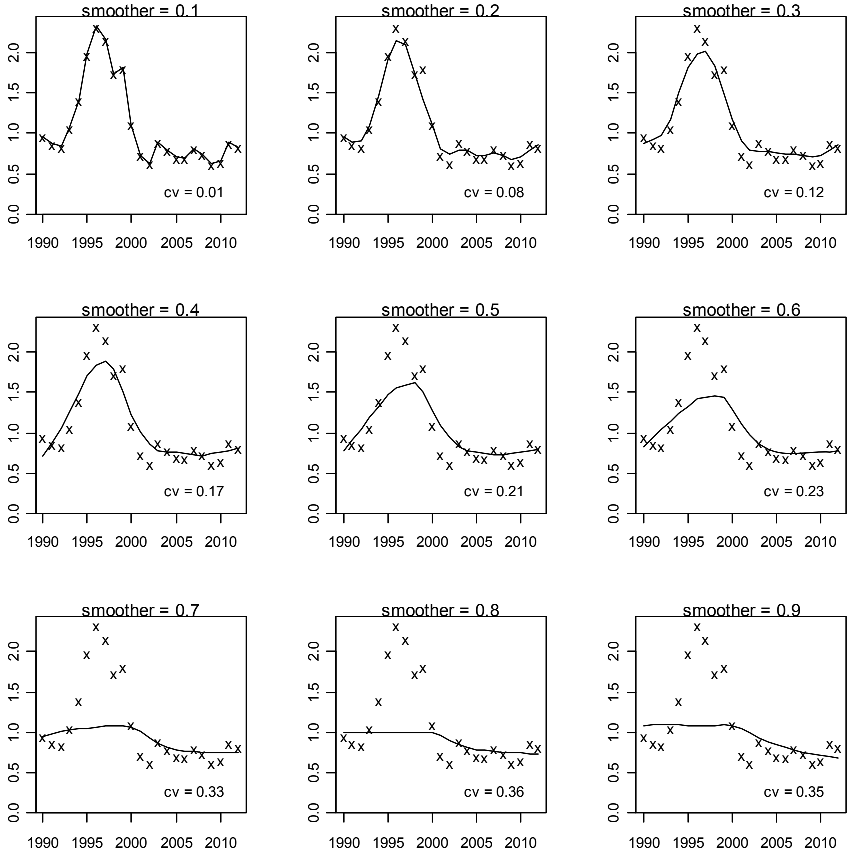

Figure 57: Lowess smoother fits to SCI 1 CPUE index for different smoother spans (proportion of points in the plot which influence the smooth at each value), and CV for lognormal error model given observed and smoother fitted values.

Fits to the abundance indices had higher standard deviations of normalised residuals than the base models, but the estimated CPUE index was better able to match the increase observed in the late 1990s than the base model. The three MCMC chains were consistent, and while the MCMC stock trajectory during the 1990s differed from the Base3 model (reweighted model showing the increase in biomass occurring later, and reaching a higher level relative to SSB_0), SSB_0, SSB_{2012} and therefore SSB_{2012}/SSB_0 were similar to the Base3 model (Figure 58). Projections conducted on the basis of this revised model (not presented) were very similar to those for the Base3 model.

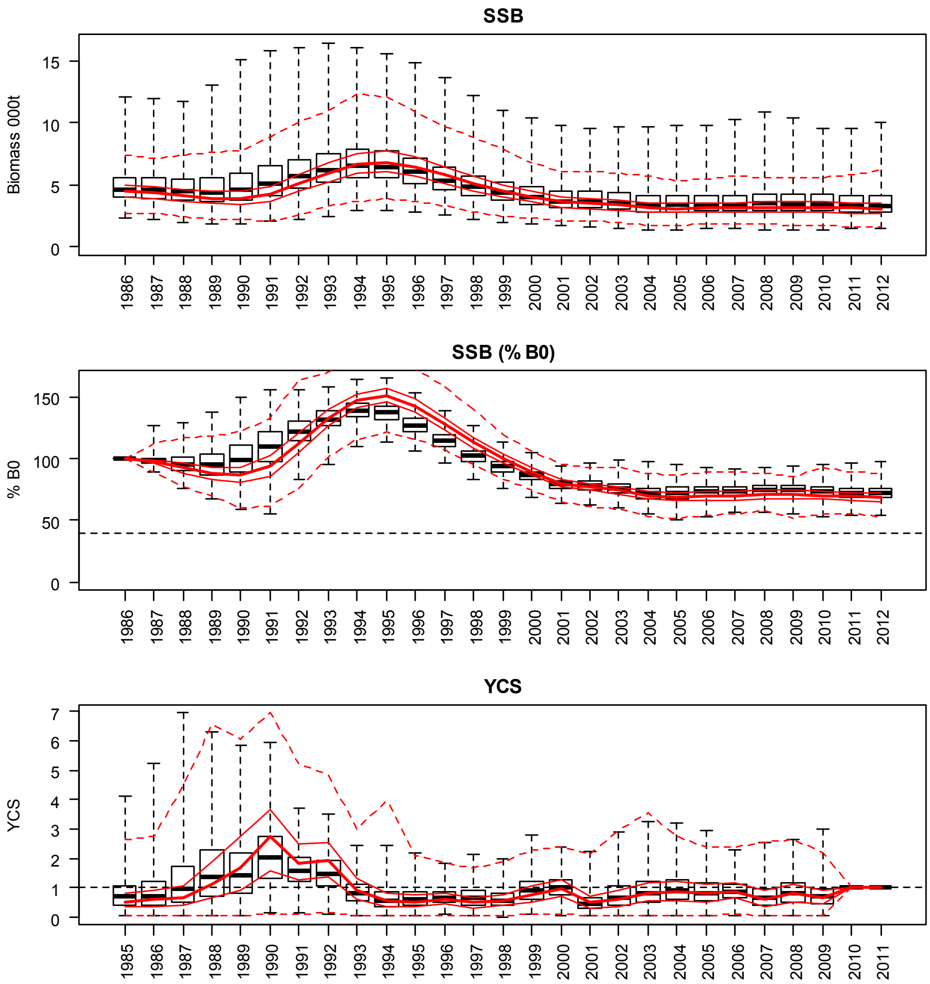

Figure 58: Posterior trajectory of SSB, SSB_{2012}/B_0 and YCS of MCMC run for SCI 1 Base3 model (black boxplots), and reweighted (CPUE CV 0.17) model (median - thick red line, quartiles - thin red line, adjacent values – red dashed line).

5. SCI 2 - ASSESSMENT MODEL RESULTS

5.1. Initial models

As described in Section 3.1, a single area model was applied, with an annual CPUE index, and the trawl survey data fitted as two separate indices in different time steps. Attempts to estimate natural mortality within the model were not considered reliable, and sensitivities to M, the shape of the commercial selectivity curve, and assumptions of equilibrium conditions at the start of the fishery, were examined. Details of differences between models examined within sensitivity analysis are presented in Table 26. Key parameter and quantity estimates from the MPD fits for the models described in Table 27, and stock and recruitment trajectories for the models are presented in Figure 59.

Table 26: General details of models examined within sensitivity analyses for SCI 2.

Model	M	Commercial selectivity	Equilibrium conditions at start of fishery
Base2	0.2	Logistic capped	Yes
Base3	0.3	Logistic capped	Yes
Base4	0.4	Logistic capped	Yes
BaseDome	0.3	Double normal capped	Yes
BaseBinit	0.3	Logistic capped	No

Trajectories of SSB/SSB_0, SSB and year class strength were reasonably consistent between the five models (Figure 59, Table 27). All models suggested an increase in SSB during the early 1990s, followed by a decline to about 2003, and an increase in more recent years, and SSB_{2012} between 60 and 86% SSB_0. There were some differences between models (e.g., model with higher M estimated faster growth), but generally little difference in the fits. The model allowing non-equilibrium conditions at the start of the fishery (BaseBinit) estimated that the stock was at about 60% SSB_0 in the mid 1980s, but estimated a similar SSB_{2012}/SSB_0 to the other models. Domed selectivity in the commercial fishery improved the fits to the observer length frequency data slightly, but did not affect our perception of the state of the stock. The pattern in the year class strengths was generally very consistent. The Base4 model estimated faster growth, and peaks in recruitment for this model were one year after the other models, since less time was required for the individuals to appear in the fishery. All models estimated a very large recruitment in the late 1990s, and higher than average recruitment in some of the most recent years estimated.

Table 27: Estimated key parameters and quantities from MPD fits for SCI 2 sensitivity model runs.

	Base2	Base3	Base4	BaseDome	BaseBinit
M	0.2	0.3	0.4	0.3	0.3
SSB_0	2664	2657	2295	2579	2268
SSB_{1986}					1334
SSB_{2012}	1612	1879	1970	1796	1425
SSB_{2012}/SSB_0	0.61	0.71	0.86	0.7	0.63
q-Photo	3.18	3.11	3.80	3.19	3.77
q-Trawl[*]	0.056	0.050	0.059	0.051	0.063
Male g20	10.36	10.44	12.20	10.46	10.78
Male g40	2.61	3.29	4.28	3.36	3.52
Female g20	11.63	11.38	12.79	11.34	10.76
Female g40	0.69	1.26	1.85	1.35	1.86
Growth min_sigma	3.58	3.49	3.63	3.43	3.36

*- *q-Trawl* for time step 1

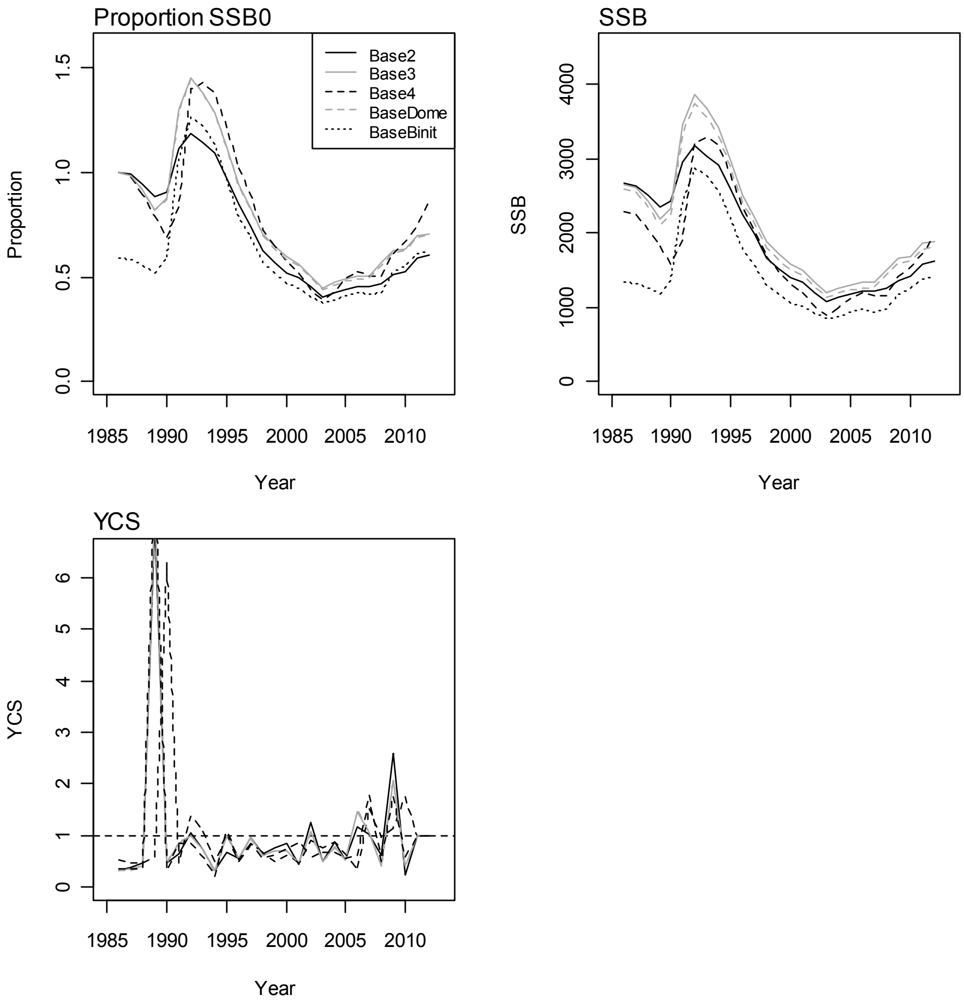

Figure 59: Plots of SSB as a proportion of SSB_0, SSB, and year class strength (YCS) for MPD fits to the SCI 2 sensitivity model runs.

5.2. Comparison with 2011 assessment

The previous assessment for SCI 2 suggested that SSB_{2010} was about 40% SSB_0. The range of current models provide a far more optimistic synopsis for the stock. As with the SCI 1 model, there have been a number of changes in model structure since the last assessment. In 2011, model 4C was accepted for SCI 2 (Tuck & Dunn 2012). This model had M fixed at 0.2, and was applied over a single area, but fitted separate CPUE indices for each time step, and trawl indices in steps 1 and 2.

In order to investigate whether the change in model structure has changed our perception of stock status, a comparable model to the 2011 assessment has been developed using the revised model structure, truncating data to 2010. Trajectories of SSB/SSB_0, SSB and year class strength for model 4C, and the equivalent new model (2013 4C) are very similar, with differences in the extent to which the biomass increases in the early 1990s likely to be related to differences in the data (particularly CPUE) weighting, but the estimates of SSB_{2010} and SSB_{2010}/SSB_0 being very similar between models (Figure 60). The models which run to 2012 show a longer term increase in biomass, which appears to be driven by better than average recruitment in 2006 and 2009. In the models with data truncated to 2010, recruitment in 2009 was not estimated (fixed at 1), and recruitment in 2006 was estimated to be below average.

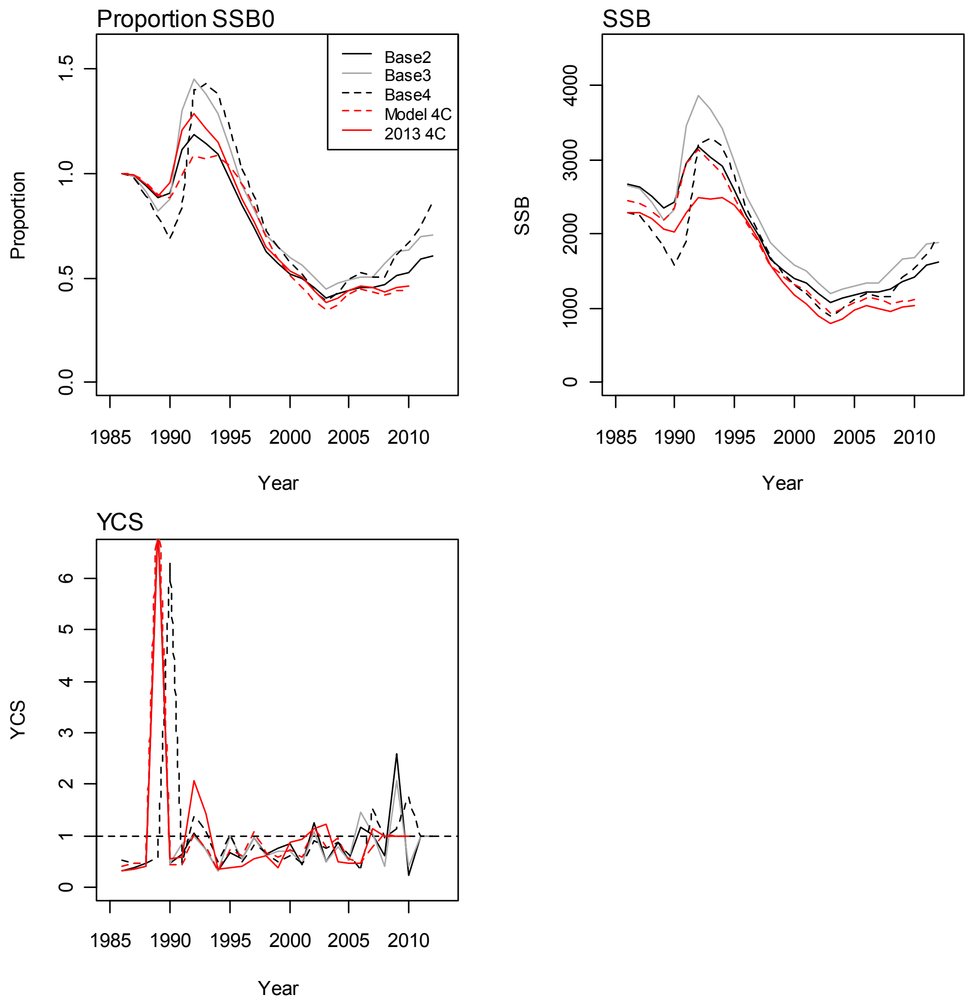

Figure 60: Plots of SSB as a proportion of SSB_0, SSB, and year class strength (YCS) for MPD fits for 2013 SCI 2 models (Base2, Base3 and Base4) for comparison with Base2 truncated to 2010 (2013 4C) and the previously accepted 2011 model (Model 4C).

5.3. Base models

On the basis of presentation of the sensitivity runs to the SFAWG, base models with M fixed at 0.2 and 0.3 were examined further. Various model output plots and diagnostics are presented as an Appendix for each model.

5.3.1. SCI 2 Base2 (Appendix 6)

The Base2 model (M = 0.2) estimated a SSB_0 at 2664 t, with SSB_{2012} 1612 t, 61% of SSB_0. Fits to the abundance indices and normalised residuals (A6. 1), show that the model was not quite able to match the timing of the observed increase and decline in CPUE in the mid 1990s, and while fits to the time step 1 trawl survey and photographic surveys were good, the model did not replicate the increase in biomass observed in the 2012 trawl survey (time step 2). SSB is estimated to have increased in the early 1990s, peaking around 1992, declining steadily until 2003, and then increasing since then (A6. 2). A strong year class strength was estimated in 1988, with an above average recruitment in 2008. Estimated selectivity curves matched observed changes in sex ratio between time steps, with males less available to trawling during time step 2 (A6. 3). MPD estimates of trawl and photo survey catchability were within the prior distribution (A6. 4). Fits to the observer length frequencies were variable (A6. 5 – A6. 7), with the data weighting generally giving observer length frequency samples low effective sample size (A6. 8 – A6. 10), while as with the SCI 1 assessments, fits to the trawl survey length frequencies were generally better (A6. 13), and effective sample size larger (A6. 14). Fits to the proportion at length from the photographic survey were also good (A6. 18).

The likelihood profile when B_0 is fixed shows a minimum at just over 2600 t (A6. 19), with a clear minimum identified in the curve. The data appear to be very consistent in their signal, particularly the trawl survey and CPUE abundance indices.

MCMC runs

Three independent MCMC chains were started a random step away from the MPD for each model, and run for 4 million simulations, with every two thousandth sample saved, giving a set of 2000 samples. The three chains were examined for evidence of lack of convergence (A6. 20 – A6. 21), and concatenated and systematically thinned to produce a 2000 sample chain for projections. There was slight divergence between the chains for SSB_0 and SSB_{2012}, but SSB_{2012}/SSB_0 was very consistent. Posterior distributions of trawl and photo survey catchability were within the prior distribution (A6. 22), with the MPD estimates also located within the posterior distributions. The posterior trajectory of SSB (Figure 61) suggests a decline from about 1992 to about 2003, with the stock remaining stable until about 2008, and increasing after this. The median estimate of current status (SSB_{2012}/SSB_0) is 63%, with 0% probability that SSB_{2012} is below 40% SSB_0.

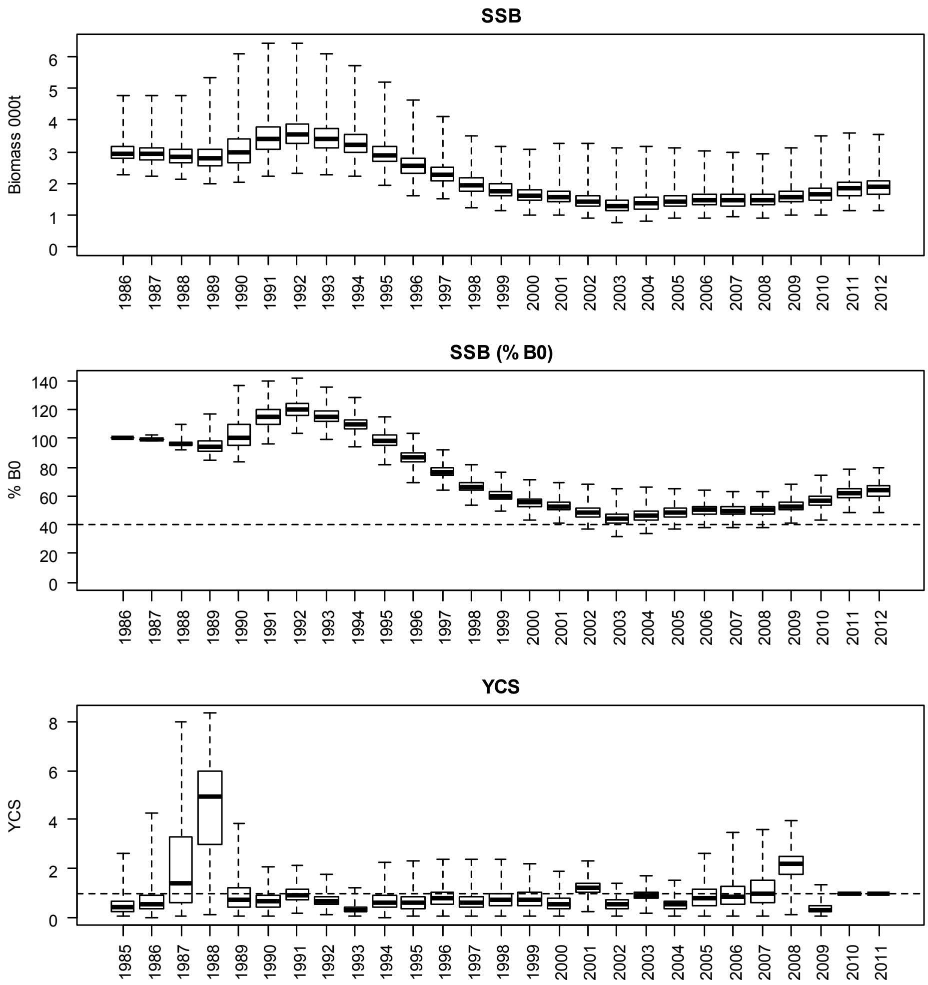

Figure 61: Posterior trajectory of SSB, SSB_{2012}/B_0 and YCS of MCMC run for SCI 2 Base2 model.

5.3.2. SCI 2 Base3 (Appendix 7)

The Base3 model (M = 0.3) estimated a SSB_0 at 2657 t, with SSB_{2012} 1879 t, 71% of SSB_0. Fits to the abundance indices and normalised residuals (A7. 1) were very similar to those for the Base2 model (A6. 1), and show the same pattern that the model was not quite able to match the timing of the observed increase and decline in CPUE in the mid 1990s, and the model appears to underestimate the biomass observed in the 2012 trawl survey (time step 2). SSB is estimated to have increased rapidly in the early 1990s, peaking around 1992, declining steadily until 2003, and then increasing since then (A7. 2). A strong year class strength was estimated in 1988, with an above average recruitment in 2008. Estimated selectivity curves were very similar to those for the Base2 model, and matched observed changes in sex ratio between time steps, with males less available to trawling during time step 2 (A7. 3). MPD estimates of trawl and photo survey catchability were within the prior distribution (A7. 4). Fits to the observer length frequencies were variable (A7. 5 – A7. 7), with the data weighting generally giving observer length frequency samples low effective sample size (A7. 8 – A7. 10), while fits to the trawl survey length frequencies were generally better (A7. 13), and effective sample size larger (A7. 14), and fits to the proportion at length from the photographic survey were good (A6. 18).

The likelihood profile when B_0 is fixed shows a minimum at just over 2600 t (A7. 19), with a clear minimum identified in the curve. As with the Base2 model, the data appear to be very consistent in their signal, particularly the trawl survey and CPUE abundance indices.

MCMC runs

Three independent MCMC chains were started a random step away from the MPD for each model, and run for 4 million simulations, with every two thousandth sample saved, giving a set of 2000 samples. The three chains were examined for evidence of lack of convergence (A7. 20 – A7. 21), and concatenated and systematically thinned to produce a 2000 sample chain for projections. The three MCMC chains were very consistent. Posterior distributions of trawl and photo survey catchability were within the prior distribution (A7. 22), with the MPD estimates also located within the posterior distributions. The posterior trajectory of SSB (Figure 62) suggests a decline from about 1992 to about 2003, with the stock increasing slightly until about 2008, with a more marked increase after this. The median estimate of current status (SSB_{2012}/SSB_0) is 74%, with 0% probability that SSB_{2012} is below 40% SSB_0.

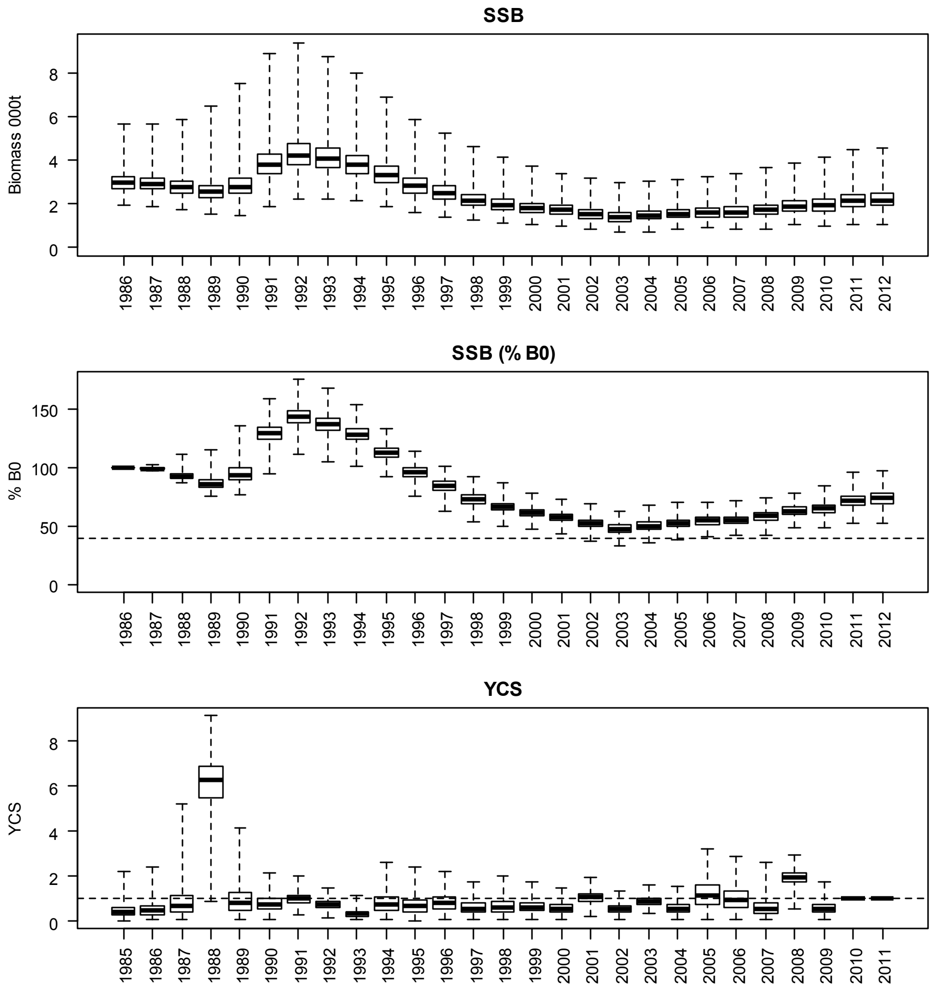

Figure 62: Posterior trajectory of SSB, SSB_{2012}/B_0 and YCS of MCMC run for SCI 2 Base3 model.

5.3.3. SCI 2 Fishing pressure

Annual fishing intensity (equivalent annual F) and the level of fishing that, if applied forever, would result in an equilibrium biomass of 40% SSB_0 (F 40% B_0) were calculated using methods described by Cordue (2012). Plots of annual fishing intensity against proportion SSB_0 for both models (Figure 63 and Figure 64) show that although SSB declined to a level close to the 40% SSB_0 target in the early 2000s, following the peak in fishing intensity observed in 2002 (which exceeded the F 40% B_0 for the

Base2 model), it has increased in more recent years, and is currently well above the 40% SSB_0 target, with annual fishing intensity well below F 40% B_0.

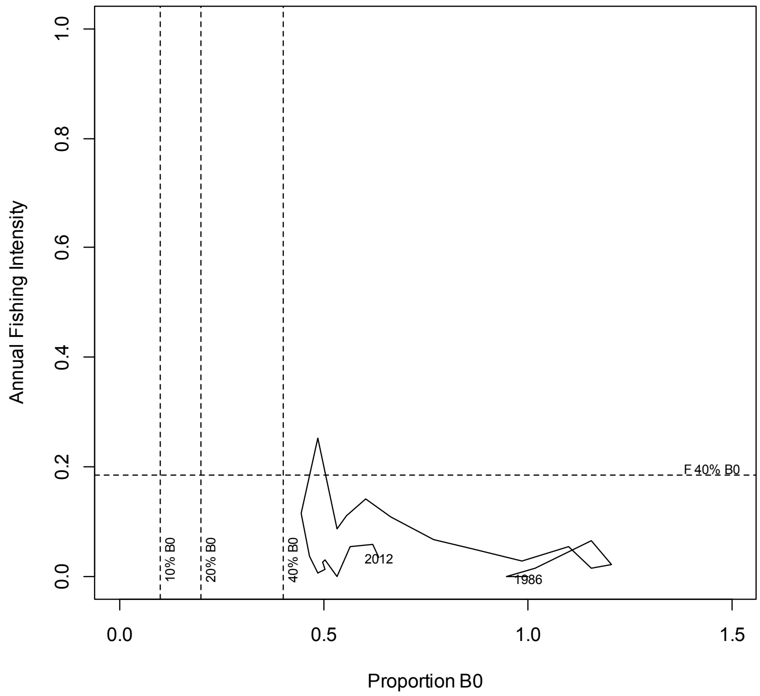

Figure 63: Trajectory of annual fishing intensity (equivalent annual F) plotted against proportion SSB_0 for the SCI 2 Base2 model, in relation to Harvest Strategy Standard target and limit reference points.

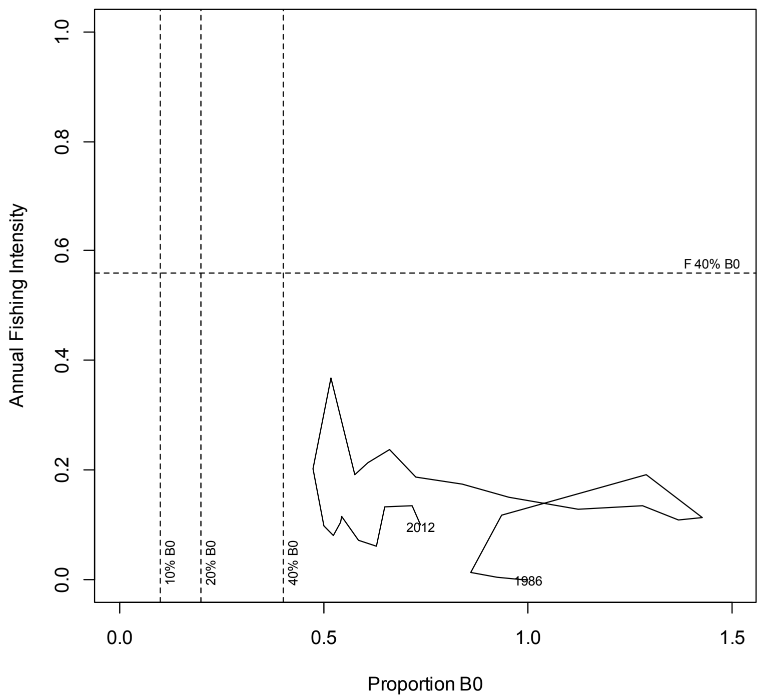

Figure 64: Trajectory of annual fishing intensity (equivalent annual F) plotted against proportion SSB_0 for the SCI 2 Base3 model, in relation to Harvest Strategy Standard target and limit reference points.

5.3.4. SCI 2 Projections

The assessments reported SSB_0 and $SSB_{current}$ and used the ratio of current and projected SSB to SSB_0 as preferred indicators. Projections were conducted up to 2018 on the basis of a range of catch scenarios (at and above the current TACC of 100 t) (Table 28). Projections have been conducted randomly resampling year class strengths from the last decade of YCS estimated within the model (2000 – 2009). The probability of exceeding the default Harvest Strategy Standard target and limit reference points are reported (Table 29).

For both models presented (M=0.2 and M=0.3), future catches between 100 and 140 tonnes are predicted to reduce the SSB relative to SSB_{2012}, but remain above 40% SSB_0 (the most pessimistic prediction giving a 92% probability of SSB exceeding 40% SSB_0 by 2018).

Table 28: Results from MCMC runs showing B_0, B_{curr}, B_{2016} and B_{2018} estimates at varying catch levels for SCI 2.

	Model	**M=0.2**	**M=0.3**
	B_0	2959	2953
	B_{curr}	1880	2168
	B_{curr}/B_0	0.63	0.74
100 tonnes (TACC)	B_{2016}/B_0	0.63	0.72
	B_{2016}/B_{curr}	0.99	0.98
	B_{2018}/B_0	0.63	0.71
	B_{2018}/B_{curr}	1.00	0.98
110 tonnes	B_{2016}/B_0	0.62	0.72
	B_{2016}/B_{curr}	0.98	0.97
	B_{2018}/B_0	0.62	0.71
	B_{2018}/B_{curr}	0.97	0.97
120 tonnes	B_{2016}/B_0	0.61	0.70
	B_{2016}/B_{curr}	0.96	0.96
	B_{2018}/B_0	0.60	0.69
	B_{2018}/B_{curr}	0.95	0.94
130 tonnes	B_{2016}/B_0	0.60	0.69
	B_{2016}/B_{curr}	0.95	0.94
	B_{2018}/B_0	0.59	0.67
	B_{2018}/B_{curr}	0.93	0.93
140 tonnes	B_{2016}/B_0	0.59	0.68
	B_{2016}/B_{curr}	0.93	0.93
	B_{2018}/B_0	0.58	0.66
	B_{2018}/B_{curr}	0.91	0.90

Table 29: Results from MCMC runs for SCI 2, showing probabilities of projected spawning stock biomass exceeding the default Harvest Strategy Standard target and limit reference points.

	100 tonnes (TACC)	110 tonnes	120 tonnes	130 tonnes	140 tonnes
M=0.2					
2016					
P(SSB<10% B0)	0.00	0.00	0.00	0.00	0.00
P(SSB<20% B0)	0.00	0.00	0.00	0.00	0.00
P(SSB>40% B0)	0.99	0.99	0.98	0.98	0.97
P(B2016 < B2012)	0.52	0.56	0.59	0.64	0.67
2018					
P(SSB<10% B0)	0.00	0.00	0.00	0.00	0.00
P(SSB<20% B0)	0.00	0.00	0.00	0.00	0.00
P(SSB>40% B0)	0.97	0.96	0.94	0.93	0.92
P(B2018 < B2012)	0.51	0.55	0.59	0.63	0.66
M=0.3					
2016					
P(SSB<10% B0)	0.00	0.00	0.00	0.00	0.00
P(SSB<20% B0)	0.00	0.00	0.00	0.00	0.00
P(SSB>40% B0)	1.00	1.00	0.99	0.99	0.98
P(B2016 < B2012)	0.55	0.56	0.60	0.62	0.66
2018					
P(SSB<10% B0)	0.00	0.00	0.00	0.00	0.00
P(SSB<20% B0)	0.00	0.00	0.00	0.00	0.00
P(SSB>40% B0)	0.99	0.99	0.98	0.97	0.97
P(B2018 < B2012)	0.55	0.56	0.60	0.64	0.67

6. DISCUSSION

Assessments of SCI 1 and SCI 2 stocks were last conducted in 2011 (Tuck & Dunn 2012), following previous investigations developing the model structure. At this time, SCI 1 was estimated to be between 40 and 50% SSB_0, while SCI 2 was estimated to be at 40% SSB_0.

The previous models for SCI 1 and SCI 2 included spatial structure, based on survey strata (Tuck & Dunn 2012), but following the characterisation and preliminary model investigation, the SFAWG recommended a single area model for both assessments. Base models were developed for both areas, with M fixed at 0.2 and 0.3. For each area, a single annual standardised CPUE index was calculated, and along with trawl survey and photo survey data were fitted as abundance indices, with associated length frequency distributions. For both areas, the new model structure provided a similar perception of stock status to that of the 2011 models, when using the same data, confirming that revising the model structure did not significantly affect model outputs. Projections were conducted for both stocks, up to 2018 on the basis of a range of catch scenarios.

For SCI 1, the MPD estimate of SSB_0 was about 4700 t, although the likelihood profiles were relatively flat in this region of the curve. The model with M fixed at 0.2 estimated slightly lower SSB_0 and general SSB trajectory than the M=0.3 model. SSB is estimated to have increased through the late 1980s or early 1990s, peaking around 1994, and then declining until the early 2000s, and remaining stable at around 70% SSB_0 thereafter. The MCMC estimate of SSB_0 was between 4400 and 4700 t. SSB_{2012} was estimated to be between 3000 and 3300 t, and MCMC posteriors suggest 0% probability that SSB_{2012} is below 40% SSB_0. Annual fishing intensity (equivalent annual F) has consistently been estimated to be below F 40% B_0. Sensitivity analysis suggested that upweighting the CPUE index to improve the fit to that dataset would not change the current perception of the stock. For both models presented, future catches between 100 and 140 tonnes are predicted to reduce the SSB relative to SSB_{2012}, but remain above 40% SSB_0 (the most pessimistic prediction giving a 98% probability of SSB exceeding 40% SSB_0 by 2018).

For SCI 2, the MPD estimate of SSB_0 was about 2600 t, with the likelihood profiles identifying a clear minimum. The two models estimated very similar SSB_0, with the M=0.3 model estimating a slightly higher stock trajectory relative to SSB_0, SSB is estimated to have increased through the early 1990s, peaking in 1992, and then declining to a minimum in 2003, increasing slightly until about 2008, with a more marked increase after this. The MCMC estimate of SSB_0 was about 2950 t. SSB_{2012} was estimated to be between 1900 and 2200 t, and MCMC posteriors suggest 0% probability that SSB_{2012} is below 40% SSB_0. Annual fishing intensity (equivalent annual F) peaked in 2002 (when it may have exceeded F 40% B_0) but has declined considerably in recent years, while SSB as a proportion of SSB_0 has increased. For both models presented, future catches between 100 and 140 tonnes are predicted to reduce the SSB relative to SSB_{2012}, but remain above 40% SSB_0 (the most pessimistic prediction giving a 92% probability of SSB exceeding 40% SSB_0 by 2018).

7. ACKNOWLEDGEMENTS

This work was funded by the Ministry for Primary Industries under project DEE201002SCIB, and builds on a series of scampi assessment projects funded by the Ministry. I thank the many NIWA and Ministry of Fisheries staff who measured scampi over the years, and the members of the NIWA scampi image reading team. Development of the model structure benefitted greatly from comments by Patrick Cordue and Paul Breen in particular, along with other members of the Shellfish Fisheries Assessment Working Group. This report was reviewed by Charles Edwards (NIWA, Wellington).

8. REFERENCES

Bell, M.C.; Redant, F.; Tuck, I.D. (2006). *Nephrops* species. *In*: Phillips, B. (ed.). Lobsters: biology, management, aquaculture and fisheries, pp. 412–461. Blackwell Publishing, Oxford.

Bentley, N.; Kendrick, T.H.; Starr, P.J.; Breen, P.A. (2012). Influence plots and metrics: tools for better understanding fisheries catch-per-unit-effort standardisations. *ICES Journal of Marine Science 69*: 84–88.

Bull, B.; Dunn, A. (2002). Catch-at-age: User manual v 1.06.2002/09/12. *NIWA Internal Report 114*.

Bull, B.; Francis, R.I.C.C.; Dunn, A.; McKenzie, A.; Gilbert, D.J.; Smith, M.H.; Bian, R. (2008). CASAL (C++ algorithmic stock assessment laboratory). *NIWA Technical Report 130*.

Charnov, E.L.; Berrigan, D.; Shine, R. (1983). The M/*k* ratio is the same for fish and reptiles. *American Naturalist 142*: 707–711.

Cordue, P.L. (2012). Fishing intensity metrics for use in overfishing determination. *ICES Journal of Marine Science: Journal du Conseil 69(4)*: 615–623. <http://dx.doi.org/10.1093/icesjms/fss036>

Cryer, M.; Coburn, R. (2000). Scampi stock assessment for 1999. *New Zealand Fisheries Assessment Report 2000/7*.

Cryer, M.; Dunn, A.; Hartill, B. (2005). Length-based population model for scampi (*Metanephrops challengeri*) in the Bay of Plenty (QMA 1). *New Zealand Fisheries Assessment Report 2005/27*. 55 p.

Cryer, M.; Hartill, B.; Drury, J.; Armiger, H.; M.D, Smith.; Middleton, C. (2003). Indices of relative abundance for scampi, *Metanephrops challengeri*, based on photographic surveys in QMA 1 (1998–2003) and QMA 2 (2003). Final Research Report for Ministry of Fisheries research project SCI2002-01. 18 p. (Unpublished report held by Ministry for Primary Industries, Wellington.)

Cryer, M.; Oliver, M. (2001). Estimating age and growth in New Zealand scampi, *Metanephrops challengeri*. Final Research Report for Ministry of Fisheries Research Project SCI98-02. p. (Unpublished report held by Ministry for Primary Industries, Wellington)

Cryer, M.; Stotter, D.R. (1997). Trawling and tagging of scampi off the Alderman Islands, western bay of Plenty, September 1995 (KAH9511). *New Zealand Fisheries Data Report 84*.

Cryer, M.; Stotter, D.R. (1999). Movement and growth rates of scampi inferred from tagging, Alderman Islands, western Bay of Plenty. *NIWA Technical Report (49)*.

Fenaughty, C. (1989). Reproduction in *Metanephrops challengeri*. Unpubl. Rep. MAF Fisheries, Wellington. 46 p. (Unpublished report held by Ministry for Primary Industries, Wellington)

Francis, R.I.C.C. (1999). The impact of correlations in standardised CPUE indices. New Zealand Fisheries Assessment Research Document 99/42. 30 p. (Unpublished report held by NIWA library, Wellington.)

Francis, R.I.C.C. (2011). Data weighting in statistical fisheries stock assessment models. *Canadian Journal Fisheries and Aquatic Science 68*: 1124–1138.

Francis, R.I.C.C.; Bian, R. (2011). Catch-at-length and -age (CALA) User Manual. 83 p. (NIWA Unpublished Report).

McCullagh, P.; Nelder, J.A. (1989). Generalised Linear Models. 2nd Ed. Chapman and Hall, London. 511 p.

Morizur, Y. (1982). Estimation de la mortalité pour quelques stocks de langoustine, *Nephrops norvegicus*. *ICES CM 1982/K:10*.

Pauly, D. (1980). On the interrelationships between natural mortality, growth parameters, and mean environmental temperature in 175 fish stocks. *Journal du Conseil International pour l'Exloration du Mer 39*: 175–192.

Starr, P.J. (2009). Rock lobster catch and effort data: summaries and CPUE standardisations, 1979–80 to 2007–08. *New Zealand Fisheries Assessment Report 2009/38*: 73p.

Starr, P.J.; Breen, P.A.; Kendrick, T.H.; Haist, V. (2009). Model and data used for the 2008 stock assessment of rock lobsters (*Jasus edwardsii*) in CRA 3. *New Zealand Fisheries Assessment Report 2009/22*: 62 p.

Tuck, I. (2013). Characterisation and length-based population model for scampi (*Metanephrops challengeri*) on the Mernoo Bank (SCI 3). *New Zealand Fisheries Assessment Report 2013/24*: 165 p.

Tuck, I.; Parkinson, D.; Drury, J.; Armiger, H.; Miller, A.; Rush, N.; Smith, M.; Hartill, B. (2013). Estimating the abundance of scampi in SCI 1 and SCI 2 (2012). Final Research Report for Ministry of Fisheries research project SCI201002A. 54p p. (Unpublished report held by Ministry for Primary Industries, Wellington.)

Tuck, I.D. (2009). Characterisation of scampi fisheries and the examination of catch at length and spatial distribution of scampi in SCI 1, 2, 3, 4A and 6A. *New Zealand Fisheries Assessment Report 2009/27*: 102 p.

Tuck, I.D. (2010) Scampi burrow occupancy, burrow emergence and catchability. Final Research Report for Ministry of Fisheries research project 2010/13. 58 p. (Unpublished report held by Ministry for Primary Industries, Wellington.)

Tuck, I.D.; Atkinson, R.J.A.; Chapman, C.J. (2000). Population biology of the Norway lobster, *Nephrops norvegicus* (L.) in the Firth of Clyde, Scotland. II. Fecundity and size at onset of maturity. *ICES Journal of Marine Science 57*: 1222–1237.

Tuck, I.D.; Dunn, A. (2006). Length based population model for scampi (*Metanephrops challengeri*) in the Bay of Plenty (SCI 1) and Wairarapa / Hawke Bay (SCI 2). Final Research Report for Ministry of Fisheries research project SCI2005-01. 93 p. (Unpublished report held by Ministry for Primary Industries, Wellington.)

Tuck, I.D.; Dunn, A. (2009). Length-based population model for scampi (*Metanephrops challengeri*) in the Bay of Plenty (SCI 1) and Wairarapa / Hawke Bay (SCI 2). Final Research Report for Ministry of Fisheries research projects SCI2006-01 & SCI2008-03W. 30 p. (Unpublished report held by Ministry for Primary Industries, Wellington.)

Tuck, I.D.; Dunn, A. (2012). Length-based population model for scampi (*Metanephrops challengeri*) in the Bay of Plenty (SCI 1), Wairarapa / Hawke Bay (SCI 2) and Auckland Islands (SCI 6A). *New Zealand Fisheries Assessment Report 2012/1*: 125 p.

Tuck, I.D.; Hartill, B.; Drury, J.; Armiger, H.; Smith, M.; Parkinson, D. (2006). Measuring the abundance of scampi - Indices of abundance for scampi, *Metanephrops challengeri*, based on photographic surveys in SCI 2 (2003-2006). Final Research Report for Ministry of Fisheries Research Project SCI200501(Objective 1). (Unpublished report held by Ministry for Primary Industries, Wellington.)

Tuck, I.D.; Hartill, B.; Parkinson, D.; Harper, S.; Drury, J.; Smith, M.; Armiger, H. (2009). Estimating the abundance of scampi - Relative abundance of scampi, *Metanephrops challengeri*, from a photographic survey in SCI 1 and SCI 6A (2008). Final Research Report for Ministry of Fisheries research project SCI2007-02. p. (Unpublished report held by Ministry for Primary Industries, Wellington.)

Vignaux, M. (1994). Catch per unit effort (CPUE) analysis of west coast South Island and Cook Strait spawning hoki fisheries, 1987–93. *New Zealand Fisheries Assessment Research Document 94/11*: 29 p.

Wear, R.G. (1976). Studies on the larval development of *Metanephrops challengeri* (Balss, 1914) (Decapoda, Nephropidae). *Crustaceana 30*: 113–122.

9. APPENDIX 1. Comparison of groomed data set with previous grooming approach.

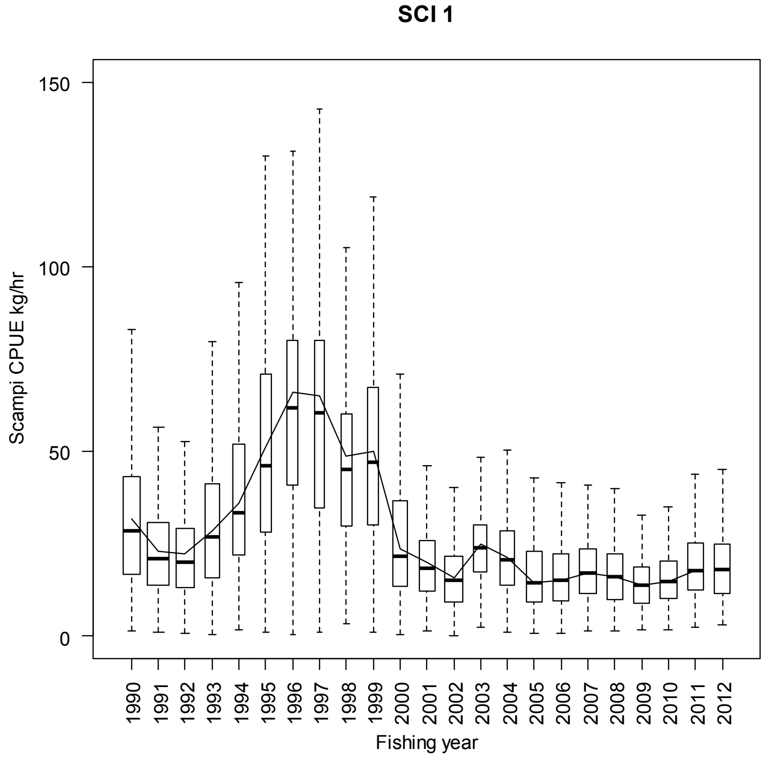

A1. 1: Comparison of groomed data set (box plots) with median CPUE for equivalent data using previous grooming approach for SCI 1.

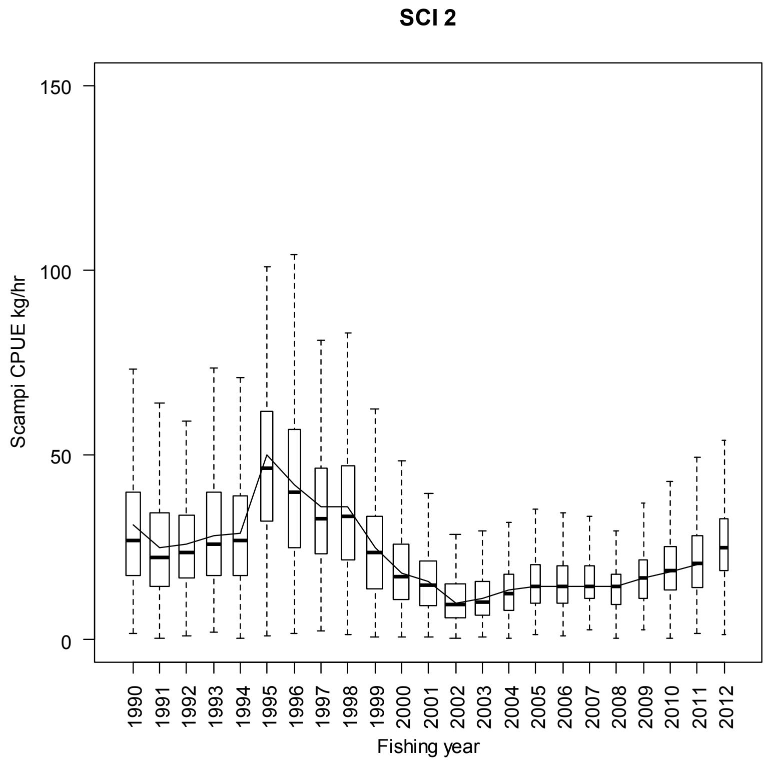

A1. 2: Comparison of groomed data set (box plots) with median CPUE for equivalent data using previous grooming approach for SCI 2.

10. APPENDIX 2. Diagnostic plots for SCI 1 final CPUE standardisation model.

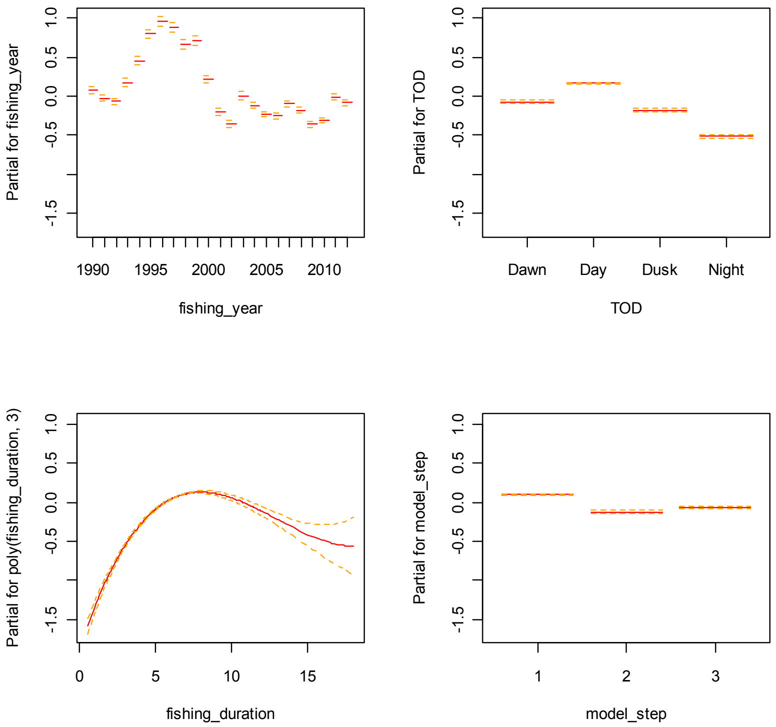

A2. 1: Termplot for final SCI 1 CPUE standardisation model (Table 7).

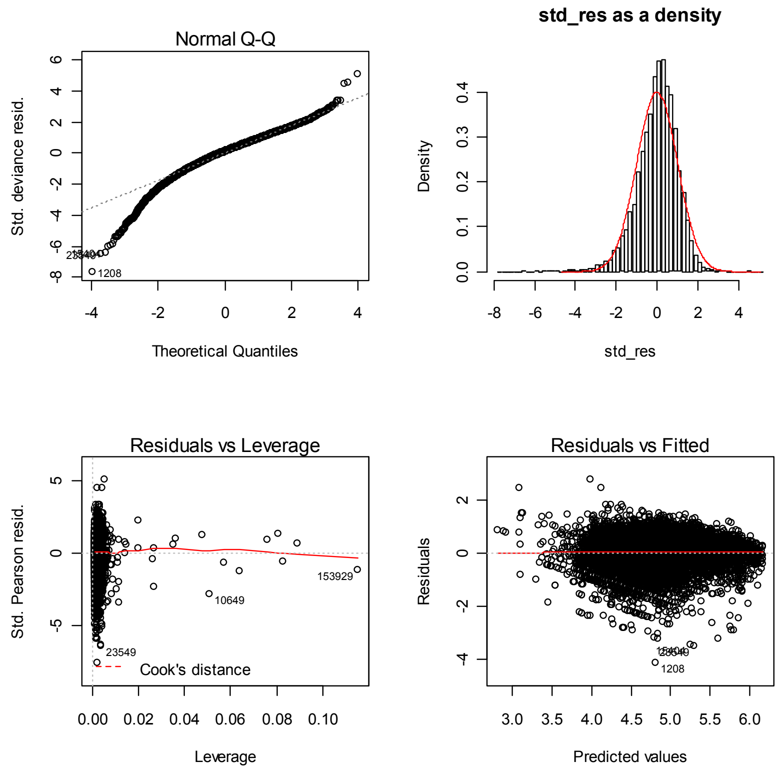

A2. 2. Diagnostic plots for final SCI 1 CPUE standardisation model (Table 7).

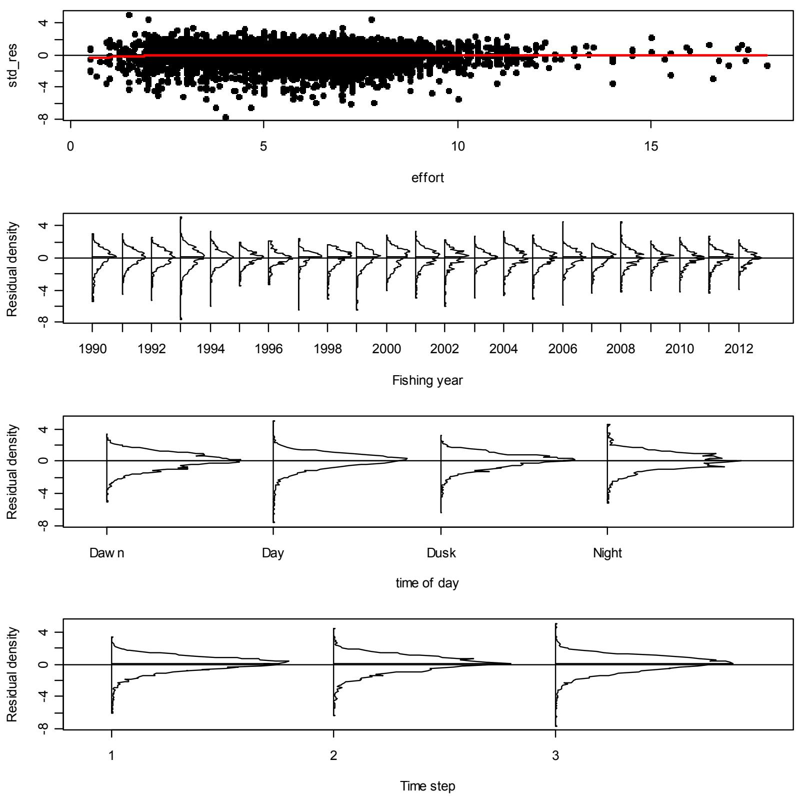

A2. 3: Distributions of residuals for final SCI 1 CPUE standardisation model (Table 7).

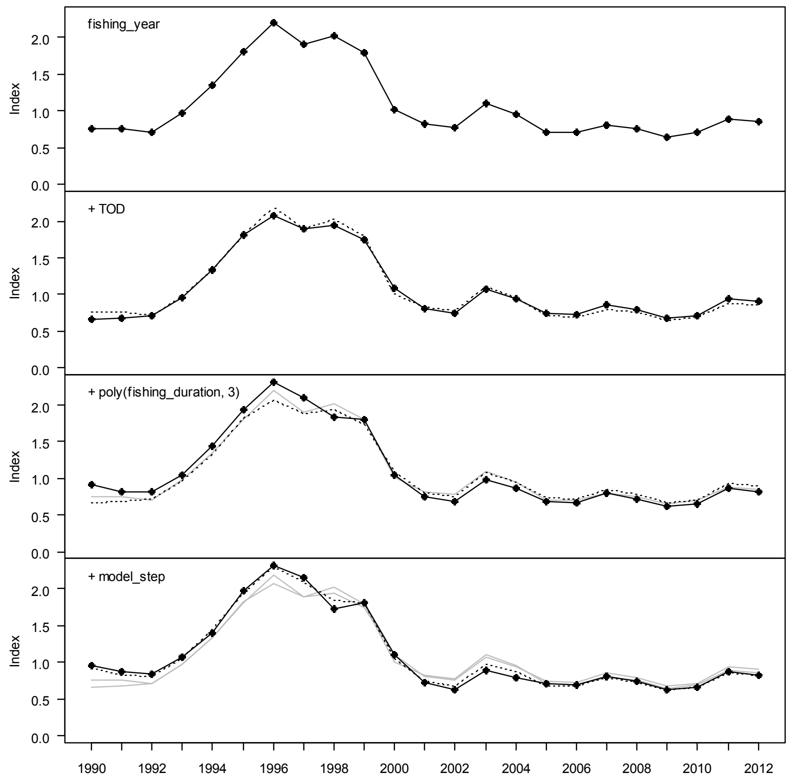

A2. 4: Step influence plot for final SCI 1 CPUE standardisation model (Table 7).

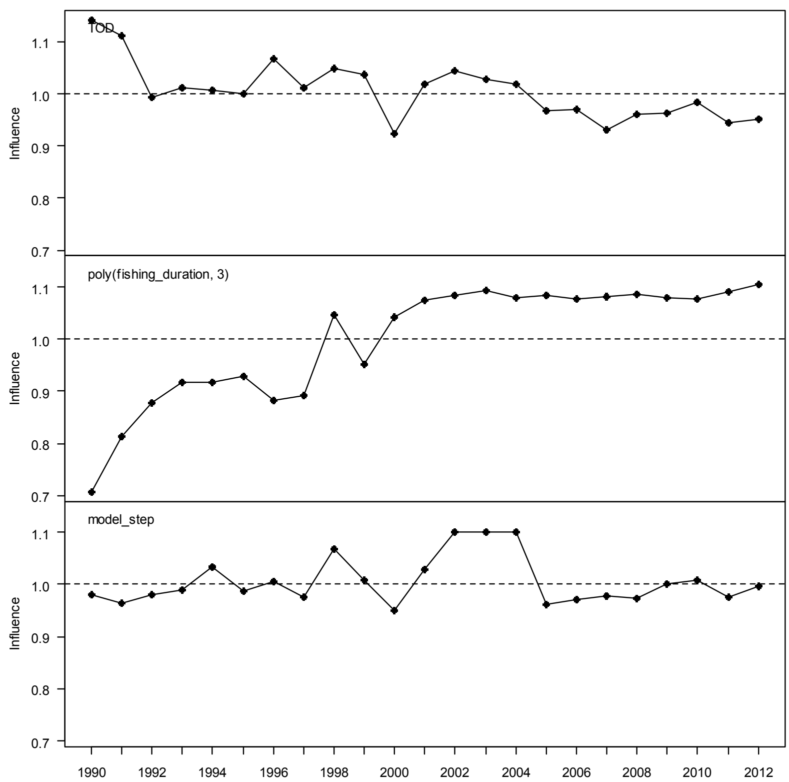

A2. 5: Year influence plots for each explanatory variable for final SCI 1 CPUE standardisation model (Table 7).

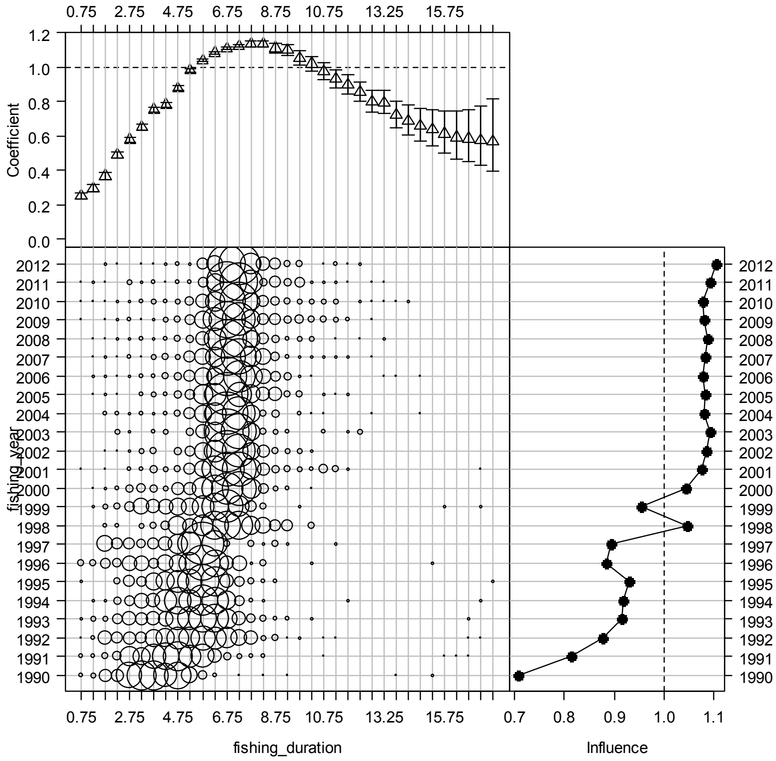

A2. 6: Coefficient-distribution influence plot for effort for final SCI 1 CPUE standardisation model (Table 7).

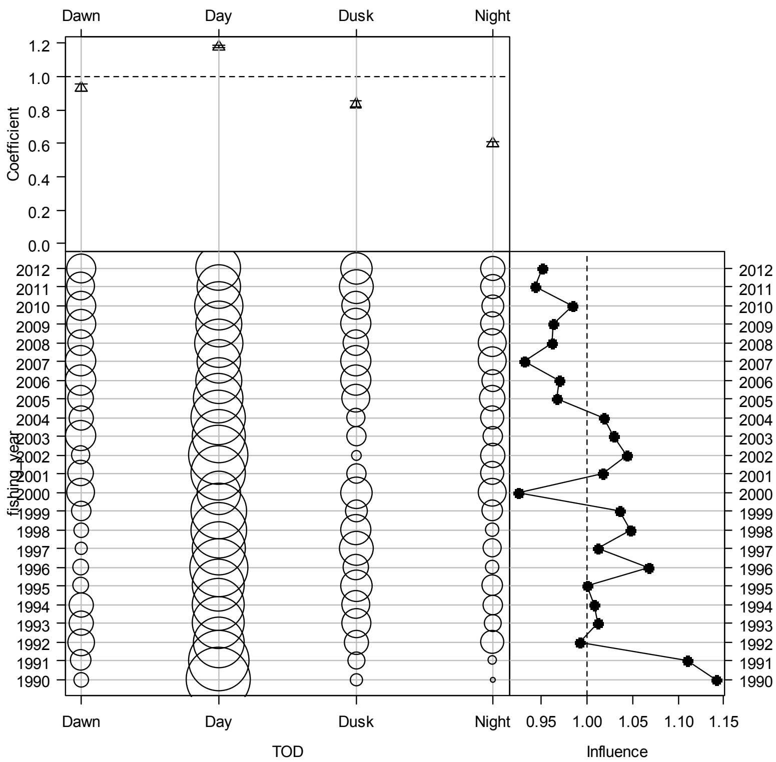

A2. 7: Coefficient-distribution influence plot for time of day for final SCI 1 CPUE standardisation model (Table 7).

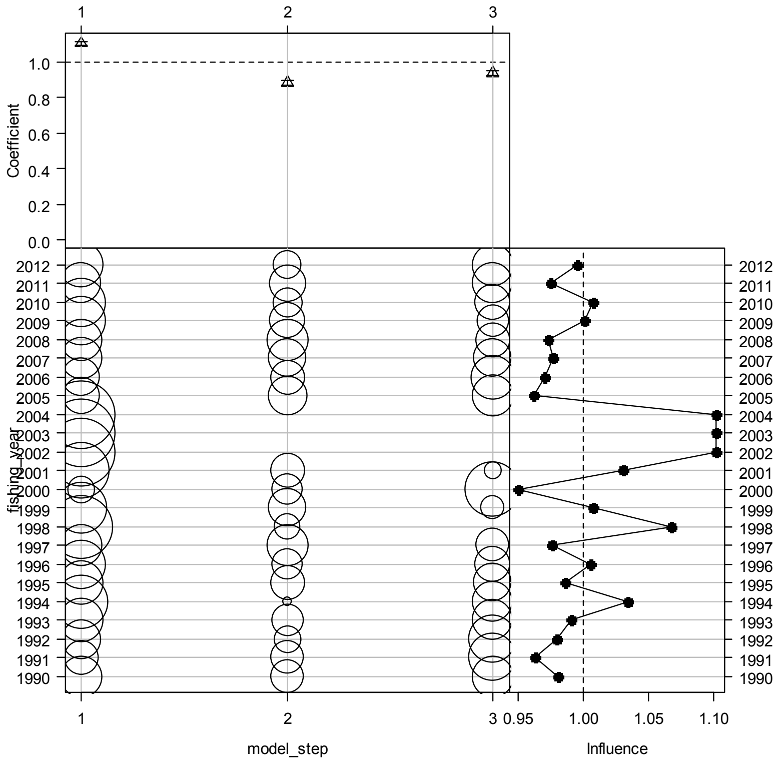

A2. 8: Coefficient-distribution influence plot for timestep for final SCI 1 CPUE standardisation model (Table 7).

11. APPENDIX 3. Diagnostic plots for SCI 2 final CPUE standardisation model.

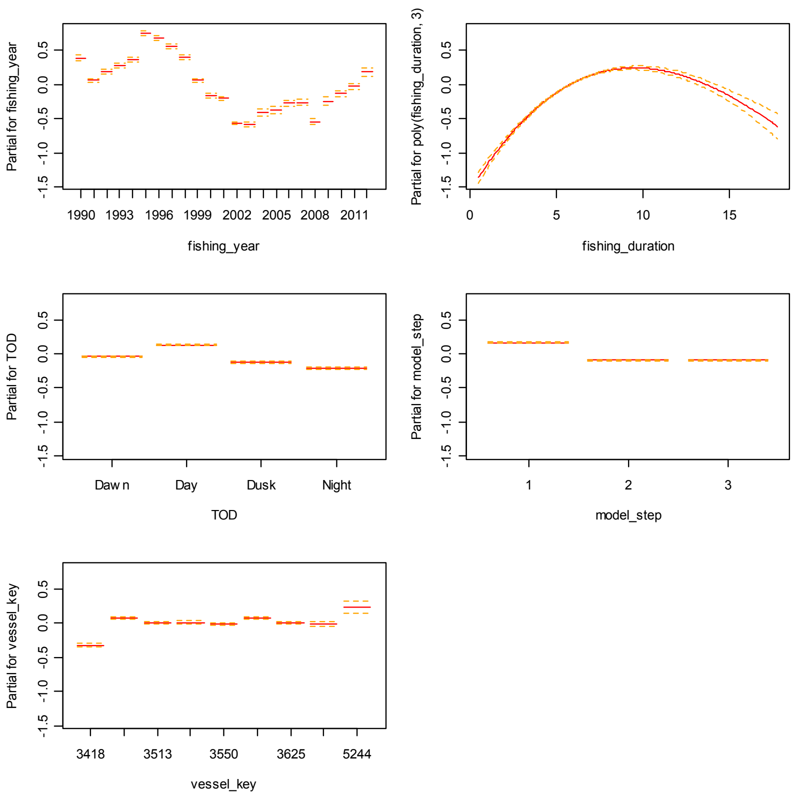

A3. 1: Termplot for final SCI 2 CPUE standardisation model (Table 10).

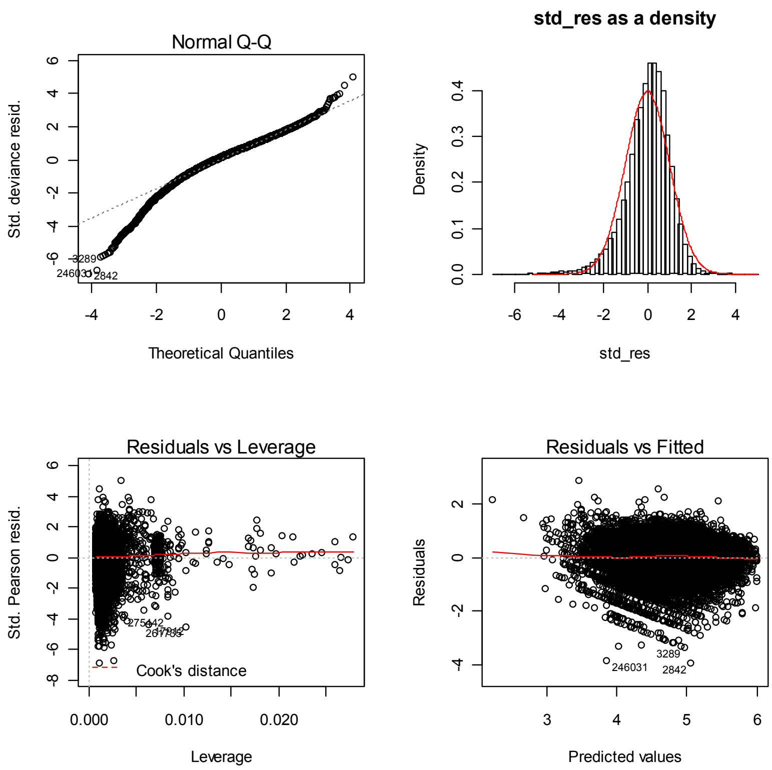

A3. 2: Diagnostic plots for final SCI 2 CPUE standardisation model (Table 10).

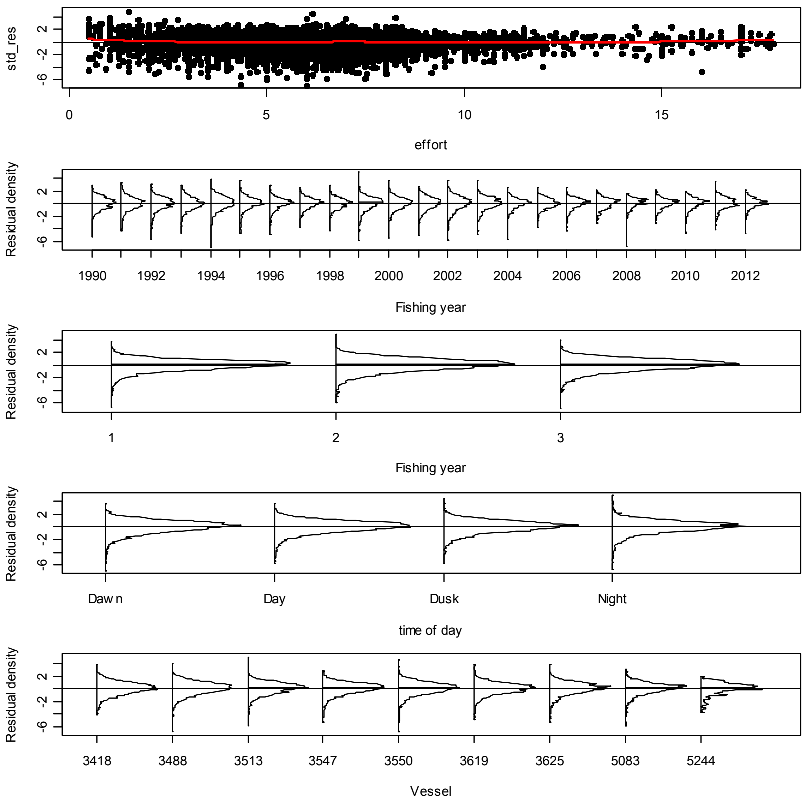

A3. 3: Distributions of residuals for final SCI 2 CPUE standardisation model (Table 10).

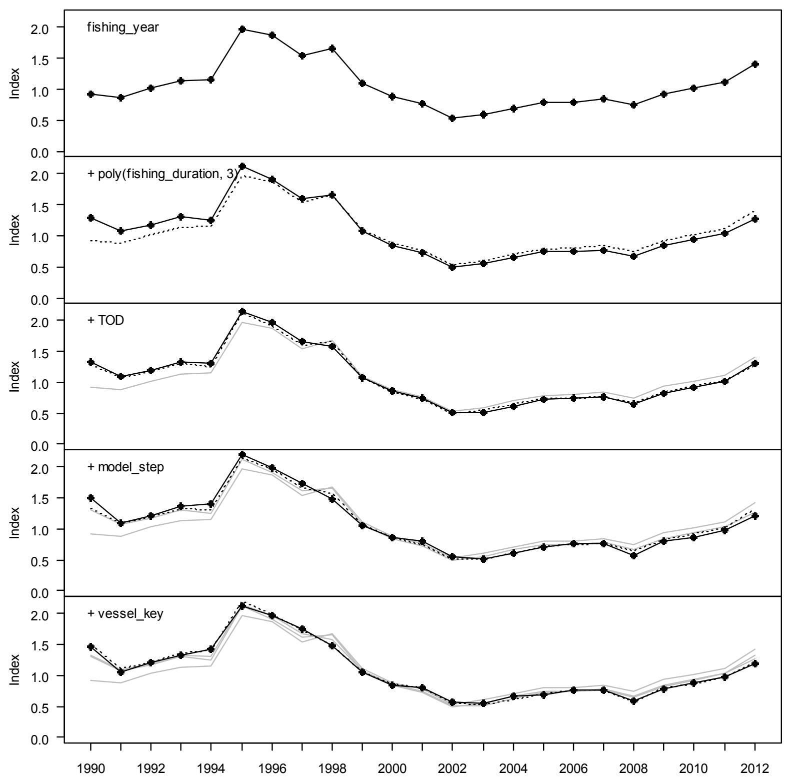

A3. 4: Step influence plot for final SCI 2 CPUE standardisation model (Table 10).

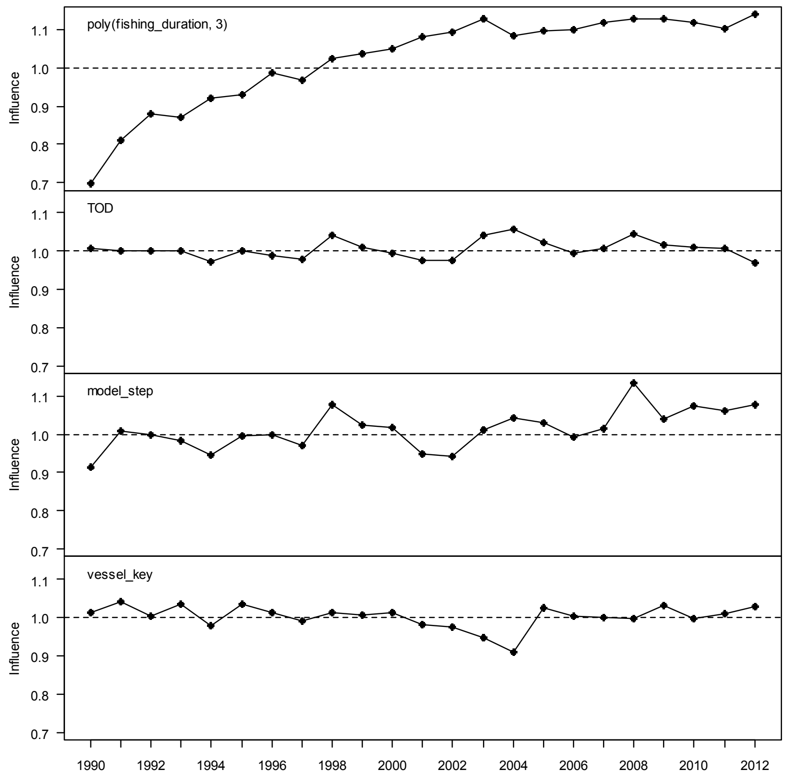

A3. 5: Year influence plots for each explanatory variable for final SCI 2 CPUE standardisation model (Table 10).

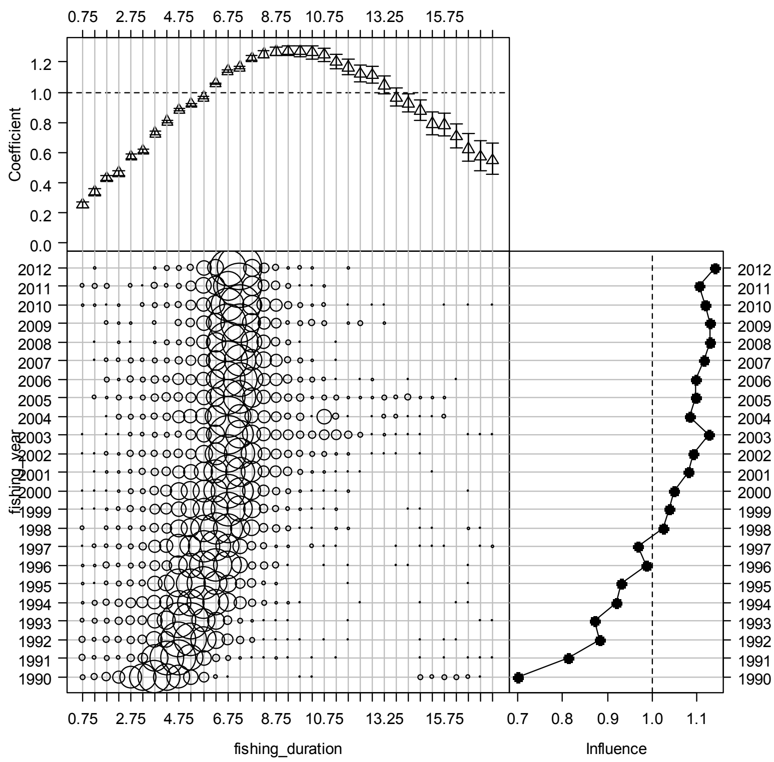

A3. 6: Coefficient-distribution influence plot for effort for final SCI 2 CPUE standardisation model (Table 10).

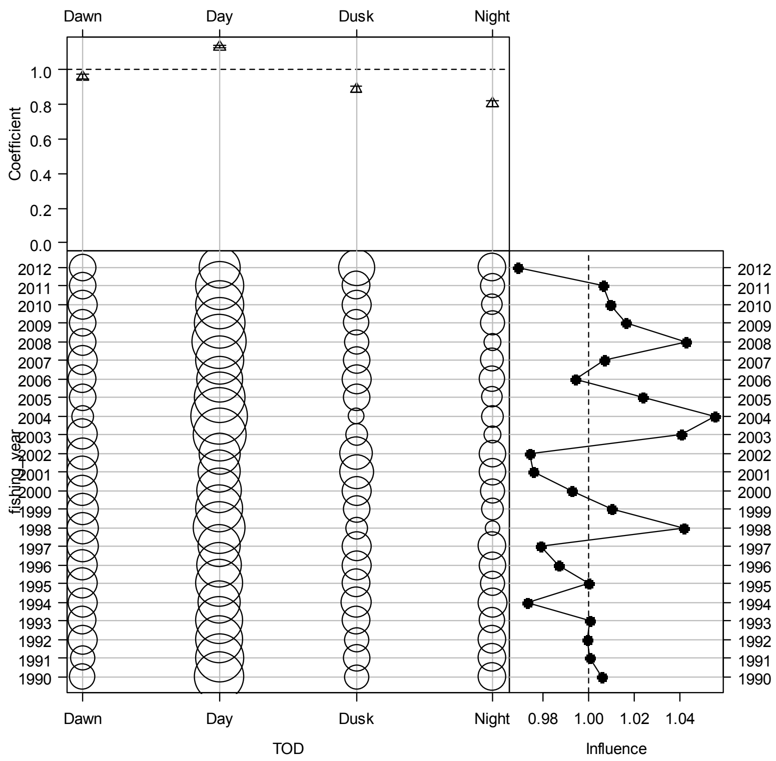

A3. 7: Coefficient-distribution influence plot for time of day for final SCI 2 CPUE standardisation model (Table 10).

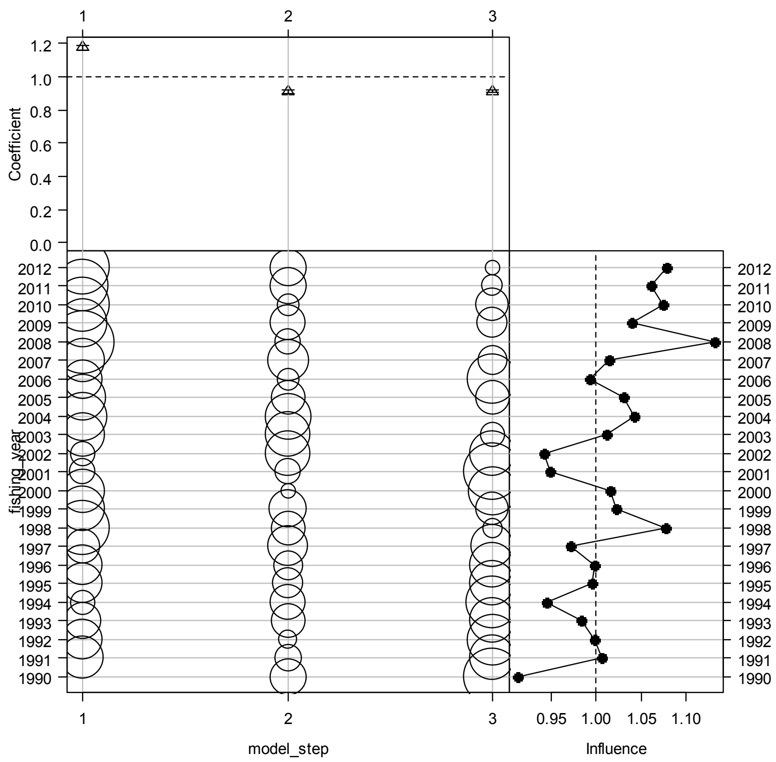

A3. 8: Coefficient-distribution influence plot for timestep for final SCI 2 CPUE standardisation model (Table 10).

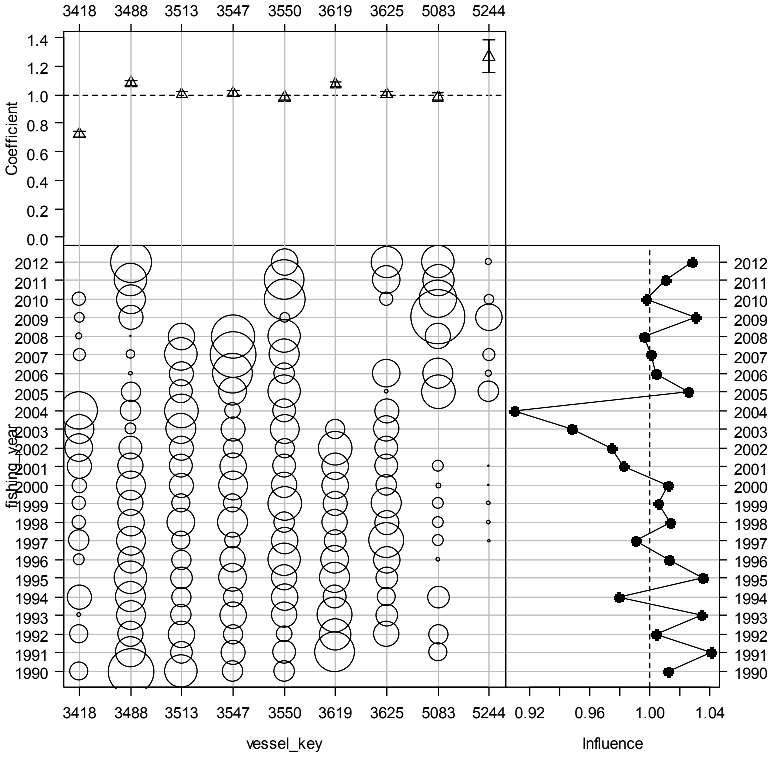

A3. 9: Coefficient-distribution influence plot for vessel for final SCI 2 CPUE standardisation model (Table 10).

12. APPENDIX 4. SCI 1 BASE2 model plots (M=0.2)

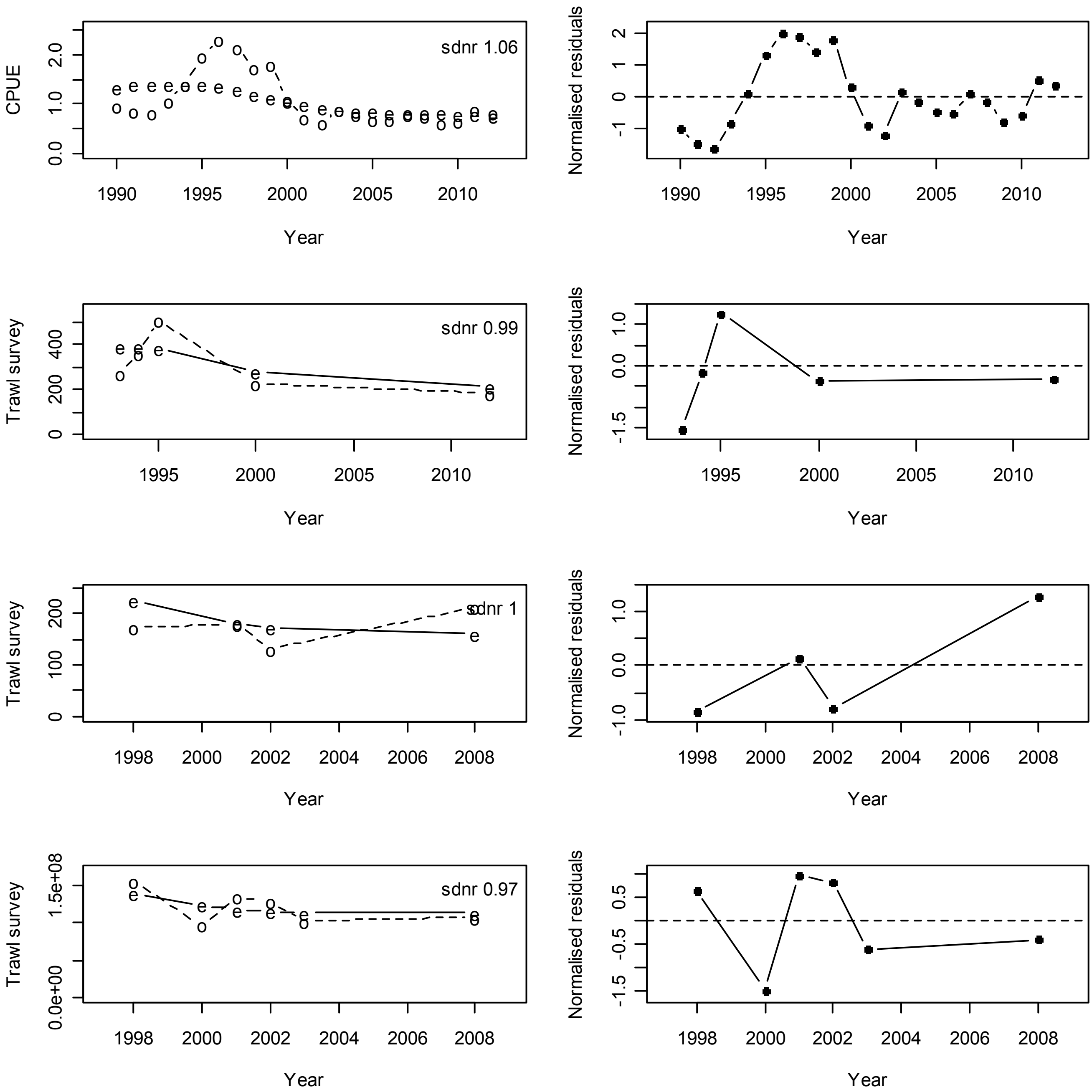

A4. 1: Fits to abundance indices (left column) and normalised residuals (right column) for standardised CPUE index (top row) trawl survey biomass index covering whole area (second row), trawl survey biomass index covering limited area (third row) and photo survey abundance index (fourth row) for SCI 1 Base2 model.

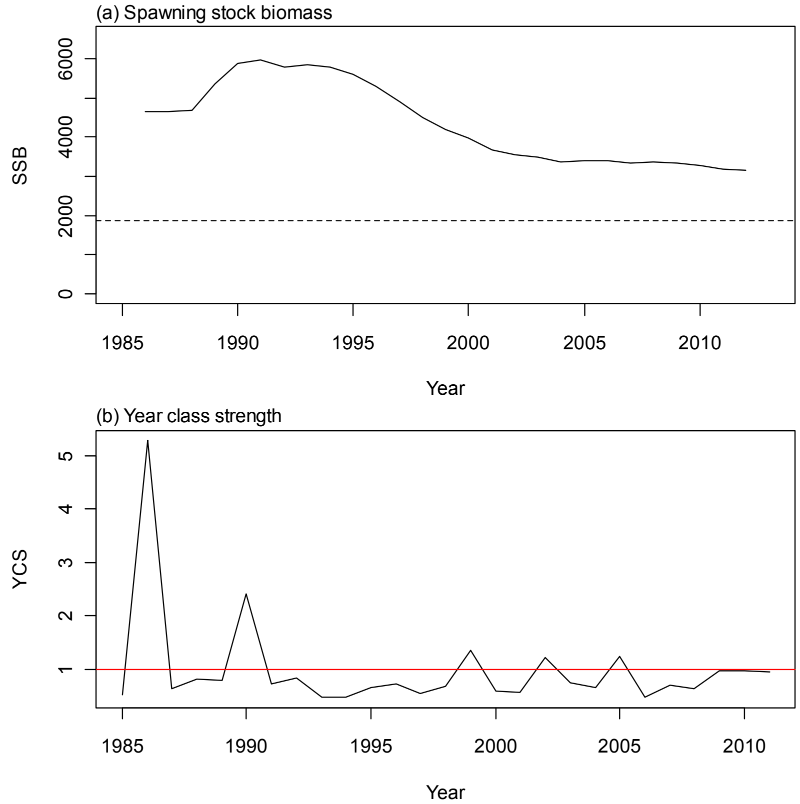

A4. 2: Spawning stock biomass trajectory (upper plot), year class strength (lower plot) for SCI 1 Base2 model.

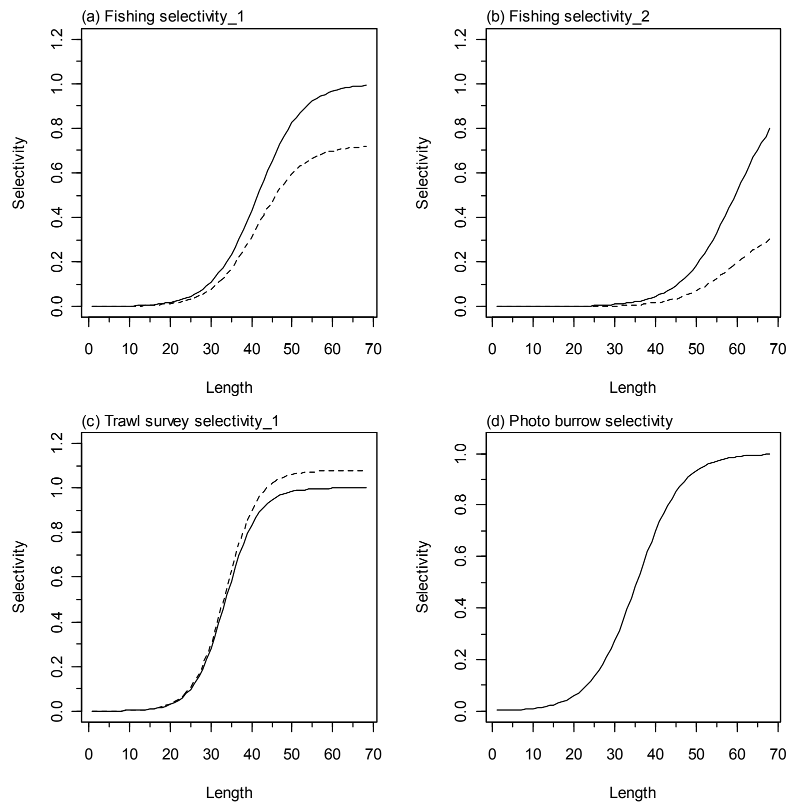

A4. 3: Fishery and survey selectivity curves. Solid line – females, dotted line – males. The scampi burrow index is not sexed, and a single selectivity applies.

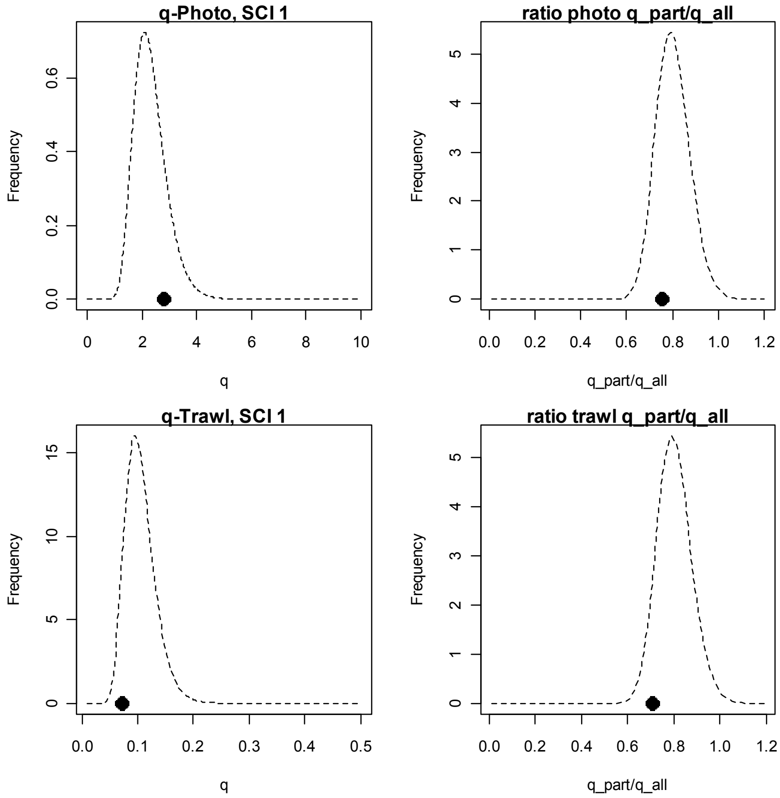

A4. 4: Catchability estimates from MPD model run, plotted in relation to prior distribution.

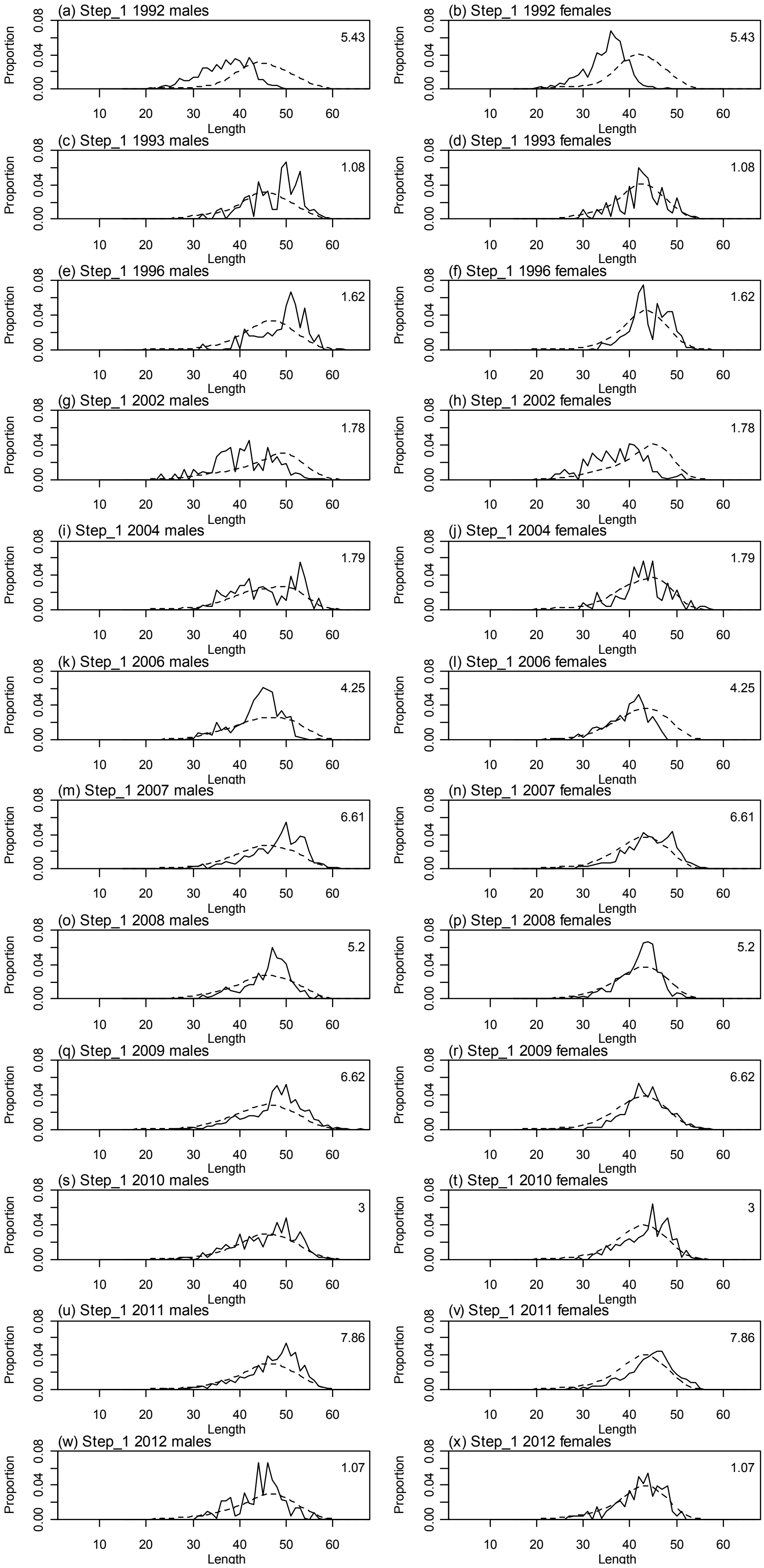

A4. 5: Observed (solid line) and fitted (dashed line) length frequency distributions for observer samples, time step 1.

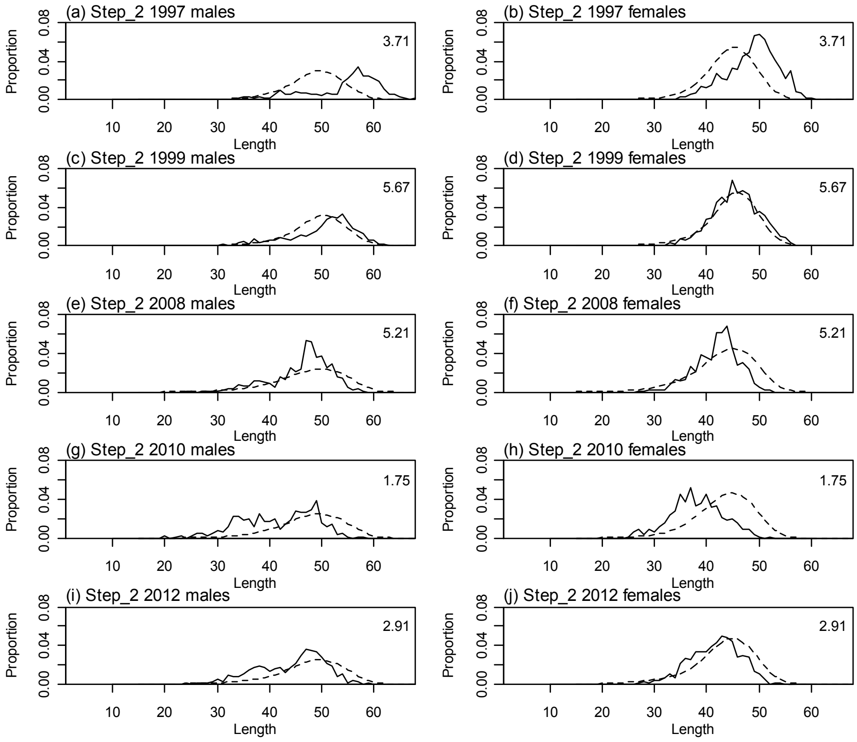

A4. 6: Observed (solid line) and fitted (dashed line) length frequency distributions for observer samples, time step 2.

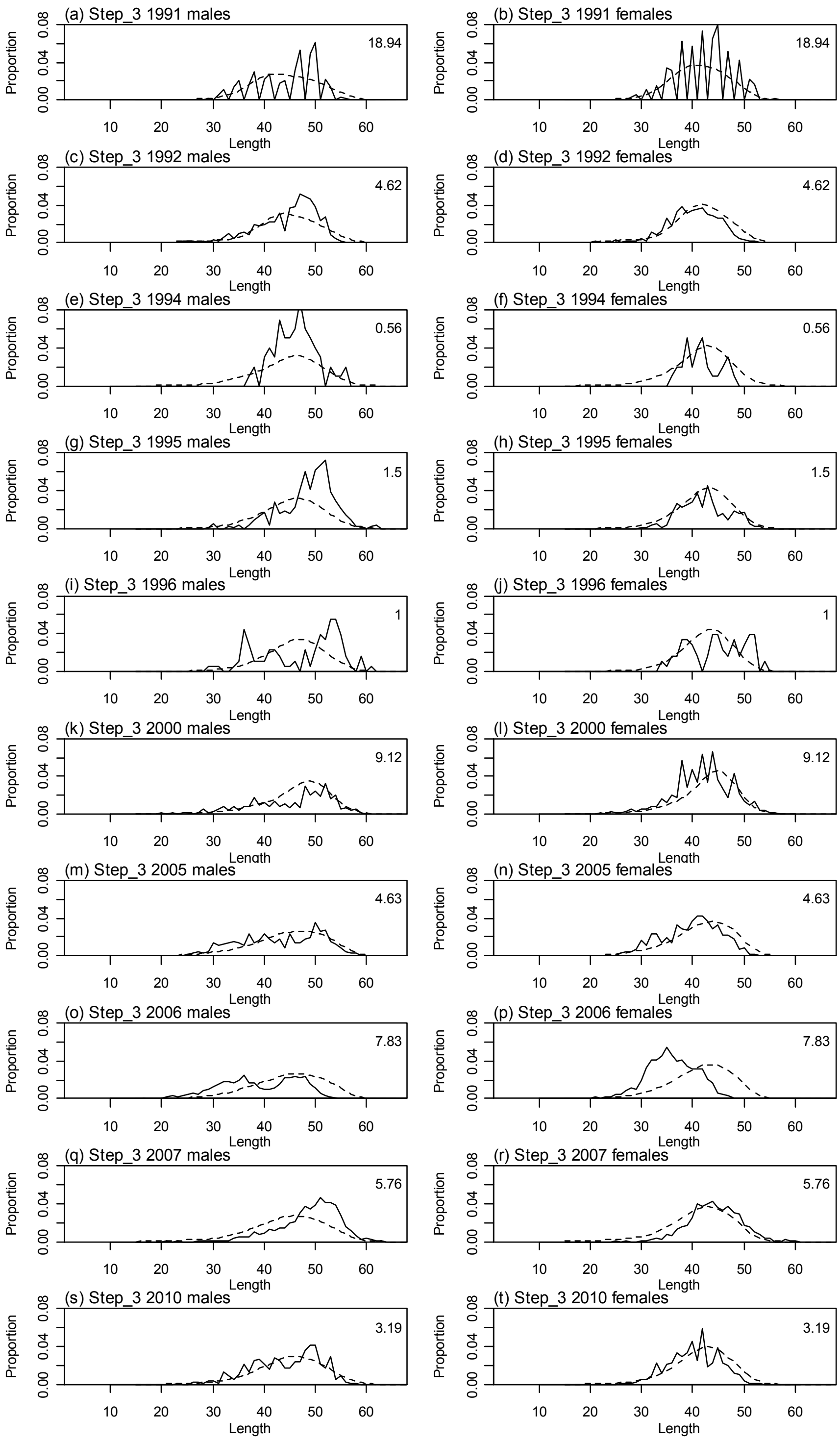

A4. 7: Observed (solid line) and fitted (dashed line) length frequency distributions for observer samples, time step 3.

A4. 8: Numbers of scampi measured, estimated multinomial N sample size, and effective sample size used within the model for length frequency distributions for observer samples, time step 1.

	Measured	Multinomial N	Effective sample size
N_1992	1717	1738	5.43
N_1993	263	345	1.08
N_1996	500	519	1.62
N_2002	454	570	1.78
N_2004	315	574	1.79
N_2006	1768	1361	4.25
N_2007	2404	2115	6.61
N_2008	2150	1662	5.20
N_2009	2475	2118	6.62
N_2010	1300	959	3.00
N_2011	2733	2513	7.86
N_2012	271	343	1.07

A4. 9: Numbers of scampi measured, estimated multinomial N sample size, and effective sample size used within the model for length frequency distributions for observer samples, time step 2.

	Measured	Multinomial N	Effective sample size
N_1997	1905	1802	3.71
N_1999	2586	2751	5.67
N_2008	2847	2528	5.21
N_2010	1013	851	1.75
N_2012	1408	1410	2.91

A4. 10: Numbers of scampi measured, estimated multinomial N sample size, and effective sample size used within the model for length frequency distributions for observer samples, time step 3.

	Measured	Multinomial N	Effective sample size
N_1991	10245	6871	18.94
N_1992	1751	1677	4.62
N_1994	100	203	0.56
N_1995	450	543	1.50
N_1996	180	363	1.00
N_2000	3891	3309	9.12
N_2005	2113	1679	4.63
N_2006	3197	2842	7.83
N_2007	2600	2090	5.76
N_2010	3325	1159	3.19
N_2011	3040	2337	6.44

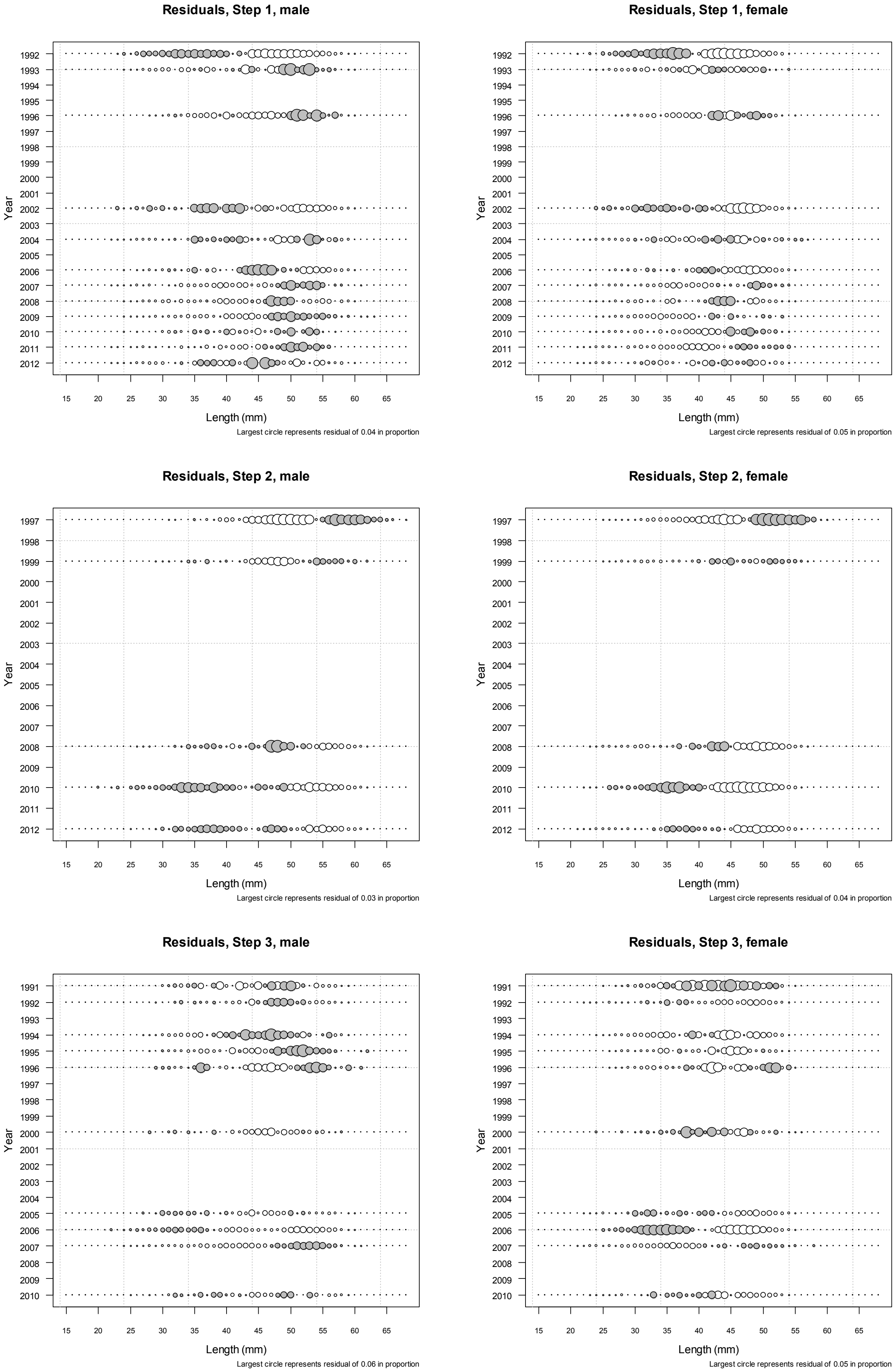

A4. 11: Bubble plots of residuals for fits to length frequency distributions for observer sampling.

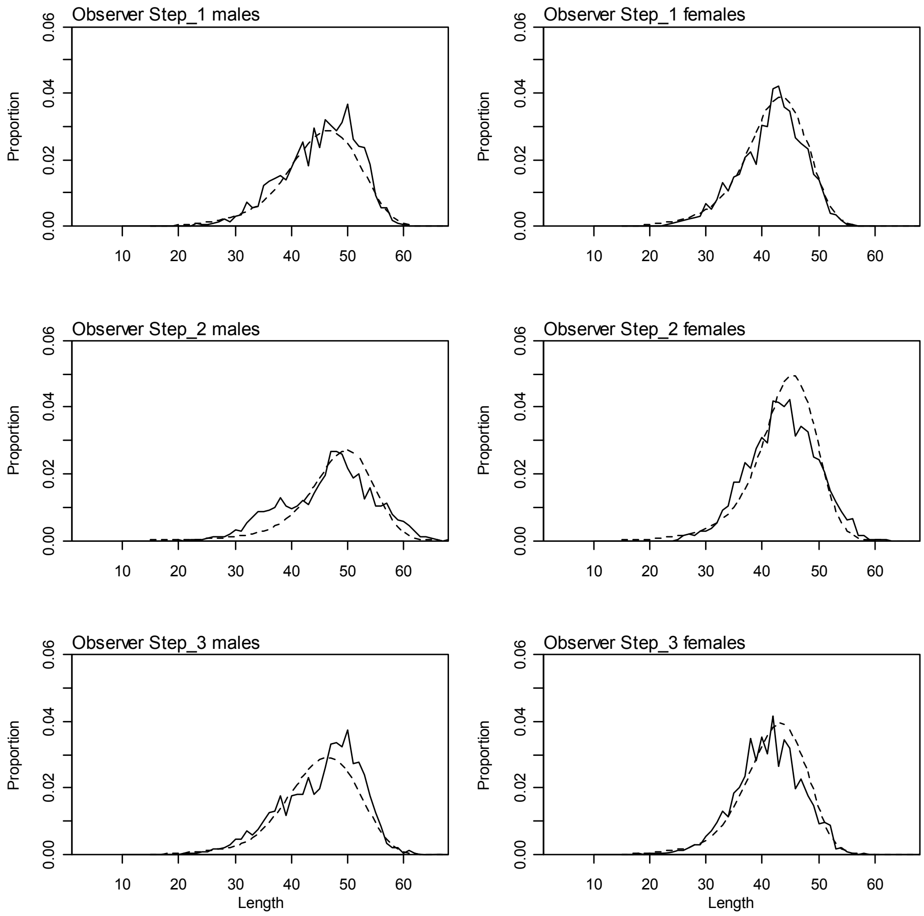

A4. 12: Average observed (solid line) and fitted (dashed line) length frequency distributions for observer samples.

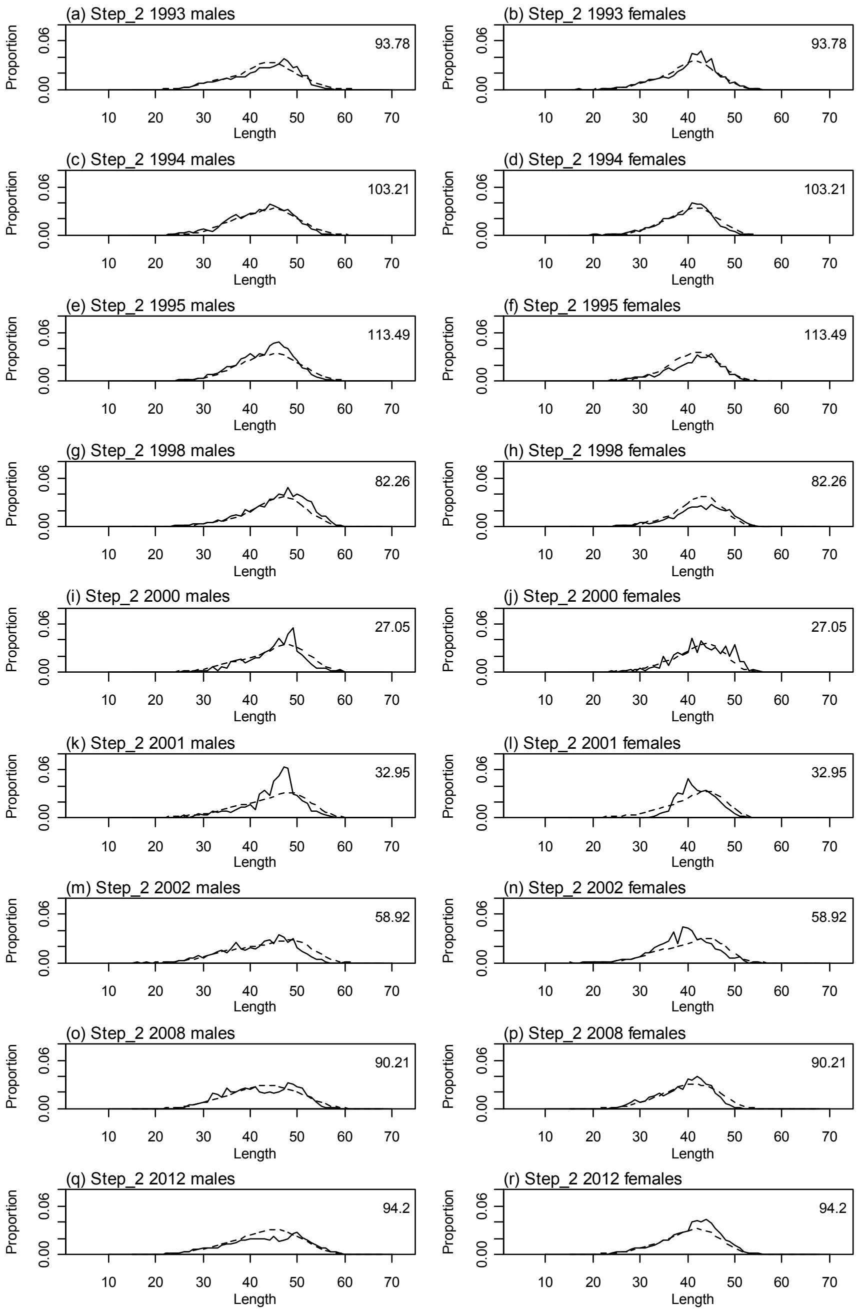

A4. 13: Observed (solid line) and fitted (dashed line) length frequency distributions for research survey samples.

A4. 14: Numbers of scampi measured, estimated multinomial N sample size, and effective sample size used within the model for length frequency distributions for research survey samples.

	Measured	Multinomial N	Effective sample size
N_1993	5710	8506	93.78
N_1994	5346	9361	103.21
N_1995	6334	10294	113.49
N_1998	4212	7461	82.26
N_2000	1360	2453	27.05
N_2001	1913	2989	32.95
N_2002	2647	5344	58.92
N_2008	3985	8182	90.21
N_2012	4353	8544	94.20

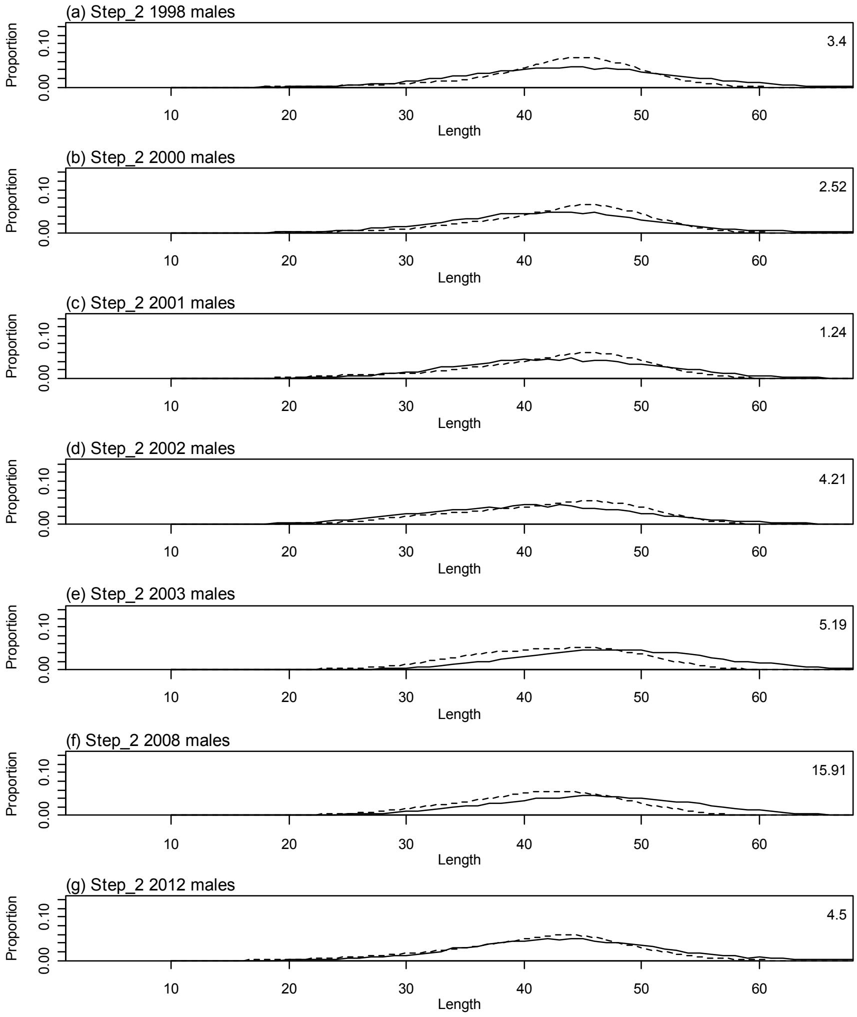

A4. 15: Observed (solid line) and fitted (dashed line) length frequency distributions for photographic survey scampi size estimation.

A4. 16: Numbers of scampi measured, estimated multinomial N sample size, and effective sample size used within the model for length frequency distributions for photographic survey samples.

	Measured	Multinomial N	Effective sample size
N_1998	46	93	3.40
N_2000	35	69	2.52
N_2001	17	34	1.24
N_2002	57	115	4.21
N_2003	73	142	5.19
N_2008	237	435	15.91
N_2012	62	123	4.50

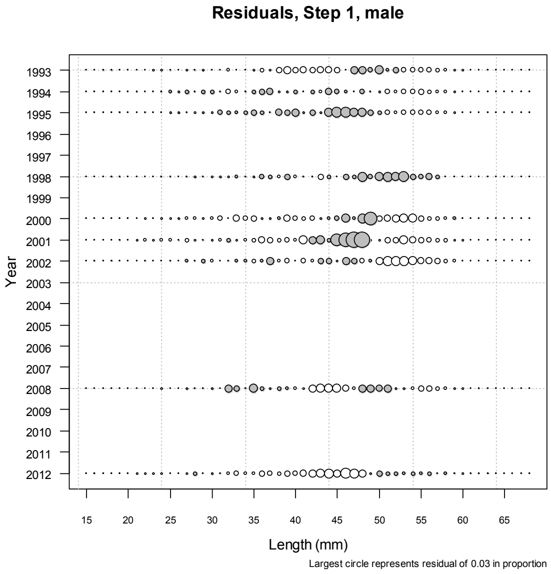

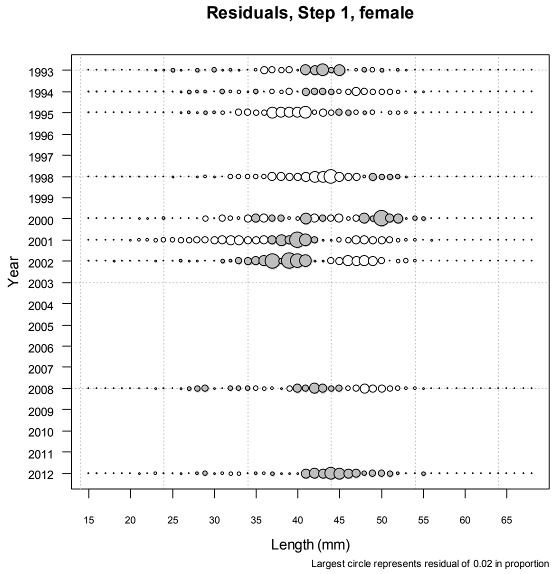

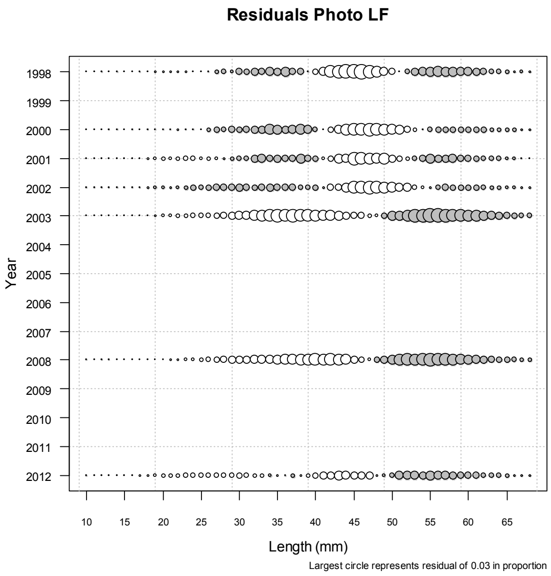

A4. 17: Bubble plots of residuals for fits to length frequency distributions for trawl survey sampling and photographic survey scampi size estimation.

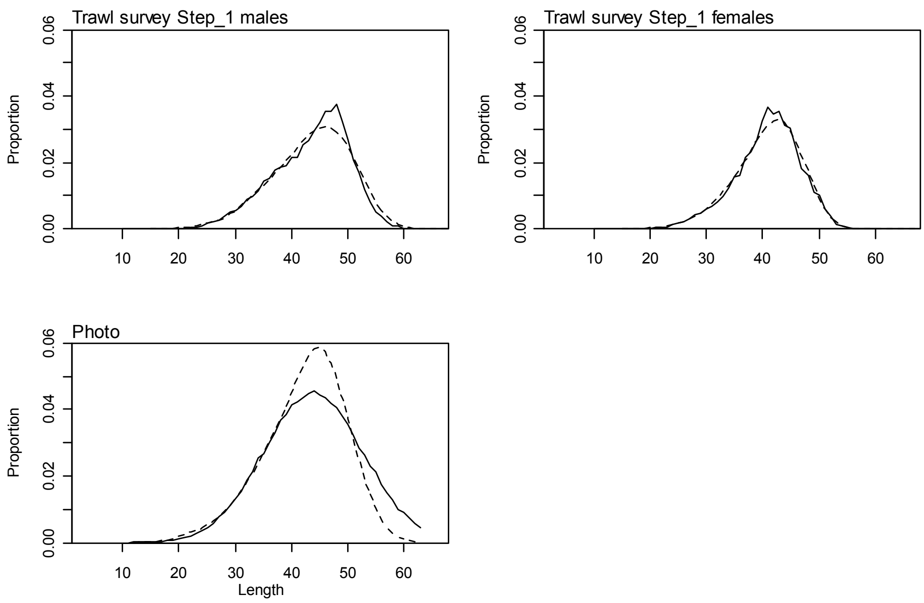

A4. 18: Average observed (solid line) and fitted (dashed line) length frequency distributions for trawl survey sampling and photographic survey scampi size estimation.

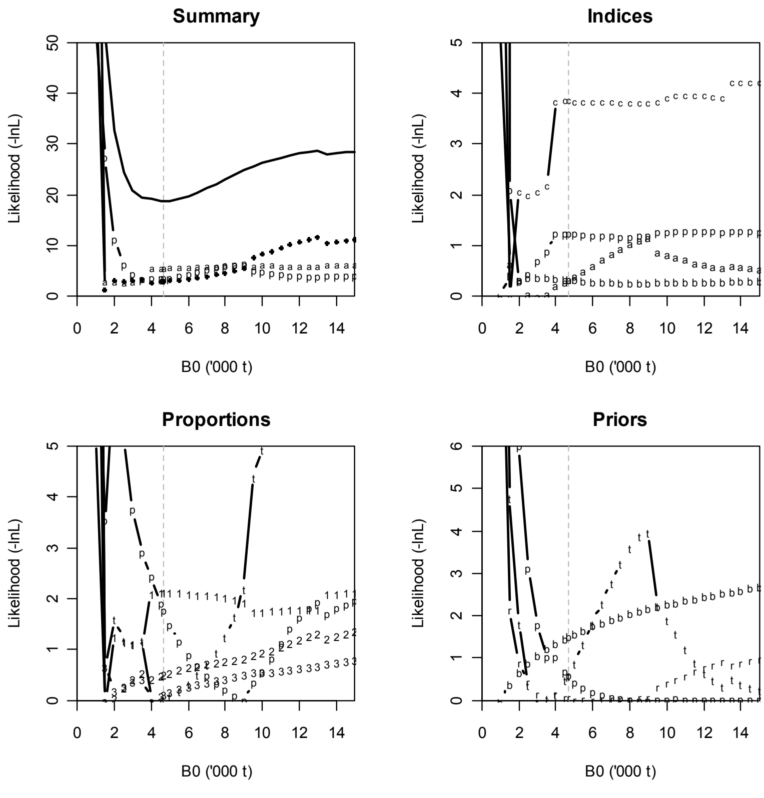

A4. 19: Likelihood profiles for model Base2 for SCI 1 when B_0 is fixed in the model. Figures show profiles for main priors (top left, p-priors, a – abundance indices, • – proportions at length), abundance indices (top right, a - trawl survey step 1, b – trawl survey step 2, c - CPUE, p – photo survey), proportion at length data (bottom left, t-trawl, 1 – observer time step 1, 2 – observer time step 2, 3 – observer time step 3) and priors (bottom right, b- B_0, YCS - r, p- *q-Photo*, t – *q-Trawl*).

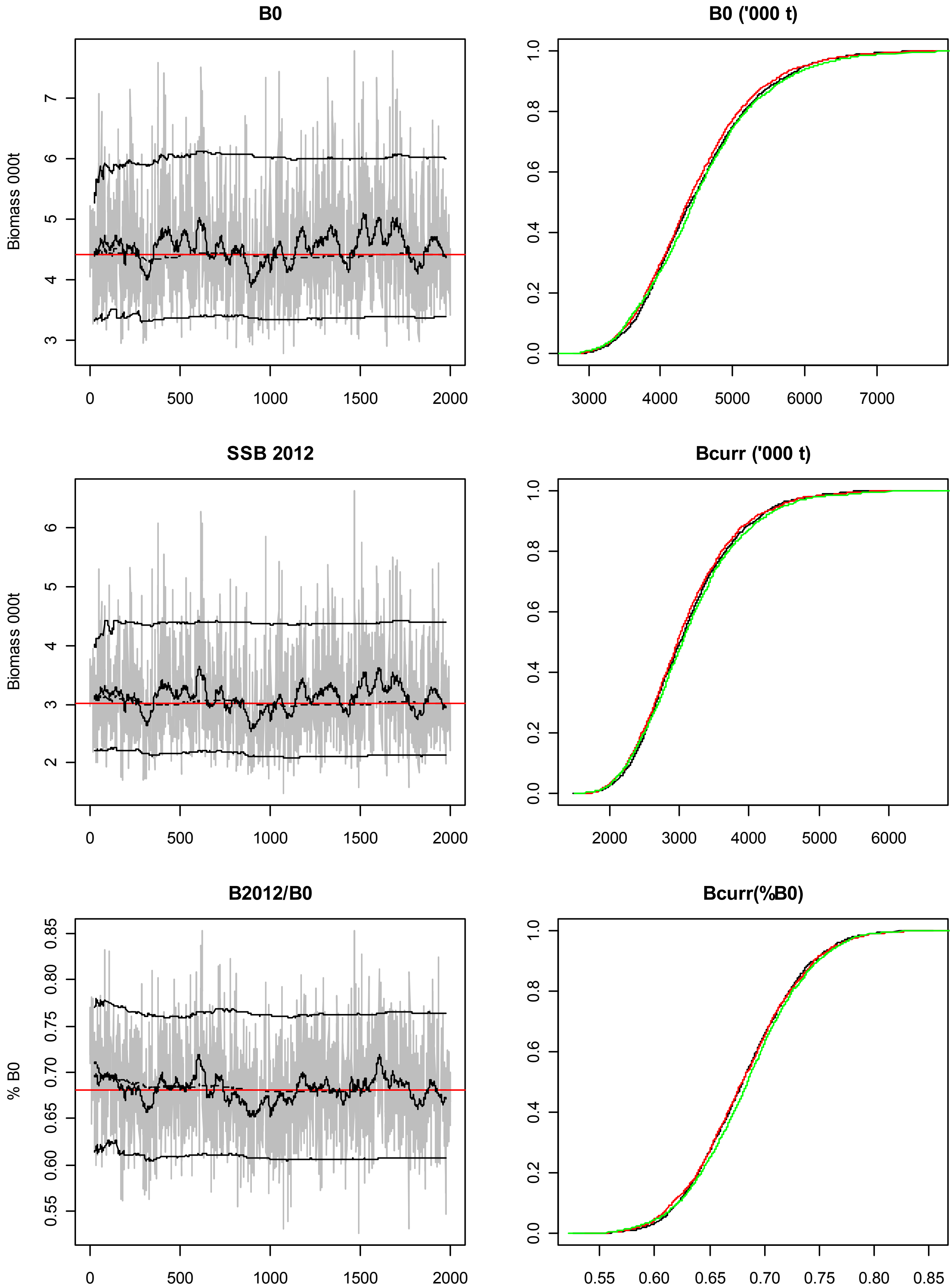

A4. 20: MCMC traces for B_0, SSB_{2012}, and SSB_{2012}/B_0 terms for the Base2 model for SCI 1, along with cumulative frequency distributions for three independent MCMC chains.

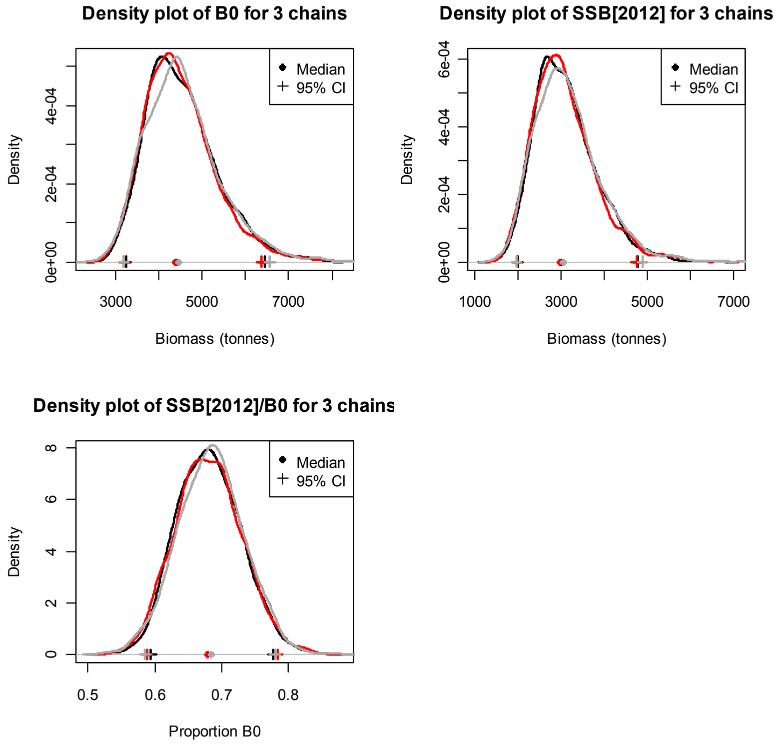

A4. 21: Density plots for B_0, SSB_{2012}, and SSB_{2012}/B_0 terms for the Base2 model for SCI 1 for three independent MCMC chains, with median and 95% confidence intervals.

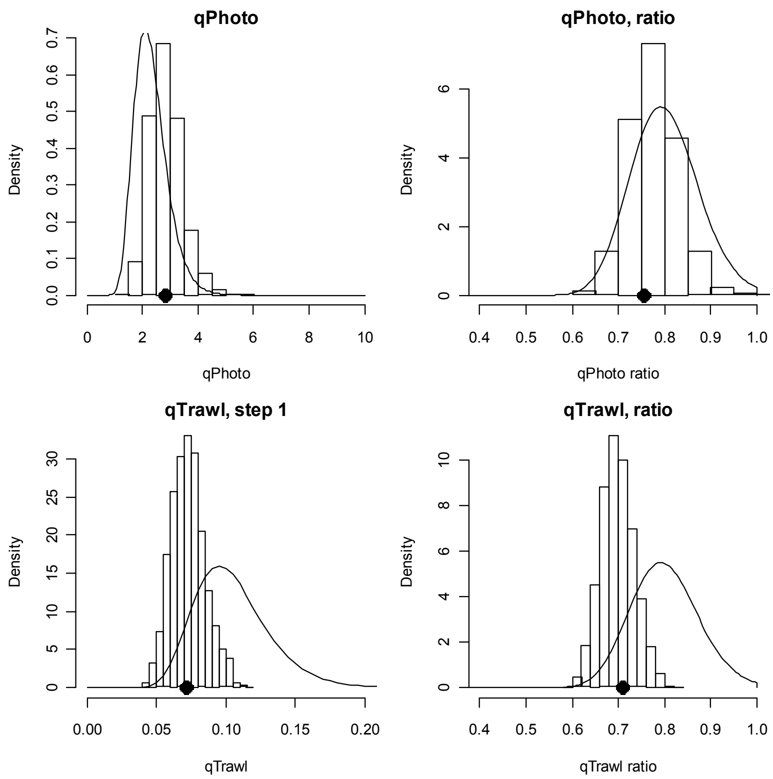

A4. 22: Marginal posterior distributions (histograms), MPD estimates (solid symbols) and distributions of priors (lines) for catchability terms.

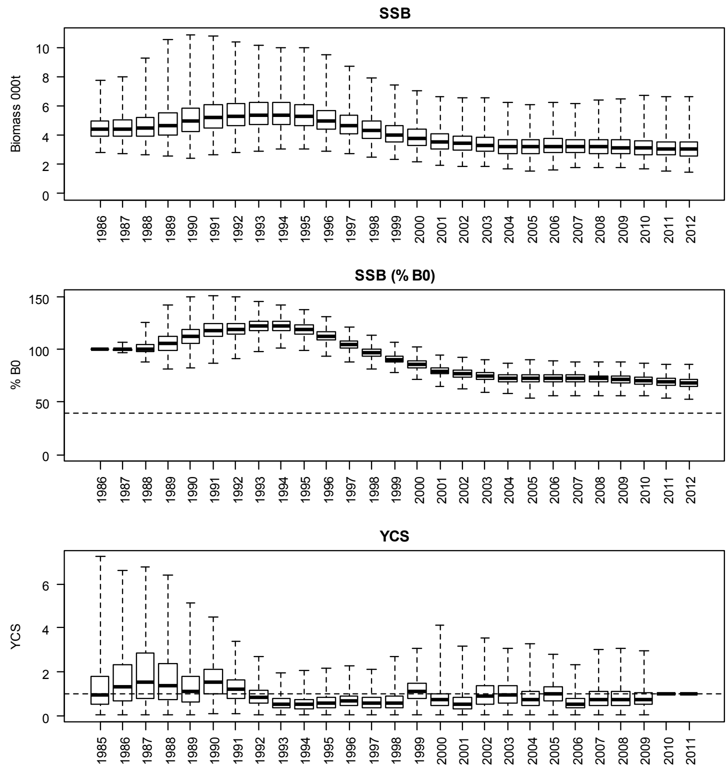

A4. 23: Posterior trajectory of SSB, SSB_{2012}/B_0 and YCS.

13. APPENDIX 5. SCI 1 Base3 model plots (M=0.3)

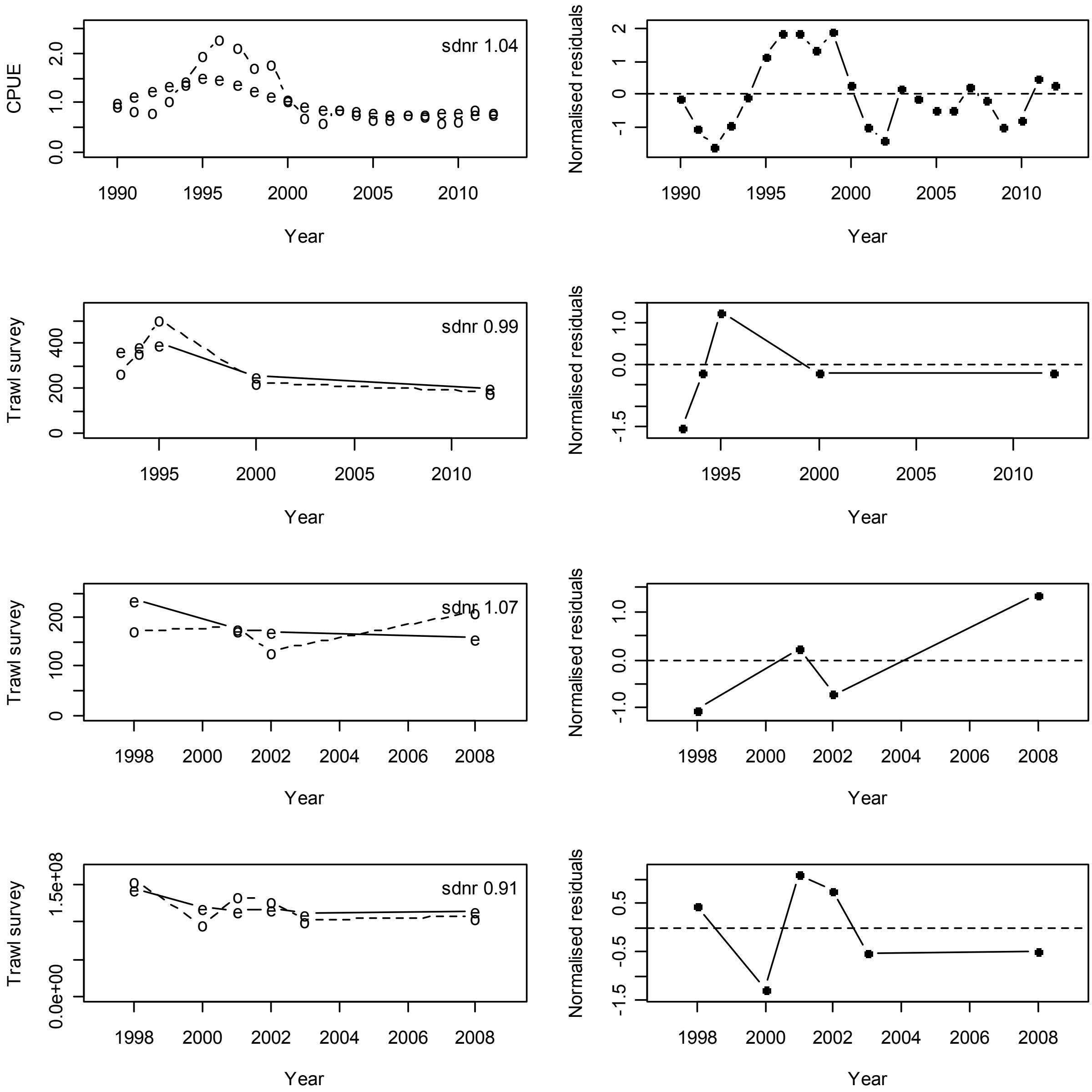

A5. 1: Fits to abundance indices (left column) and normalised residuals (right column) for standardised CPUE index (top row) trawl survey biomass index covering whole area (second row), trawl survey biomass index covering limited area (third row) and photo survey abundance index (fourth row) for SCI 1 Base3 model.

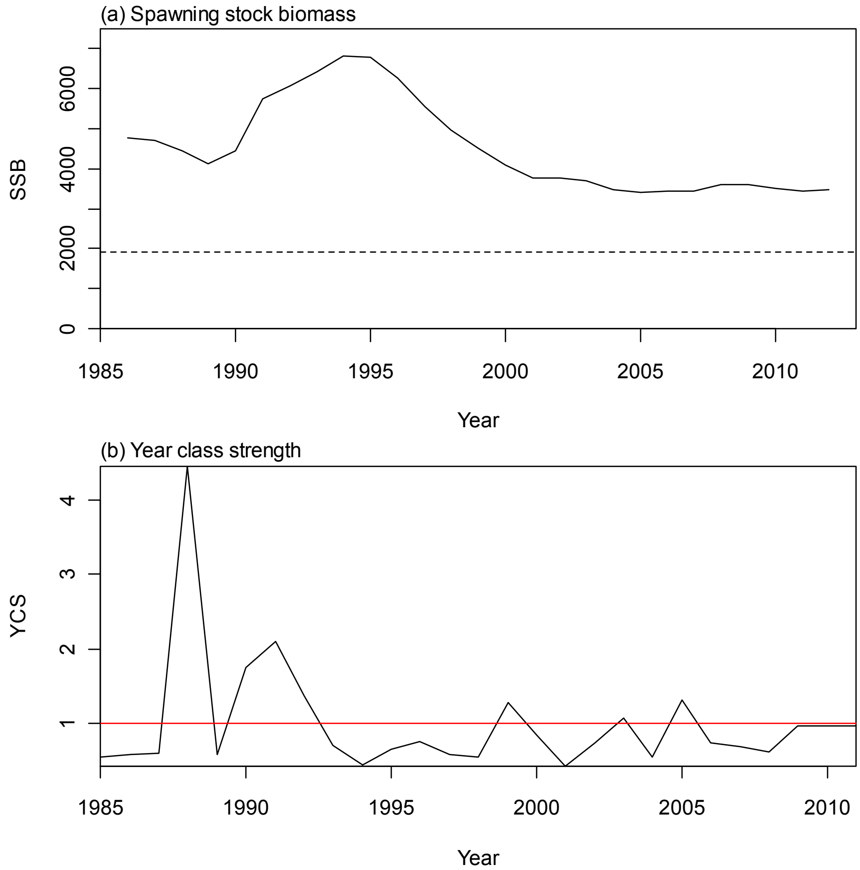

A5. 2: Spawning stock biomass trajectory (upper plot), year class strength (lower plot) for SCI 1 Base3 model.

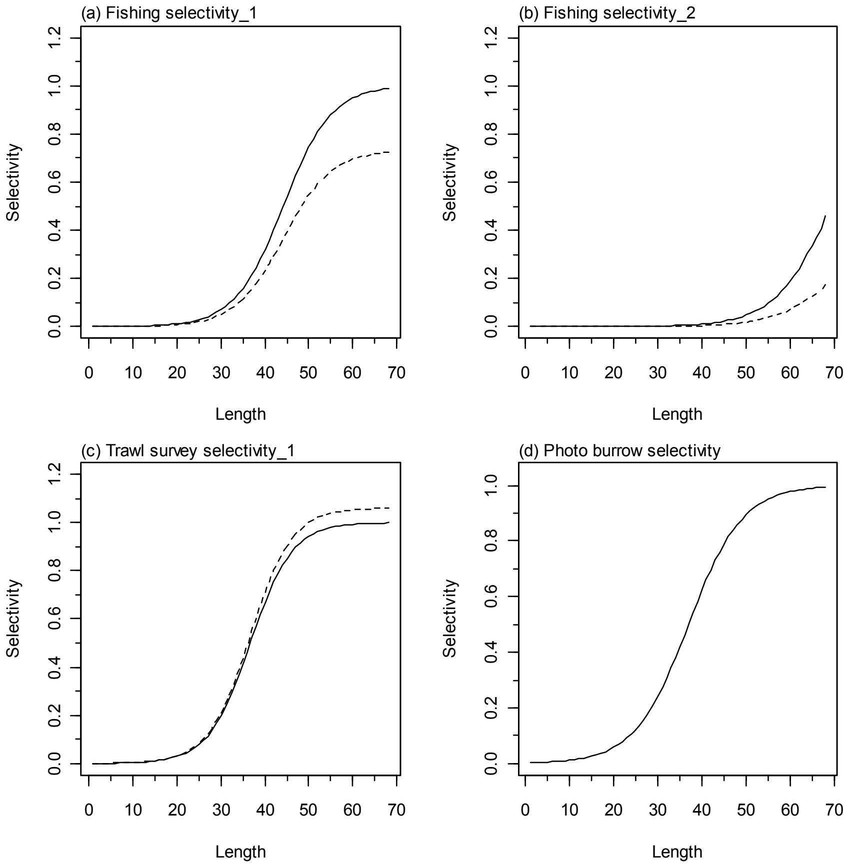

A5. 3: Fishery and survey selectivity curves. Solid line – females, dotted line – males. The scampi burrow index is not sexed, and a single selectivity applies.

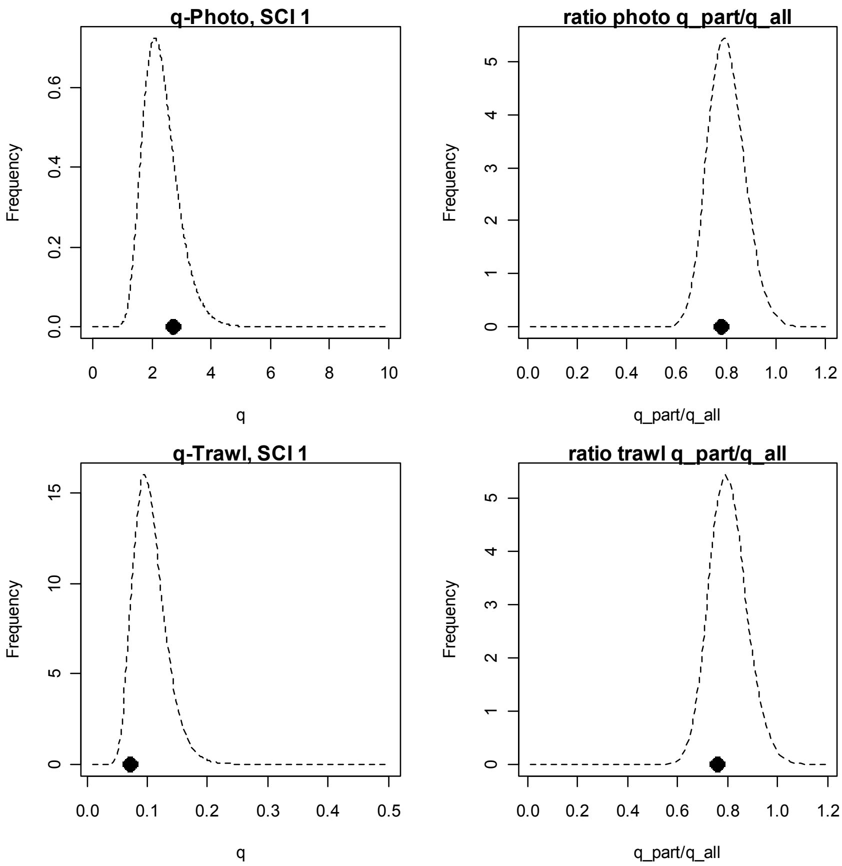

A5. 4: Catchability estimates from MPD model run, plotted in relation to prior distribution.

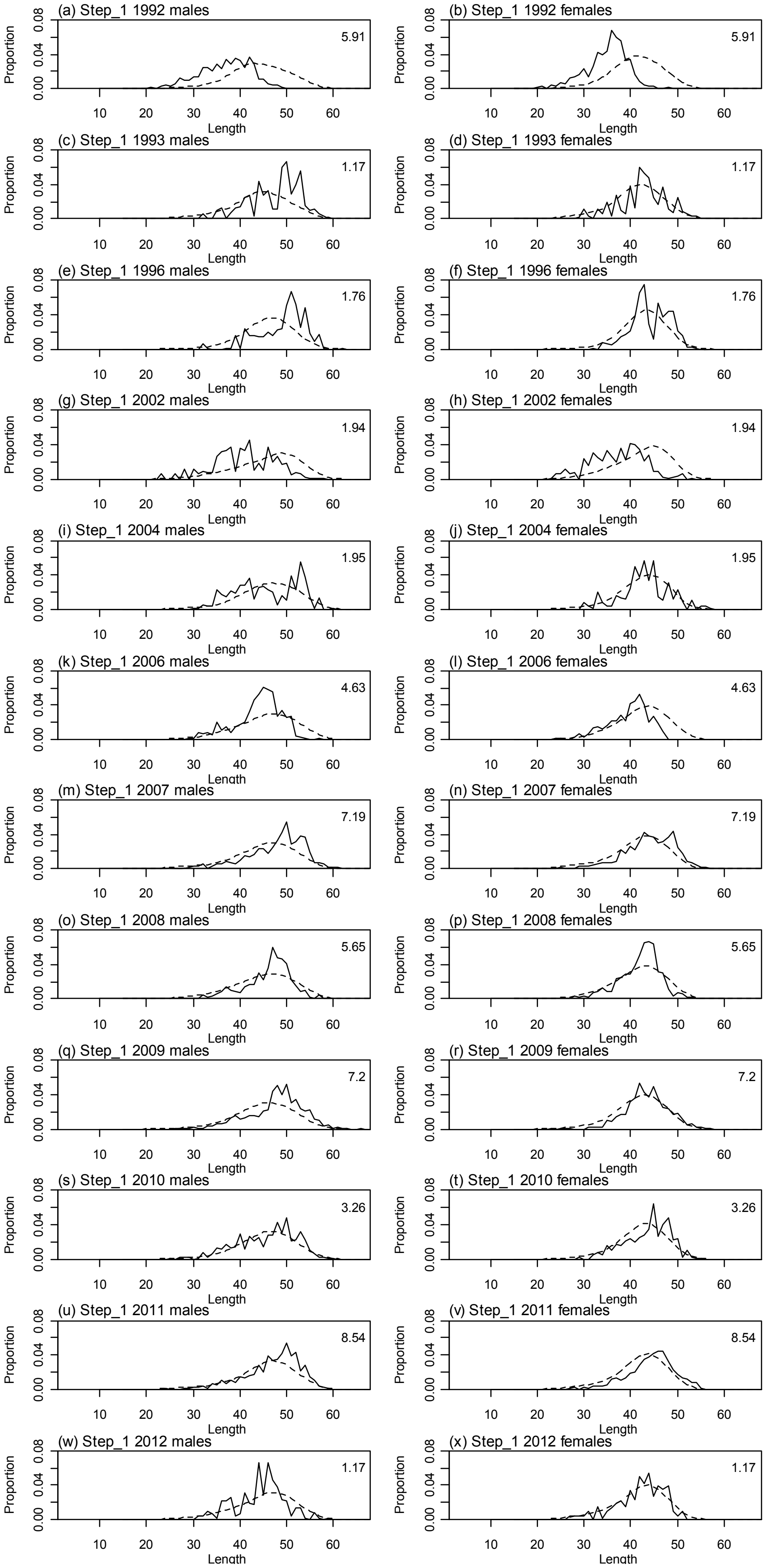

A5. 5: Observed (solid line) and fitted (dashed line) length frequency distributions for observer samples, time step 1. Number in top right of each plot is effective sample size.

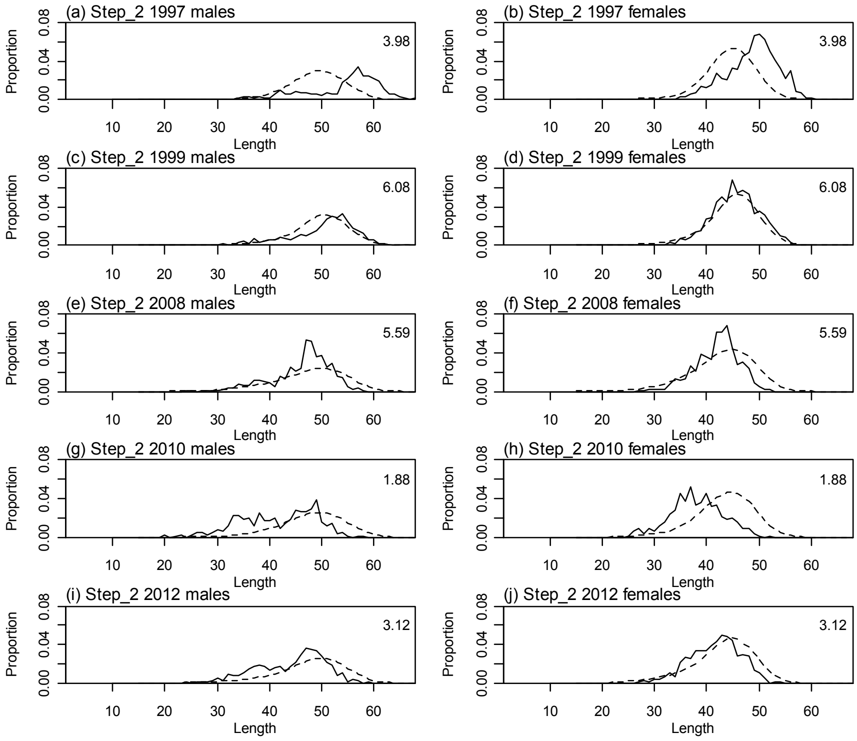

A5. 6: Observed (solid line) and fitted (dashed line) length frequency distributions for observer samples, time step 2. Number in top right of each plot is effective sample size.

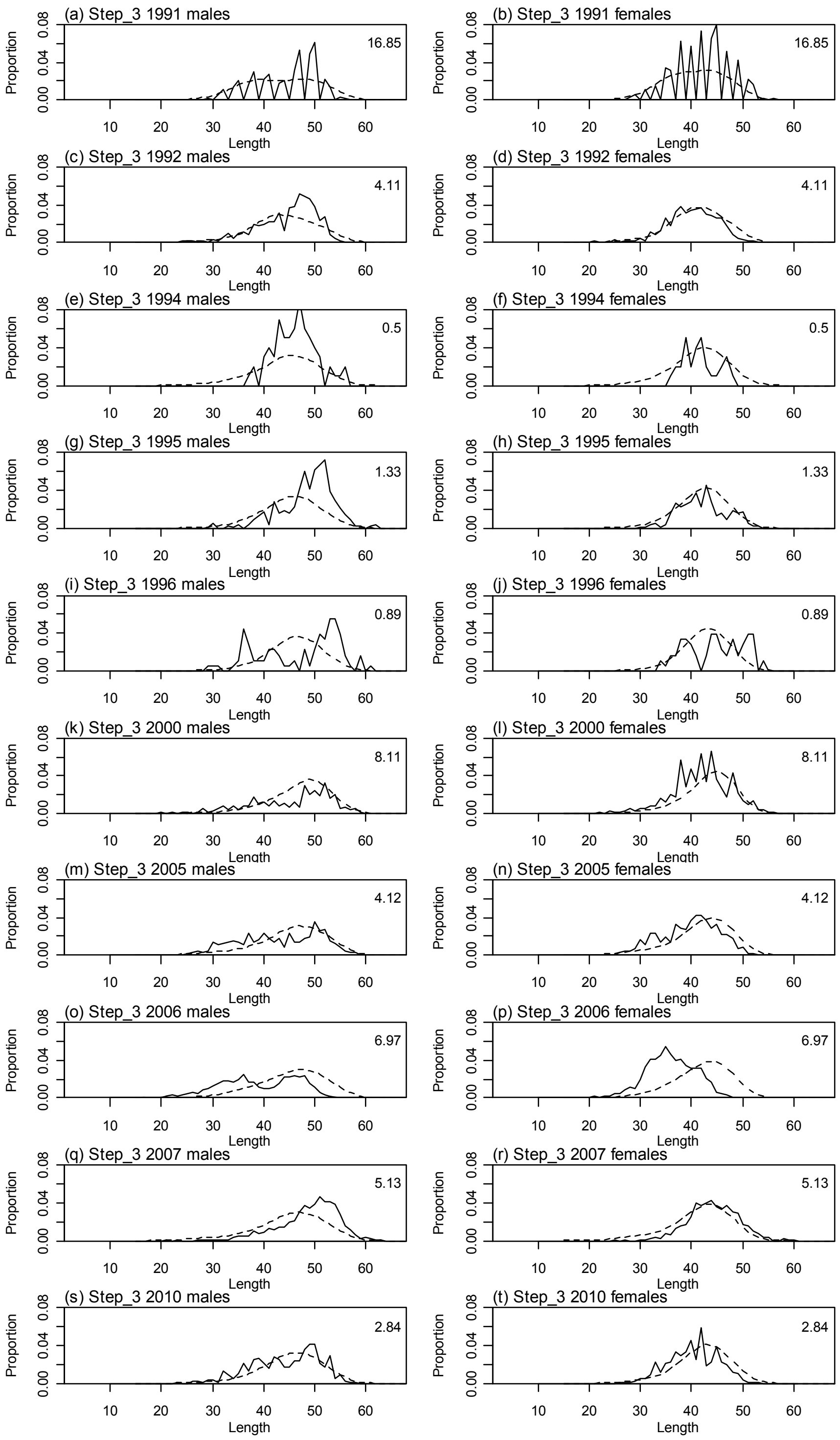

A5. 7: Observed (solid line) and fitted (dashed line) length frequency distributions for observer samples, time step 3. Number in top right of each plot is effective sample size.

A5. 8: Numbers of scampi measured, estimated multinomial N sample size, and effective sample size used within the model for length frequency distributions for observer samples, time step 1.

	Measured	Multinomial N	Effective sample size
N_1992	1717	1738	5.91
N_1993	263	345	1.17
N_1996	500	519	1.76
N_2002	454	570	1.94
N_2004	315	574	1.95
N_2006	1768	1361	4.63
N_2007	2404	2115	7.19
N_2008	2150	1662	5.65
N_2009	2475	2118	7.20
N_2010	1300	959	3.26
N_2011	2733	2513	8.54
N_2012	271	343	1.17

A5. 9: Numbers of scampi measured, estimated multinomial N sample size, and effective sample size used within the model for length frequency distributions for observer samples, time step 2.

	Measured	Multinomial N	Effective sample size
N_1997	1905	1802	3.98
N_1999	2586	2751	6.08
N_2008	2847	2528	5.59
N_2010	1013	851	1.88
N_2012	1408	1410	3.12

A5. 10: Numbers of scampi measured, estimated multinomial N sample size, and effective sample size used within the model for length frequency distributions for observer samples, time step 3.

	Measured	Multinomial N	Effective sample size
N_1991	10245	6871	16.85
N_1992	1751	1677	4.11
N_1994	100	203	0.50
N_1995	450	543	1.33
N_1996	180	363	0.89
N_2000	3891	3309	8.11
N_2005	2113	1679	4.12
N_2006	3197	2842	6.97
N_2007	2600	2090	5.13
N_2010	3325	1159	2.84

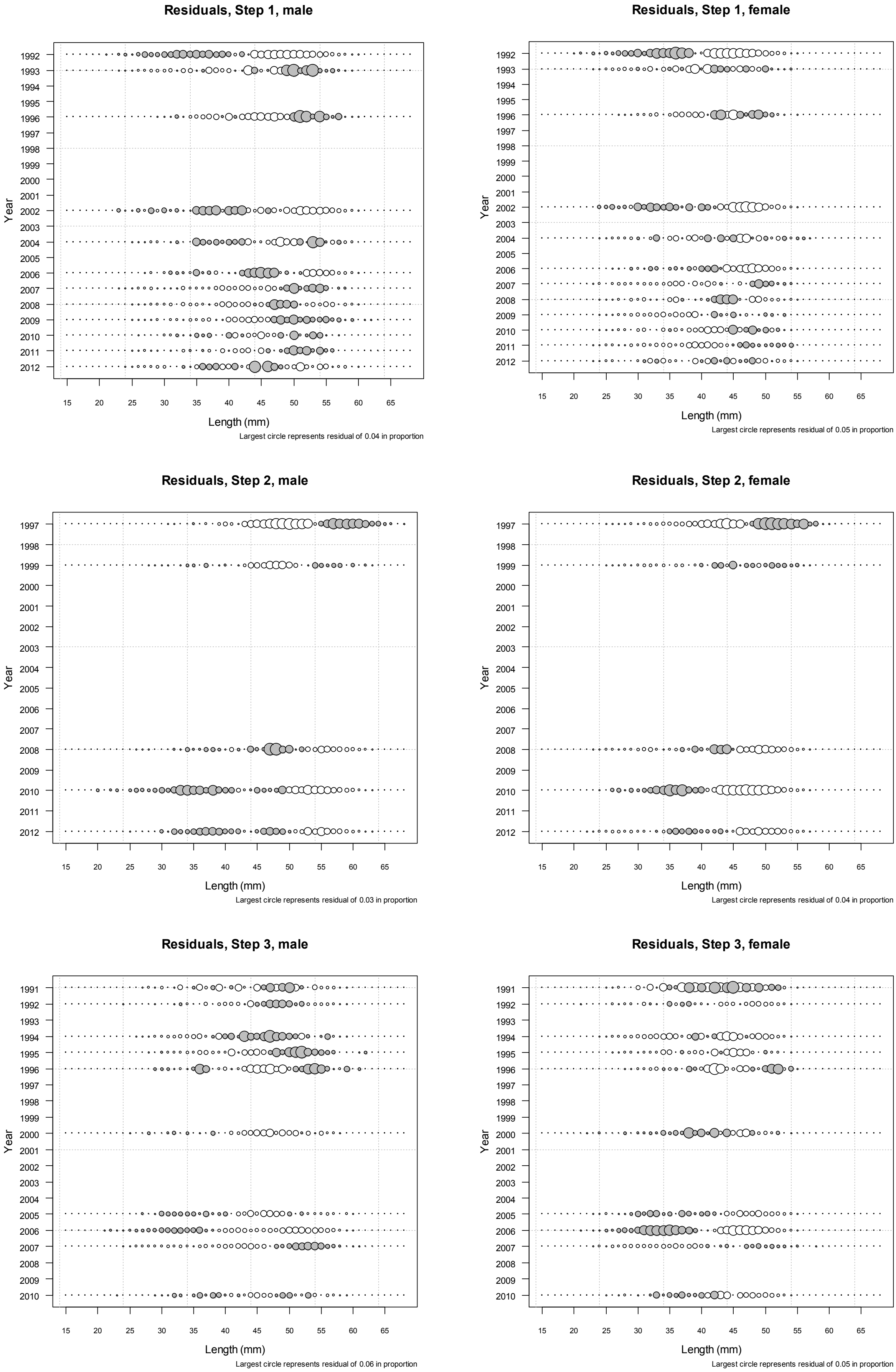

A5. 11: Bubble plots of residuals for fits to length frequency distributions for observer sampling.

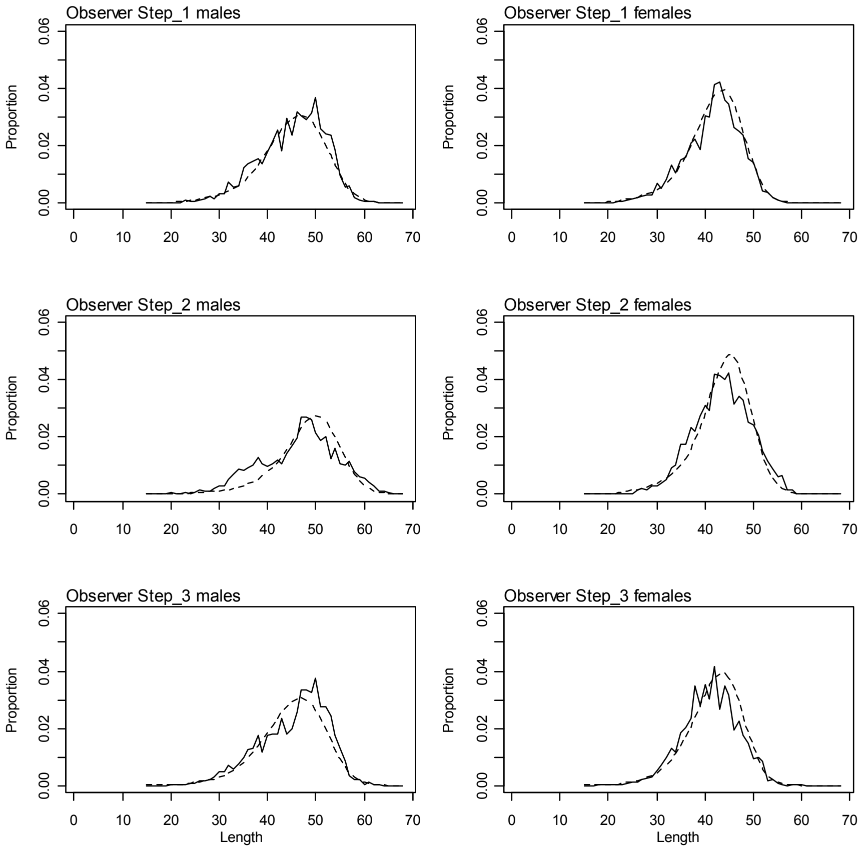

A5. 12: Average observed (solid line) and fitted (dashed line) length frequency distributions for observer samples.

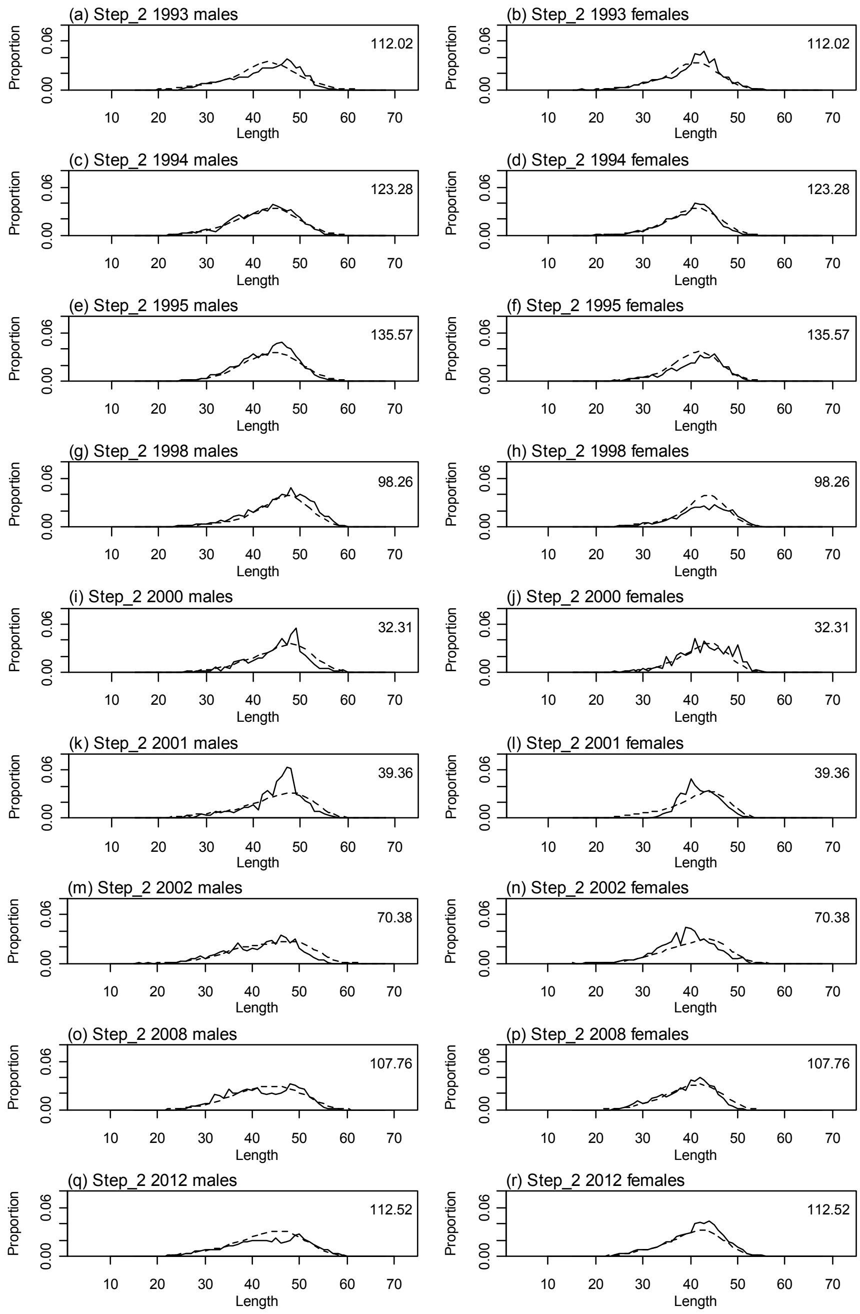

A5. 13: Observed (solid line) and fitted (dashed line) length frequency distributions for research survey samples. Number in top right of each plot is effective sample size.

A5. 14: Numbers of scampi measured, estimated multinomial N sample size, and effective sample size used within the model for length frequency distributions for research survey samples.

	Measured	Multinomial N	Effective sample size
N_1993	5710	8506	112.02
N_1994	5346	9361	123.28
N_1995	6334	10294	135.57
N_1998	4212	7461	98.26
N_2000	1360	2453	32.31
N_2001	1913	2989	39.36
N_2002	2647	5344	70.38
N_2008	3985	8182	107.76
N_2012	4353	8544	112.52

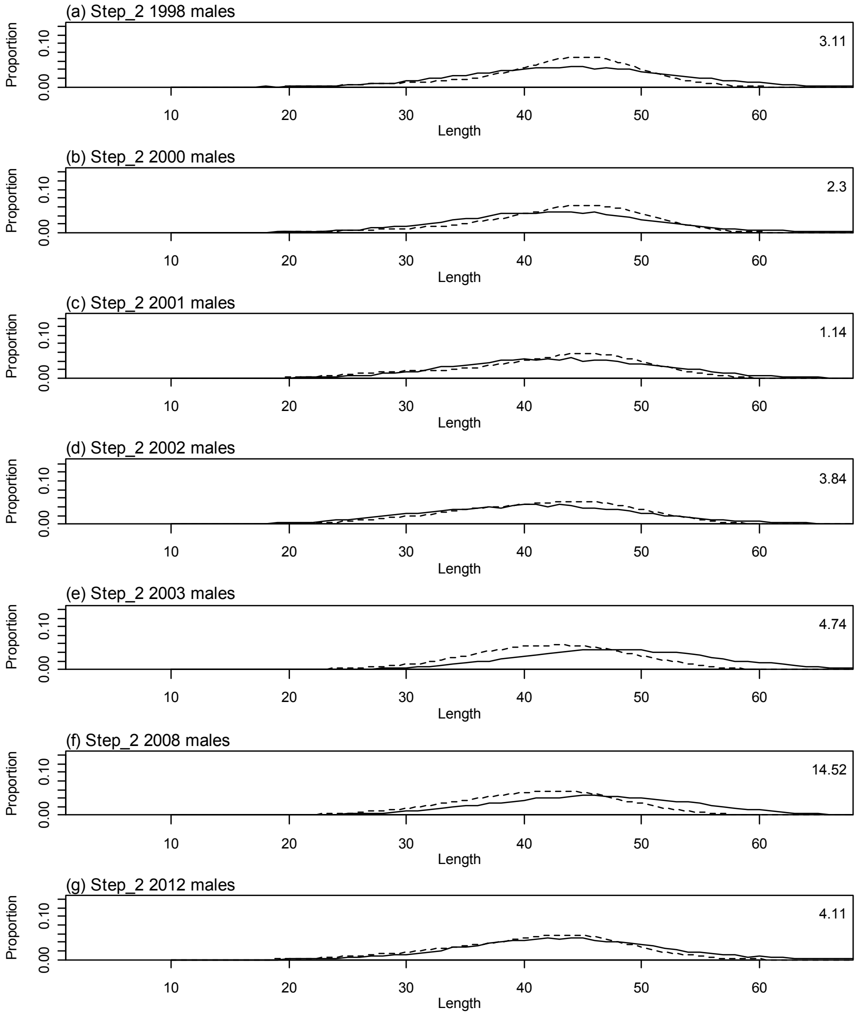

A5. 15: Observed (solid line) and fitted (dashed line) length frequency distributions for photographic survey scampi size estimation. Number in top right of each plot is effective sample size.

A5. 16: Numbers of scampi measured, estimated multinomial N sample size, and effective sample size used within the model for length frequency distributions for photographic survey samples.

	Measured	Multinomial N	Effective sample size
N_1998	46	93	3.11
N_2000	35	69	2.30
N_2001	17	34	1.14
N_2002	57	115	3.84
N_2003	73	142	4.74
N_2008	237	435	14.52
N_2012	62	123	4.11

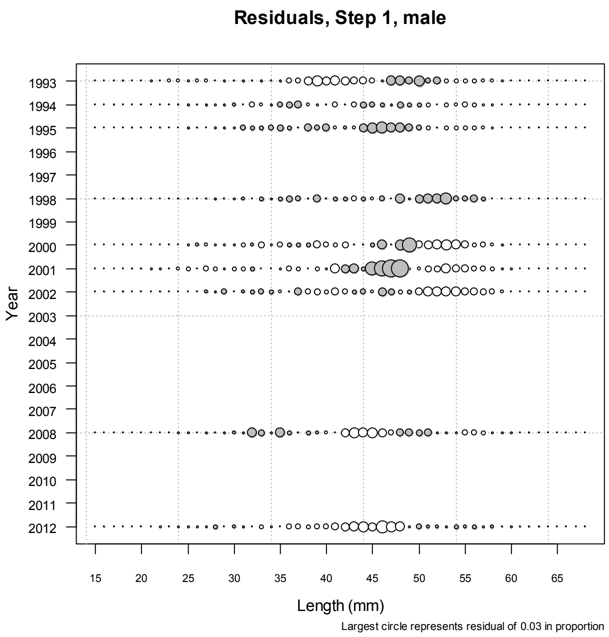

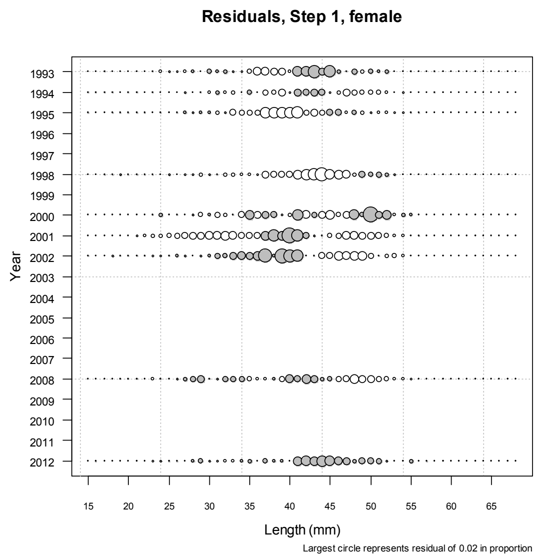

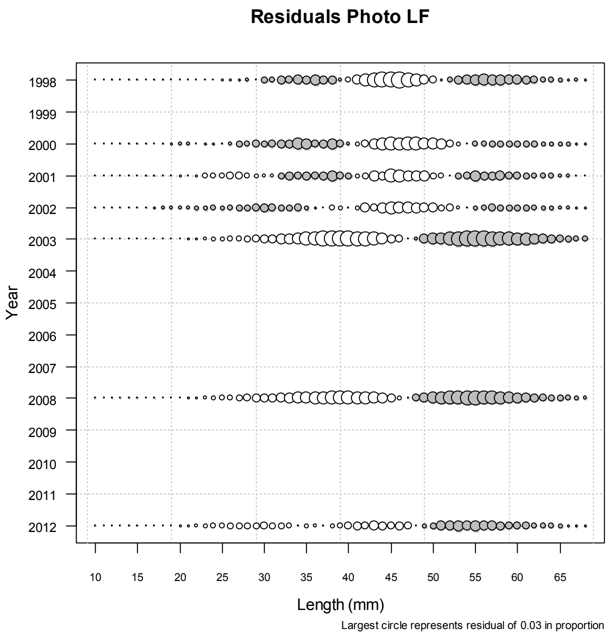

A5. 17: Bubble plots of residuals for fits to length frequency distributions for trawl survey sampling and photographic survey scampi size estimation.

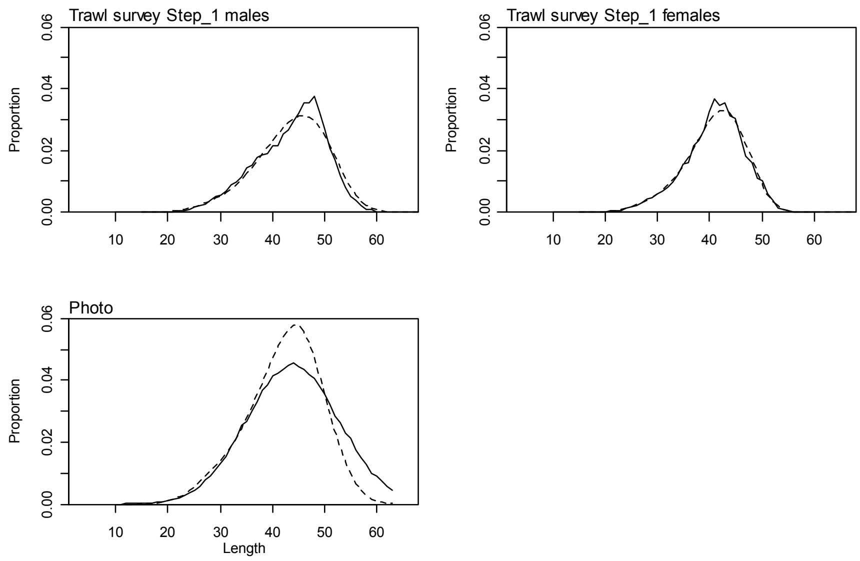

A5. 18: Average observed (solid line) and fitted (dashed line) length frequency distributions for trawl survey sampling and photographic survey scampi size estimation.

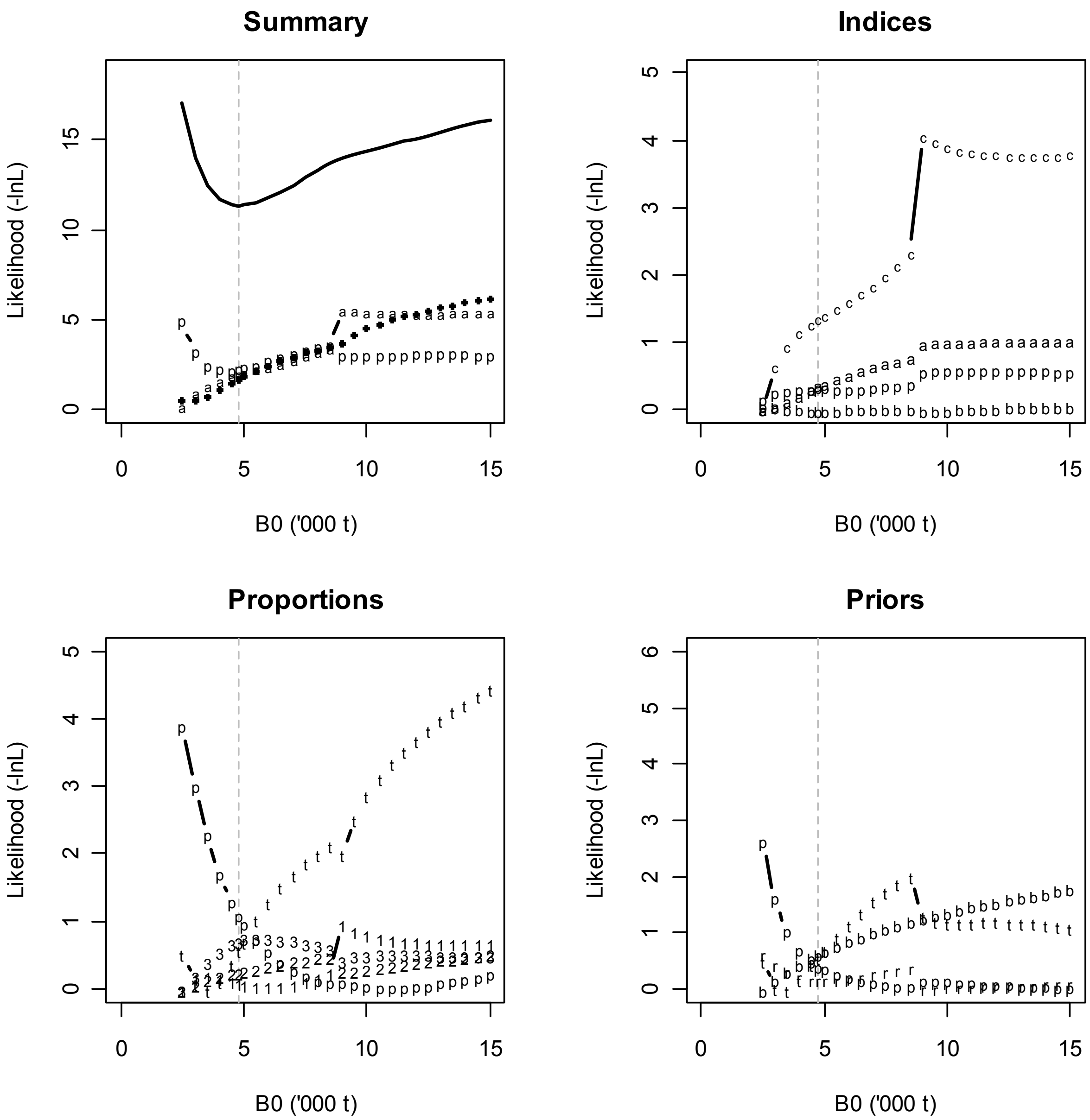

A5. 19: Likelihood profiles for model Base3 for SCI 1 when B_0 is fixed in the model. Figures show profiles for main priors (top left, p-priors, a – abundance indices, • – proportions at length), abundance indices (top right, a - trawl survey step 1, b – trawl survey step 2, c - CPUE, p – photo survey), proportion at length data (bottom left, t-trawl, 1 – observer time step 1, 2 – observer time step 2, 3 – observer time step 3) and priors (bottom right, b- B_0, YCS - r, p- *q-Photo*, t – *q-Trawl*).

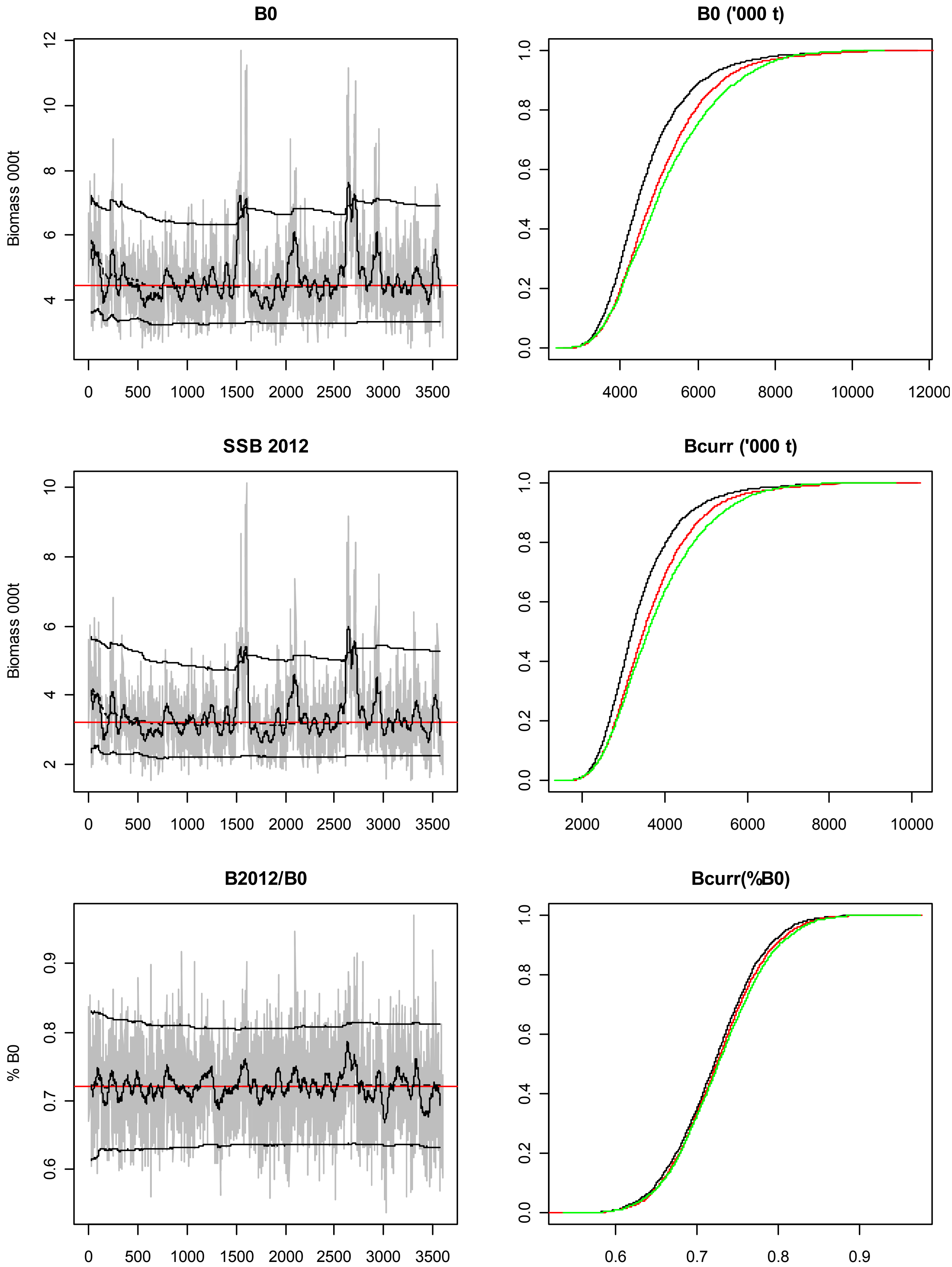

A5. 20: MCMC traces for B_0, SSB_{2012}, and SSB_{2012}/B_0 terms for the Base3 model for SCI 1, along with cumulative frequency distributions for three independent MCMC chains.

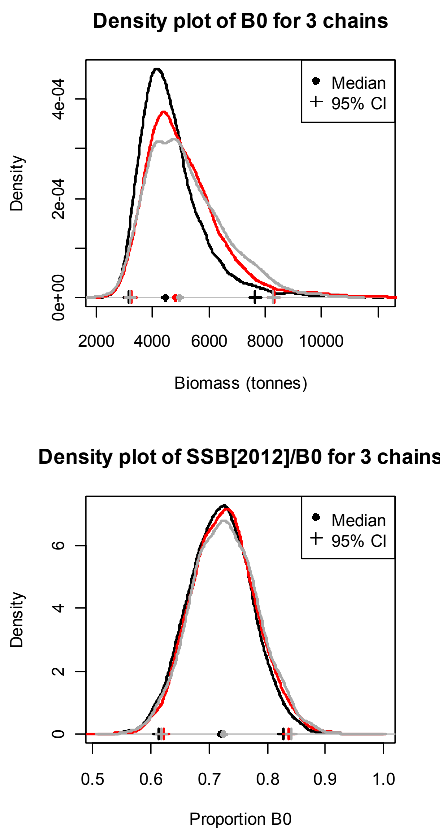

A5. 21: Density plots for B_0, SSB_{2012}, and SSB_{2012}/B_0 terms for the Base3 model for SCI 1 for three independent MCMC chains, with median and 95% confidence intervals.

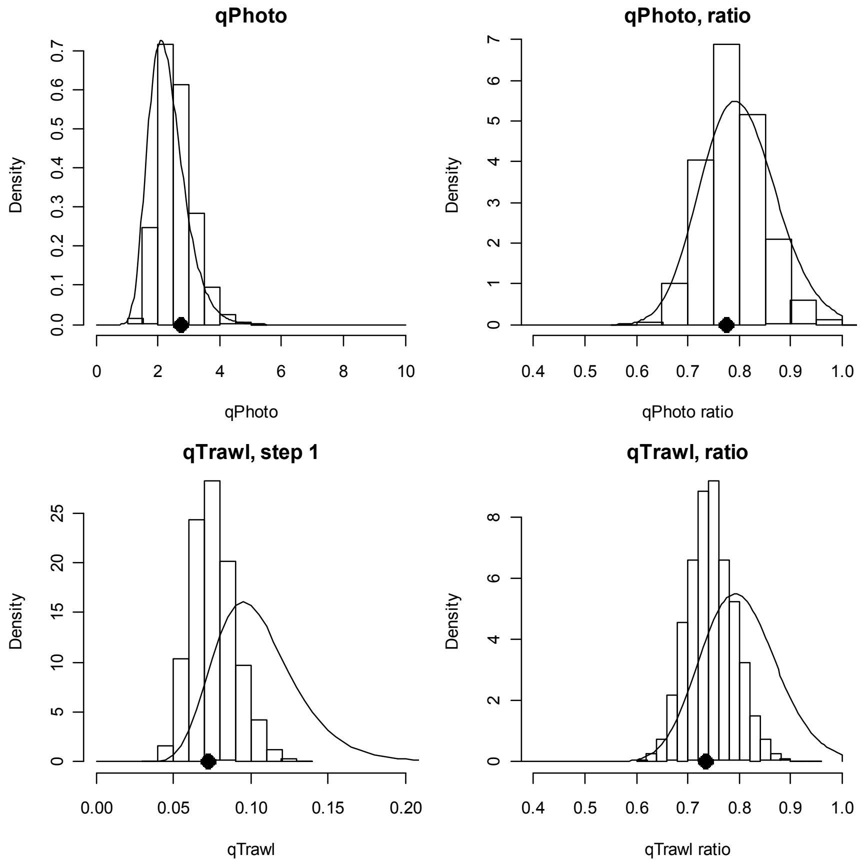

A5. 22: Marginal posterior distributions (histograms), MPD estimates (solid symbols) and distributions of priors (lines) for catchability terms.

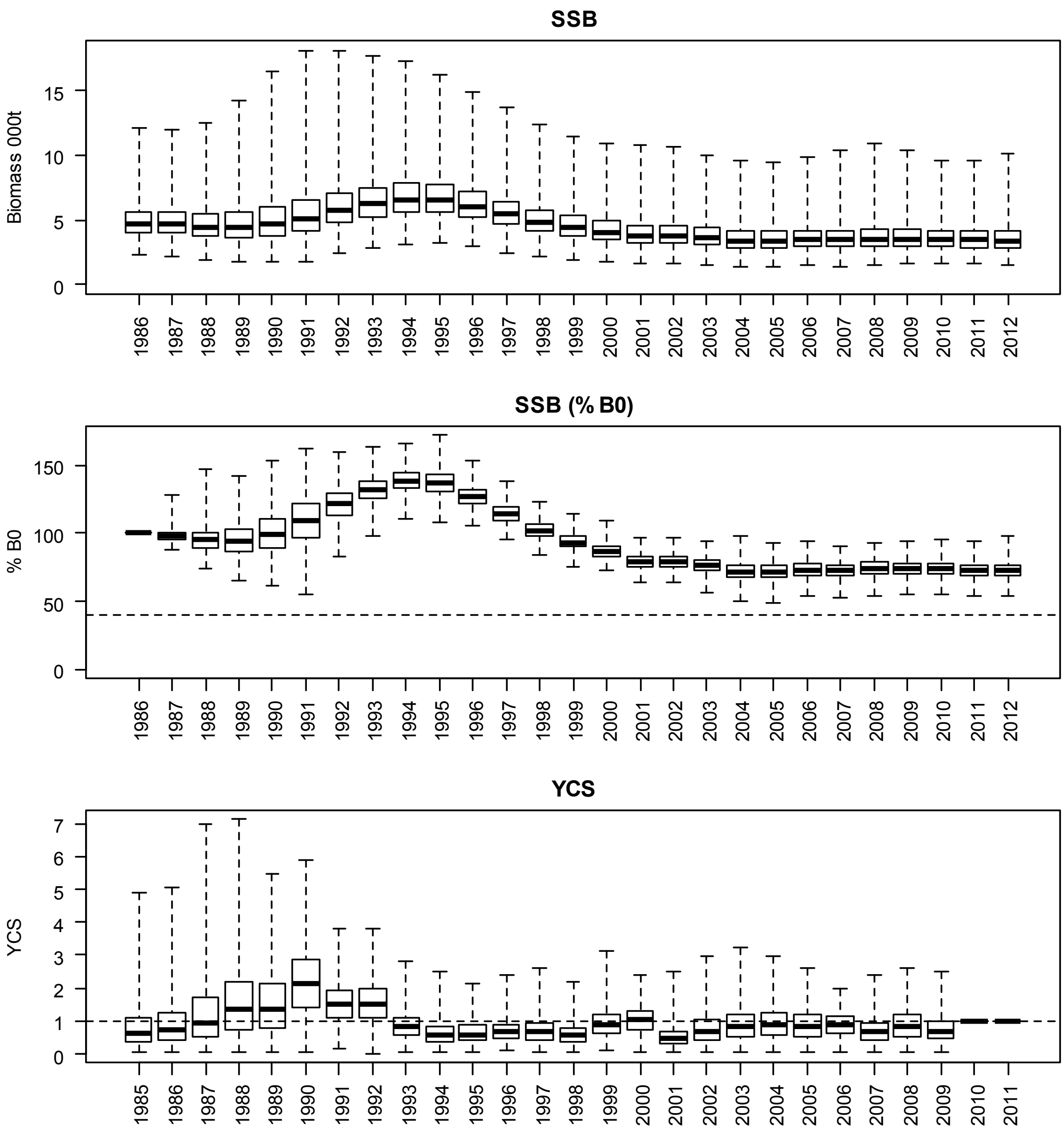

A5. 23: Posterior trajectory of SSB, SSB_{2012}/B_0 and YCS.

14. APPENDIX 6. SCI 2 model plots (M=0.2)

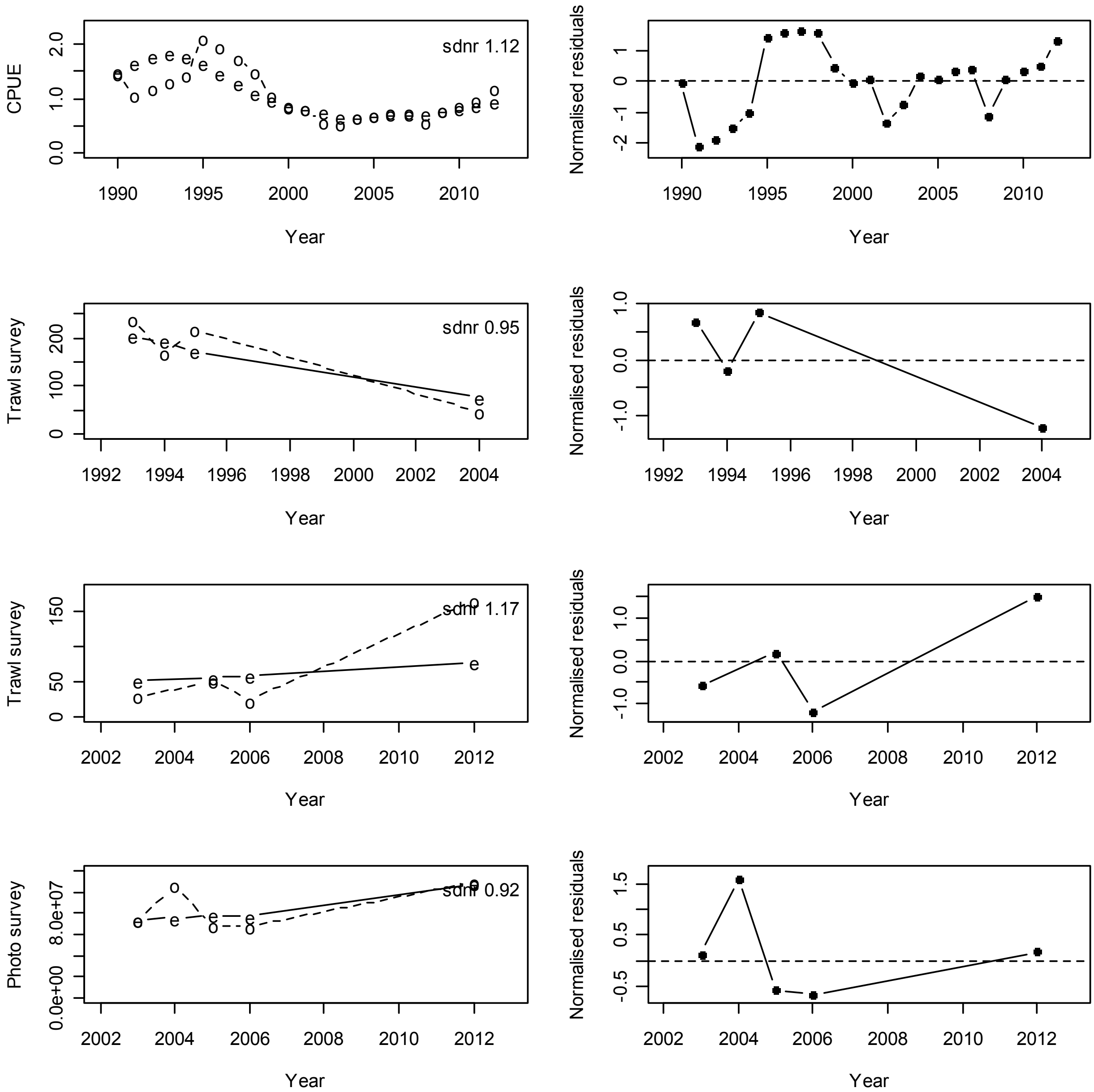

A6. 1: Fits to abundance indices (left column) and normalised residuals (right column) for standardised CPUE index (top row) trawl survey biomass index covering whole area (second row), trawl survey biomass index covering limited area (third row) and photo survey abundance index (fourth row) for SCI 2 Base2 model.

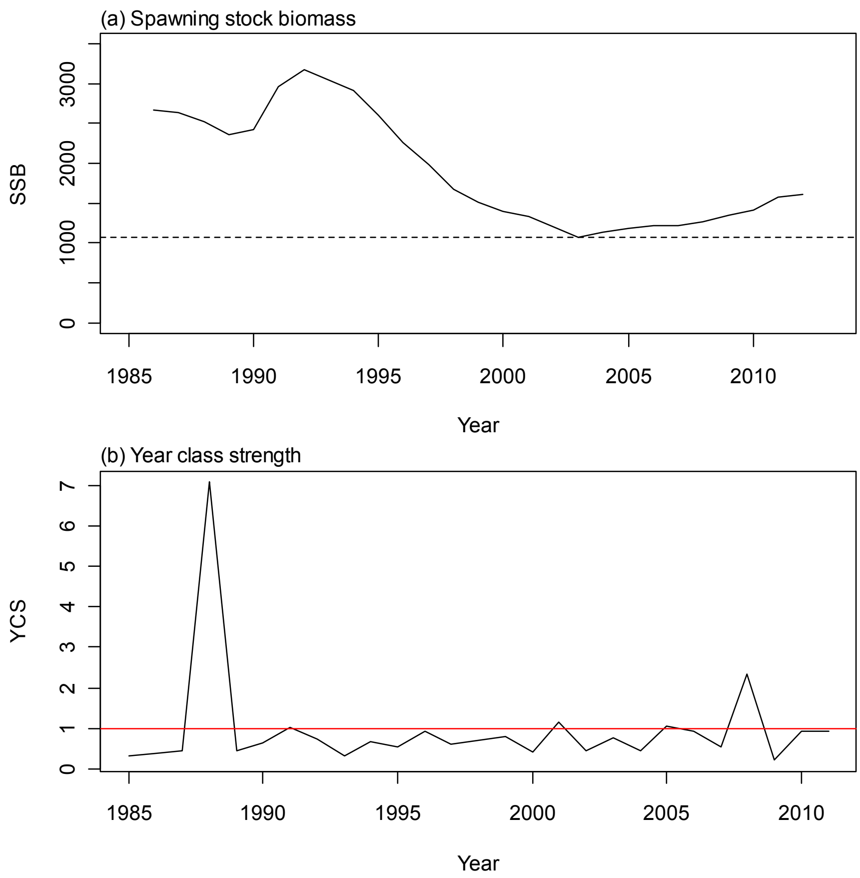

A6. 2: Spawning stock biomass trajectory (upper plot), year class strength (lower plot) for SCI 2 Base2 model.

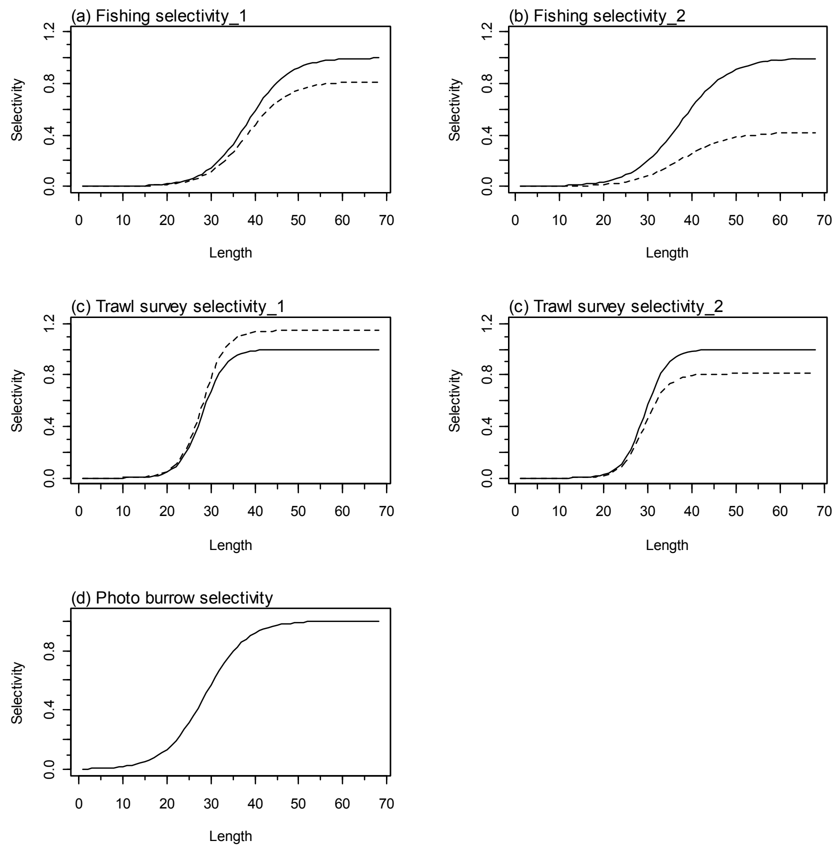

A6. 3: Fishery and survey selectivity curves. Solid line – females, dotted line – males. The scampi burrow index is not sexed, and a single selectivity applies.

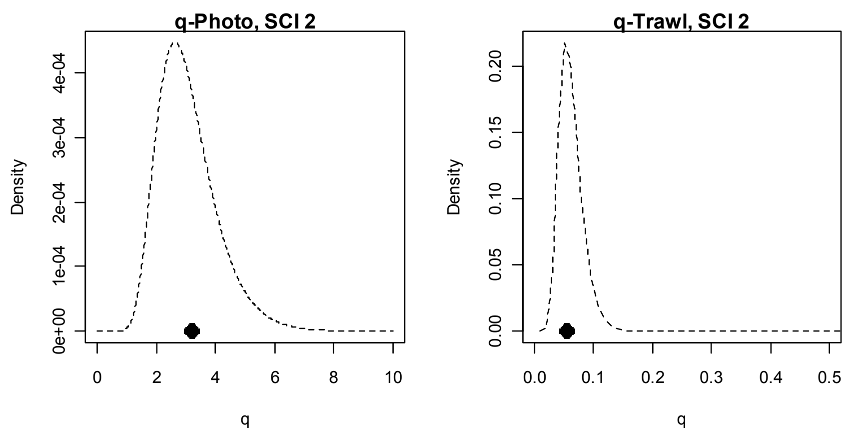

A6. 4: Catchability estimates from MPD model run, plotted in relation to prior distribution.

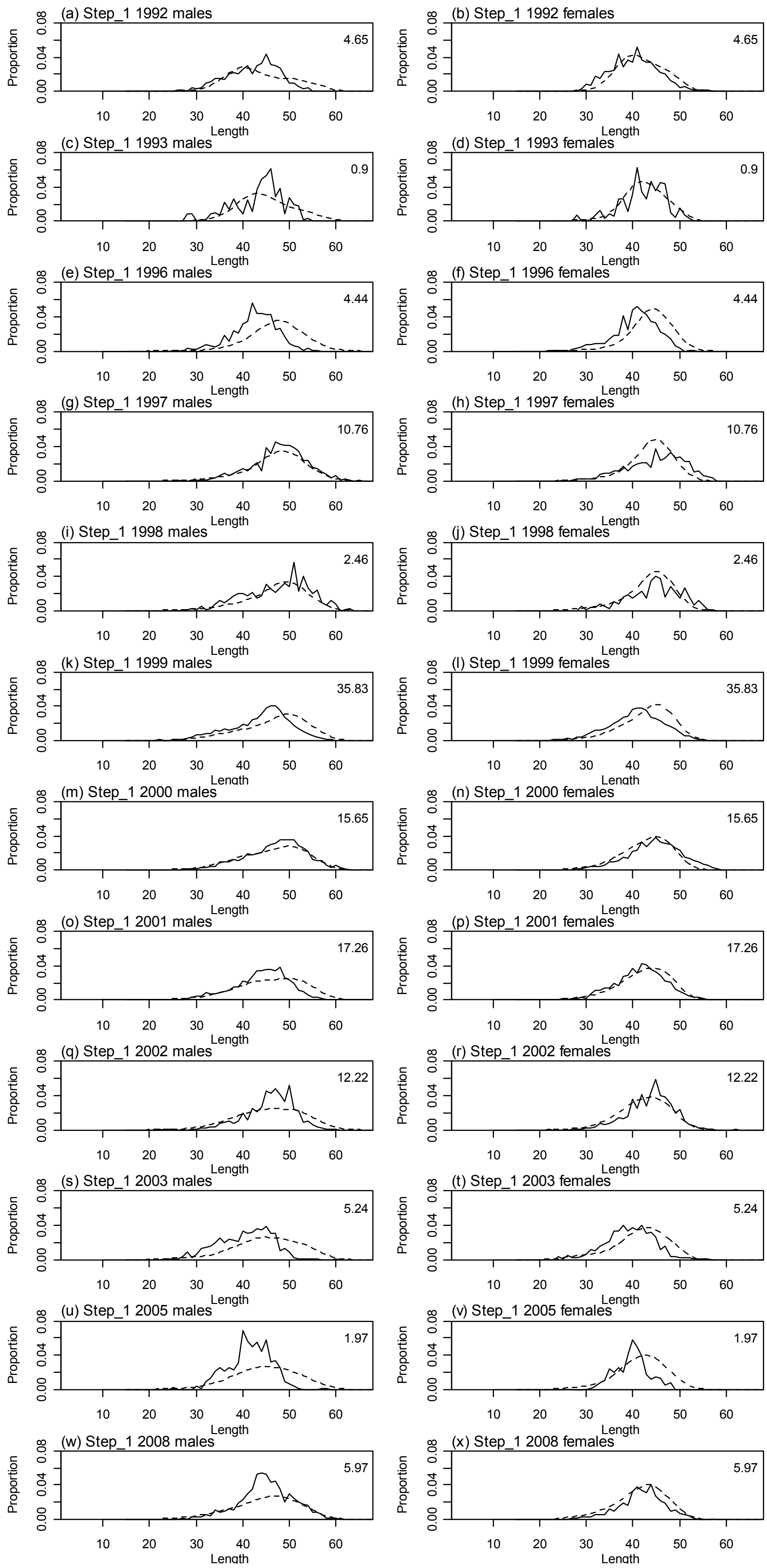
(a) Step_1 1992 males
(b) Step_1 1992 females
(c) Step_1 1993 males
(d) Step_1 1993 females
(e) Step_1 1996 males
(f) Step_1 1996 females
(g) Step_1 1997 males
(h) Step_1 1997 females
(i) Step_1 1998 males
(j) Step_1 1998 females
(k) Step_1 1999 males
(l) Step_1 1999 females
(m) Step_1 2000 males
(n) Step_1 2000 females
(o) Step_1 2001 males
(p) Step_1 2001 females
(q) Step_1 2002 males
(r) Step_1 2002 females
(s) Step_1 2003 males
(t) Step_1 2003 females
(u) Step_1 2005 males
(v) Step_1 2005 females
(w) Step_1 2008 males
(x) Step_1 2008 females
4.65
0.9
4.44
10.76
2.46
35.83
15.65
17.26
12.22
5.24
1.97
5.97
Proportion
Length

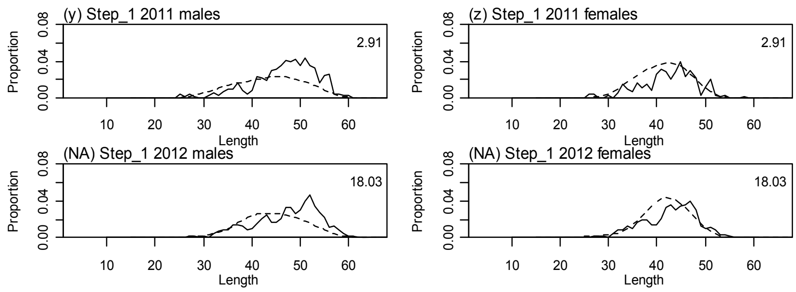

A6. 5: Observed (solid line) and fitted (dashed line) length frequency distributions for observer samples, time step 1. Number in top right of each plot is effective sample size.

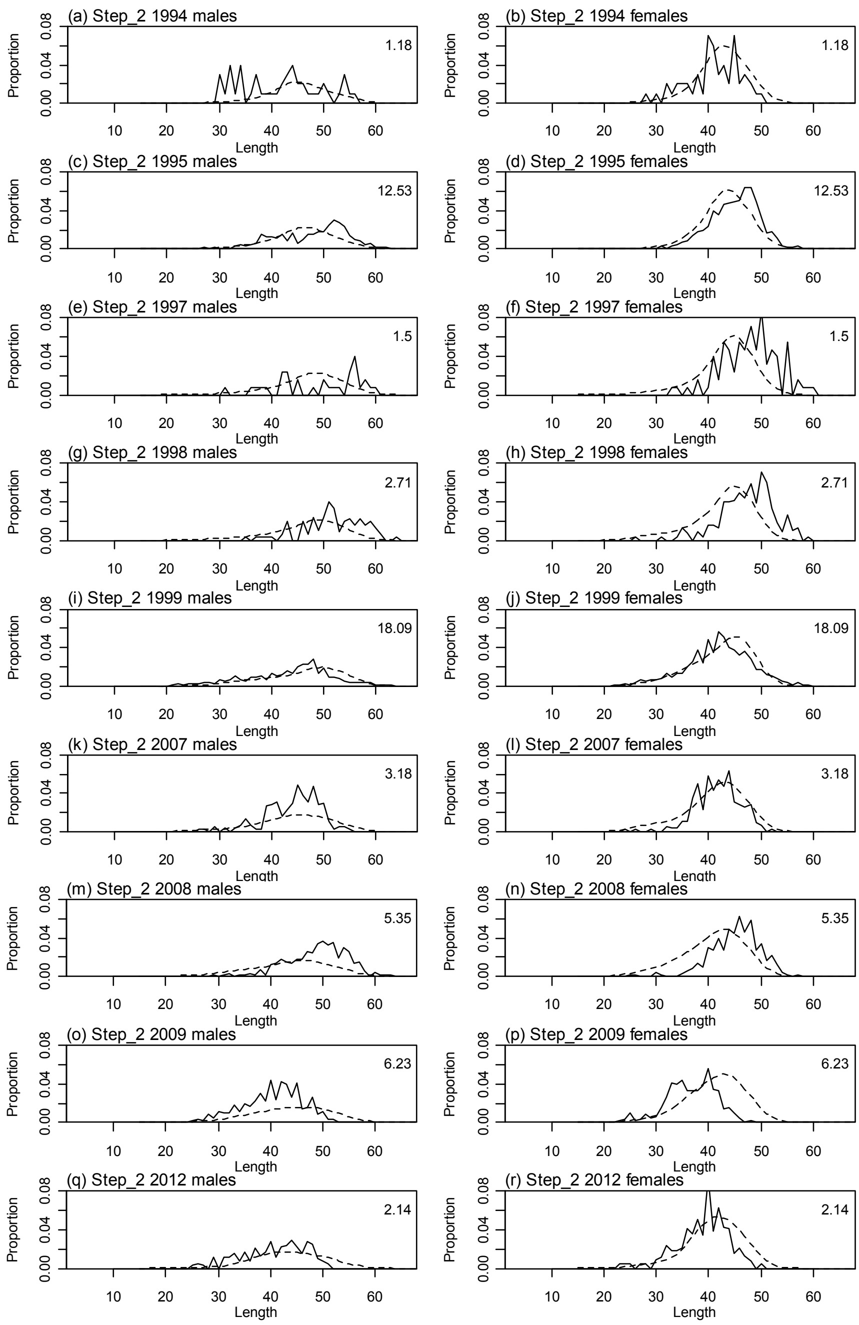

A6. 6: Observed (solid line) and fitted (dashed line) length frequency distributions for observer samples, time step 2. Number in top right of each plot is effective sample size.

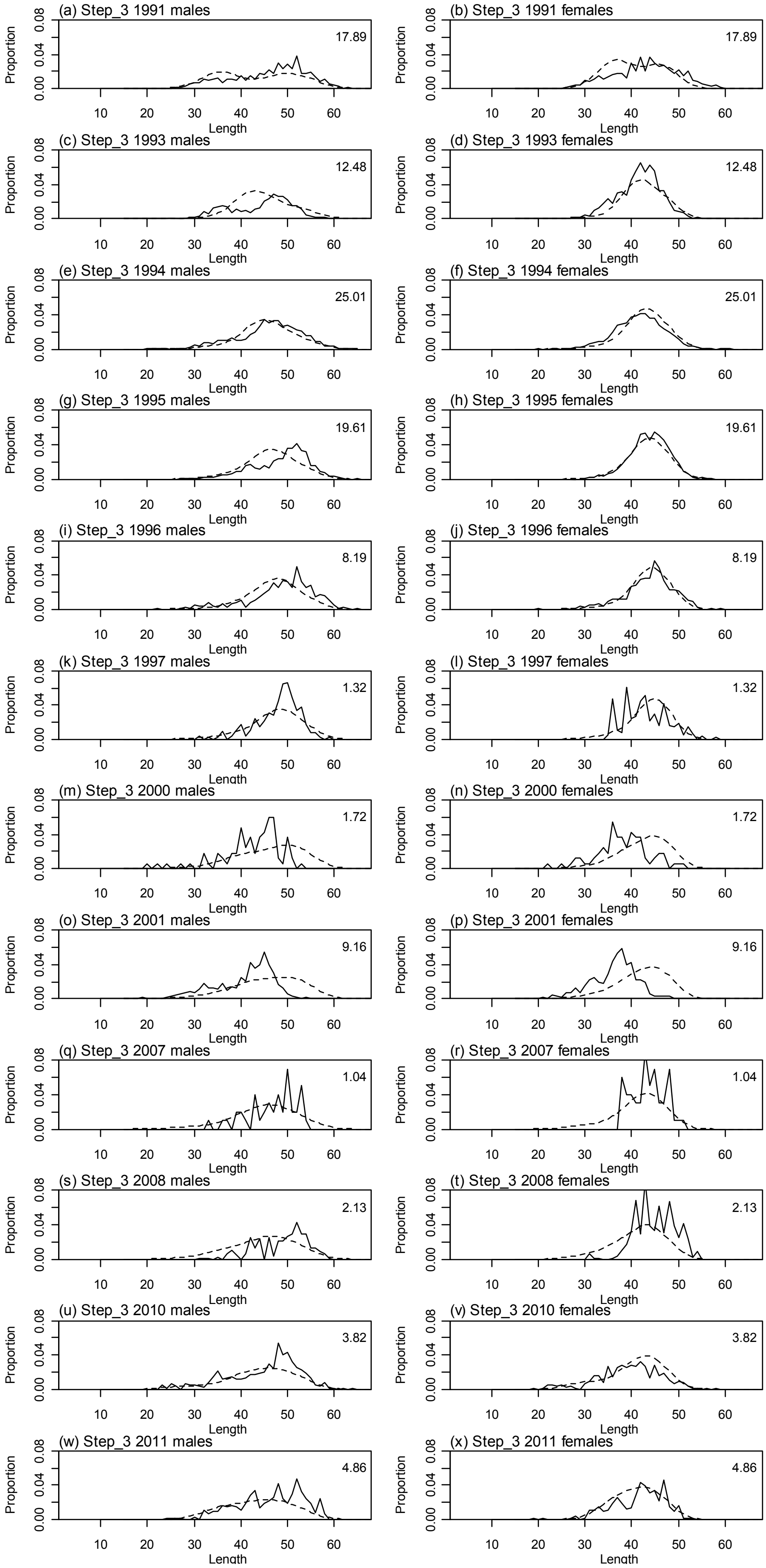

A6. 7: Observed (solid line) and fitted (dashed line) length frequency distributions for observer samples, time step 3. Number in top right of each plot is effective sample size.

A6. 8: Numbers of scampi measured, estimated multinomial N sample size, and effective sample size used within the model for length frequency distributions for observer samples, time step 1.

	Measured	Multinomial N	Effective sample size
N_1992	1591	1599	4.65
N_1993	286	311	0.90
N_1996	1666	1526	4.44
N_1997	4040	3698	10.75
N_1998	737	847	2.46
N_1999	14831	12320	35.83
N_2000	7453	5382	15.65
N_2001	7510	5934	17.25
N_2002	4847	4201	12.21
N_2003	2078	1803	5.24
N_2005	630	677	1.97
N_2008	2364	2051	5.96
N_2011	1884	1002	2.91
N_2012	7256	6198	18.02

A6. 9: Numbers of scampi measured, estimated multinomial N sample size, and effective sample size used within the model for length frequency distributions for observer samples, time step 2.

	Measured	Multinomial N	Effective sample size
N_1994	100	204	1.18
N_1995	3306	2162	12.53
N_1997	127	259	1.50
N_1998	300	467	2.71
N_1999	4550	3120	18.09
N_2007	400	549	3.18
N_2008	1001	922	5.34
N_2009	1330	1074	6.23
N_2012	254	369	2.14

A6. 10: Numbers of scampi measured, estimated multinomial N sample size, and effective sample size used within the model for length frequency distributions for observer samples, time step 3.

	Measured	Multinomial N	Effective sample size
N_1991	5821	3498	17.89
N_1993	2699	2440	12.48
N_1994	7087	4889	25.00
N_1995	4250	3833	19.60
N_1996	2006	1602	8.19
N_1997	257	259	1.32
N_2000	166	336	1.72
N_2001	1550	1791	9.16
N_2007	100	203	1.04
N_2008	300	416	2.13
N_2010	1177	746	3.81
N_2011	810	950	4.86

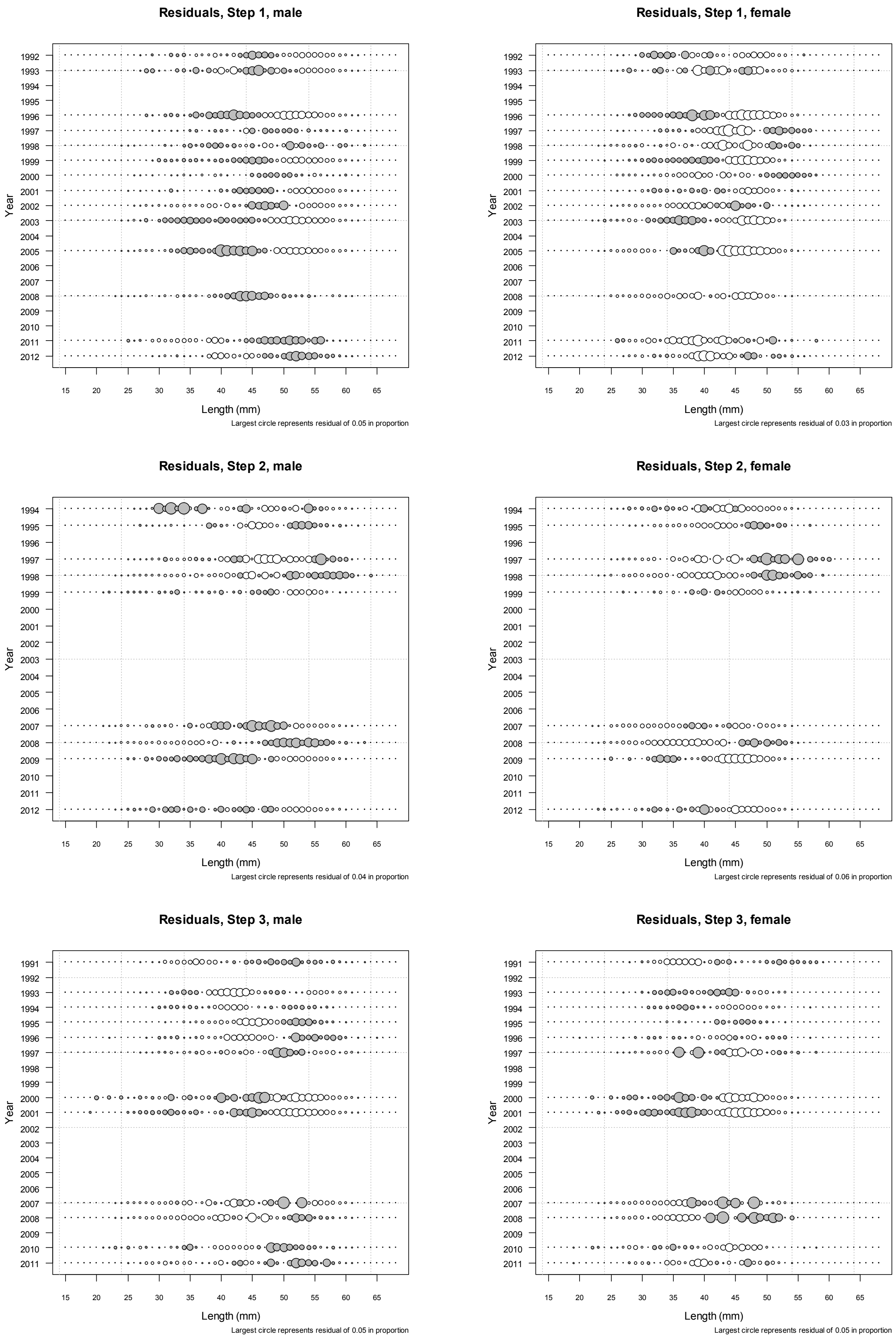

A6. 11: Bubble plots of residuals for fits to length frequency distributions for observer sampling.

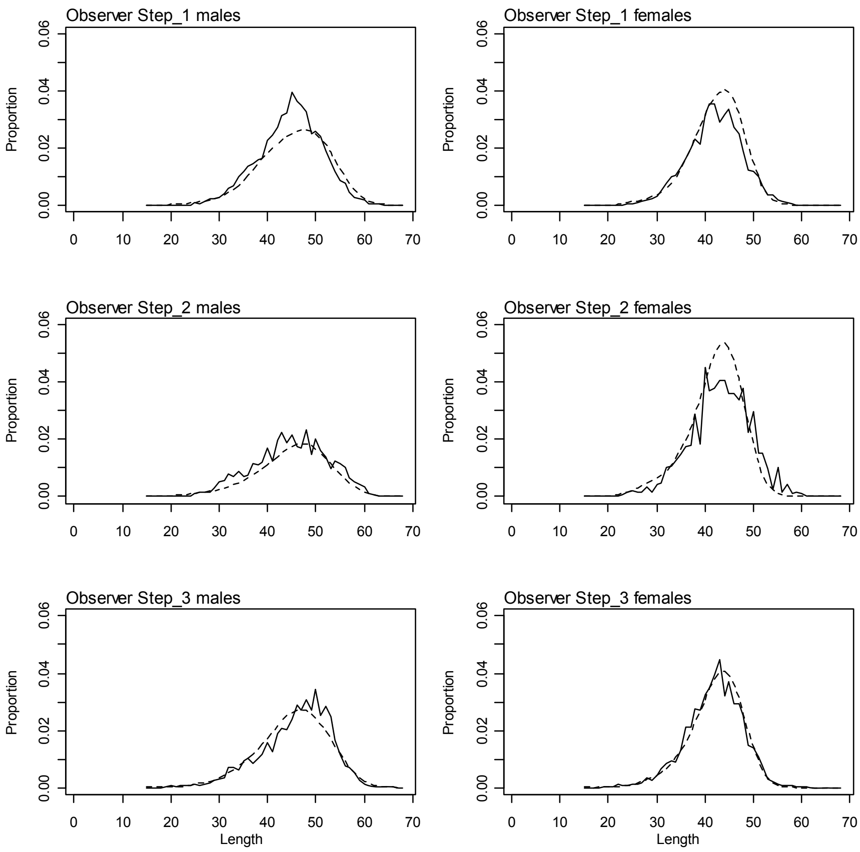

A6. 12: Average observed (solid line) and fitted (dashed line) length frequency distributions for observer samples.

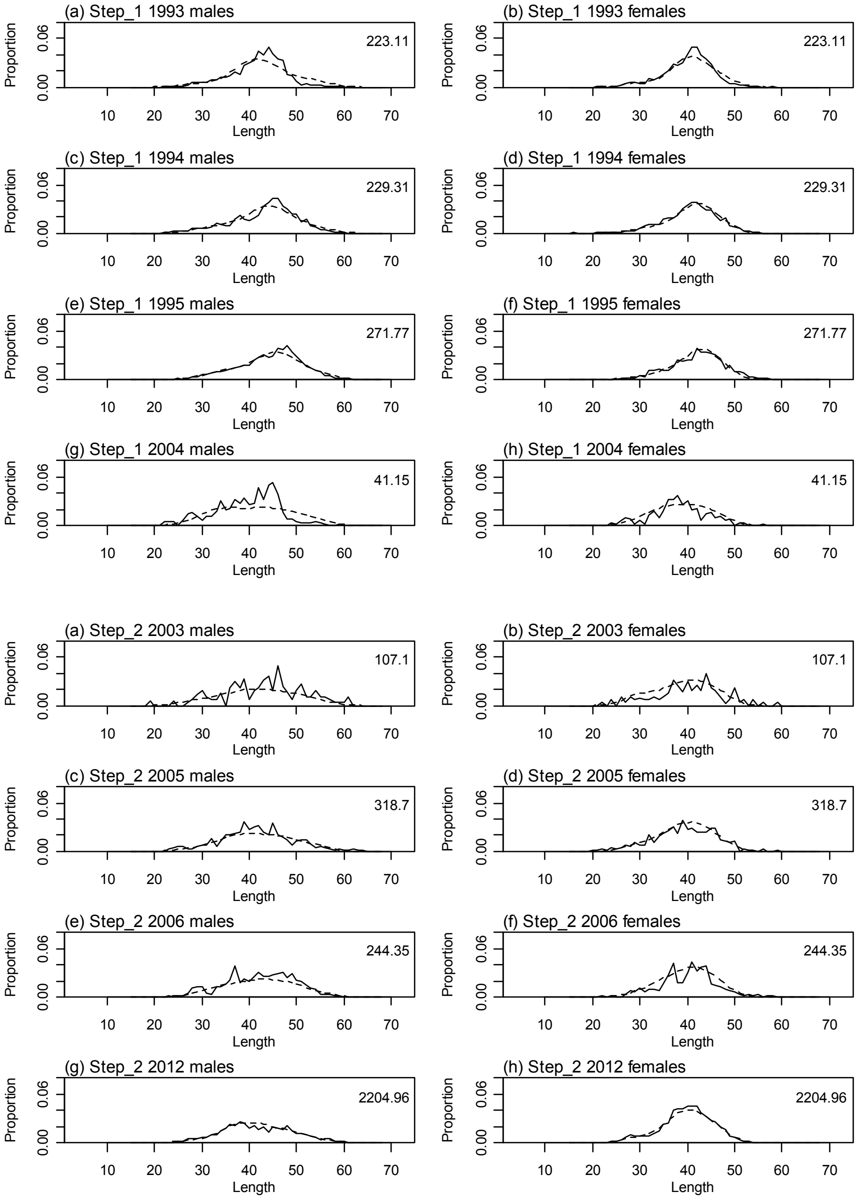

A6. 13: Observed (solid line) and fitted (dashed line) length frequency distributions for research survey samples Samples from time step 1 plotted in block above those from time step 2. Number in top right of each plot is effective sample size.

A6. 14: Numbers of scampi measured, estimated multinomial N sample size, and effective sample size used within the model for length frequency distributions for research survey samples. Samples from time step 1 in block above those from time step 2.

	Measured	Multinomial N	Effective sample size
N_1993	3384	6295	223.11
N_1994	3847	6470	229.31
N_1995	4611	7668	271.77
N_2004	564	1161	41.149
N_2003	260	533	107.10
N_2005	800	1586	318.70
N_2006	596	1216	244.35
N_2012	5480	10973	2204.96

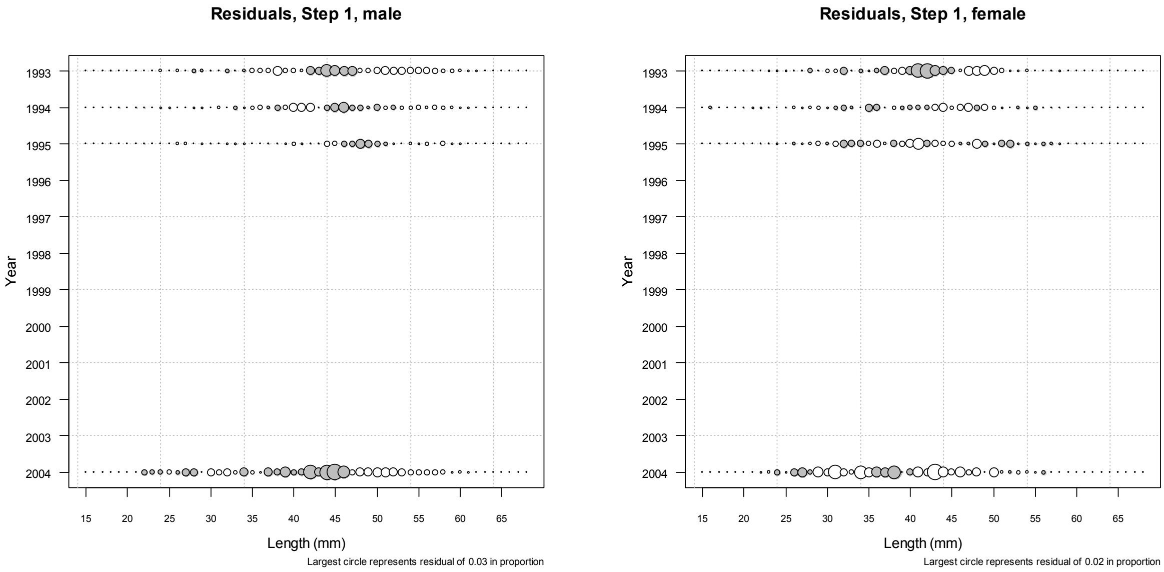

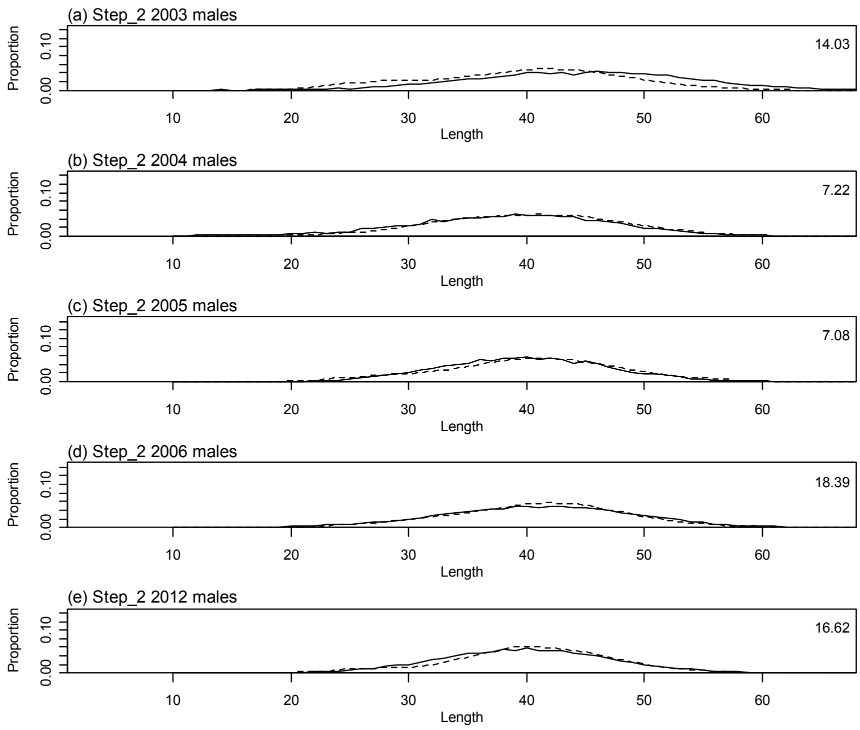

A6. 15: Observed (solid line) and fitted (dashed line) length frequency distributions for photographic survey scampi size estimation. Number in top right of each plot is effective sample size.

	Measured	Multinomial N	Effective sample size
N_2003	53	103	14.03
N_2004	26	53	7.22
N_2005	26	52	7.084
N_2006	69	135	18.39
N_2012	104	122	16.62

A6. 16: Numbers of scampi measured, estimated multinomial N sample size, and effective sample size used within the model for length frequency distributions for photographic survey samples.

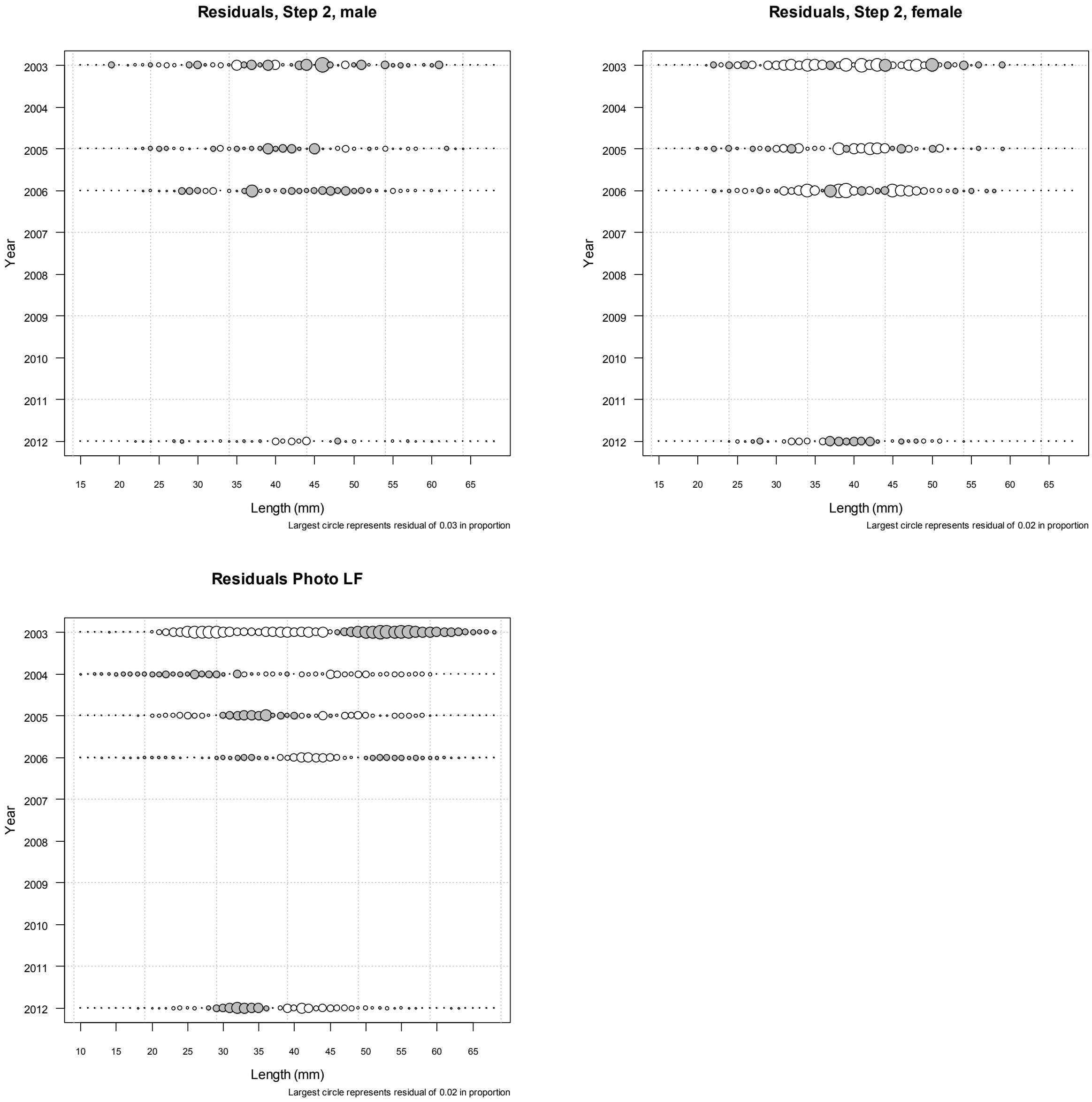

A6. 17: Bubble plots of residuals for fits to length frequency distributions for trawl survey sampling and photographic survey scampi size estimation.

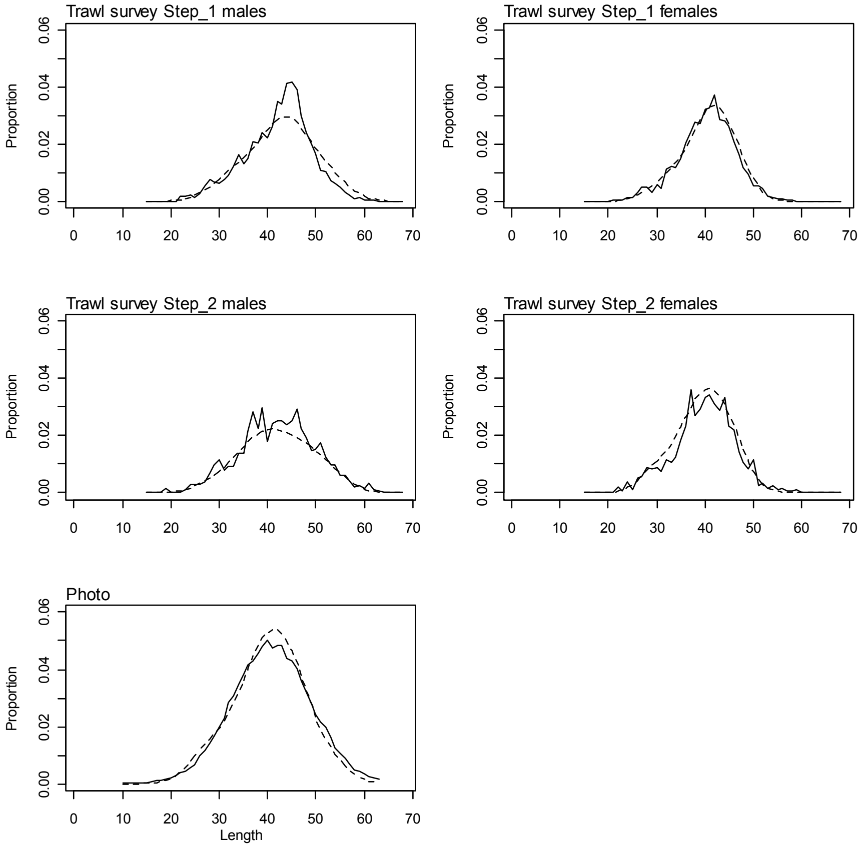

A6. 18: Average observed (solid line) and fitted (dashed line) length frequency distributions for trawl survey sampling and photographic survey scampi size estimation.

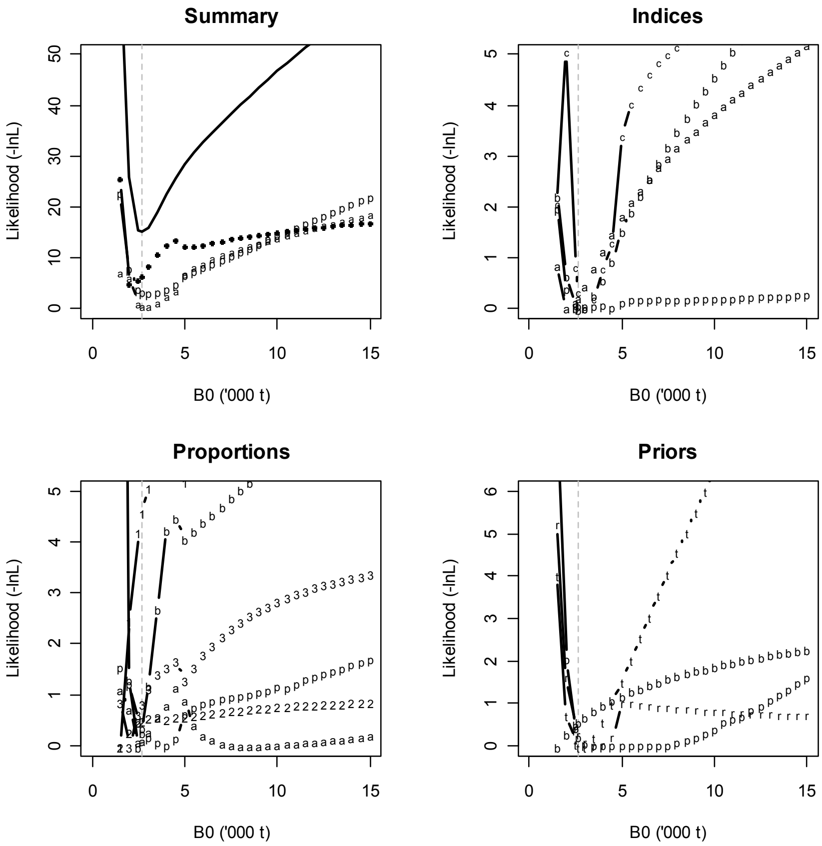

A6. 19: Likelihood profiles for model Base2 for SCI 2 when B_0 is fixed in the model. Figures show profiles for main priors (top left, p-priors, a – abundance indices, • – proportions at length), abundance indices (top right, a - trawl survey step 1, b – trawl survey step 2, c - CPUE, p – photo survey), proportion at length data (bottom left, t-trawl, 1 – observer time step 1, 2 – observer time step 2, 3 – observer time step 3) and priors (bottom right, b- B_0, YCS - r, p- *q-Photo*, t – *q-Trawl*).

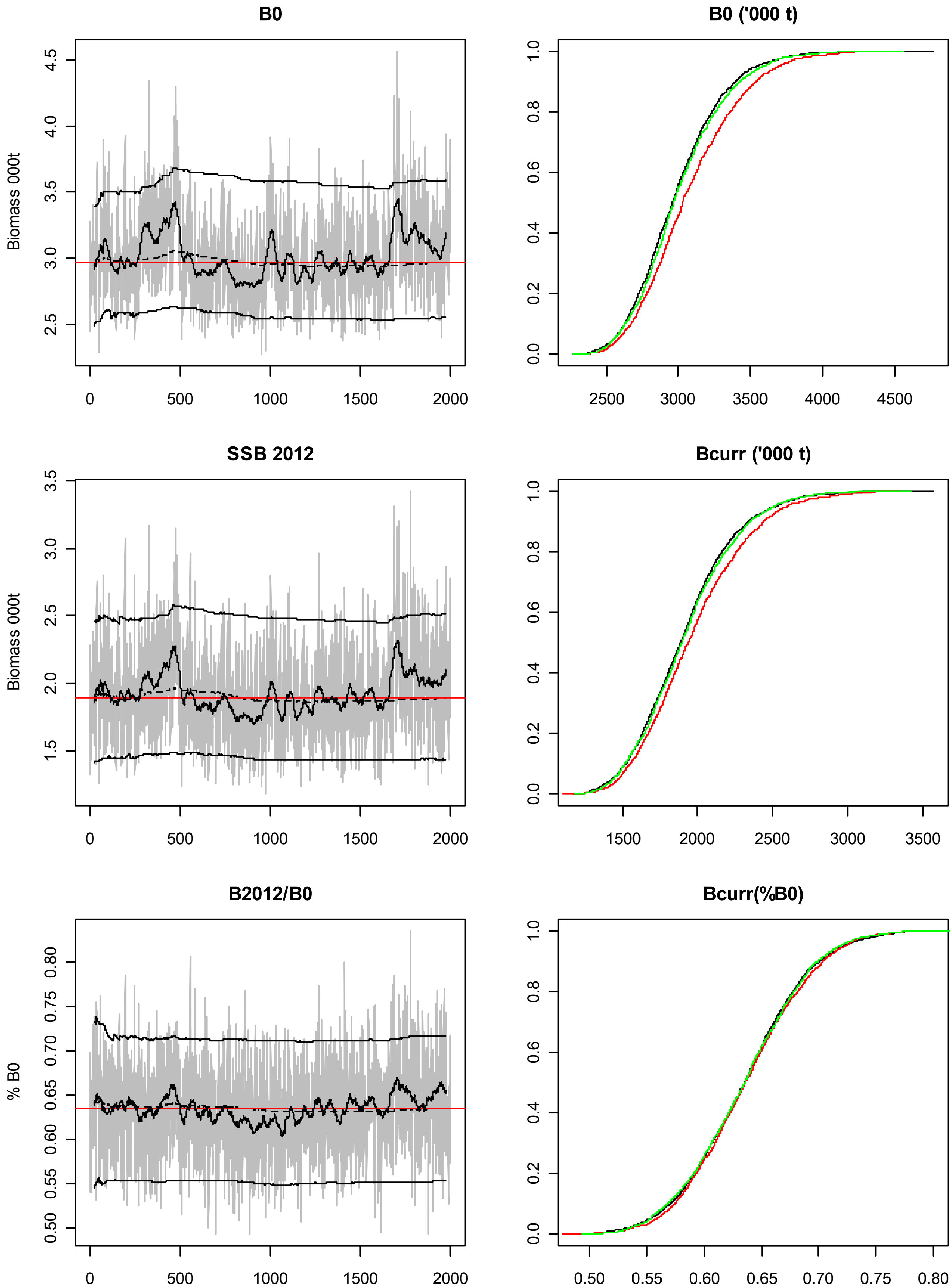

A6. 20: MCMC traces for B_0, SSB_{2012}, and SSB_{2012}/B_0 terms for the Base2 model for SCI 2, along with cumulative frequency distributions for three independent MCMC chains.

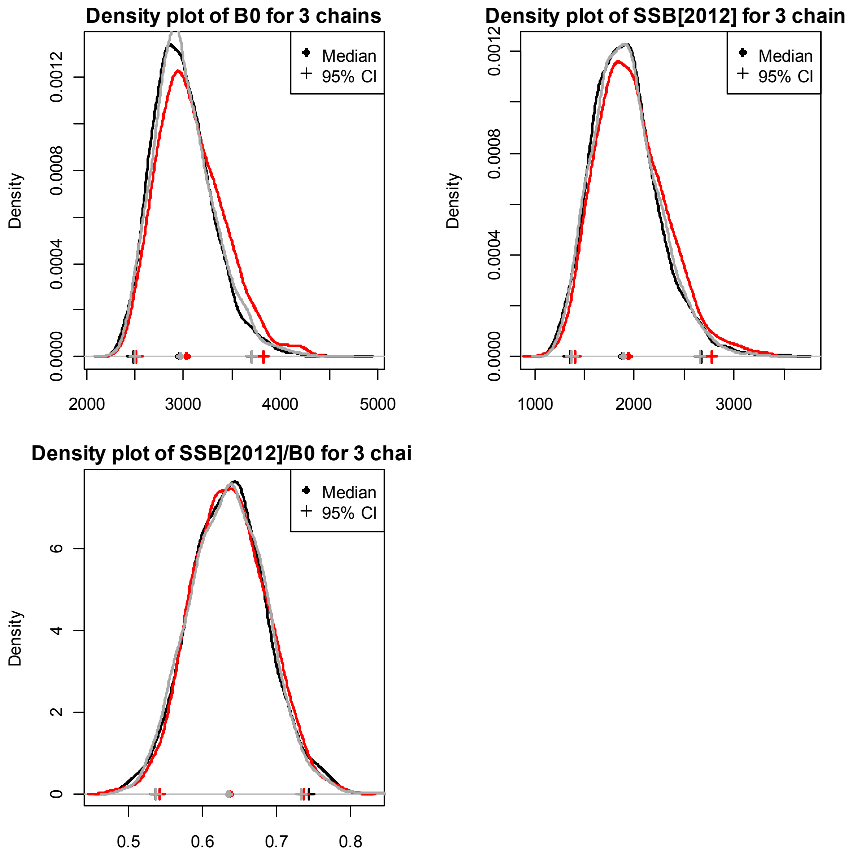

A6. 21: Density plots for B_0, SSB_{2012}, and SSB_{2012}/B_0 terms for the Base2 model for SCI 2 for three independent MCMC chains, with median and 95% confidence intervals.

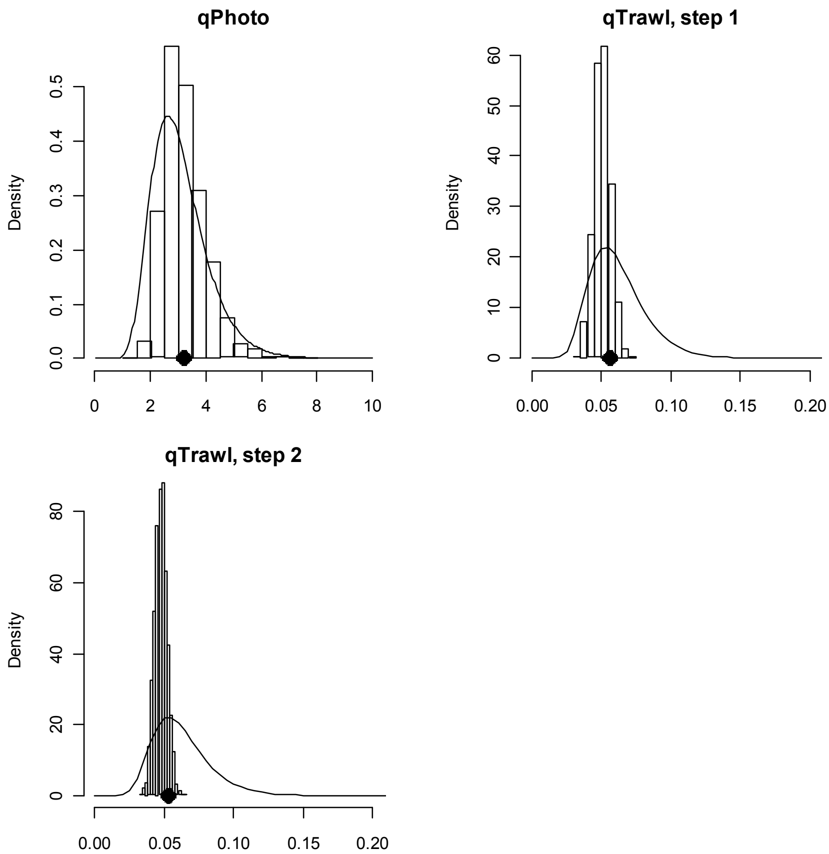

A6. 22: Marginal posterior distributions (histograms), MPD estimates (solid symbols) and distributions of priors (lines) for catchability terms.

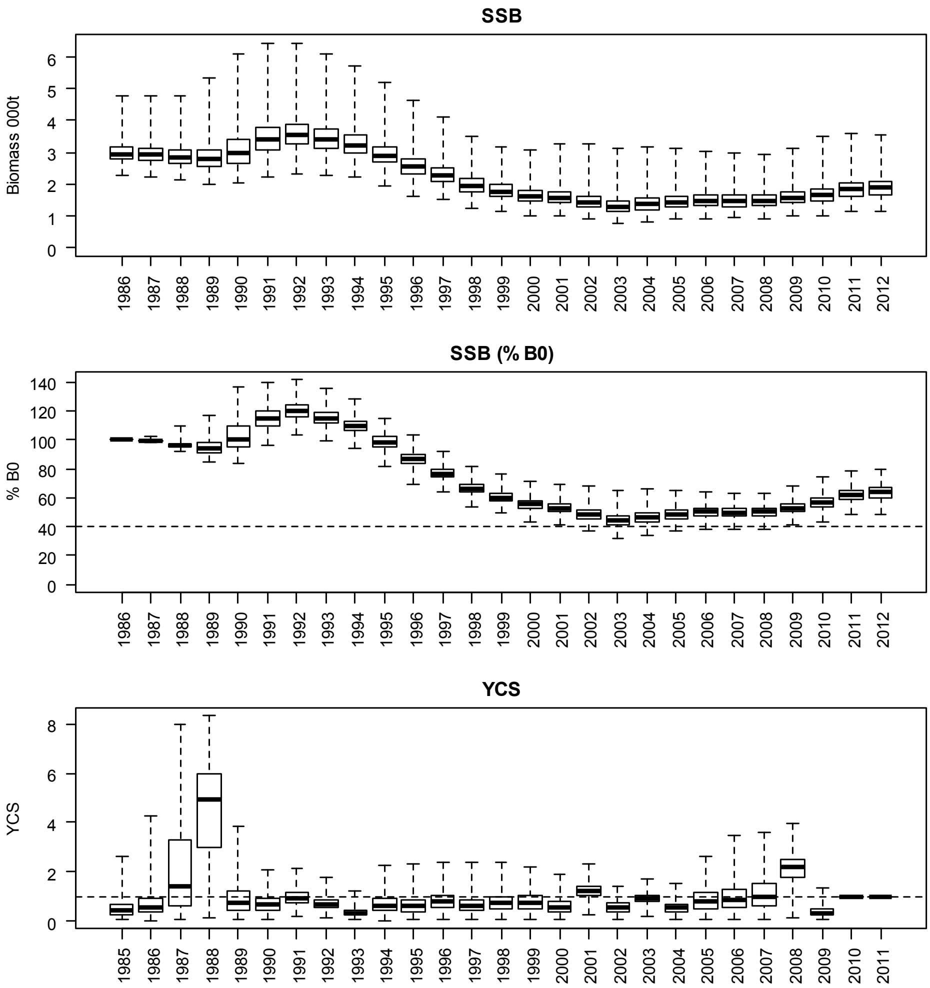

A6. 23: Posterior trajectory of SSB, SSB_{2012}/B_0 and YCS.

15. APPENDIX 7. SCI 2 model plots (M=0.3)

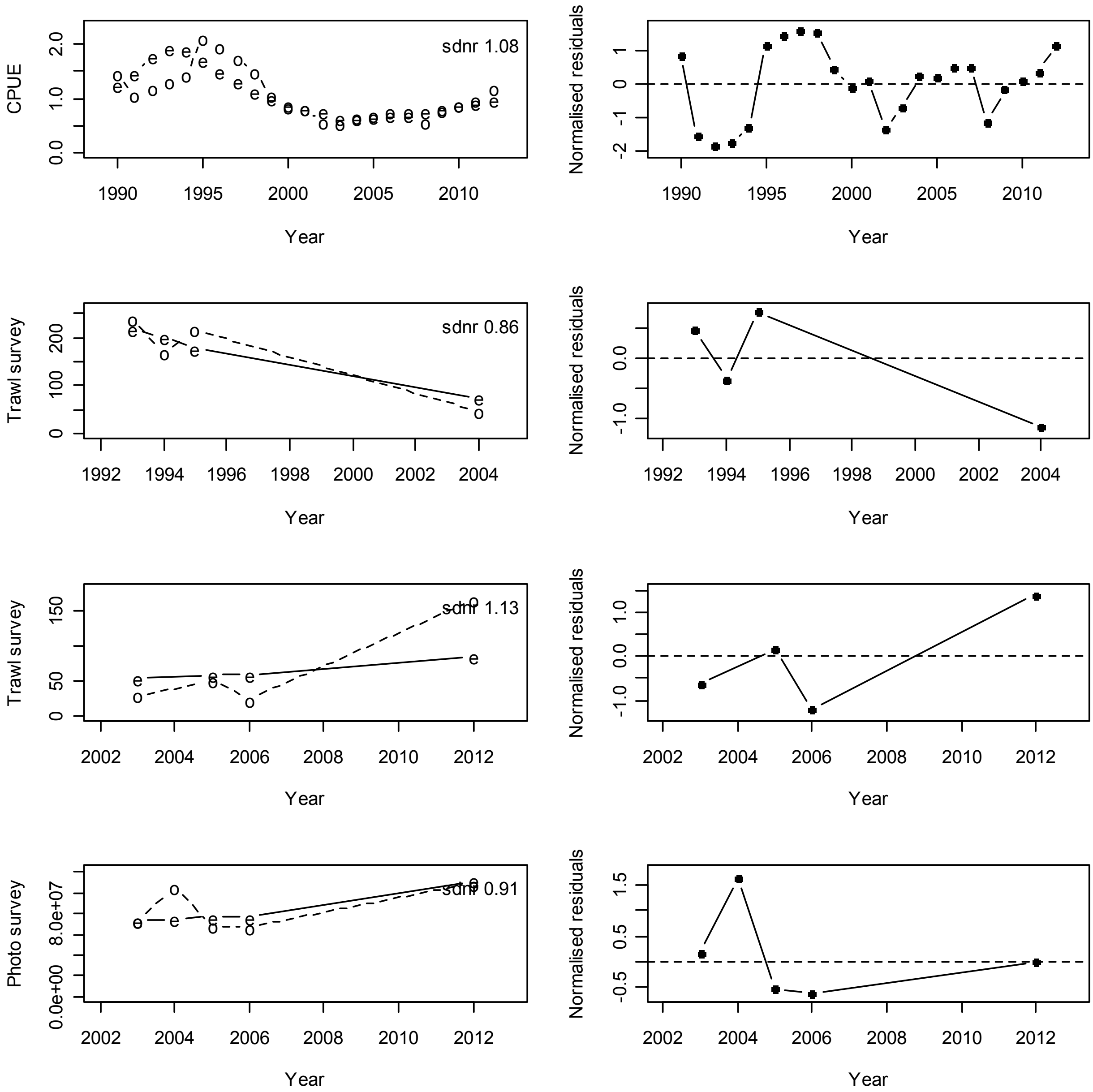

A7. 1: Fits to abundance indices (left column) and normalised residuals (right column) for standardised CPUE index (top row) trawl survey biomass index covering whole area (second row), trawl survey biomass index covering limited area (third row) and photo survey abundance index (fourth row) for SCI 2 Base3 model.

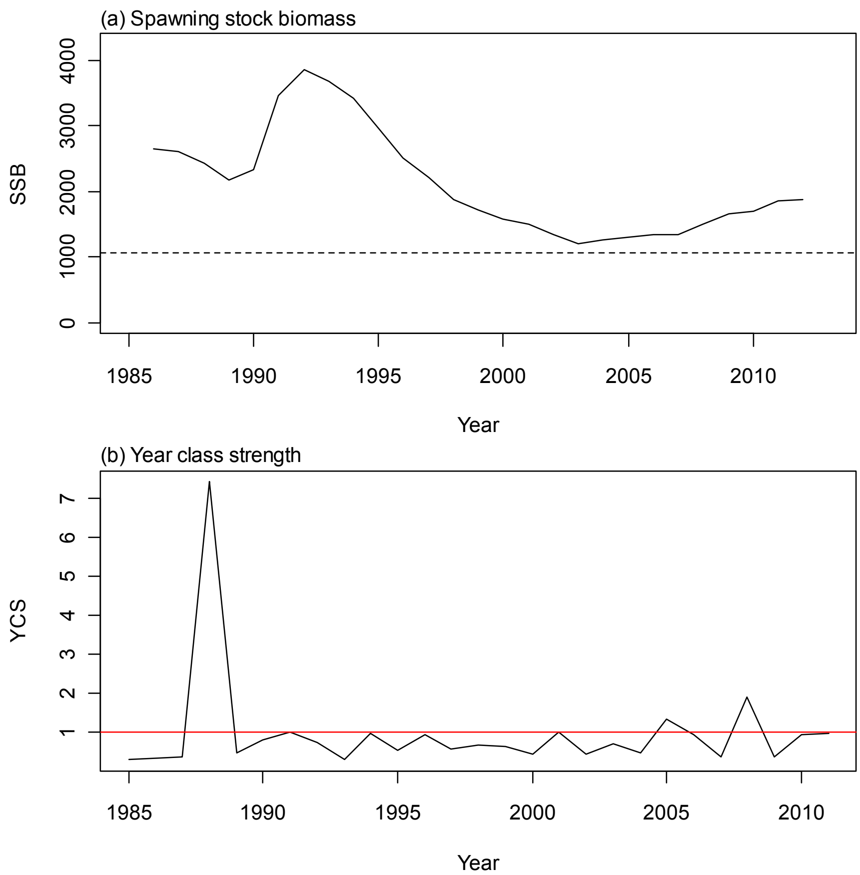

A7. 2: Spawning stock biomass trajectory (upper plot), year class strength (lower plot) for SCI 2 Base3 model.

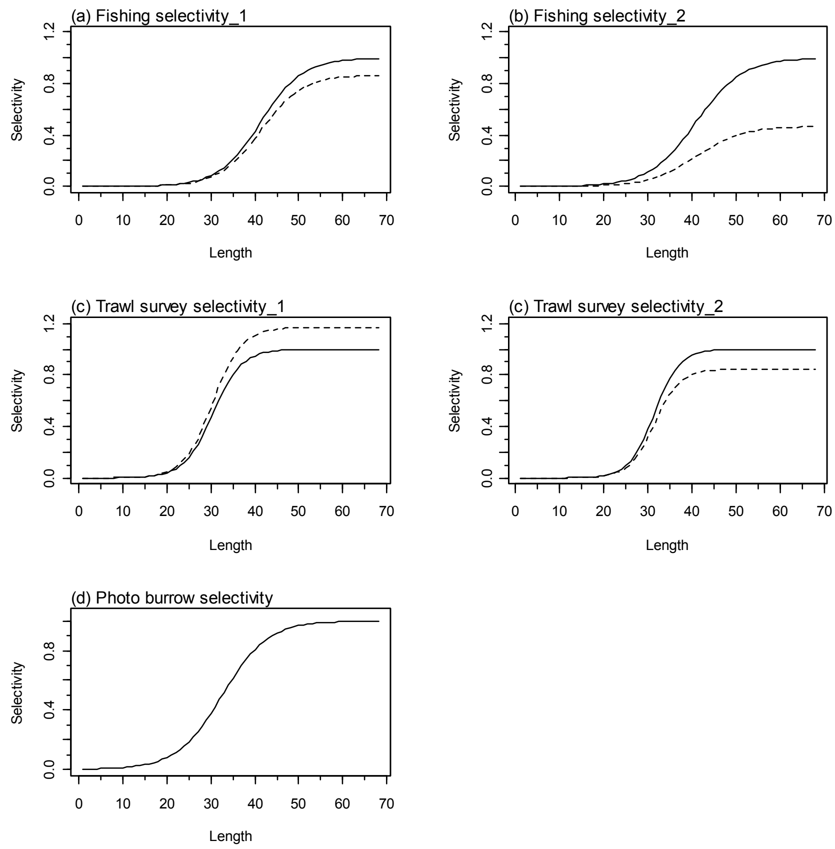

A7. 3: Fishery and survey selectivity curves. Solid line – females, dotted line – males. The scampi burrow index is not sexed, and a single selectivity applies.

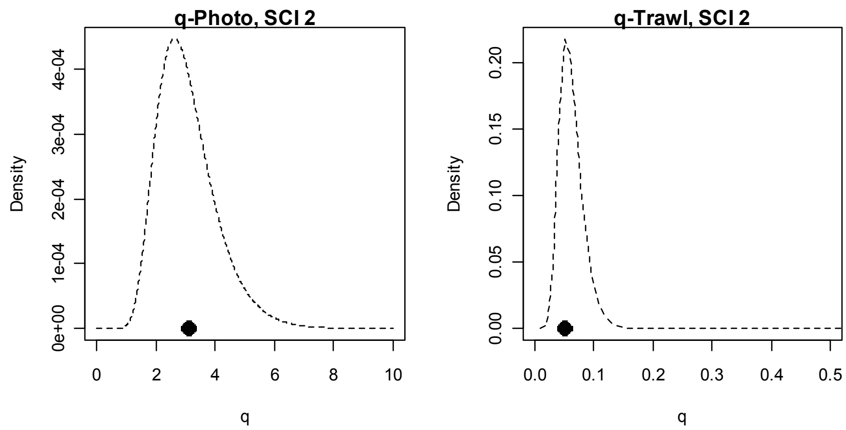

A7. 4: Catchability estimates from MPD model run, plotted in relation to prior distribution.

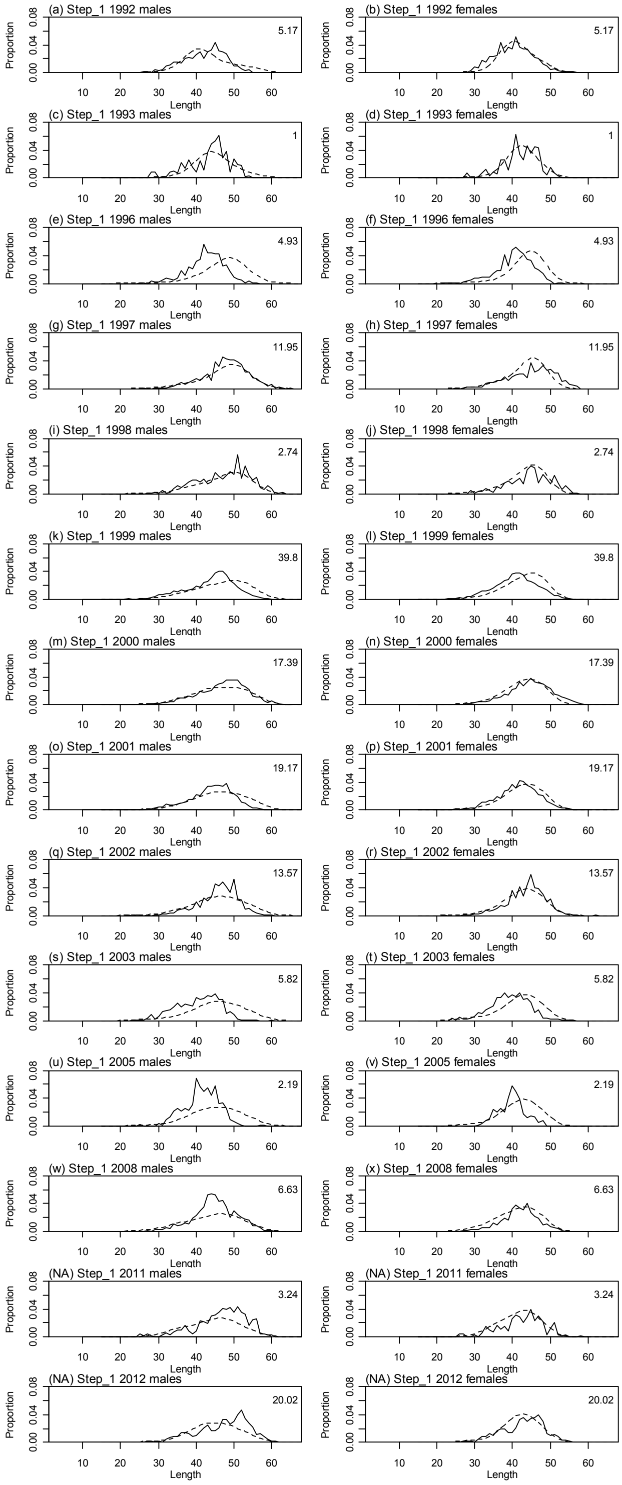

A7. 5: Observed (solid line) and fitted (dashed line) length frequency distributions for observer samples, time step 1. Number in top right of each plot is effective sample size.

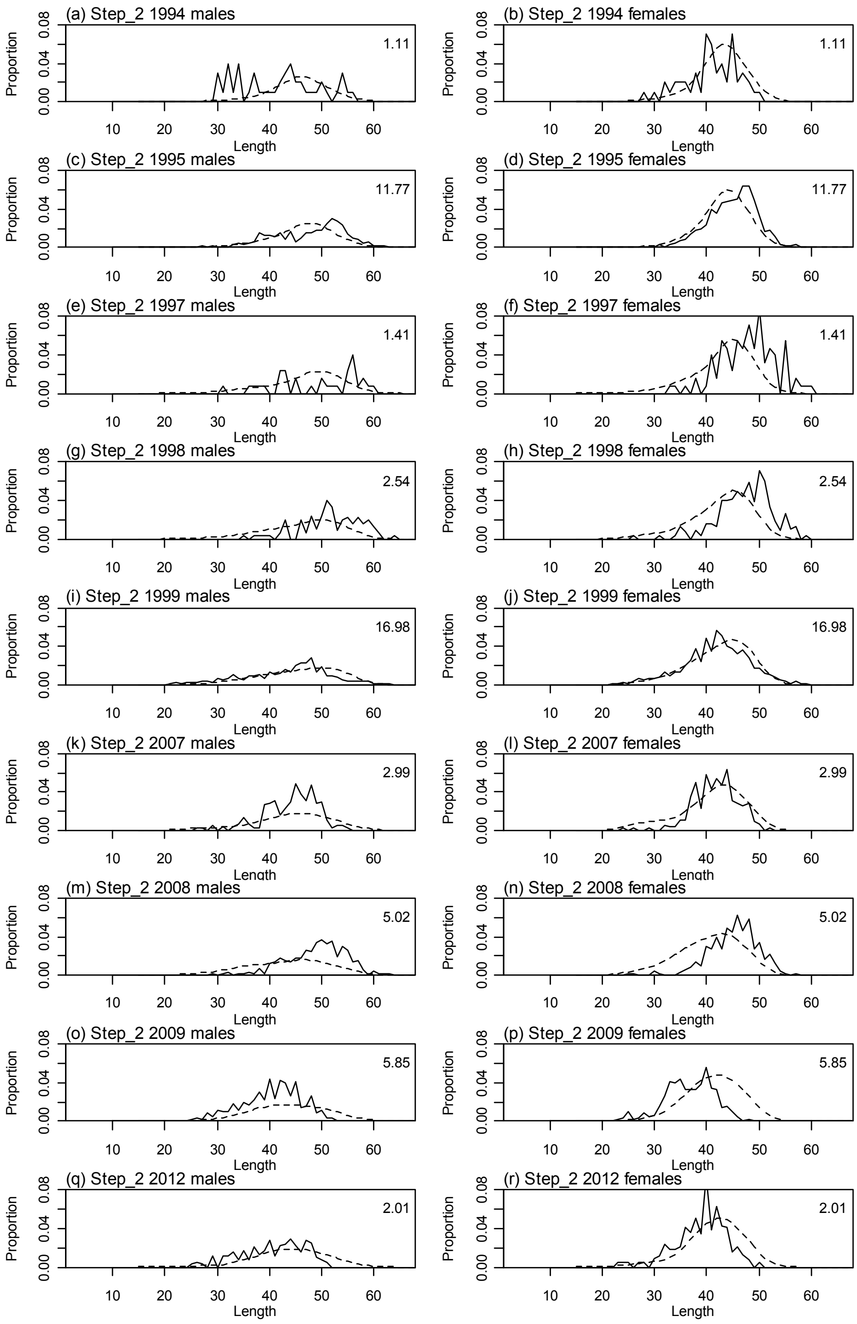

A7. 6: Observed (solid line) and fitted (dashed line) length frequency distributions for observer samples, time step 2. Number in top right of each plot is effective sample size.

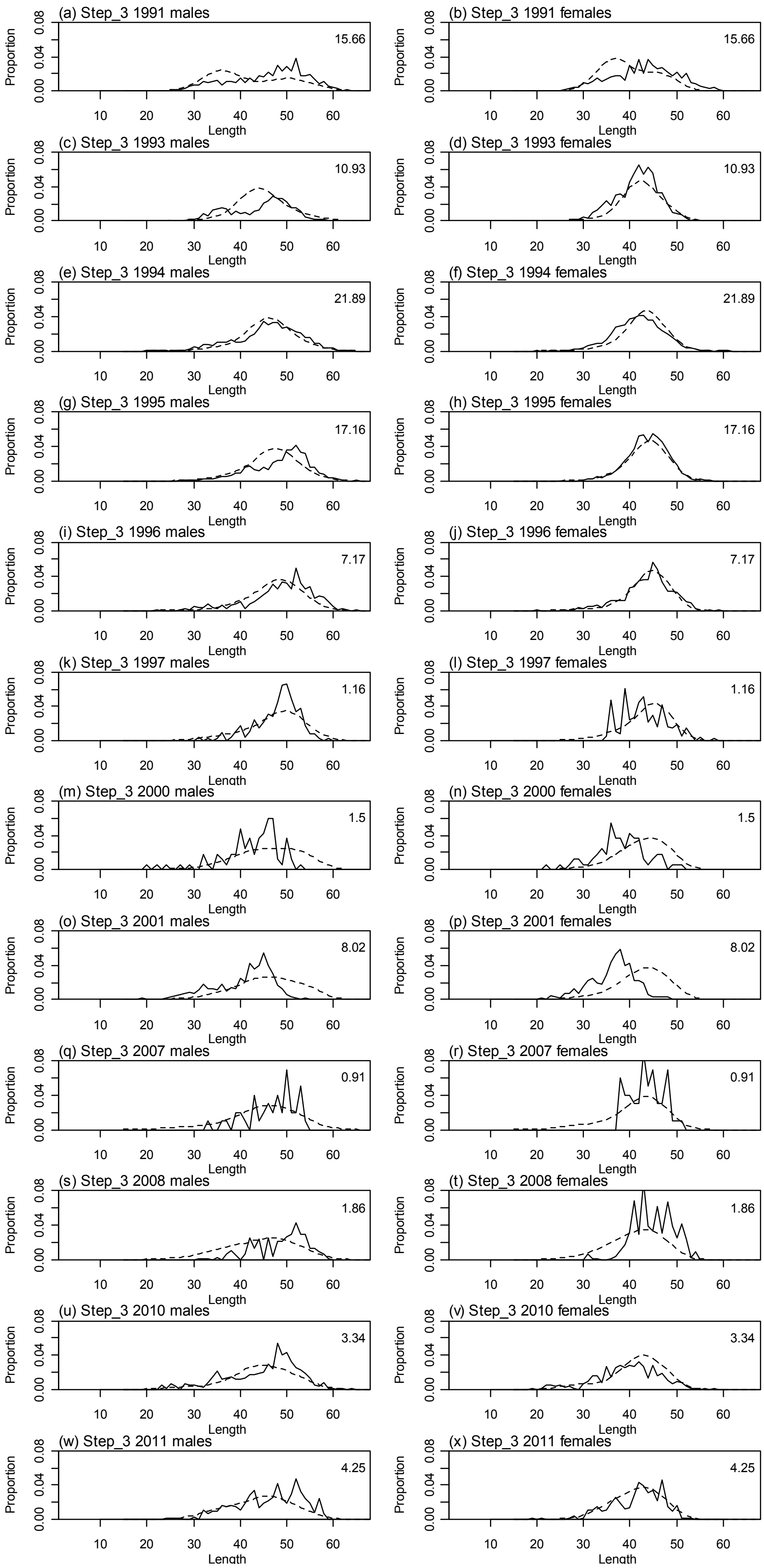

A7. 7: Observed (solid line) and fitted (dashed line) length frequency distributions for observer samples, time step 3. Number in top right of each plot is effective sample size.

A7. 8: Numbers of scampi measured, estimated multinomial N sample size, and effective sample size used within the model for length frequency distributions for observer samples, time step 1.

	Measured	Multinomial N	Effective sample size
N_1992	1591	1599	5.17
N_1993	286	311	1.00
N_1996	1666	1526	4.93
N_1997	4040	3698	11.94
N_1998	737	847	2.74
N_1999	14831	12320	39.80
N_2000	7453	5382	17.38
N_2001	7510	5934	19.17
N_2002	4847	4201	13.57
N_2003	2078	1803	5.82
N_2005	630	677	2.19
N_2008	2364	2051	6.63
N_2011	1884	1002	3.24
N_2012	7256	6198	20.02

A7. 9: Numbers of scampi measured, estimated multinomial N sample size, and effective sample size used within the model for length frequency distributions for observer samples, time step 2.

	Measured	Multinomial N	Effective sample size
N_1994	100	204	1.11
N_1995	3306	2162	11.77
N_1997	127	259	1.41
N_1998	300	467	2.54
N_1999	4550	3120	16.98
N_2007	400	549	2.99
N_2008	1001	922	5.02
N_2009	1330	1074	5.85
N_2012	254	369	2.01

A7. 10: Numbers of scampi measured, estimated multinomial N sample size, and effective sample size used within the model for length frequency distributions for observer samples, time step 3.

	Measured	Multinomial N	Effective sample size
N_1991	5821	3498	15.66
N_1993	2699	2440	10.93
N_1994	7087	4889	21.89
N_1995	4250	3833	17.16
N_1996	2006	1602	7.17
N_1997	257	259	1.16
N_2000	166	336	1.50
N_2001	1550	1791	8.02
N_2007	100	203	0.91
N_2008	300	416	1.86
N_2010	1177	746	3.34
N_2011	810	950	4.25

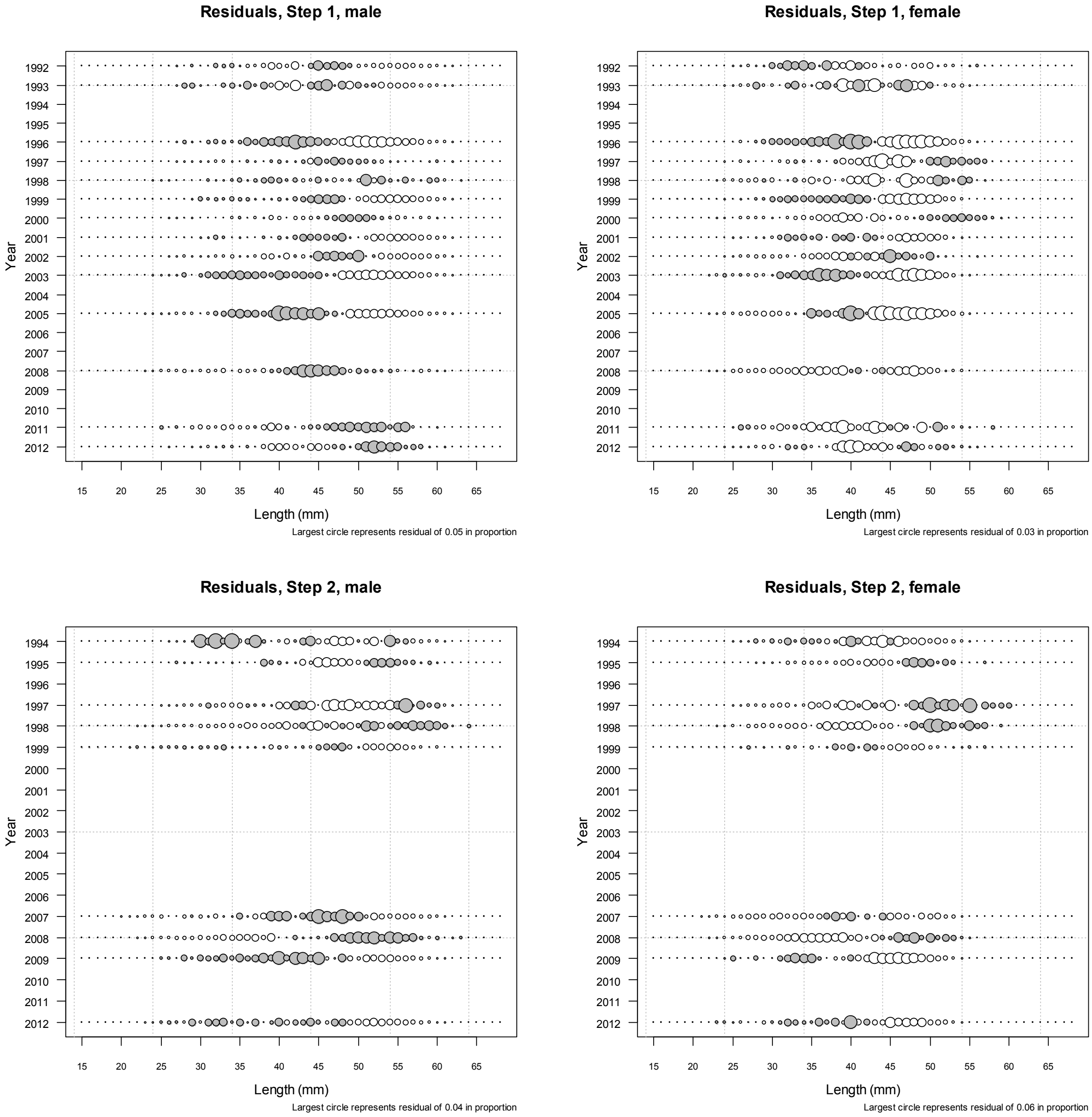
Residuals, Step 1, male
Residuals, Step 1, female
Residuals, Step 2, male
Residuals, Step 2, female
Year
Length (mm)
Largest circle represents residual of 0.05 in proportion
Largest circle represents residual of 0.03 in proportion
Largest circle represents residual of 0.04 in proportion
Largest circle represents residual of 0.06 in proportion

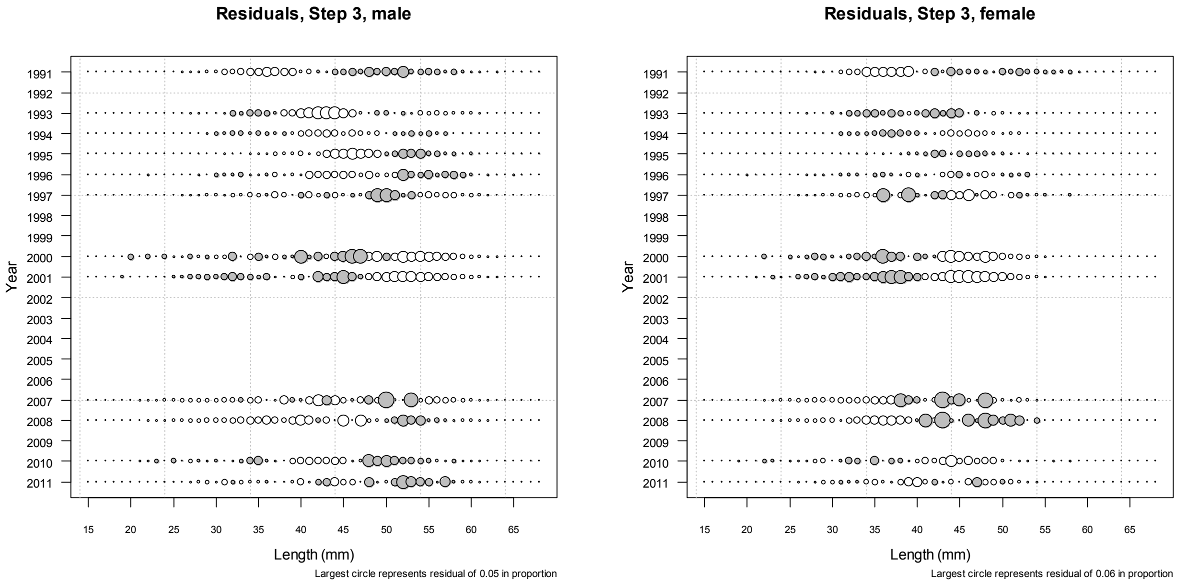

A7. 11: Bubble plots of residuals for fits to length frequency distributions for observer sampling.

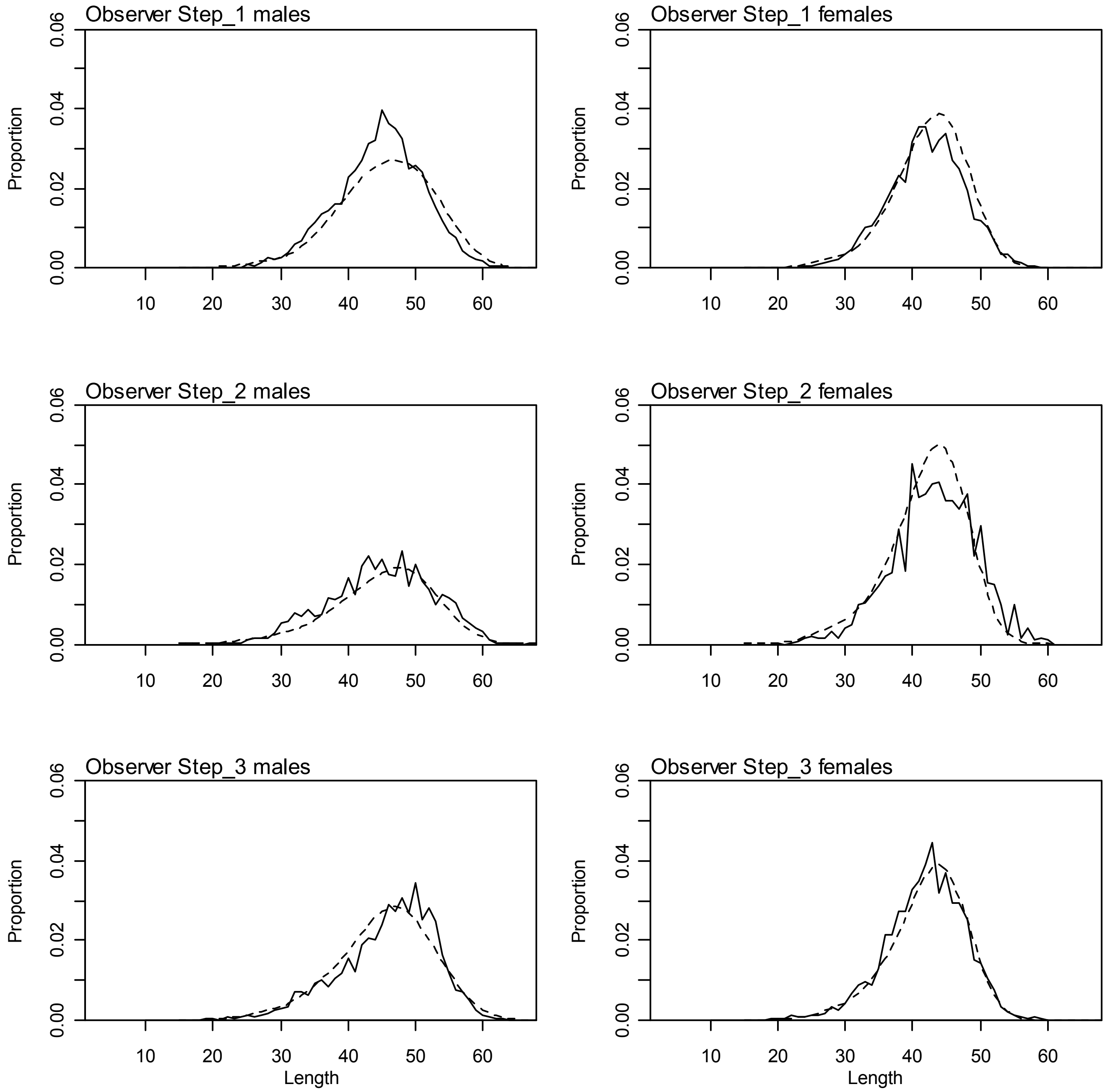

A7. 12: Average observed (solid line) and fitted (dashed line) length frequency distributions for observer samples.

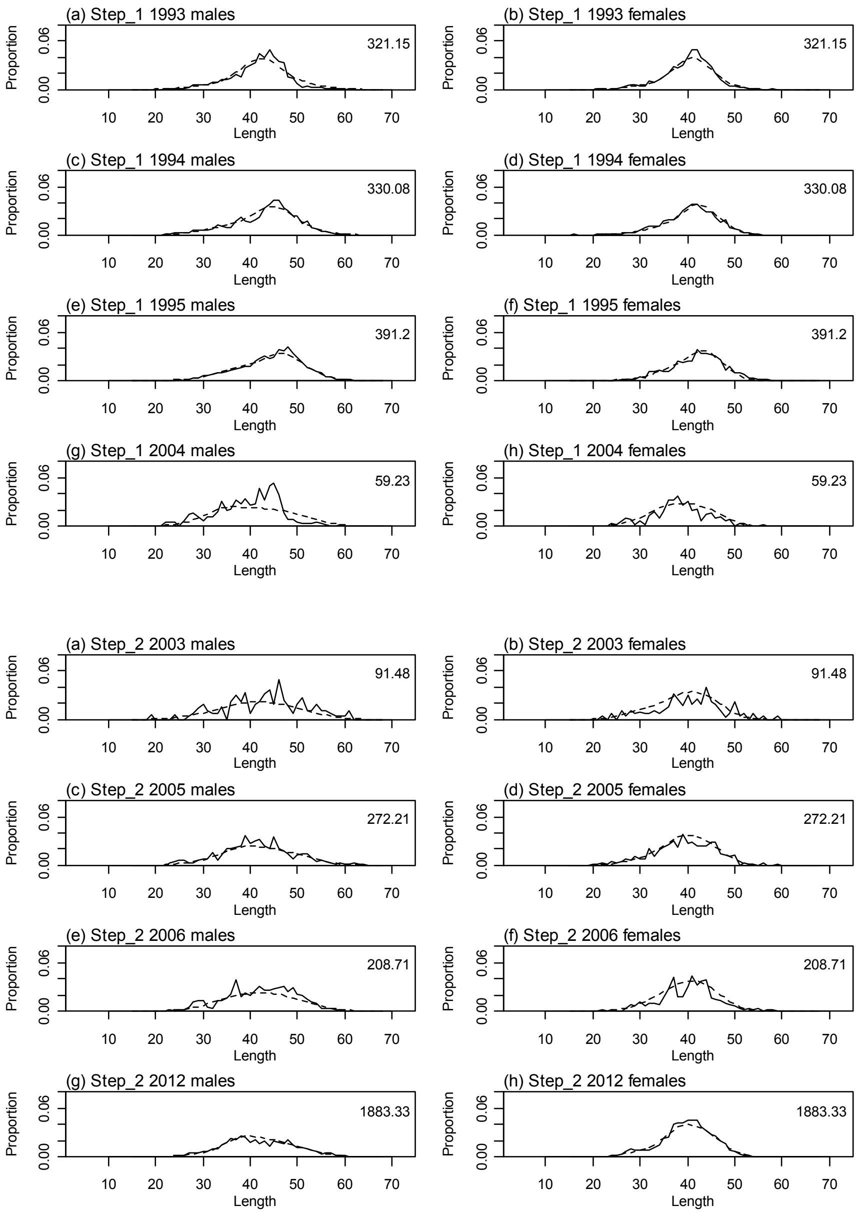

A7. 13: Observed (solid line) and fitted (dashed line) length frequency distributions for research survey samples Samples from time step 1 plotted in block above those from time step 2. Number in top right of each plot is effective sample size.

A7. 14: Numbers of scampi measured, estimated multinomial N sample size, and effective sample size used within the model for length frequency distributions for research survey samples. Samples from time step 1 in block above those from time step 2.

	Measured	Multinomial N	Effective sample size
N_1993	3384	6295	321.15
N_1994	3847	6470	330.08
N_1995	4611	7668	391.20
N_2004	564	1161	59.23
N_2003	260	533	91.48
N_2005	800	1586	272.21
N_2006	596	1216	208.71
N_2012	5480	10973	1883.33

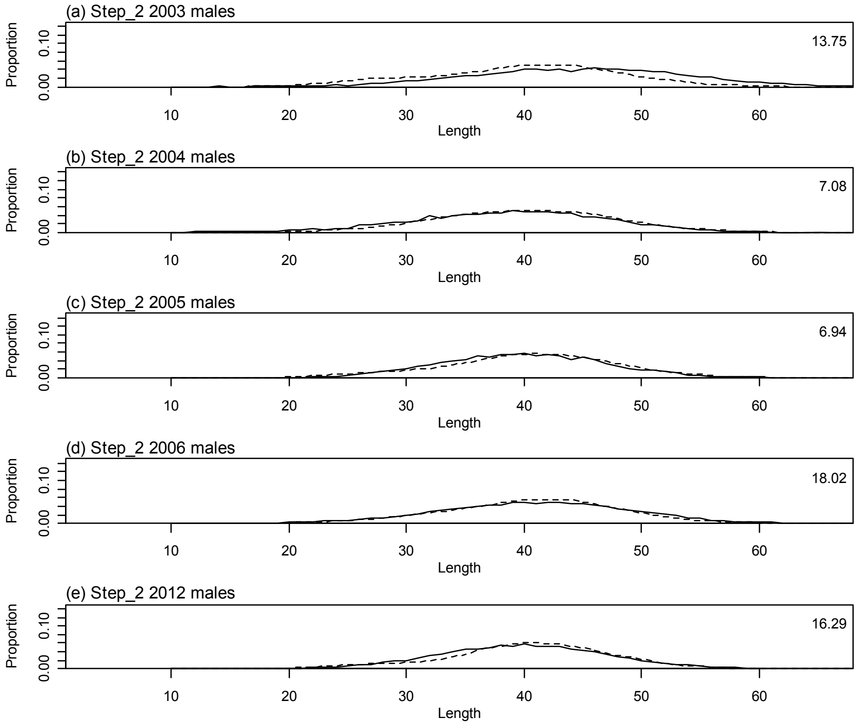

A7. 15: Observed (solid line) and fitted (dashed line) length frequency distributions for photographic survey scampi size estimation. Number in top right of each plot is effective sample size.

A7. 16: Numbers of scampi measured, estimated multinomial N sample size, and effective sample size used within the model for length frequency distributions for photographic survey samples.

	Measured	Multinomial N	Effective sample size
N_2003	53	103	13.75
N_2004	26	53	7.08
N_2005	26	52	6.94
N_2006	69	135	18.02
N_2012	104	122	16.29

A7. 17: Bubble plots of residuals for fits to length frequency distributions for trawl survey sampling and photographic survey scampi size estimation.

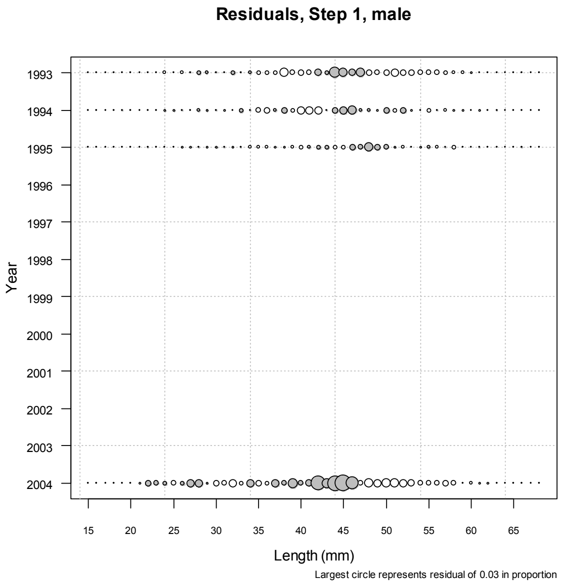

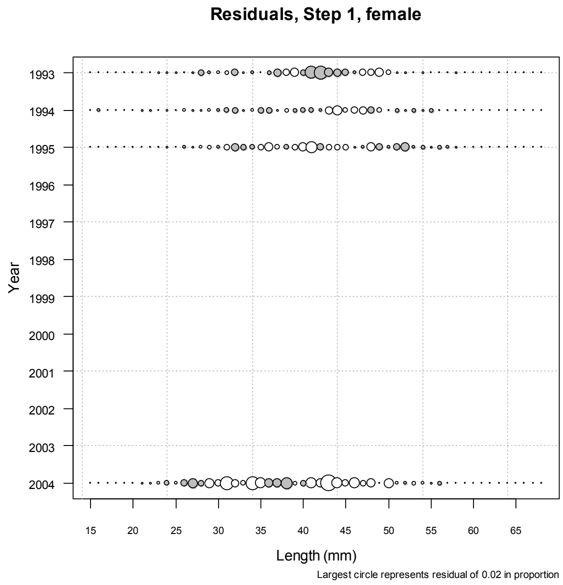

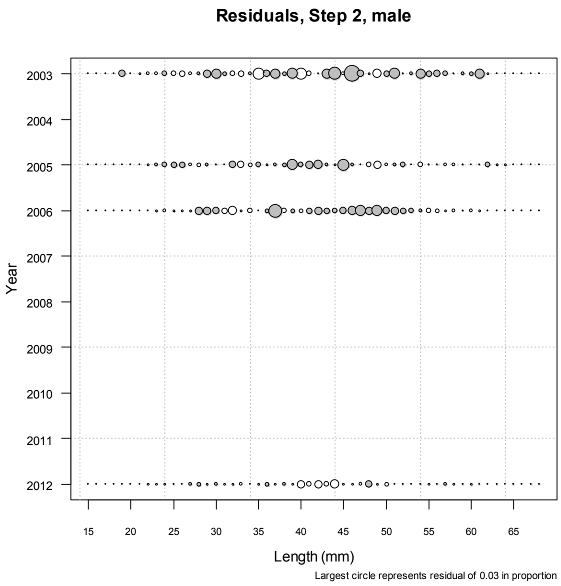

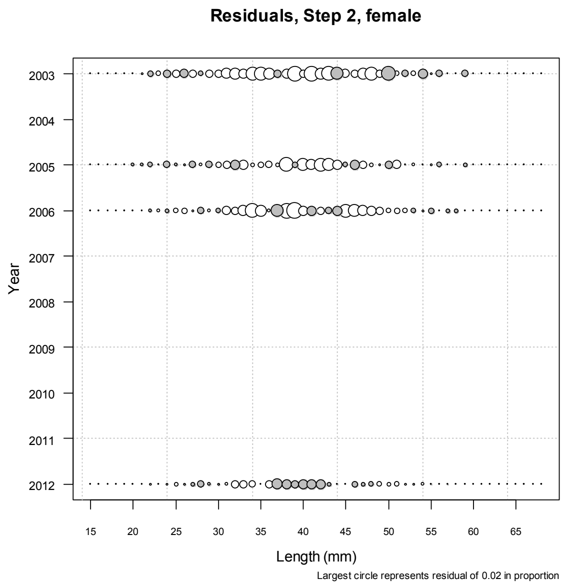

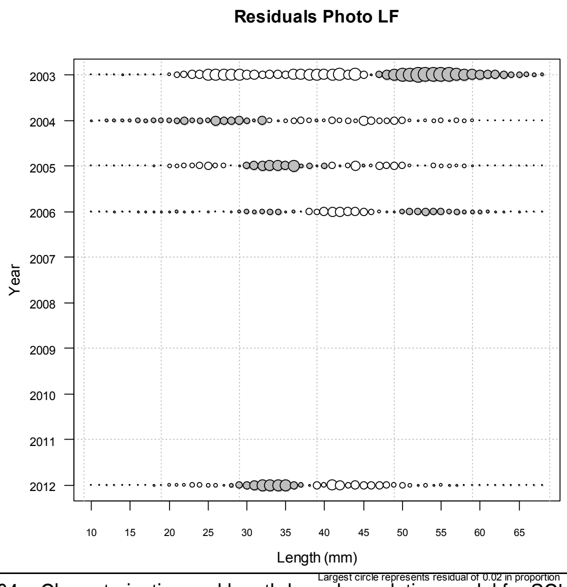

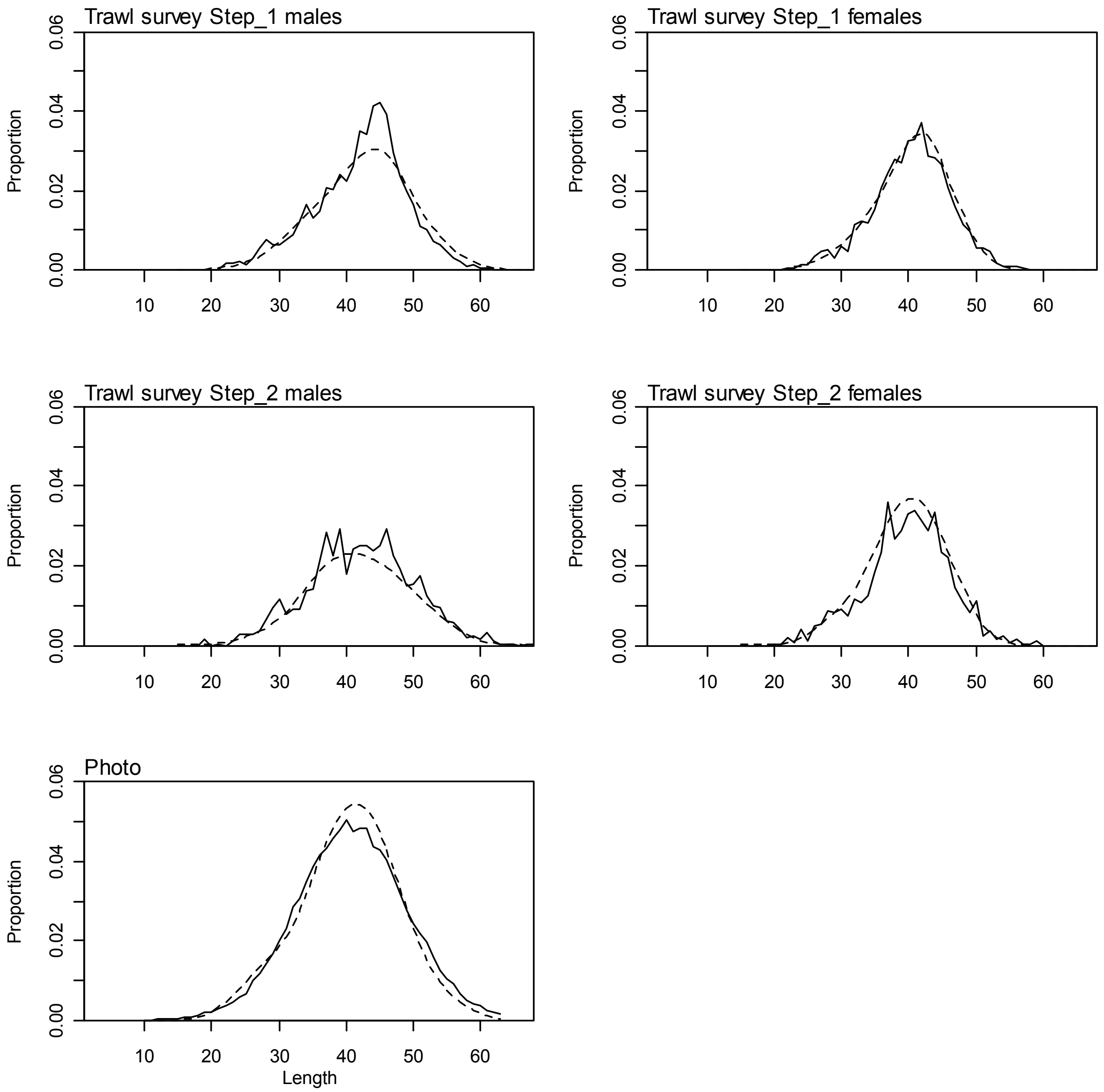

A7. 18: Average observed (solid line) and fitted (dashed line) length frequency distributions for trawl survey sampling and photographic survey scampi size estimation.

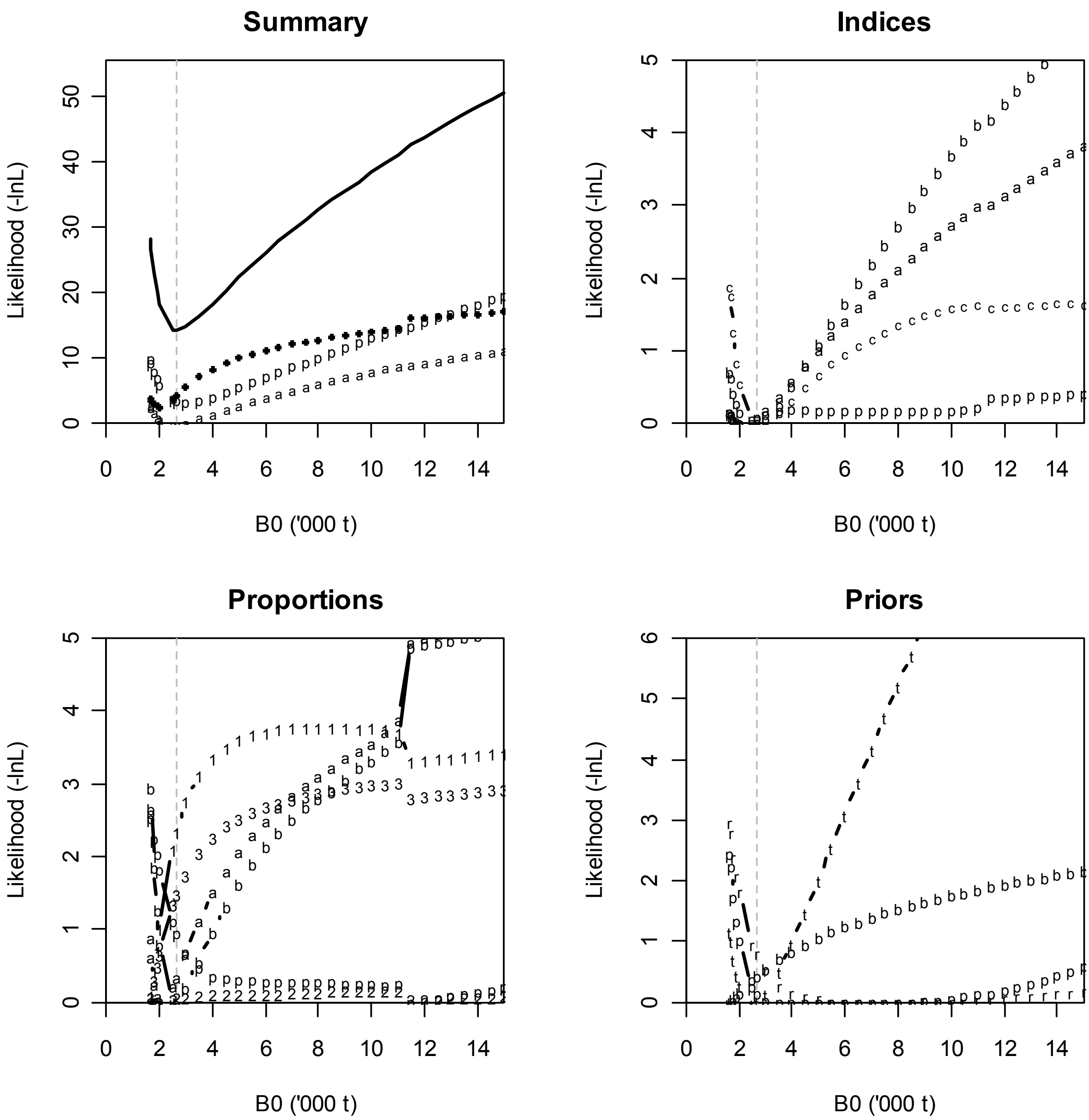

A7. 19: Likelihood profiles for model Base3 for SCI 2 when B_0 is fixed in the model. Figures show profiles for main priors (top left, p-priors, a – abundance indices, • – proportions at length), abundance indices (top right, a - trawl survey step 1, b – trawl survey step 2, c - CPUE, p – photo survey), proportion at length data (bottom left, t-trawl, 1 – observer time step 1, 2 – observer time step 2, 3 – observer time step 3) and priors (bottom right, b- B_0, YCS - r, p- *q-Photo*, t – *q-Trawl*).

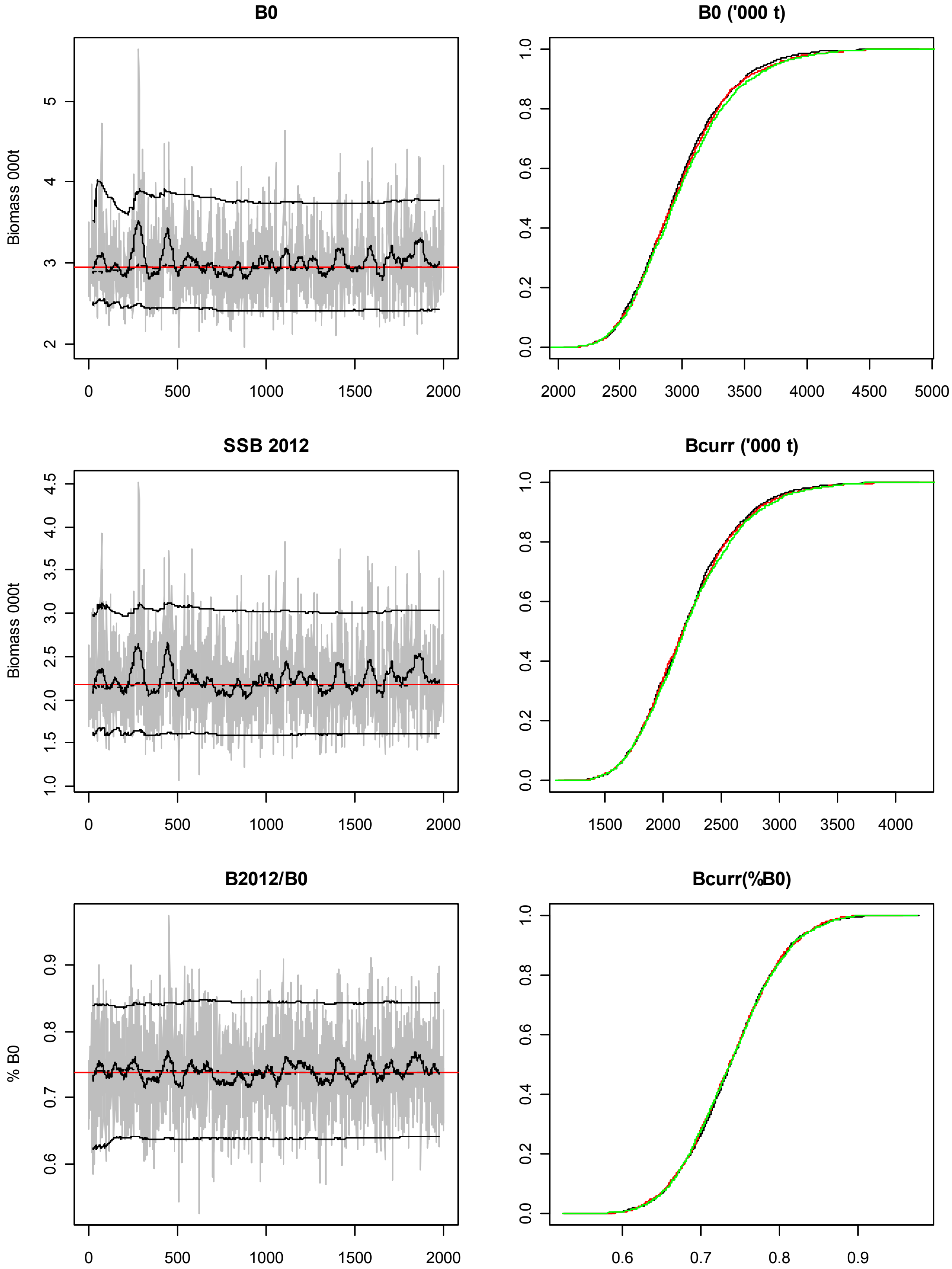

A7. 20: MCMC traces for B_0, SSB_{2012}, and SSB_{2012}/B_0 terms for the Base3 model for SCI 2, along with cumulative frequency distributions for three independent MCMC chains.

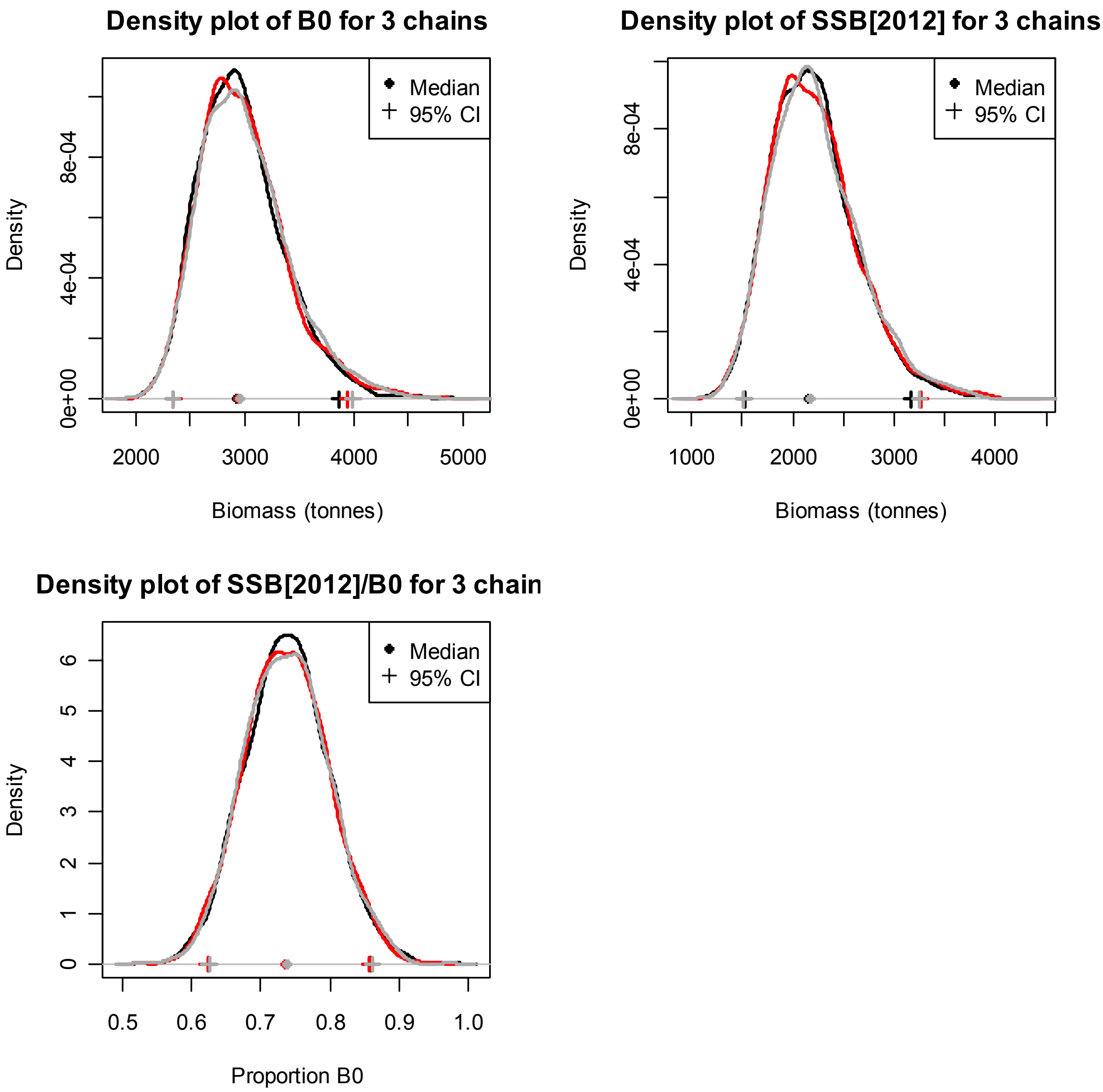

A7. 21: Density plots for B_0, SSB_{2012}, and SSB_{2012}/B_0 terms for the Base3 model for SCI 2 for three independent MCMC chains, with median and 95% confidence intervals.

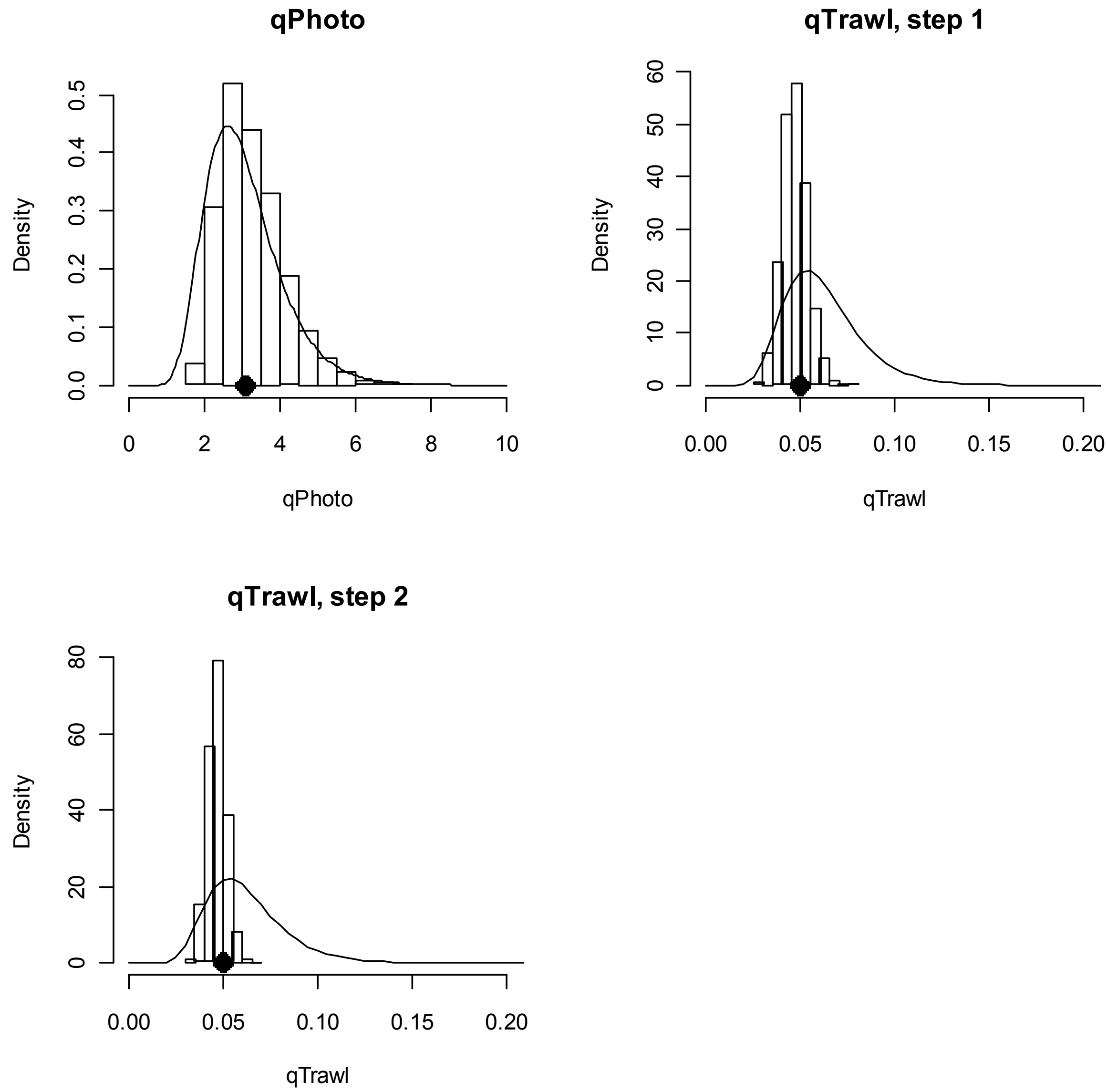

A7. 22: Marginal posterior distributions (histograms), MPD estimates (solid symbols) and distributions of priors (lines) for catchability terms.

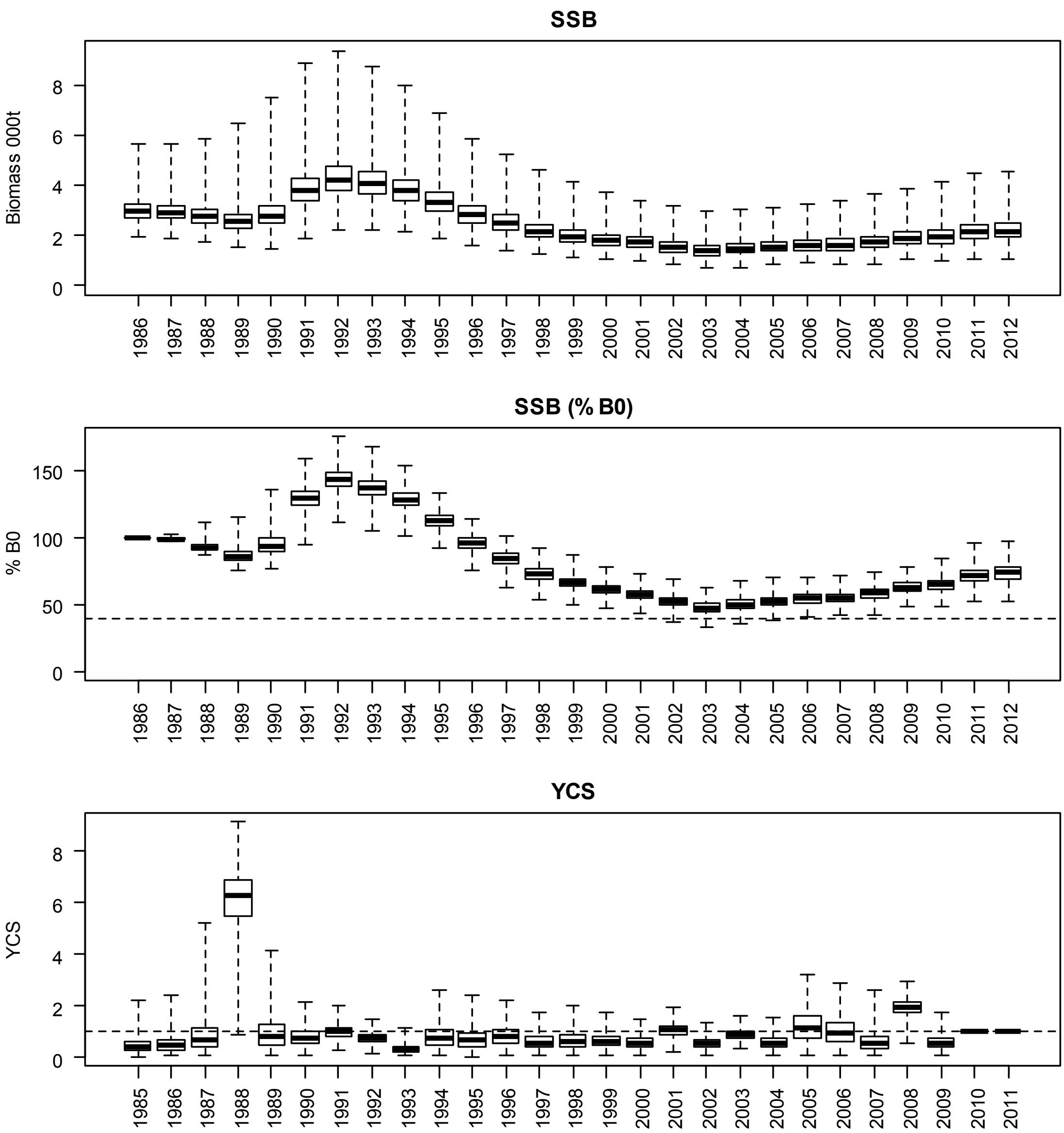

A7. 23: Posterior trajectory of SSB, SSB_{2012}/B_0 and YCS.